Australian Government
Geoscience Australia

Government of South Australia
Primary Industries and Resources SA

South Australian Seismic and MT Workshop 2010

Extended Abstracts

Edited by R.J Korsch & N. Kositcin

Record
2010/10
GeoCat #70149

South Australian Seismic and MT Workshop 2010

Extended Abstracts

GEOSCIENCE AUSTRALIA
RECORD 2010/10

Edited by R.J. Korsch[1] & N. Kositcin[1]

Australian Government
Geoscience Australia

Government of South Australia
Primary Industries and Resources SA

1. Onshore Energy and Minerals Division, Geoscience Australia, GPO Box 378, Canberra, ACT 2601, Australia

Department of Resources, Energy and Tourism
Minister for Resources and Energy: The Hon. Martin Ferguson, AM MP
Secretary: Mr Drew Clarke

Geoscience Australia
Acting Chief Executive Officer: Dr Chris Pigram

ISSN: 1448-2177
ISBN Print: 9781921672743
ISBN Web: 9781921672750

GeoCat # 70149

Bibliographic references:

Korsch, R.J., and Kositcin, N., editors, 2010. South Australian Seismic and MT Workshop 2010. *Geoscience Australia, Record,* **2010/10**.

Fomin, T., Holzschuh, J., Nakamura, A., Maher, J., Duan, J. and Saygin, E., 2010. 2008 Gawler-Curnamona-Arrowie (L189) and 2009 Curnamona-Gawler link (L191) seismic surveys – acquisition and processing. In: Korsch, R.J. and Kositcin, N., editors, South Australian Seismic and MT Workshop 2010. *Geoscience Australia, Record,* **2010/10,** 1-10.

Contents

2008 Gawler-Curnamona-Arrowie (L189) and 2009 Curnamona-Gawler Link (L191) seismic surveys – acquisition and processing

T. Fomin[1], J.Holzschuh[1], A. Nakamura[1], J. Maher[1], J. Duan[1] and E. Saygin[2]

[1] *Onshore Energy & Minerals Division, Geoscience Australia, GPO Box 378, Canberra, ACT 2601, Australia*
[2] *Research School of Earth Sciences, Jaeger Building, 61, The Australian National University, Canberra, ACT 0200, Australia*
tanya.fomin@ga.gov.au

Introduction

Deep seismic reflection surveys were carried out in South Australia for Geoscience Australia (GA) and the Department of Primary Industries and Resources, South Australia (PIRSA) by Terrex Seismic Pty Ltd in June-July 2008 (L189) and in January 2009 (L191). A total of 720.5 km of 2D seismic reflection and gravity data were acquired along four traverses across the Gawler Craton (Line 08GA-G1), the Curnamona Province (Line 08GA-C1), the Arrowie Basin (Line 08GA-A1) and between the Gawler Craton and the Curnamona Province (Line 09GA-CG1) (Figure 1). Line 09GA-CG1 linked to the 2003-2004 (Line 03GA-CU1) seismic survey, which was conducted under the Australian National Seismic Imaging Resource (ANSIR) program across the Curnamona Province.

Magnetotelluric data were also acquired along three of the seismic traverses (Thiel et al., 2010) and wide-angle seismic reflection data were collected on a 150 km central section of the Gawler Line 08GA-G1 (Figure 1).

The surveys were undertaken as a component of the Onshore Energy Security Program, funded by the Australian Government, and as part of the ongoing cooperation under the National Geoscience Agreement with the states and territories of Australia. They were designed primarily to provide an understanding of the crustal-scale geodynamics of the Proterozoic Gawler Craton, Curnamona Province and the Adelaide Rift System, and to encourage exploration for energy resources.

Seismic Reflection Data

Seismic reflection acquisition

A summary of the deep seismic reflection traverses collected in 2008 and 2009 is listed in Table 1. Line pegging, surveying and gravity data for the surveys were carried out by Dynamic Satellite Surveys Pty Ltd (DSS). Stations were pegged and surveyed using 40 m station intervals. Gravity readings were made at every 10th station (400 m spacing). Gravity data for the Curnamona-Gawler Link Line 09GA-CG1 were collected by PIRSA. DSS reports describe the operational and technical details of the surveying (Dynamic Satellite Surveys, 2008, 2009). The seismic line followed existing tracks and minor roads. Further details are provided in the Operations Report by Price et al. (2010).

Acquisition parameters used to collect the regional scale vibroseis reflection data were based on previous GA experience in hard rock seismic data environments and an experimental program, which was implemented prior to seismic acquisition, to determine the optimum parameters for the Gawler-Curnamona region. A summary of acquisition parameters is listed in Table 2.

2D 75 fold seismic reflection data were acquired to 20 s Two-Way-Travel Time (TWT) (approximately 60 km depth), using three HEMI-60 Vibroseis trucks as the energy source, and a multi channel Sercel SN388 recording system. The DISCO/FOCUS seismic processing software was used to QC the field data on a daily basis. Brute stacks were routinely produced in the field to further monitor data quality.

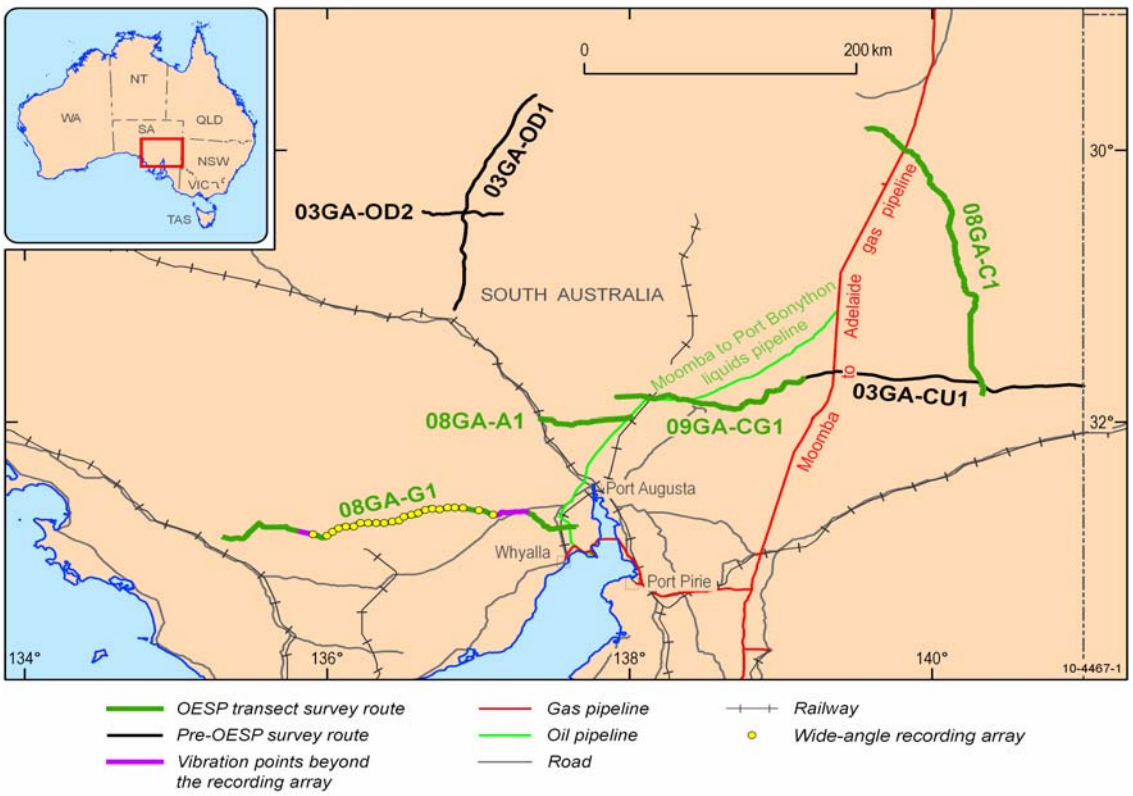

Figure 1. Location of 2008 Gawler-Curnamona-Arrowie and 2009 Curnamona Gawler Link Seismic Surveys (green lines). The wide-angle seismic line (150 km) coincides with the Gawler reflection transect. Deep seismic reflection lines acquired by Geoscience Australia in 2003 and 2004 are also shown (in black).

Seismic reflection processing

Seismic data were processed using DISCO/FOCUS seismic processing software. An example of the general processing stream used to process these data is summarised in Table 3. A description of some of the major processing steps is given below.

Line geometry and crooked line definition

The geometry for the seismic line is defined according to the location of the vibe-points and receivers. As the lines followed existing roads or tracks the lines were crooked. In order to perform optimal common mid-point stacking (CMP), it is necessary to define a CDP (common depth point) line, which is essentially a curve of best fit to the common midpoints generated by the various shot-receiver pairs which exist. This CDP line is less contorted than the actual seismic traverse and depends on the severity of the bends in the roads and tracks used.

All seismic sections, which are produced for display and interpretation, refer to this CDP line, and not the traverse used during acquisition.

Table 1. Summary of deep seismic reflection transects collected in South Australia in 2008 and 2009.

Survey Name	Line Name	Date, start to finish	Stations	Line Length
Gawler-Curnamona-Arrowie	Gawler 08GA-G1	6–23 June 2008	1313-7650	253.48 km
Gawler-Curnamona-Arrowie	Arrowie 08GA-A1	25–29 June 2008	1000-2510	60.4 km
Gawler-Curnamona-Arrowie	Curnamona 08GA-C1	3–23 July 2008	1000-7554	262.16 km
Curnamona-Gawler Link	Link 09GA- CG1	11–19 January 2009	1000-4611	144.44 km
			Total	**720.48 Km**
Gawler-Curnamona-Arrowie	Gawler Wide-Angle 08GAG1WA	3–21 June 2008	**Total**	**~150 Km**

Table 2. Summary of seismic reflection acquisition parameters.

LINE	08GA-G1, 08GA-A1, 08GA-C1, 09GA- CG1
AREA	Gawler Craton, Curnamona Province (SA)
DIRECTION	W to E (08GA-G1, 08GA-A1, 09GA-CG1), S to N (08GA-C1)
CDP RANGE	2002-14446(08GA-C1), 2002-4892(08GA-A1), 2628-14582 (08GA-G1), 2002-8497 (09GA-CG1)
SOURCE TYPE	3 x IVI Hemi-60
SOURCE ARRAY	15 m moveup, 15 m pad-to-pad
VIBRATION POINT (VP) INTERVAL	80 m
SWEEP	6-64 Hz, 12-96 Hz, 8-72 Hz; 3 x 12 sec
RECIEVER GROUP PATTERN	12 in-line @ 3.33 m spacing
GROUP INTERVAL	40 m
CHANNELS	300
FOLD (NOMINAL)	75
RECORD LENGTH	20 sec (approx. 60 km depth)
SAMPLE RATE	2 ms
RECORDING FORMAT	SEGD

Table 3. An example of the seismic reflection processing stream.

1. Line geometry and crooked line definition (CDP interval 20 m)
2. Field SEG-D to SEG-Y, SEG-Y to Disco/Focus format, resample to 4 ms
3. Quality control of the data and trace editing
4. Common midpoint (CMP or CDP) sort
5. Gain balance (spherical divergence corrections based on velocity function)
6. Spectral equalisation
7. Application floating datum residual refraction and automatic residual statics
8. Band pass filter
9. Velocity analysis
10. Normal moveout (NMO) correction with stretch mute
11. Offset regularisation and dip moveout (DMO) correction
12. Velocity analysis
13. Common mid-point stack of the data
14. Migration of the data (Finite Difference and Time-Space Kirchhoff)
15. Band pass filter
16. Signal enhancement (digistack)
17. Application of CDP mean datum statics
18. Amplitude balancing
19. Display data

Refraction statics corrections

The near-surface layers are often weathered (regolith) and exhibit substantial variations in thickness and seismic velocity. These effects cause variable travel times from one seismic trace to the next, which are not related to the configuration of the deep-seated reflectors. If these variations are not accounted for prior to CDP stack, a poor seismic section will result. Refraction statics computation is a technique used to determine such corrections, based on the travel times picked from the first arrivals on the shot records. These times are assigned to the appropriate refracting horizon(s) and solutions are obtained for the depth variation(s) and the velocity distribution(s) of the various horizons. Refraction statics corrections are applied in two stages, first floating datum statics (smaller static corrections) before NMO, and then the mean static corrections to the final datum before display of the data (datum 100 m for 08GA-G1 and 09GA-CG1, 130 m for 08GA-A1, 150 m for 08GA-C1). The application of the statics corrections improved the quality of the seismic data, especially in the upper 2 s TWT.

Velocity analysis and common midpoint stack of the data

Velocity analysis is a very important step in the processing of seismic reflection data, as the velocities are used to apply normal moveout (NMO) and dip moveout (DMO) corrections prior to CDP stacking of the seismic data.

Velocity analysis is usually carried out at two stages during the processing of the seismic data: after statics corrections and after DMO corrections. DMO corrections allow horizontal and dipping seismic events to stack at the same velocity (Figure 2). Velocities are picked on the basis of coherency of seismic events observed in a small range of post-stack data. Velocity functions, spaced on average at ~2-4 km intervals along the line, are used to produce the velocity model. Constraining a stacking velocity model in a hard rock environment is difficult, as the continuity of individual reflections is low.

The common midpoint (CMP) stacking procedure sums seismic traces to improve the signal-to-noise ratio, by suppressing noise and multiples, and therefore improving the quality of the data.

Migration of the seismic data

The main purpose of seismic migration is to bring reflections to their true spatial position in the seismic section, and to collapse diffraction waves. As a result of the migration procedure, reflections seen on a stacked section become steeper, shorter and closer to the surface on the migrated section. Unfortunately, in the areas with severe bends in the line, or some spikes (large amplitude events) in the data, migration can partly reduce data quality by producing artefacts. Migrated sections were used primarily in the geological interpretation of the seismic data.

Display of the seismic data

It is very important to choose appropriate display parameters for the final presentation of the data. It is difficult to present small features and large scale crustal structures in the same display with the same display parameters. Consequently two scales, using different display parameters, are used to display the seismic sections:

- A 1:50 000 scale section to interpret the upper crust (down to 6 s or ~18 km in depth);
- A 1:100 000 scale section (to 20 s TWT or ~60 km depth) for interpretation of crustal scale features including the Moho boundary.

All sections are displayed at vertical to horizontal scale ratio equal to 1, assuming average crustal velocity of 6000 m s^{-1}. After all the processing steps had been completed, signal enhancement and trace amplitude balancing procedures were used to improve the appearance of the plotted seismic data.

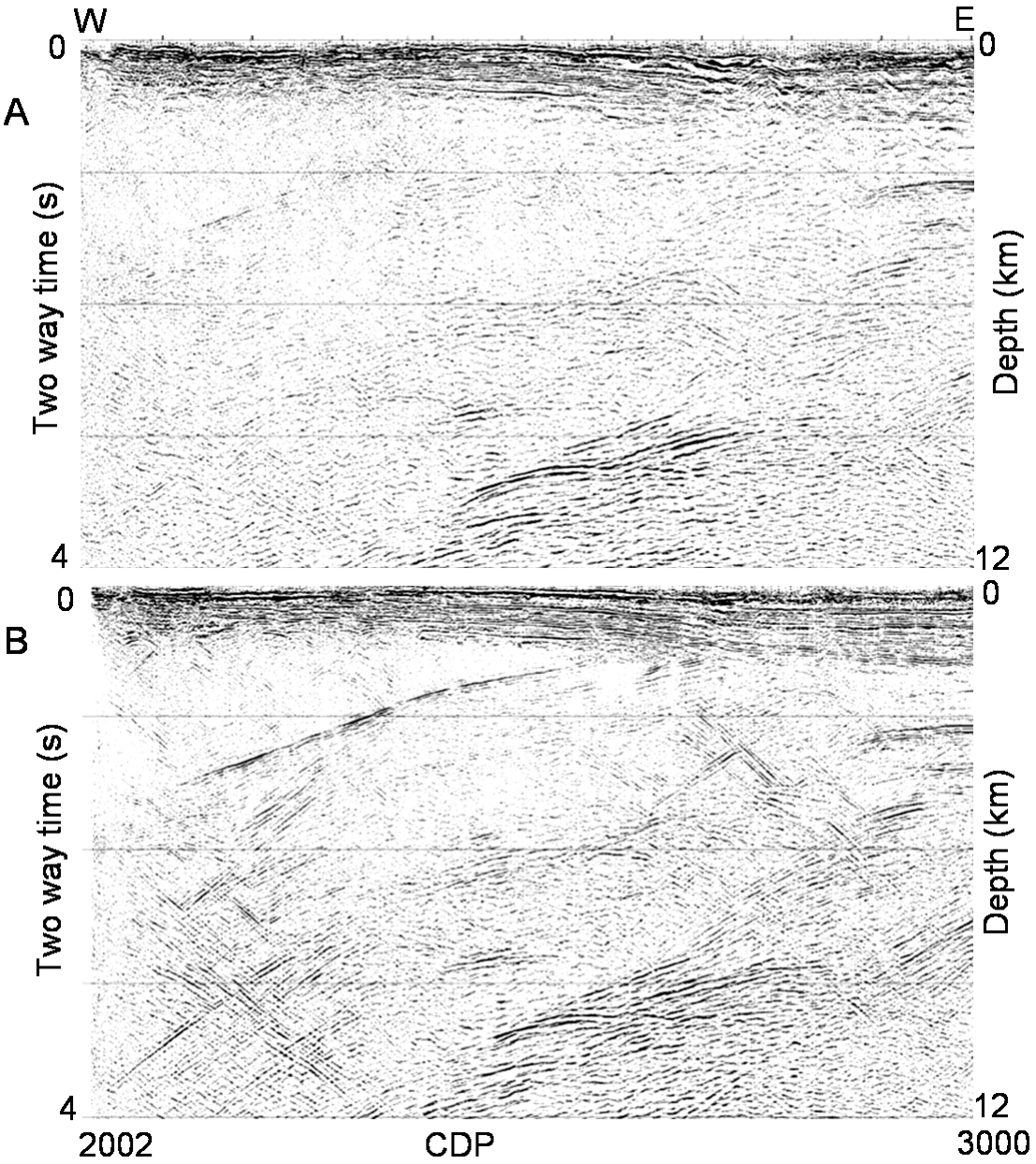

Figure 2. Fragment of stack section for seismic transect 08GA-A1. (A) Before DMO applied; (B) After DMO applied. 1 CDP equal 20 m; V:H=1 for a crustal velocity 6000 m s^{-1}. Dipping seismic events are imaged after DMO has been applied (B).

Wide-angle Seismic Reflection Data

Wide-angle seismic technique and acquisition parameters

A wide-angle reflection survey was carried out to supplement the deep seismic reflection studies, providing velocity information for the upper crust (10-15 km). The wide-angle Vibroseis experiment was conducted simultaneously with the 08GA-G1 Gawler reflection transect, using the same Vibroseis sources. The energy from these sources is sufficient to collect wide-angle data at 70-80 km offsets (Fomin et al., 2003; Fomin and Goleby, 2006). The wide-angle line, with a total length of 150 km (Table 1), was focused on the central part of the 08GA-G1 transect and crossed the western boundary of the South Australian Heat Flow Anomaly (SAHFA), which

is the boundary between the high-heat-producing granites in eastern part of the Gawler Craton and normal heat flow granites in the central Gawler Craton.

The 120 km long wide-angle recording array (yellow dots in Figure 1) was extended by 10 km to the west with vibration points and 25 km to the east with vibration points (purple line in Figure 1). As a result of positioning vibration points beyond the recording array on both ends of the line, maximum offsets in excess of the 150 km line were achieved (Figure 1). The acquisition parameters for the wide-angle reflection experiment were selected to ensure that the parameters would fit into the schedule and the technology used in the conventional seismic reflection survey, and, at the same time, ensure that high quality wide-angle data were collected, while utilising acquisition parameters of the reflection survey. The seismic source parameters are listed in Table 2.

The Australian National University (ANU) and the National Research Facility for Earth Sounding (ANSIR) provided the recording equipment to collect the wide-angle reflection data. 23 Earth Data recorders were deployed as a fixed recording array, with 5 and 10 km interval spacing. Three-component seismometers, with one vertical (Z) and two horizontal components (E) and (N), were used to collect the wide-angle data. The recording parameters used for this survey are specified in Table 4.

The survey ran for three weeks, and included three major stages: deployment of instruments, servicing the sites, and retrieving the equipment. These stages overlapped due to the complex nature of the work schedule. The program was designed to enable the most efficient utilisation of the recording equipment and GA personnel. Further details are provided in the Operations Report by Price et al. (2010).

The Earth Data recorders operated continuously during the wide-angle reflection survey, and not just at the time of vibration action which occurred during the reflection survey. The Sercel SN388 Recording System, which was used during the Gawler-Curnamona-Arrowie Seismic Survey, was developed in the early 1990's, at which time when GPS was not used with recording systems. Subsequently, it was not possible to connect the GPS unit to the Sercel SN388 system. To be able to extract uncorrelated sweeps produced by vibroseis trucks from collected wide-angle data, a stand-alone Data Logger designed and supplied by Monitor Sensors Company was used to obtain a True Time File from the Recording System. The Data Logger was designed to trigger the starting sweep time and log this time (with 1 ms accuracy) when an event occurs.

At the end of the survey, the internal hard disks were removed from the recorders and the data were downloaded to an external hard disk using a docking station. A copy of all raw data was written to DVDs.

Table 4. Seismic wide-angle recording parameters.

LINE	08GA G1WA
TYPE OF RECORDERS	24 Earth Data recorders 3 and 6 channels
SPACING INTERVAL	~ 5 and 10 km
RECORDING ARRAY	120 km fixed array, 23 stations from 3000 to 6126
STATION RANGE	2750-6750
CDP RANGE	5259-12909
RECEIVER-SOURCE DISTANCE	In an average from 30 to 100 km
SAMPLE RATE	250 samples per second (4 ms)
TYPE OF SEISMOMETERS	Mars-Lite 3-component 1 Hz seismometers
LISTENING TIME	Continuous
RECORDING FILE SIZE	15 min
GAIN LEVEL	High
GPS CORRECTION	15 min
RECORDING FORMAT	MiniSeed

Table 5. Summary of the processing sequence of wide-angle data.

1. Download raw data as continuous records from internal hard disk to intermediate media
2. Quality control of the data
3. Conversion from MiniSeed to SAC, extraction of one minute traces for every vibration, rotation of horizontal components to radial and transverse components, conversion SAC to SEG-Y format
4. Input SEG-Y data into Disco/Focus processing software
5. Line geometry
6. Sorting data into common receiver gathers
7. Cross-correlation with appropriate reference sweep
8. Stacking (vertical summing) of every three sweeps generated at the same vibration point
9. Spectral equalisation
10. Application of a minimum-phase band-pass filter
11. Reduction of data using a velocity of 8 km/s
12. Signal enhancement (digistack)
13. Amplitude balancing prior to final display
14. Output in SEG-Y format for loading to GeoFrame interpretation software

Wide-angle data processing

Wide-angle data were recorded along the central part of the Gawler line (08GA-G1) with 5 and 10 km spacing interval by using 23 Earth Data Loggers and 3-component seismometers. A multistep processing stream was used to prepare data for seismic velocity modelling. A detailed description of processing of the wide-angle data is given by Fomin et al. (2003) and Fomin and Goleby (2006). Some of the major processing steps are explained below. A summary of the processing sequence of wide-angle data is given in Table 5.

Conversion of the field data to SEG-Y format

An average 8000 single vibrations were recorded by each Earth Data Logger, from 2700 vibration points generated by the vibroseis vibrator trucks. Since there is no standard commercial software for processing vibroseis wide-angle data, several software packages and stand-alone programs were used at different stages of the processing. Software for conversion of MiniSeed format to standard SEG-Y was developed by the Seismology and Geomagnetism Group at the Research School of Earth Sciences, Australian National University. The conversion and extraction procedure consists of two steps: conversion from MiniSeed to SAC, with extraction of a minute of data for every sweep using ‘true time file’ (Price et al, 2010), and then conversion from SAC to SEG-Y (Fomin, 2010a, 2010b). Horizontal components north-south and east-west were rotated to radial and transverse components before conversion to SEG-Y format (E. Saygin, 2009, unpublished procedure). SEG-Y data obtained from that stage were processed in the DISCO/FOCUS commercial software package.

Sorting, cross-correlation and stacking data

Wide-angle data were sorted into the common receiver gathers, where each trace corresponds to a single vibration, with the spacing interval of 80 m between traces. Uncorrelated sweeps from the vibrator trucks were recorded on the tape during the experimental program, and were used for cross-correlation instead of generic sweeps which are generated in FOCUS. After the cross-correlation has been performed with appropriate recorded reference sweeps (Table 2), the obtained gathers were stacked (vertically summed) on an assumption that every three sweeps belong to the same vibration point.

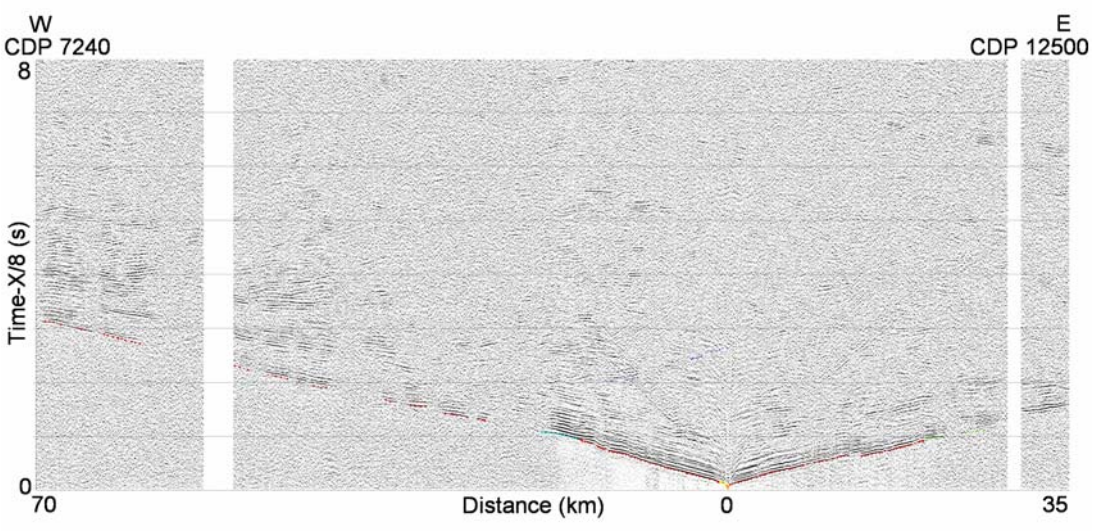

Figure 3. Example of the common receiver gather for Station 5625 at CDP 10740 (0 km) derived from wide-angle data collected along the Gawler reflection transect (08GA-G1). Colour lines show interpreted seismic events. Missing traces, that is, gaps in the section, were due to acquisition problems.

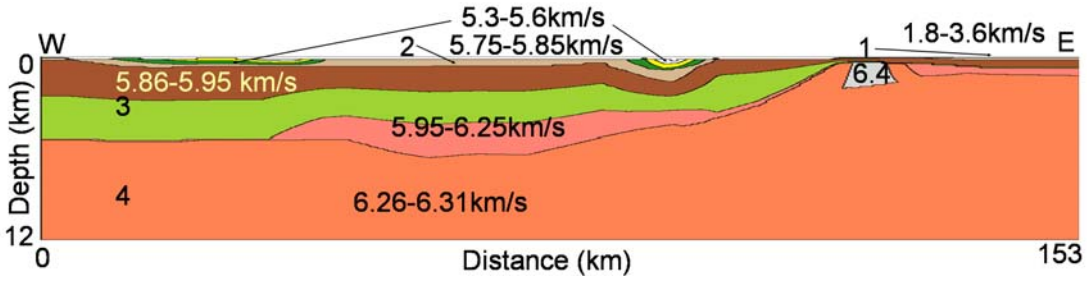

Figure 4. Velocity model of the upper crust derived from wide-angle data along the central part of the Gawler transect.

Enhancement of the data

Spectral equalisation was used to suppress low frequency noise. At the final stage, a minimum-phase bandpass filter was applied, knowing that the frequency of the useful signal was within 10-15 Hz. The data were then reduced using a velocity of 8000 m s^{-1}. The signal enhancement and amplitude balance were applied prior to a final display.

Figure 3 shows an example of common receiver data after all the processing steps were performed. Data quality is generally very good. High amplitude arrivals were observed up to 60-70 km offsets. Unfortunately, wide-angle reflection events from the lower crust are not observed clearly on the sections.

Final sections were converted to SEG-Y format, and loaded to GeoFrame Seismic Interpretation software for field analysis and interpretation of seismic events, and further velocity modelling using ray-tracing software (Fomin, 2010).

Velocity modelling

Travel time data from 23 stations were used to develop the seismic velocity model for the upper crust along the Gawler Craton traverse. Travel times were picked from common receiver gathers, including up to three seismic events from different boundaries in the first arrivals (colour lines in Figure 3).

The process of developing the velocity model included two steps: (1) designing a starting model based on wave field analysis of wide-angle data, and (2) iterative ray-tracing to achieve a match between computed and recorded travel times. The forward modelling software, based on the ray-tracing algorithm of Zelt and colleagues (Zelt and Smith, 1992; Zelt et al., 2003) was employed.

The final velocity model shows a range of seismic velocity variations in the upper crust (Figure 4). The model consists of three layers over basement (6.26 - 6.31 km s^{-1}):

(1) A thin upper layer from 4 to 200 m depth, with velocity 1.8-3.6 km s^{-1};
(2) A 200-900 m thick layer, with 5.75-5.85 km s^{-1} velocity; with two local bodies having a relatively lower velocity of 5.3-5.6 km s^{-1};
(3) A thick layer with 5.86-6.25 km s^{-1} velocity (possibly granite-gneissic composition) down to 5.5 km depth in the western part of the line and only 1.3 km in the east; and
(4) Basement with 6.26-6.31 km s^{-1} and 6.4 km s^{-1} high velocity body.

The wide-angle reflections for the deep crust were not prominent on common receiver gathers (Figure 3), therefore it was not possible to build a velocity model for lower crust.

The final results of the wide-angle data is in preparation (see Fomin, 2010a, 2010b; Fraser et al., 2010).

Conclusions

Approximately 720 km of high quality 2D deep seismic reflection data were acquired using vibroseis sources along four seismic traverses during the 2008 Gawler-Curnamona-Arrowie and 2009 Curnamona Gawler Link Seismic Surveys. As a part of this project, a wide-angle vibroseis experiment was carried out along central part of the Gawler transect, simultaneously with recording of seismic reflection data. Seismic data processed by Geoscience Australia imaged the entire crust from the shallow upper crust down to the Moho.

Knowledge of the acquisition parameters and processing steps helps to resolve differences in these seismic datasets and also helps to understand their advantages and limitations. An understanding of the acquisition, processing, analysis and modelling technologies has improved the quality of the geological interpretation of data over the Gawler Craton.

Acknowledgements

We thank colleagues in the Geoscience Australia Seismic Acquisition and Processing project for their support. The authors are grateful to Prof. Brian Kennett, The Australian National University and ANSIR (National Research Facility for Earth Sounding) for providing the wide-angle recording equipment to collect the data. We especially thank Mondo Arcidiaco and Erdinc Saygin from the Seismology and Geomagnetism Group of the Research School of Earth Sciences, Australian National University, for providing the software to convert the raw data into SEG-Y format. We also thank Richard Chopping and Russell Korsch for their reviews of the manuscript.

References

Dynamic Satellite Surveys, 2008. Final Operations Report on the 2008 Gawler, Arrowie, Curnamona 2D Seismic Survey for Terrex Seismic Pty Ltd and Geoscience Australia, June-July 2008. *Report DSS08030.*

Dynamic Satellite Surveys, 2009. Final Operations Report on the 2008 Gawler–Officer-Musgrave–Amadeus GOMA & Curnamona, Gawler Link CGL 2D Seismic Survey for Terrex Seismic Pty Ltd and Geoscience Australia, October-December 2009. *Report DSS08057.*

Fomin, T., Crawford, A.R. and Johnstone D.W., 2003. A wide-angle reflection experiment with vibroseis sources as part of a multidisciplinary seismic study of the Leonora-Laverton tectonic zone, Northeastern Yilgarn Craton. *Exploration Geophysics*, **34**, 147-150.

Fomin, T. and Goleby, B.R., 2006. Lessons from joint interpretation of Vibroseis wide-angle and near-vertical reflection data in the Northeastern Yilgarn, Western Australia. *Tectonophysics,* **420**, 301-316.

Fomin, T., 2010a. Gawler Wide-Angle Vibroseis Seismic Survey, Gawler Craton, South Australia, 2008. *Geoscience Australia, Record, in preparation.*

Fomin, T., 2010b. Combining wide-angle and reflection vibroseis surveys: advantages and limitations of these techniques, northern Eyre Peninsula, Gawler Craton. 14th International Symposium on Deep Seismic Profiling of the Continents and their Margins - Cairns, Australia, 29 August - 4 September 2010. *in preparation.*

Fraser, G.L., Blewett, R.S., Reid, A.J., Korsch R.J., Dutch, R., Neumann, N.L., Meixner, A.J., Skirrow, R.G., Cowley, W.M., Szpunar, M., Preiss, W.V., Nakamura, A., Fomin, T., Holzschuh J., Milligan, P.R. and Bendall, B.R., 2010. Geological interpretation of deep seismic reflection and magnetotelluric line 08GA-G1: Eyre Peninsula, Gawler Craton, South Australia. *Geoscience Australia, Record,* **2010/10**, this volume.

Price, J., Fomin, T. and Duan, J., 2010. Gawler, Curnamona, Arrowie and Curnamona Gawler Link Seismic Surveys, (L189 & 191), South Australia, 2008-2009, Operations Report. *Geoscience Australia, Record, in preparation*.

Thiel, S., Milligan, P.R., Heinson, G., Boren, G., Duan, J., Ross, J., Adam, H., Dhu, T., Fomin, T., Craven, E., and Curnow, S., 2010. Magnetotelluric acquisition and processing, with examples from the Gawler, Curnamona and Link transects in South Australia. *Geoscience Australia, Record,* **2010/10**, this volume.

Zelt, C.A., Sain, K., Naumenko, J.V., and Sawyer, D. S., 2003. Assessment of crustal velocity models using seismic refraction and reflection tomography. *Geophysical Journal International*, **153**, 609-626.

Zelt, C.A. and Smith, R.B., 1992. Seismic travel time inversion for 2-D crustal velocity structure. *Geophysical Journal International*, **108**, 16-34.

Magnetotelluric acquisition and processing, with examples from the Gawler Craton, Curnamona Province and Curnamona-Gawler Link transects in South Australia

S. Thiel[1], P.R. Milligan[2], G. Heinson[1], G. Boren[1], J. Duan[2], J. Ross[1], H. Adam[1], T. Dhu[3], T. Fomin[2], J. Maher[2], E. Craven[3], S. Curnow[2]

[1] School of Earth & Environmental Sciences, The University of Adelaide, Adelaide, SA 5005, Australia
[2] Onshore Energy & Minerals Division, Geoscience Australia, GPO Box 378, Canberra, ACT 2601, Australia
[3] Geological Survey Branch, Primary Industries and Resources South Australia (PIRSA), GPO Box 1671, Adelaide, SA 5001, Australia

Stephan.Thiel@adelaide.edu.au

Introduction

The magnetotelluric (MT) geophysical survey method uses natural time variations of the magnetic and electric fields of the Earth to measure its electrical conductivity distribution. Ratios of electric to magnetic field measurements, made over a range of frequencies, provide estimates of conductivity with depth; the lower the frequency the greater the depth of the estimate. Whereas the actual depth of measurement also depends upon the conductivity distribution itself, MT data acquired over a wide range of frequencies can provide conductivity information from very near surface to hundreds of kilometres into the mantle (Simpson and Bahr, 2005).

The MT method utilises the diffusion of the time variations of the magnetic field of the Earth into the ground, to provide a source signal, with the electric field variations being the induced response. It differs in this respect from the seismic method, which utilises the reflection of acoustic energy at property boundaries within the Earth, and is thus a wave propagation process. This fundamental difference in the physics of the two methods is why the resolution of conductivity by the MT method is low, compared with the seismic method, particularly as the depth of penetration increases and the signal diffuses into a larger volume.

MT data are acquired at ground sites, either by a single instrument or by several instruments recording concurrently. Although information from single instrument sites can be analysed and ultimately combined with data from other sites, concurrent recording is preferable, to enable remote referencing for the removal of uncorrelated noise. Multisite distributions are commonly along profiles, as in the examples referred to below, in which a 1D or 2D conductivity distribution with depth is assumed. 3D arrays of instruments provide the best information for analysing the 3D conductivity distribution of the Earth, but the modelling of data from such arrays with 3D code is still in its infancy.

Geoscience Australia (GA), The University of Adelaide, and Primary Industries and Resources South Australia (PIRSA) have acquired MT data along three seismic transects in South Australia, as part of the Onshore Energy Security Program funded by the Australian Government, and as part of the National Geoscience Agreement (NGA) with the states and territories of Australia (Figure 1). Data along the east-west Gawler Craton seismic line (08GA-

G1) were acquired in a collaborative project between the University of Adelaide and GA in 2008 and 2009, data along the Curnamona-Gawler Link seismic line (09GA-CG1) were acquired in a collaborative project between PIRSA (main funding from the Plan for Accelerating Exploration (PACE) initiative), GA and the University of Adelaide in 2009, and data along the north-south Curnamona Province seismic line (08GA-C1) were acquired for GA in 2008 by Quantec Geoscience on behalf of Terrex Seismic Pty Ltd. Examples from these three surveys are used here to illustrate data acquisition and processing of the MT method. Interpretation results for each specific seismic line are provided in other papers of this volume (Korsch et al., 2010; Preiss et al., 2010; Fraser et al., 2010).

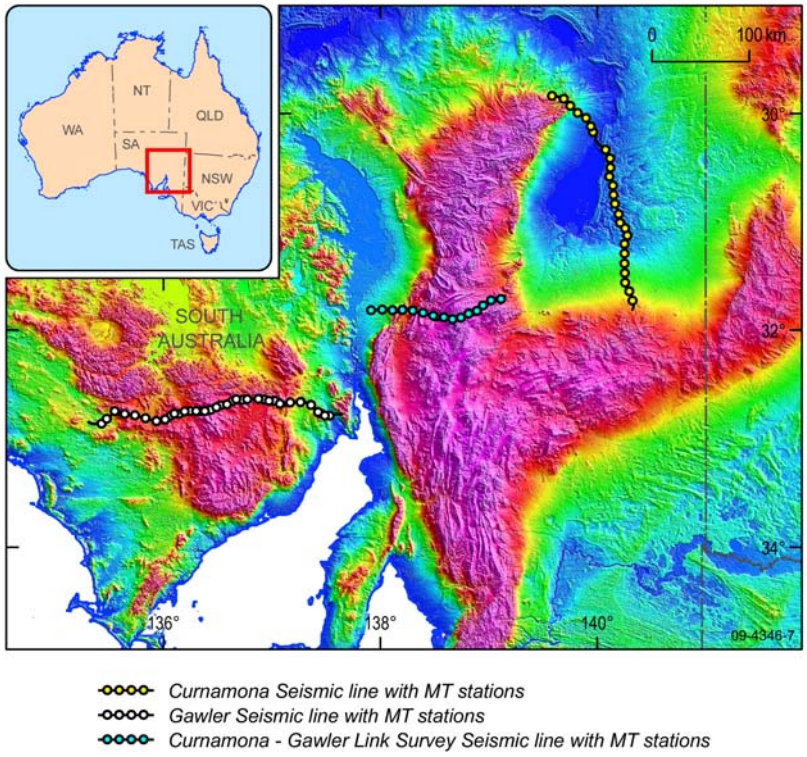

Figure 1. Locations of the three seismic lines in South Australia along which magnetotelluric measurements have been made at the sites indicated by the circles. Base map is a digital elevation model derived from the Shuttle Radar Topography Mission (Farr et al., 2007).

Electrical Conductivity of the Earth

The electrical conductivity of Earth materials has a large range, across 14 orders of magnitude, from dry crystalline rocks, with very low conductivity, to highly saline fluids, with very high conductivity. In order to be useful in a geological interpretation context, measured conductivity must be related to other rock properties, such as composition, porosity, permeability, fluids, mineralisation, fractures and faults, and temperature. The electrical conductivity of a volume of rock can be complex, for example, a granite pluton with few fractures will be highly resistive, but if the same rock material is highly fractured and permeable, then saline, percolating fluids will greatly increase the bulk conductivity. For Earth material other than uniform sediments, and perhaps the mantle, it is difficult to relate small volume sample conductivity measurements to the bulk conductivity, as sensed by methods such as MT (Simpson and Bahr, 2005).

Four different conduction mechanisms contribute to the bulk conductivity of rocks. In fluid-saturated porous rocks, *electrolytic* conduction plays the major role. Fractured rock or fluid-filled sediments are an example where electrolytic conduction is important. Porosity, permeability and the connectivity of the pore system are the physical parameters governing the bulk resistivity of the rock (Archie, 1942). Moreover, the concentrations of the pore fluid, as well as temperature, are chemical contributing factors. If an abundance of graphite or sulfides exist, even along thin

films of micrometre scale, in an interconnected network, *electronic* conduction can increase the bulk conductivity by several orders of magnitude.

Semiconduction is the most common electrical transport process in the Earth's crust and mantle. Temperature is the main controlling factor, and conductivity rises exponentially with temperature (Arrhenius-type behaviour). At room temperature, most rock-forming minerals are almost insulators. An increase in temperature leads to lattice defects, and an increase in mobility of charge carriers. Two conduction mechanisms can be differentiated, depending on temperature. Extrinsic charge transport dominates at low temperatures, with movement of impurities on interstitial lattice positions. Intrinsic conduction is dominant for high temperatures, with ions of the crystal lattice moving from their regular position to an interstitial position (Nover, 2005). At depths of 400 km and 670 km, olivine experiences phase transitions, into the spinel phase, by changing its crystallographic structure. The phase transitions are associated with an increase in conductivity by a factor of 1.5. Semiconduction is less dependent on pressure compared to the electronic and electrolytic conduction processes.

Partial melts also increase the conductivity by several orders of magnitude. Their formation depends on the temperature, chemical composition of the rocks, hydrous mineral phases and abundance of free water (Nover, 2005). Partial melts play a major role in volcanic systems, although across Archean cratons such as the Gawler Craton, semiconduction of olivine is the main contributing factor to the resistivities seen. Fault zones can connect graphite phases through intense shearing, and may be a cause for enhanced conductivity.

Method

The MT method is a passive electromagnetic (EM) technique which measures natural changes in the magnetic field of the Earth, as well as their secondary responses of the induced electric field (Tikhonov, 1950; Cagniard, 1953). The magnetic field B and electric field E are measured in orthogonal directions at the surface of the Earth. Surveys conducted in mid latitudes, away from the geomagnetic equator and poles, have a uniform and planar source B-field {Bx, By, 0}, also referred to as the primary field. The measured components of the E-field {Ex, Ey}, and the vertical magnetic field component Bz, contain information about the subsurface, and are regarded as the secondary fields. The ratio between the primary and secondary fields is a function of the conductivity σ of the subsurface (or its inverse resistivity $\rho = 1/\sigma$). As the conductivity of rocks ranges by several orders of magnitude (Guéguen and Palciauskas, 1994), the MT method is a tool of choice for imaging structures from tens of metres to hundreds of kilometres.

As the MT method uses natural sources it is, therefore, relatively low-cost. The fluctuations of the magnetic field are generated by lightning discharges for periods shorter than 1 s, which travel as an EM wave in the ionospheric waveguide between the surface of the Earth and the ionosphere. Signals in the period range between 10 s and 10^4 s originate from interaction between the solar wind and the magnetosphere and ionosphere (Vozoff, 1991). The dead band dominates for periods around 1 s, where there is little naturally-occurring signal. Sufficiently long deployments and remote referencing are usually needed to obtain meaningful estimates for that period band.

The MT fields behave diffusively, and are distinctly different to the potential field methods, for example, gravity and magnetics, as well as the wave methods (seismics, ground-penetrating radar (GPR)). The diffusive EM fields are non-reversible, and behave similar to, for example, heat diffusion. Geophysical wave methods, such as seismics and GPR, have a dominant wave part, and usually achieve a higher resolution at the expense of penetration, particularly for the EM method GPR. The depth of penetration obeys the skin-depth relation, and is essentially dependent on the frequency of the signal and the bulk conductivity of the subsurface. Low frequencies or long periods penetrate deeper into the crust and high conductivities (low resistivities) of the rock matrix inhibit penetration of the signal. The relationship between the inducing horizontal magnetic field components {Bx, By} and the induced electric field components {Ex, Ey} is expressed through a transfer function, the impedance tensor Z. The complex impedance tensor Z contains all information about the subsurface, and is commonly expressed as apparent resistivity ρa and phase φ. The impedance tensor is calculated for a

range of frequencies equally spaced across the period log-scale. Broadband MT deployments range between periods of 10^{-3} to 10^{3} s, while long-period MT measurements range between 10 to 10^{5} s. MT data are usually displayed as apparent resistivity and phase plots as a function of period (Figure 2), and as pseudosections with distance along the horizontal axis and period along the vertical axis (Figure 3).

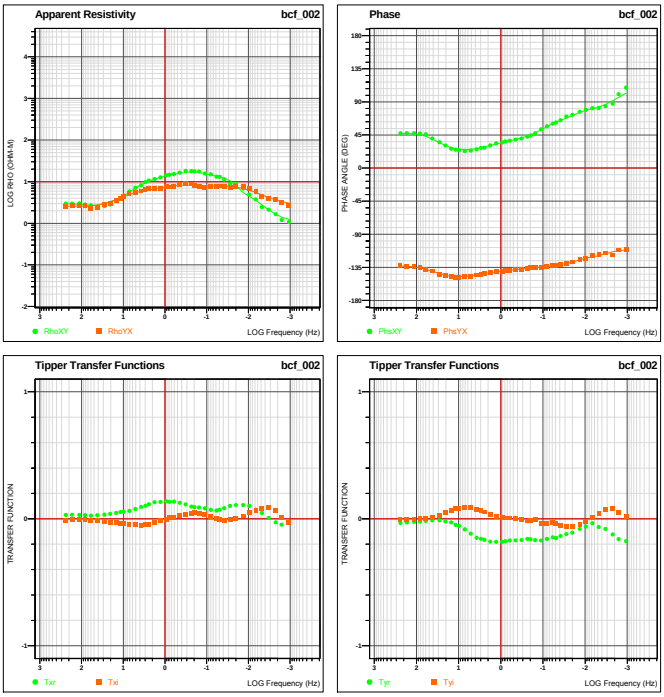

Figure 2. An example from site BC02 (Curnamona MT acquisition along seismic line 08GA-C1) of apparent resistivity, phase (XY, red and YX, green) and tipper transfer function (Txr, Txi, red, Tyr, Tyi, green) sounding curves (from Stockill et al., 2009).

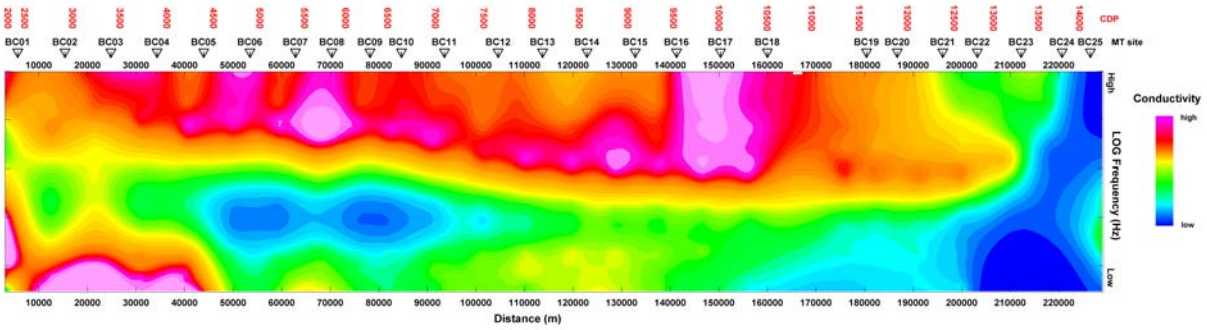

Figure 3. An example pseudosection of TE apparent resistivity from broadband acquisition along the Curnamona Province traverse. Section is south (left) to north (right), with $\log_{10}$ frequency for the vertical axis.

Analysis and interpretation of the subsurface distribution contained in the impedance tensor simplify, in some cases, where the resistivity distribution of the lithosphere can be approximated by a 1D or 2D Earth. For a 1D Earth, the orientation of the electrodes (E-field) and the magnetometer (B-field) in the field are irrelevant; the estimates of apparent resistivity and phase will always be the same for a given period. In a 2D setting (for example, faults), the impedance tensor is fully occupied for a general coordinate system. If the measurement coordinate system aligns with the strike of the fault, however, the tensor separates into two modes, the TE-mode (transverse electric) and the TM-mode (transverse magnetic). The TE-mode describes the ratio between the electric field along strike and the magnetic field across strike, while the TM-mode is the ratio of the electric field across strike and the magnetic field along strike. As a general rule, the TE-mode is better at estimating the resistivities either side of a fault, whereas the TM-mode

delineates vertical boundaries well due to the electric currents crossing the boundary perpendicular. In a 3D environment, the impedance tensor cannot be simplified in any coordinate system. A summary of the dimensionality behaviour is shown in Table 1.

As mentioned above, the vertical Bz field is also regarded as a secondary field generated from induced currents in the Earth. Over a uniform conducting half-space, no vertical induced magnetic field is generated from induction by the horizontal source fields. When there is a lateral change in the conductivity, however, for example along a fault boundary, then induced electric currents do have a vertical field component. Thus, information regarding lateral variations in subsurface conductivity can be gained from analysing the ratio of the vertical induced magnetic field variations to the horizontal source field variations, and this provides additional information to the MT measurements about the Earth conductivity distribution.

Table 1. Dimensionality behaviour of the impedance tensor. The impedance tensor becomes more complex for increasing subsurface dimensionality.

	Dimensionality		
	1-D	2-D	3-D
tensor components	$Z_{xx} = Z_{yy} = 0$ $Z_{xy} = -Z_{yx}$	$Z_{xx} = -Z_{yy}$ $Z_{xy} \neq -Z_{yx}$	$Z_{xx} \neq -Z_{yy} \neq Z_{xy} \neq Z_{yx}$
impedance tensor Z	$\begin{pmatrix} 0 & Z_n \\ -Z_n & 0 \end{pmatrix}$	$\begin{pmatrix} 0 & Z_{\parallel} \\ Z_{\perp} & 0 \end{pmatrix}$	$\begin{pmatrix} Z_{xx} & Z_{xy} \\ Z_{yx} & Z_{yy} \end{pmatrix}$

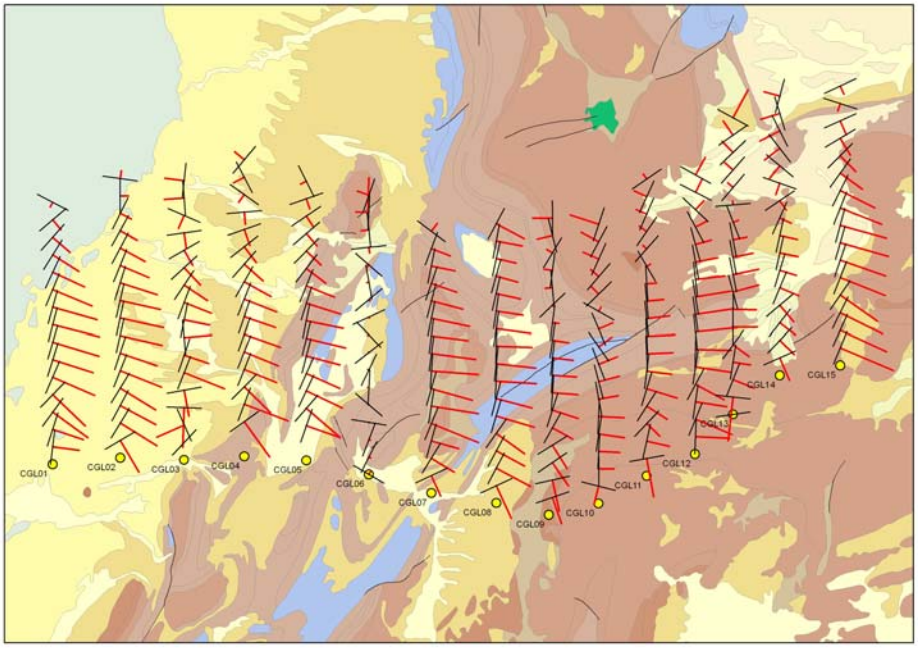

Figure 4. In-phase Parkinson arrows (red) and strike symbols (black) for MT long-period data acquired along the Curnamona-Gawler Link seismic traverse at the yellow circle site locations, and overlaid on the 1:1 000 000 scale Geology of Australia (Whitaker et al., 2008). The longest period data is represented at the site itself, and the shortest period furthest to the top from the site. The arrows show a consistency in direction predominantly east-southeast, with longer periods tending more southerly. Thus, they generally point towards the axis of the Flinders Anomaly conductor, previously mapped to the south-east of this traverse (Gough et al., 1972; Chamalaun, 1986).

Parkinson Arrows (Parkinson, 1959) are a useful graphical way of showing the relationship between the vertical magnetic field and the horizontal field as a function of frequency, and are oriented by convention to point towards lateral regions of higher conductivity. The length of the arrow is a function both of the strength of the currents, which give rise to the vertical field variations, and the distance of the measuring site from the induced currents. As with the MT tensor, the transfer functions which define the arrows are complex functions of frequency; thus two arrows are defined, an in-phase arrow and a quadrature-phase arrow. If there is a well-defined arrow for a particular measurement site, then the direction at 90^0 to the arrow direction defines the regional electrical strike, and this is an additional strike measure to the strike determined by the MT tensor. It should be noted that for responses from shallow sources, which are essentially 1D, the arrows are very small, and both strike directions and arrow directions become meaningless. Figure 4 shows in-phase Parkinson arrows for the long-period data acquired along the Curnamona-Gawler Link traverse.

Instrumentation and Data Acquisition

At each MT site, magnetic data are acquired in either two or three orthogonal directions, depending upon whether the vertical field is measured, and electric data are acquired in the two orthogonal horizontal directions. The instruments used for recording magnetic data include induction coils for the higher frequencies (broadband) and fluxgate magnetometers for the lower frequencies. The precise mix of each depends upon the survey specifications and the frequency responses of the instruments. For example, data collected by contractors in Australia use only induction coils with a wide frequency range (including a vertically deployed coil), whereas the AuScope instrumentation provides a mixture of two horizontal induction coils and a three-component fluxgate magnetometer for the low frequency measurements. Electric field data are acquired by two orthogonal sets of electrodes, with electrode separation typically between 20 m and 100 m. There are several types of electrode; for example, contractors acquiring broadband data in Australia use steel spikes driven into the ground, whereas the AuScope equipment provides copper–copper sulphate electrodes. The latter are non-polarisable electrodes, and are, therefore, not prone to drifts in the electric field. The drifts are only relevant for long-period MT data with deployments of the order of days. Figure 5 shows examples of AuScope instruments deployed along the Gawler seismic traverse.

For broad-band deployments, the components of magnetic and electric field are typically recorded at a sampling rate of 500 Hz, allowing a bandwidth of approximately 100−0.001 Hz, and stored on a local hard-drive. At frequencies lower than 0.001 Hz, the induction coils lose much of their sensitivity. The fluxgate magnetometers, however, are sensitive well below that frequency, but are limited in the high frequency band (> 0.1 Hz). For long-period MT deployments, the sampling frequency is usually of the order of 10 Hz, and the measured time-series is subsequently sub-sampled into 1 s blocks. Modern equipment uses GPS-syncing for precise time-stamping of the observed electric and magnetic field measurements. Thus, remote referencing procedures in the processing stage become more accurate, especially in the high-frequency range, where synchronous measurements between stations are critical.

The length of deployment usually depends on the depth of the target. Broadband surveys are used for targets within the top few 10s of kilometres of the crust, and deployments between 1 to 3 days are sufficient. Long-period surveys are used for identifying regional features in the crust and upper mantle. The necessity of having longer periods for deeper EM signal penetration requires deployments of between 3 days to several weeks.

Figure 5. Examples of AuScope instrumentation, as deployed along the Gawler and Curnamona-Gawler Link traverses. Top left, broadband induction coil. Top right, Fluxgate magnetometer in housing. Bottom left, control and logging instrumentation. Bottom right, burial of electrode.

Analysis

The time-series data are converted into the frequency domain using robust remote reference codes (Chave and Thomson, 1989, 2004; Egbert, 1997), which remove outliers in the measured time-series (for example, from passing cars) and calculate Fourier coefficients for varying time window lengths across the measured time-series. Typically, two Fourier coefficients are calculated for each window and a decimation process changes the window lengths, yielding about seven Fourier coefficients per frequency decade. The Fourier coefficients are the transfer functions between the electric and magnetic field, the impedance tensor Z.

Noise in the predicting magnetic field channels can lead to a downward bias of the impedance amplitudes (or the apparent resistivities) in the period range of 1−10 s. The estimates of the impedance tensor Z can be improved using a remote referencing procedure. Synchronous horizontal magnetic field measurements from an adjacent site are used as a remote reference. In practice, more than one station is usually deployed at a time to enable remote-referencing. The underlying idea is that noise is usually random, and cross-correlation with the magnetic field fluctuations of a remote site and the observation site enables distinction between coherent signal and noise (Egbert, 2002). Alternatively, geomagnetic observatory data are also used successfully for remote referencing long-period data. Local coherent noise, for example, from electric trains, in the vicinity of tens of kilometres, may contaminate the signal, giving preference to observatory data, which is usually collected from a distance much farther away (> 500 km).

Before modelling can be attempted, it is important to define the dimensionality of the data set, and if two-dimensionality has been established (as is usually the case for at least a certain period bandwidth), the correct geoelectric strike has to be determined. The strike angle defines the coordinate system in which the impedance tensor separates into the TE- and TM-mode. The separation into the independent modes is a necessary requirement for 2D modelling.

The dimensionality of the subsurface is determined using either a variety of decomposition methods (Groom and Bailey, 1989; Bahr, 1991; Lilley, 1998; Ledo et al., 1998; Utada and

Munekane, 2000; McNeice and Jones, 2001) and/or MT invariant methods (Weaver et al., 2000; Caldwell et al., 2004; Marti et al., 2005). The decomposition methods make assumptions about the regional resistivity distribution, in most cases 2D, to determine the local galvanic distortion, which can be subtracted from the measured impedance response. MT invariant methods, such as phase tensor analysis (Caldwell et al., 2004), are defined so that the phase tensor is independent of the galvanic distortion matrix. It can be shown that the phase tensor behaves independently from influences of local galvanic (non-inductive) perturbations, and is identical to the regional phase tensor at all times.

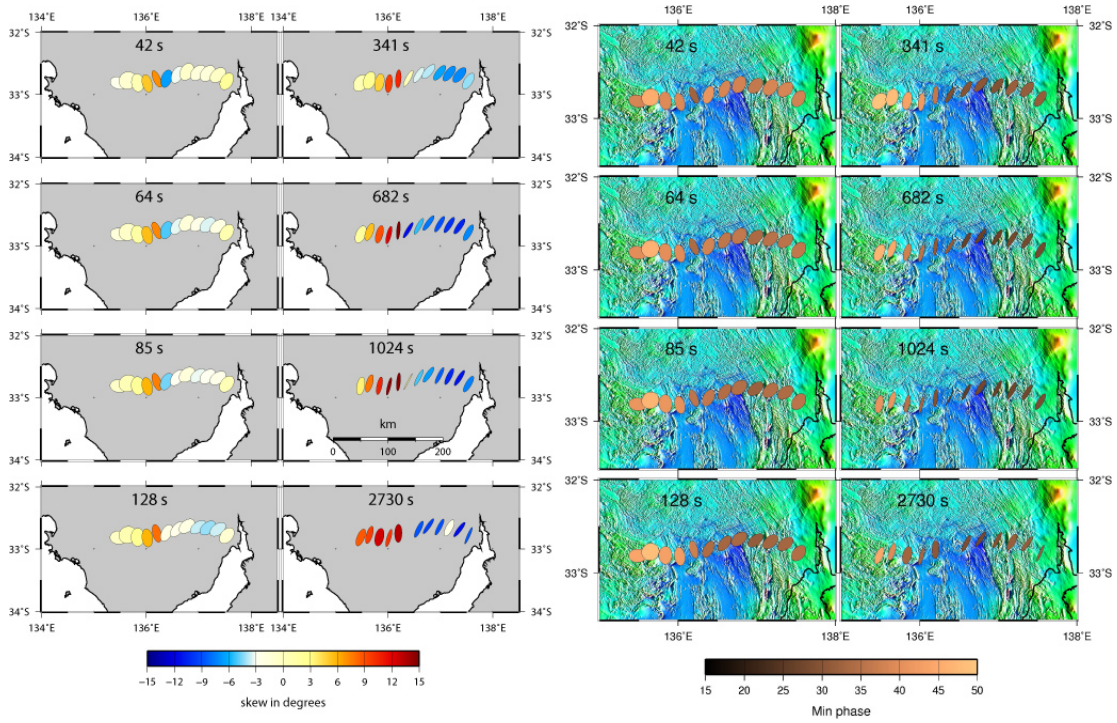

Figure 6. Phase tensor ellipses for the 12 long-period responses along the Gawler transect. For periods up to a few 100 s, there is a clear distinction between the western and eastern sites with varying major current flow as depicted by the major orientation of the ellipses. Skew values indicate mostly two-dimensionality for periods up to 300 s with increasing complexity for longer periods (left image). Ellipses on right image are shaded according to minimum phase; the base image is of total magnetic intensity.

The phase tensor, therefore, is a simple and useful tool to determine the dimensionality and the strike of the subsurface. Three invariants define the phase tensor ellipse: the minimum phase, the maximum phase, and the skew angle β. The maximum phase defines the orientation of the current flow for the respective frequency. In a 2D setting the maximum phase is either parallel or perpendicular to the geoelectric strike of, for example, a fault. At the same time the skew angle β = 0. The skew angle is a measure of three-dimensionality. As a rough guide, if the skew angle is within 5 degrees for a certain period bandwidth and across adjacent stations, then the corresponding subsurface can be regarded as predominantly 2D (Thiel et al., 2009). Figure 6 shows phase tensor ellipses and minimum phase values for the Gawler MT data. Minimum phase values are generally large for the western sites and small for the eastern sites. The minimum phase value indicates a qualitative measure of change in resistivity with depth. Low phases below 45 degrees indicate a transition from conductive to more resistive crust with increasing depth. On the other hand, high phases point toward a transition from resistive to conductive crust for the penetration depth of the given period.

Modelling

Modelling of MT data can be divided into two main approaches. Forward modelling assumes a simplified resistivity distribution in the modelling domain, from which the responses at the station locations are computed. This is usually a trial-and-error approach, with the aim of reproducing

induction arrow responses and/or apparent resistivities and phases (Brasse et al., 2009; Thiel et al., 2009). Inverse modelling is more common, and MT responses are used to change the model space in an automated way until a minimum misfit between model and observation responses is achieved (deGroot Hedlin and Constable, 1990; Siripunvaraporn and Egbert, 2000; Rodi and Mackie, 2001).

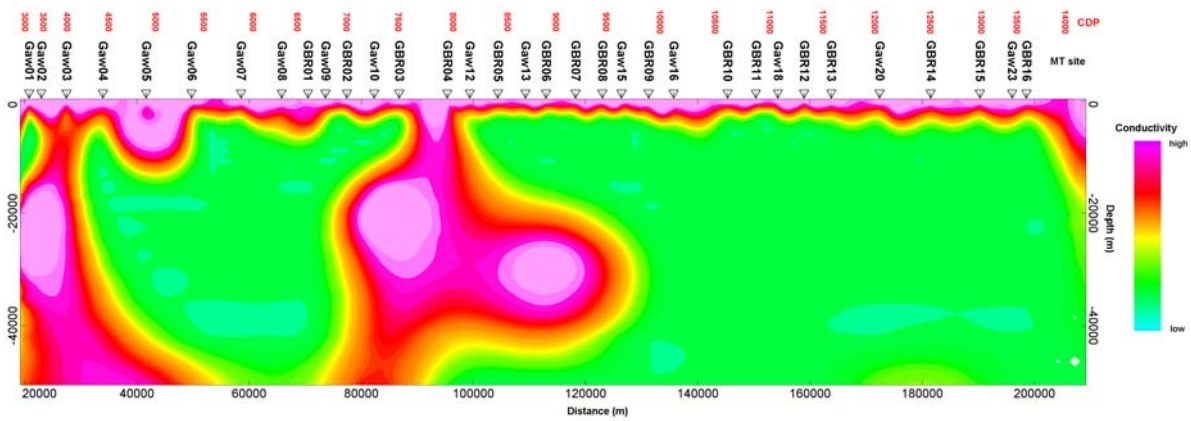

Figure 7. 2D model of the Gawler MT data, west (left), east (right). Depth of the section is approximately 50 km.

Currently, 2D inverse modelling is standard in the academic community, complemented by 3D forward modelling for hypothesis testing. 3D inverse modelling is still in its infancy, but promising results have been obtained for targets ranging from geothermal exploration to deeper lithospheric structures (Heise et al., 2007; Patro and Egbert, 2008; Thiel and Heinson, 2009). Achieving a reliable model from a non-linear and regularized inversion procedure requires careful tests of inversion parameters. It is important to test the robustness of features in the model to varying parameters and to avoid getting trapped in local minima. The inversion minimises the regularised penalty functional. The trade-off parameter balances the data misfit functional and the structure penalty term. Commonly, bathymetry information and knowledge of sedimentary basins can be included in the *a priori* model. Figure 7 shows a 2D model of the Gawler traverse broadband data using the method of Rodi and Mackie (2001).

Conclusions

Magnetotelluric data have been acquired by Geoscience Australia, the University of Adelaide and Primary Industries and Resources South Australia along three seismic transects in South Australia as part of the Onshore Energy Security Program of the Australian Government and the NGA. To aid geological understanding of results of the MT method, and its limitations, an overview of the method has been presented, using selected examples of data acquisition, presentation, processing and preliminary analysis and modelling results from each of the three surveys. More detailed analyses of the data and modelling are in progress.

Acknowledgements

The MT equipment deployed along the Gawler Craton and Curnamona-Gawler Link transects was supplied under ANSIR (Australian National Research Facility for Earth Sounding) agreement for the use of AuScope equipment funded by NCRIS (National Collaborative Research Infrastructure Strategy). Colleagues of our organisations are thanked for their help in field data acquisition. We thank Russell Korsch and Richard Blewett for their comments on the manuscript.

References

Archie, G.E., 1942. The electrical resistivity log as an aid in determining some reservoir characteristics. *Petroleum Transactions of AIME*, **146**, 54–62.

Aster, R., Borchers, B. and Thurber, C., 2005. Parameter Estimation and Inverse Problems (International Geophysics). Academic Press, har/cdr edition.

Bahr, K., 1991. Geological noise in magnetotelluric data: a classification of distortion types. *Physics of the Earth and Planetary Interiors*, **66**, 24–38.

Brasse, H., Kapinos, G., Li, Y., Mütschard, L., Soyer, W. and Eydam, D., 2009. Structural electrical anisotropy in the crust at the south-central Chilean continental margin as inferred from geomagnetic transfer functions. *Physics of the Earth and Planetary Interiors*, **173(1-2)**, 7–16.

Cagniard, L., 1953. Basic theory of the magneto-telluric method of geophysical prospecting. *Geophysics*, **18**, 605–635.

Caldwell, T.G., Bibby, H.M. and Brown, C., 2004. The magnetotelluric phase tensor. *Geophysical Journal International*, **158**, 457–457.

Chamalaun, F.H., 1986. Extension of the Flinders Ranges anomaly. *Exploration Geophysics*, **17**, 31.

Chave, A.D. and Thomson, D.J., 1989. Some comments on magnetotelluric response function estimation. *Journal of Geophysical Research*, **94**, 14215–14225.

Chave, A.D. and Thomson, D.J., 2004. Bounded influence magnetotelluric response function estimation. *Geophysical Journal International*, **157(3)**, 988–1006.

deGroot Hedlin, C. and Constable, S., 1990. Occam's inversion to generate smooth, two-dimensional models from magnetotelluric data. *Geophysics*, **55**, 1613–1624.

Egbert, G.D., 1997. Robust multiple-station magnetotelluric data processing. *Geophysical Journal International*, **130**, 475–496

Egbert, G.D., 2002. Processing and interpretation of electromagnetic induction array data. *Surveys in Geophysics*, **23**, 207–249.

Farr, T. G., Rosen, P.A., Caro, E., Crippen, R., Duren, R., Hensley, S., Kobrick, M., Paller, M., Rodriguez, E., Roth, L., Seal, D., Shaffer, S., Shimada, J., Umland, J., Werner, M., Oskin, M., Burbank, D. and Alsdorf, D., 2007. The Shuttle Radar Topography Mission. *Reviews in. Geophysics*, **45**, RG2004, doi:10.1029/2005RG000183.

Fraser, G.L., Blewett, R.S., Reid, A.J., Korsch R.J., Dutch, R., Neumann, N.L., Meixner, T., Skirrow, R.G., Cowley, W., Szpunar, M., Preiss, W.V., Nakamura, A., Fomin, T., Holzschuh J., Milligan, P.R. and Bendall, B., 2010. Geological interpretation of deep seismic reflection and magnetotelluric line 08GA-G1: Eyre Peninsula, Gawler Craton, South Australia. *Geoscience Australia, Record,* **2010/10**, this volume.

Gough, D.I., McElhinny, M.W. and Lilley, F.E.M., 1974. A magnetometer array study in southern Australia*. Geophysical Journal of the Royal astronomical Society*, **36**, 345-362.

Groom, R.W. and Bailey, R.C., 1989. Decomposition of magnetotelluric impedance tensors in the presence of local three-dimensional galvanic distortion. *Journal of Geophysical Research*, **94**, 1913–1925.

Guéguen, Y. and Palciauskas, V., 1994. *Introduction to the physics of rocks.* Princeton University Press, New Jersey.

Heise, W., Caldwell, T.G. and Bibby, H.M, 2007. 3D inversion of magnetotelluric data from the Rotokawa geothermal field, Taupo Volcanic Zone, New Zealand. In: *Proceedings of the 4th International Symposium on Three-Dimensional Electromagnetics*.

Ledo, J., Queralt, P. and Pous, J., 1998. Effects of galvanic distortion on magnetotelluric data over a three-dimensional regional structure. *Geophysical Journal International*, **132**, 295–301.

Lilley, F.E.M., 1998. Magnetotelluric tensor decomposition: Part I, Theory for a basic procedure. *Geophysics*, **63**, 1885–1897.

Korsch, R.J., Preiss, W.V., Blewett, R.S., Fabris, A.J., Neumann, N.L., Fricke, C.E., Fraser, G.L., Holzschuh, J., Milligan, P.R. and Jones, L.E.A., 2010. Geological interpretation of deep seismic reflection and magnetotelluric line 08GA-C1: Curnamona Province, South Australia. *Geoscience Australia, Record,* **2010/10**, this volume.

Martí, A., Queralt, P., Jones, A.G. and Ledo, J., 2005. Improving Bahr's invariant parameters using the WAL approach, *Geophysical Journal International,* **163**, 38-41

McNeice, G.W. and Jones, A.G., 2001. Multisite, multifrequency tensor decomposition of magnetotelluric data. *Geophysics,* **66**, 158–173.

Nover, G., 2005. Electrical Properties of Crustal and Mantle Rocks: A Review of Laboratory Measurements and their Explanation. *Surveys in Geophysics*, **26**, 593-651.

Parkinson, W.D., 1959. Directions of rapid geomagnetic fluctuations. *Geophysical Journal Royal Astronomical Society*, **2**, 1-14.

Patro, P.K. and Egbert, G.D., 2008. Regional conductivity structure of Cascadia: Preliminary results from 3D inversion of USArray transportable array magnetotelluric data. *Geophysical Research Letters*, **35**, **20**, doi:10.1029/2008GL035326.

Preiss, W.V., Korsch, R.J., Blewett, R.S., Fomin, T., Cowley, W.M., Neumann, N.L. and Meixner, A.J., 2010. Geological interpretation of deep seismic reflection line 09GA-CG1: the Curnamona Province-Gawler Craton Link Line, South Australia. *Geoscience Australia, Record,* **2010/10**, this volume.

Rodi, W. and Mackie, R.L., 2001. Nonlinear conjugate gradients algorithm for 2-D magnetotelluric inversion. *Geophysics*, **66**, 174–187.

Simpson, F. and Bahr, K., 2005. *Practical Magnetotellurics.* The University Press, Cambridge, 2005.

Siripunvaraporn, W. and Egbert, G., 2000. An efficient data-subspace inversion method for 2-D magnetotelluric data. *Geophysics*, **65**, 791–803.

Stockill, J., Brown, D., Scappin, S., Retallick, T. and Gharibi, M., 2009. Geophysical Survey Logistics report (v.2), regarding the Quantec Spartan Tensor Magnetotelluric Survey over the Curnamona MT Project, near Arkaroola, South Australia, Australia, on behalf of Terrex Seismic Pty Ltd, Perth, WA, Australia.

Thiel, S. and Heinson, G., 2009. Regional MT survey across an Archaean Craton in South Australia – influence of sedimentary basins and plate boundaries. In*: Proceedings of the 11th IAGA Scientific Assembly*, Sopron, Hungary.

Thiel, S., Heinson, G., Gray, D.R. and Gregory, R.T., 2009. Ophiolite emplacement in NE Oman: constraints from magnetotelluric sounding. *Geophysical Journal International*, **176(3)**, 753–766.

Tikhonov, A.N., 1950. The determination of the electrical properties of deep layers of the Earth's crust. *Doklady Academii Nauk. SSSR*, **73**, 295–297.

Utada, H. and Munekane, H., 2000. On galvanic distortion of regional 3-D MT impedances On galvanic distortion of regional three-dimensional magnetotelluric impedances. *Geophysical Journal International*, **140**, 385–398.

Vozoff, K., 1991. The Magnetotelluric Method, In: Nabighian, M.N., editor, Electromagnetic methods in applied geophysics. *Society of Exploration Geophysicists*, 641–711.

Weaver, J.T., Agarwal, A.K. and Lilley, F.E.M., 2000. Characterization of the magnetotelluric tensor in terms of its invariants. *Geophysical Journal International*, **141**, 321–321.

Whitaker, A.J., Glanville, H.D., English, P.M., Stewart, A.J., Retter, A.J., Connolly, D.P., Stewart, G.A. and Fisher, C.L., 2008. Surface Geology of Australia 1:1 000 000 scale, South Australia [Digital Dataset] Canberra: The Commonwealth of Australia, Geoscience Australia. http://www.ga.gov.au.

Curnamona Province: a Paleo- to Mesoproterozoic time slice

C.E. Fricke[1], W.V. Preiss[1] and N.L. Neumann[2]

[1]Geological Survey Branch, Primary Industries and Resources South Australia (PIRSA), GPO Box 1671, Adelaide, SA 5001, Australia
[2]Onshore Energy & Minerals Division, Geoscience Australia, GPO Box 378, Canberra, ACT 2601, Australia

Claire.Fricke@sa.gov.au

Introduction

The Curnamona Province is a near-circular Paleo- to Mesoproterozoic crustal element that extends from central eastern South Australia to western New South Wales that is bounded by much younger structural boundaries (Robertson et al., 1998, Conor and Preiss, 2008) (Figures 1, 2). Rocks of the Paleoproterozoic Willyama Supergroup (1720–1640 Ma) were deposited in an intracontinental rift, accompanied by synsedimentary mafic and felsic magmatism (Conor and Preiss, 2008) and were intruded by the early Mesoproterozoic Ninnerie Supersuite (Fricke, 2006). The substrate of the supracrustal Willyama Supergroup is unknown, and inferences can be drawn only from analogy with other provinces (e.g., Mt Isa), and from three deep seismic transects (Gibson et al., 1998; Goleby et al., 2006; Korsch et al., 2009). The shallow-water facies and stratigraphic relationships of some of the oldest exposed sediments, preserved despite Olarian deformation and metamorphism, suggest deposition upon continental crust in rift basins (Preiss, 2009).

The Curnamona Province is largely buried by younger sedimentary cover of Neoproterozoic to Holocene age. In the southern Curnamona Province, however, the Willyama Supergroup is exposed, occupying the Olary Domain and the Broken Hill Domain. In the northwestern portion (Mount Babbage and Mount Painter Inliers), it crops out as early Mesoproterozoic basement to Neoproterozoic age rocks. Two major orogenic events have been recorded in the Curnamona Province: the ~1600 Ma Olarian Orogeny and the ~500 Ma Delamerian Orogeny.

Curnamona Province in relation to other late Paleoproterozoic provinces in Australia

Northern Australia

Deposition of the Willyama Supergroup was at least partly coeval with deposition of units of the Calvert and Isa Superbasins in the North Australian Craton (Page et al., 2005; Betts and Giles, 2006). Isotopic and detrital zircon evidence has been used to suggest a central Australian source region for the sediments of the Willyama Supergroup (Barovich, 2003; Page et al., 2005).

Gawler Province

On the eastern Gawler Province, the ~1760 Ma metasedimentary and metavolcanic rocks of the Wallaroo Group overlap in age with the older rift packages at Mt Isa, and, although they are 30 Ma older, show considerable lithological similarity to the younger Willyama Supergroup (Conor, 2000). Metamorphic grade and intensity of deformation in the Wallaroo Group decrease to the east, so it is possible that equivalents could extend eastward, with little evidence of pre-Olarian

deformation, beneath the Willyama Supergroup (Preiss, 2009). Such successions are potentially much thicker than the exposed Willyama Supergroup, and may account for much of the layered mid-crust imaged on the Curnamona seismic transects (Goleby et al., 2006; Korsch et al., 2009).

Basement to the Adelaide Geosyncline

Basement to the Neoproterozoic sediments includes the Mount Painter Inlier, which contains an early Mesoproterozoic metasedimentary and metavolcanic package (Teale, 1993). In the basement inliers of the Mount Lofty Ranges, the Barossa Complex contains a granitic orthogneiss, recently dated at 1718 Ma, similar in age, though not chemistry, to syn-Willyama magmatism of the Basso Suite (Belousova et al., 2006, Szpunar et al., 2006).

Subdivision of the Curnamona Province

The Curnamona Province is divided into domains based on age, sedimentary facies and thickness, magmatism and metamorphism (Figure 1):

- Broken Hill Domain: relatively thicker, more complete stratigraphy, with well-developed lode-bearing Broken Hill Group (Conor and Preiss, 2008). Metamorphism from lower amphibolite facies in the north to granulite in the south (Phillips, 1980). Synsedimentary mafic and S-type felsic magmatism related to rifting.
- Redan Domain: characterised by calcalbitic Redan Gneiss, granulite metamorphism, and a high Total Magnetic Intensity signature and it contains the oldest rocks known within the Broken Hill Inlier (Conor and Preiss, 2008).
- Olary Domain: thinner, less complete stratigraphy; restricted development of Broken Hill Group equivalents and only locally developed; oldest known rocks in the Willyama Supergroup (Curnamona Group). Synsedimentary A-type felsic (~1715 Ma Basso Suite) and minor mafic magmatism (~1685 Ma Lady Louise Suite). Polyphase deformation and metamorphism from greenschist facies in north to upper amphibolite facies in south (Clarke et al., 1987; Webb and Crooks, 2005).
- Mulyungarie Domain: characterised by a thick sulfidic succession; relatively weakly deformed greenschist facies metasedimentary rocks with significant stratigraphic differences from both the Broken Hill and Olary Domains. May be transitional between Broken Hill and Olary Domains (Conor and Preiss, 2008). Boundaries are poorly defined, apart from the Mundi Mundi Fault to the east (Conor and Preiss, 2008).
- Moolawatana Domain: Early Mesoproterozoic rocks of the Mount Painter and Mount Babbage Inliers and extending eastward as a buried ridge. Delamerian and possible Proterozoic high-grade metamorphic events are recorded in the basement.
- Mudguard Domain: a relatively undeformed sheet of ~1580 Ma volcanics inferred from geophysics to unconformably overlie folded Willyama Supergroup on the Benagerie Ridge.
- Erudina and Quinyambie Domains: unknown basement deeply buried by thick Cambrian and Neoproterozoic cover of the Moorowie and Yalkalpo Sub-basins west and east of the Benagerie Ridge, respectively.

Domain boundaries are subject to further refinement based on new mapping, drilling and seismic data. In particular, the Olary-Broken Hill Domain boundary is currently being re-assessed, based on solid geology and stratigraphic interpretation on the Mingary 1:100 000 map sheet (Crooks and Fricke, 2010).

Broken Hill–Olary Domain Boundary

On the Mingary 1:100 000 map area, early work settled on a boundary based on geophysical patterns associated with both TMI and gravity, on which a prominent north-northeast-trending feature was recognised as the domain boundary. Detailed mapping on the ground covering the Mingary 1:100 000 map area, however, determined that the broad lithological differences used to define each of the subdomains can be found on either side of this geophysically-derived boundary (Crooks, 2001). The broad tectonic history is also repeated on both sides. As a domain boundary, the geophysically defined boundary is therefore not supported on geological grounds.

Crooks (2001) noted that the geological criteria for province subdivision suggested not one but two possible domain boundaries. The first possible domain boundary is based on the regional influence of a 1690 Ma thermal event, related to early basin development and thinning and wedging out of the Broken Hill Group lithologies (Crooks, 2001). Of particular importance is the distribution of the Hores Gneiss and Potosi Gneiss, quartz–gahnite rocks and restriction in the distribution of the coeval amphibolite bodies. Recent U-Pb SHRIMP dating has identified the Hores Gneiss on the eastern side of Mingary 1:100 000 map sheet, implying that the domain boundary occurs west of this outcrop.

The alternative domain boundary is a metamorphic-grade zonation established at 1590 Ma (Crooks, 2001). A domain boundary can be drawn based on the degree of exhumation of the two domains, exposing different crustal levels. Such a domain boundary would have to be drawn across the very northern and northwestern margins of the Mingary map area. Although most rocks from the Mingary sheet have seen the same upper amphibolite to low granulite-grade peak metamorphic conditions, which has taken them into the sillimanite => kyanite stability fields, the rocks in the northwest are probably the lowest grade. This is in line with the regional metamorphic gradient mapped by Clarke et al. (1986, 1987) for the Olary Domain (Crooks, 2001). The outcrop zonation of the migmatites and S-type granites on Mingary is also consistent with the same pattern of crustal level shallowing to the north and northwest, based on the model of D'Lemos et al. (1992).

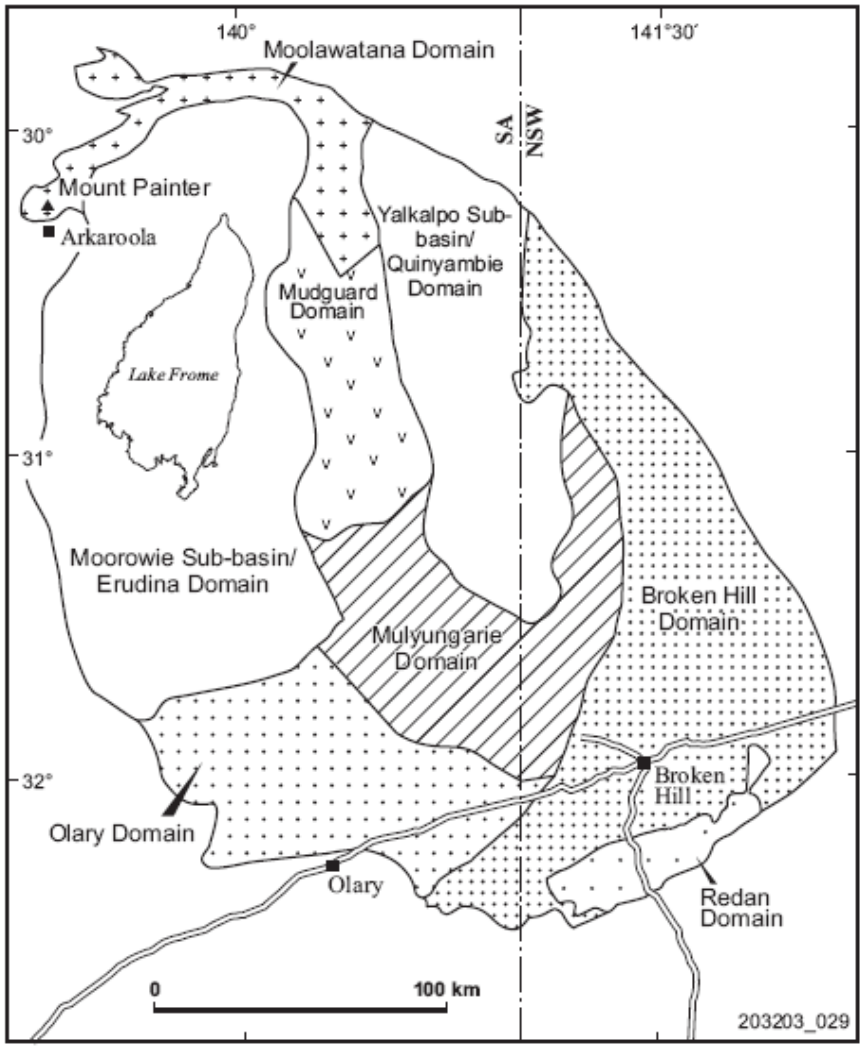

Figure 1. Location and geological domains of the Curnamona Province.

Since these two events are 100 Ma apart, they define two separate domain boundary conditions, and neither of these possible domain boundaries correlates with the TMI feature.

More recently, Petrie et al. (2009) used magnetotelluric traverses, and worms derived from upward continuation of the regional aeromagnetic data, to define a structure or structures which would define the rift boundary between the Olary and Broken Hill Domains. Three sets of major, steeply-dipping, deeply-penetrating, slightly curvilinear, northeast-striking structures were identified, but how these features relate to the domain boundary still remains unclear.

Tectonic evolution of the 1720–1640 Ma Willyama depositional basin

Early crustal extension, mafic and felsic magmatism, ~1720–1700 Ma

The oldest known metasedimentary rocks of the Willyama Supergroup (Stevens et al., 1988) are variably albitised fine- to medium-grained clastics of the Curnamona Group of the Olary Domain (Conor, 2000). The lithologically similar Thackaringa Group of the Broken Hill Domain (Willis et al., 1983) has traditionally been correlated with the Curnamona Group (e.g., Laing, 1996), but recent geochronology shows that the Curnamona Group is 10-15 Ma older (Page et al., 2003; Stevens et al., 2008). The Redan Gneiss (Redan Domain), the lowest part of the exposed Broken Hill stratigraphy, may partly overlap in age with the uppermost part of the Curnamona Group; however relationships with the adjacent Broken Hill Domain and the Olary Domain are poorly understood largely due to poor outcrop (Conor and Preiss, 2008). A-type felsic volcanic and subvolcanic (Basso Suite) units are intercalated with the Curnamona Group, and include widespread quartz-phenocryst-rich flows and volcaniclastic sedimentary rocks, high-level granitic intrusives, and restricted mafic magmatism in the form of locally pillowed basalt flows. Although predominantly metasedimentary, the associated bimodal A-type magmatism indicates crustal extension and lithospheric thinning during deposition of the Curnamona Group (Conor and Preiss, 2008). Laing (1996) identified different stratigraphic relationships within separate subdomains, and attributed this variation to juxtaposition of different facies belts by nappe-thrusting during the Olarian Orogeny. More recent mapping support concepts of growth faulting, and onlap of sediments onto tilted fault blocks, consistent with crustal extension (Conor and Preiss, 2008).

Following deposition of the Curnamona Group, little sedimentation was recorded between 1715 Ma and 1693 Ma (Plumbago Formation) in the Olary Domain, although, in the Broken Hill and Redan Domains, this time interval saw the deposition of the Rantyga Group, Thackaringa Group and possibly the Clevedale Migmatite and Thorndale Composite Gneiss (Conor and Preiss, 2008). Magmatism also shifted eastward, dominated by felsic, S-type intrusives and volcaniclastic units (Silver City Suite; Conor and Preiss, 2008), derived from melting of sediments of similar composition to the Thackaringa Group (Barovich and Hand, 2004). These S-type igneous rocks (e.g., Alma Granite Gneiss) intruded into, and were extruded as, minor felsic volcanic-volcaniclastic rocks (in the Cues Formation) within the Thackaringa Group (Conor and Preiss, 2008). This suggests that the older Curnamona Group (?and still older Wallaroo Group) could extend into the Broken Hill Domain beneath outcrops of Thackaringa Group and Redan Gneiss, and thus could have been the source of the S-type magmas generated during deposition of the Thackaringa and Broken Hill Groups (Preiss, 2009).

Upper rift packages and magmatism, ~1700–1670 Ma

The Broken Hill Group is best developed in the Broken Hill Domain, where it probably represents rift fill, with the Olary Domain as the rift flank where Broken Hill Group equivalents are thinner or missing (Conor and Preiss, 2008). The Broken Hill Group consists of siliciclastic metasedimentary rocks with Potosi-type Gneiss at two levels, and minor calcsilicates, garnet-rich banded iron formation, quartz-gahnite rock and garnet-quartz rock (Stevens et al., 2008). In the western part of the Broken Hill Domain, a thin calcsilicate marker unit (Ettlewood Calc-silicate Member), near the base of the Broken Hill Group, continues into the Olary Domain (Bimba Formation) as the base of the Saltbush Group (Conor and Preiss, 2008). Correlation is strongly supported by the ~1693 Ma age obtained on the inferred volcaniclastic metasiltstone of the Plumbago Formation, which directly overlies the Bimba Formation, and its equivalent in the Broken Hill Domain (Page et al., 2005). While the Bimba/Ettlewood-Plumbago couplet forms a through-going link between the two domains, the overlying stratigraphies differ markedly, reflecting the different tectonic settings of the Olary and Broken Hill Domains. Pelite-dominated metasedimentary rocks of the Saltbush Group overlie the Plumbago Formation in the Olary

Domain and may be equivalent to the upper Broken Hill Group and/or the Sundown Group, but they lack the distinctive lode rocks found in the Broken Hill Group. The volcaniclastic Potosi-type gneisses, such as the Hores Gneiss, have no known equivalent in the Olary Domain. Mafic intrusives of the same age as those of the Broken Hill Domain do occur in the Olary Domain (Lady Louise Suite), but are mostly seen intruding the Curnamona Group (Conor and Fanning, 2001). The only known correlative of the Broken Hill Group in the Olary Domain is found in the Kalabity Inlier, where manganiferous banded quartz-magnetite-grunerite-garnet iron formations, quartz-garnetite and occasional mafic sills occur within a pelitic unit (Oonartra Creek Formation) (Conor and Preiss, 2008). These observations support earlier concepts that the Broken Hill Group represents rift fill, and that its sediments lap out against an uplifted rift shoulder in the Olary Domain (Conor and Page, 2003), but the precise geometry of this rift and, indeed, the location of the bounding normal faults, are yet to be elucidated.

Sag-phase sedimentation, ~1660–1640 Ma

The Paragon Group (Broken Hill Domain) and Strathearn Group (Olary Domain) are the youngest known successions, and are broadly stratigraphically equivalent (Conor and Preiss, 2008). The lower part of the succession (Cartwrights Creek Metasediments, Broken Hill Domain and Alconie Formation, Olary Domain) consists of thickly-interlayered graphitic metasiltstone and chiastolite-bearing pelite (Conor and Preiss, 2008).

A tectonic origin (extensional excision) has been invoked for such juxtaposition (Noble et al., 2003), but Conor and Page (2003) preferred sedimentary onlapping models. Such a relationship would be consistent with other evidence that the stratigraphic succession in the Olary Domain is less complete than in the Broken Hill Domain. Moreover, if the Paragon Group is considered to have resulted from sag-phase sedimentation, it may have been very widespread originally, overstepping the earlier rift packages, and may also have been much thicker than what is currently preserved, thus contributing to the depth of burial of the Willyama Supergroup required by its metamorphic grade. Interpretation of geophysics suggests that such thick successions of uppermost Willyama Supergroup are likely to be preserved under cover in the Mulyungarie and northernmost Olary Domains. Being at least partly coeval with the Mount Isa Group, they must be regarded as having high Pb-Zn mineralisation potential, and warrant extensive exploration.

Tectonics of the Olarian Orogeny, ~?1620–1580 Ma

Deformation and metamorphism

The Olarian Orogeny was a polyphase, ductile deformation event, which occurred during the period ~1620 Ma–1580 Ma, and its effects being highly variable across the Curnamona Province (Conor and Preiss, 2008). The most intense deformation is observed in the southeast, in the Broken Hill and Olary Domains, where extreme shortening produced early recumbent folds with extensive overturned limbs (over tens of kilometres), and later upright buckle folds and thrust faulting (Conor and Preiss, 2008).

Several structural schemes have been proposed for the Olarian Orogeny, but the paucity of hard evidence for correlating locally-derived structural sequences has resulted in a lack of consensus. However, some elements are common to most observations:

- Ubiquitous layer-parallel foliation.
- Evidence of very early heating in the form of migmatitic veining parallel to this foliation, and early pegmatites.
- Relatively early isoclinal recumbent folds of markedly different orientations and vergences, and the formation of near-regional scale overturned limbs.
- Relatively late upright folds that refold the isoclinal folds.
- S-type (and locally I-type) granite intruded late in the structural sequence.
- Retrograde shear zones cut across all the earlier structures and affect the late granites.

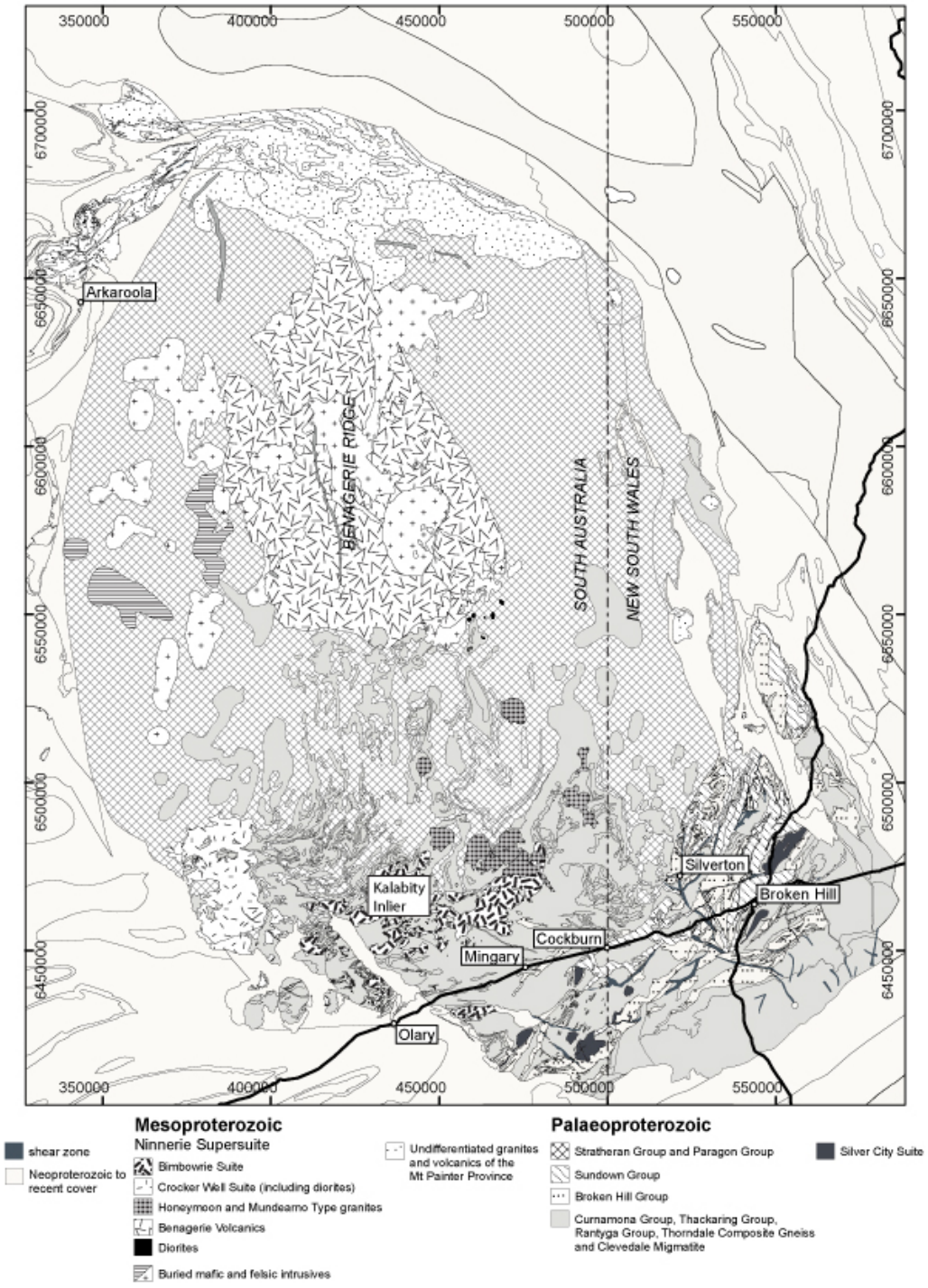

Figure 2. Solid geology of the Curnamona Province.

The implication is that the sedimentary pile was subjected to heating very early in its deformation history (W.P. Laing, 1995, pers. comm.; Stevens, 2006). Extensional tectonics have been invoked to explain this heating, but critical geochronological evidence does not support ideas of metamorphism coeval with sedimentation as proposed by Gibson and Nutman (2004), that is, prior to the Olarian Orogeny, which began at ~1600 Ma, and possibly as early as 1620 Ma. Although the data permit extension, immediately before the onset of contractional deformation, to produce the early heating and layer-parallel foliation, the evidence for such extension is not strong, and there are no associated mafic magmas of that age. One possibility is that burial under a thick, largely pelitic, and hence insulating, sedimentary blanket under

conditions of high heat-flow, perhaps resulting from radioactive heating (Stevens, 2006), might produce an early, horizontal high-grade fabric. Another is that recumbent folding may have accompanied this heating, producing horizontal axial-plane fabrics, as suggested by Marjoribanks et al. (1980).

Available metamorphic data indicate peak Olarian metamorphism at 1610-1590 Ma (Page et al., 2005; Rutherford et al., 2007). Until geochronology is able to resolve discrete deformation events within this narrow interval, the simplest hypothesis is to view the deformation as continuous and progressive under a thick sedimentary cover. By this process, earliest isoclinal recumbent folds in the internal part of the orogen, probably in the southeast, would be associated with flat-lying foliations. As deformation propagates to the more external zones in the northwest, the early-formed foliations would themselves be folded isoclinally. Discovery of true F1 folds (that is, folds which do not fold a pre-existing foliation) would be highly improbable. The variable orientation of isoclinal folds may be explained by a sheath-like geometry within a regime of overall northwest-directed tectonic transport (Forbes et al., 2004).

Repeated isoclinal folding greatly thickened the sedimentary pile and led to peak metamorphic conditions. Subsequently, the pile reacted to the contraction by more upright folding, traditionally termed F2 in the Broken Hill Domain (Marjoribanks et al., 1980) and F3 in the Olary Domain (Berry et al., 1978). While there is likely to have been a continuum between sheath folding and cylindrical folding in the Olarian Orogeny, the later folds have more consistent orientations than the early isoclinal folds, forming a sweeping arc from east-northeast (in the southern Olary Domain) through northeast- to north-south-trending axial traces (in the Broken Hill and Mulyungarie Domains). Plunge and plunge directions vary greatly, and even these later folds are clearly not all cylindrical. The vergence of the upright folds is also not consistent, though northwest vergence is common in the Olary Domain. Upright folds in the Broken Hill area have been reconstructed with a slight easterly vergence (Stevens, 2004), and the tectonic relationships remain unclear. Metamorphic grade during upright folding also varies in different areas, being retrograde in much of the Olary Domain, but still very high grade in the southern Broken Hill Domain, where a later phase of minor upright folding is considered retrograde (F_3 of Marjoribanks et al., 1980). At least some of these, with north-south trends, could be associated with deformation of the Neoproterozoic cover, and thus be of Delamerian age.

Granites ~1595–1580 Ma

During the early Mesoproterozoic (ca. 1610–1550 Ma), a continental-scale thermal event characterised by regional high-temperature metamorphism and bimodal magmatism was recorded in eastern Proterozoic Australia. This orogenesis and high-grade metamorphism is interpreted to be related to contractional phases in a long-lived accretionary orogen (Rutherford et al., 2007). In the Curnamona Province, vast quantities of A-, I- and S-type magma (Ninnerie Supersuite; Fricke, 2006) (Figure 2) were generated as a response to this event but reflect deep crustal heating of source rocks of different compositions in a variety of tectonic environments. In the Gawler Craton, the extrusion of the bimodal Gawler Range Volcanics (GRV) (ca. 1592 Ma), followed by the intrusion of the Hiltaba Granite Suite (ca. 1590–1580 Ma; Creaser et al., 1991; Flint et al., 1993; Allen et al., 2003), occurred and was responsible for the formation of the Olympic Dam and other Cu-Au-U deposits. In the Cloncurry district of the Mt Isa Province, this event included the A-type magmatism (gabbros to granites) of the Williams-Naraku Batholith (ca. 1550–1500 Ma) (Page and Sun, 1998; Oliver et al., 2001).

The Ninnerie Supersuite consists of several suites, which span across several domains in the Curnamona Province (Figure 2). The most widespread granites are found in the Olary Domain, where at least three individual granite suites have been identified. The granite suites in the Olary Domain include the:

- 2-mica, S-type granites of the Bimbowrie Suite,
- Sodic to biotite-only S- and I-type granites of the Crocker Well Suite, and
- Hornblende-biotite I-type granodiorites to diorites coeval with the Crocker Well Suite.

Several other types of mafic and felsic intrusives and volcanic rocks have been identified in the Mulyungarie Domain and Mudguard Domain, including:

- Buried magnetic gabbros to granodiorites and nonmagnetic granodiorites to monzogranites (Mulyungarie Domain and Mudguard Domain),
- Buried non-magnetic granites (so called Honeymoon Type; Mulyungarie Domain),
- Magnetic, anatectic granites (so called Mundaerno Type; Mulyungarie Domain), and the
- Benagerie Volcanics (Mudguard Domain).

The S-type magmas were likely derived from partial melting of the Willyama Supergroup (?and perhaps the underlying Wallaroo Group), which were at sufficient depth due to a combination of sedimentary and tectonic burial. The presence of more mafic I-type magmas in the western Olary Domain and the southern Mudguard Domain indicates input from a mantle source, which could also represent a heat source. The Benagerie Ridge is dominated by bimodal A-type volcanics and granites, indicating a different or mixed source from the deep crust or mantle. Nd isotopic compositions are consistent with these observations, indicating a mantle source, possibly related to a moving mantle hot-spot or plume, was present during the early Mesoproterozoic (Betts et al., 2007). The GRV and Hiltaba Granite Suite are believed to have been formed by the interaction of such a mantle plume with the continental lithosphere, which resulted in intracratonic extension, partial melting of the lower crust and shallow pluton emplacement (Giles, 1988; Creaser and White, 1991). The mantle plume has been inferred from the Gawler Craton through the Curnamona Province, to the Mt Isa Province (Betts et al., 2007), suggesting a possible linkage of these provinces.

Two pluses of magmatism have been recognised in the Mt Painter Inlier. The first pulse occurred from ~1585–1575 Ma, and includes the megacrystic Mount Neill Granite, Pepegoona Porphyry, augen gneiss Box Bore Granite and gneisses from the Paralana Hot Springs area (Teale, 1993; Neumann et al., 2009).

Granites ~1565–1555 Ma

New SHRIMP geochronology has helped resolve a slightly younger, second magmatic event known only in the Mount Painter Inlier. This younger magmatic event was the main phase of magmatism in the Mount Painter Inlier where the Terrapinna, Wattleowie and Yerila Granites were intruded only in the north of the Inlier at ~1565-1555 Ma (Teale, 1993; Neumann et al., 2009). This phase of magmatism was followed by high-temperature metamorphism with associated granodiorite magmatism (e.g., Paralana Granodiorite; Neumann et al., 2009).

Late Olarian deformation <~1580 Ma

Late Olarian deformation took the form of dominantly west-east to northwest-trending retrograde shear zones (Conor and Preiss, 2008). Determining the age range for the shearing has been difficult, as garnet Sm-Nd geochronology records only later tectonic reworking during the Delamerian Orogeny (~500 Ma) (Dutch et al., 2005). Ninnerie Supersuite granites provide some constraint on the timing of shearing, where some granites are within shear zones, suggesting possible intrusion during shearing, whereas other granites have been cut by shear zones, and are therefore >1580 Ma (Conor and Preiss, 2008). Associated east-west folds are locally quite intense. It is possible that exhumation of high-grade rocks in the southern part of the Curnamona Province took place at this time, since the overall trend of metamorphic isograds is east-west, consistent with uplift on a network of such retrograde shears. The Curnamona Province thus probably underwent overall northward tilting as a result, which allowed extrusion and subsequent preservation of ~1580 Ma volcanics over eroded, folded, low-grade Willyama Supergroup in the Mudguard Domain, while the southern regions continued to be exhumed.

The large-scale arcuate trends of the upright Olarian folds, which define its overall tectonic grain, may be partly inherited from the original rift geometry of the basin or, if these trends were originally straighter, may have been imparted or modified during late Olarian deformation to form an orocline. These arcuate trends were already in place by the time of Neoproterozoic rifting.

Radium Creek Metamorphics and felsic magmatism of the Moolawatana Domain

Dating of detrital zircons in quartzitic metasedimentary rocks of the Radium Creek Metamorphics in the Mount Painter Inlier indicates a maximum depositional age of ~1590 Ma (Fanning et al., 2003; Ogilvie, 2006; Neumann et al., 2009). As noted above, new geochronological data indicates felsic magmas were intruded in two pluses: ~1585–1575 Ma (Mount Neill Granite, Pepegoona Porphyry, Box Bore Granite and gneisses from Paralana Hot Springs area) and ~1565–1555 Ma (Terrapinna, Wattleowie and Yerila Granites; Neumann et al., 2009). The structural relationships of the intrusives are subject to considerable debate. It is also difficult at present to prove Proterozoic deformation and metamorphism in the Radium Creek Metamorphics because of intense Paleozoic overprinting.

Acknowledgements

The above summary is based on the work of many generations of geologists who have studied the Curnamona Province; only a small fraction of these could be referenced. Discussions over more than a decade with colleagues and collaborators, in particular Paul Ashley, Karin Barovich, Pete Betts, Andy Burtt, Chris Clark, Colin Conor, Wayne Cowley, Alistair Crooks, Mark Fanning, George Gibson, David Giles, Martin Hand, Steve Hore, Liz Jagodzinski, Russell Korsch, Bill Laing, Mark McGeough, Rod Page, Ian Plimer, Stuart Robertson, Lachlan Rutherford, Barney Stevens, Mike Szpunar and Graham Teale, have helped to crystallise the ideas expressed about Curnamona tectonics, but in no way does the abstract purport to represent their very diverse views.

References

Allen, S., Simpson, C.J., McPhie, J. and Daly, S.J., 2003. Stratigraphy, distribution and geochemistry of widespread felsic volcanic units in the Mesoproterozoic Gawler Range Volcanics, South Australia. *Australian Journal of Earth Sciences,* **50**, 91–112.

Barovich, K.M., 2003. Geochemical and Nd isotopic evidence for sedimentary source changes in the Willyama basin, Curnamona Province. In: Peljo, M., compiler, Broken Hill Exploration Initiative. Abstracts from the July 2003 Conference. *Geoscience Australia Record*, **2003/13**, 3–5.

Barovich, K. and Hand, M., 2004. A geochemical and isotopic perspective on the early development of the Willyama Supergroup, Curnamona Province. In: McPhie, J. and McGoldrick, P., editors, *Dynamic Earth; past, present and future.* Geological Society of Australia Abstracts, **73**, 144.

Belousova, E. A., Preiss, W. V., Schwarz, M. P. and Griffin, W. L., 2006. Tectonic affinities of the Houghton Inlier, South Australia: U - Pb and Hf-isotope data from zircons in modern stream sediments *Australian Journal of Earth Sciences,* **53**, 971–989.

Berry, R. F., Flint, R. B. and Grady, A. E., 1978. Deformation history of the Outalpa area and its application to the Olary Province, South Australia. *Transactions of the Royal Society of South Australia,* **102, 1-2**, 43-53.

Betts, P. and Giles, D., 2006. The 1800-1100 Ma tectonic evolution of Australia. *Precambrian Research,* **144**, 92–125.

Betts, P., Giles, D., Schaefer, B. and Mark, G., 2007. 1600–1500 Ma hotspot track in eastern Australia: implications for Mesoproterozoic continental reconstructions. *Terra Nova,* **19**, 496–501.

Clarke, G. L., Burg, J. P. and Wilson, C. J. L., 1986. Stratigraphic and structural constraints on the Proterozoic tectonic history of the Olary Block, South Australia. *Precambrian Research,* **34**, 107-137.

Clarke, G. L., Guiraud, M., Powell, R. and Burg, J. P., 1987. Metamorphism in the Olary Block, South Australia; compression with cooling in a Proterozoic fold belt. *Journal of Metamorphic Geology,* **5**, 291-306.

Conor, C. H. H., 2000. Definition of major sedimentary and igneous units of the Olary Domain, Curnamona Province. *MESA Journal,* **19**, 51-56.

Conor, C. H. H. and Fanning, C. M., 2001. Geochronology of the Woman-in-White Amphibolite, Olary Domain. *MESA Journal,* **20**, 41-43.

Conor, C. and Page, R., 2003. Depositional architecture of the upper Willyama Supergroup, Curnamona Province. In: Peljo, M., compiler, Broken Hill Exploration Initiative; abstracts from the July 2003 conference. *Geoscience Australia, Record,* **2003/13**, 30-31.

Conor, C. H. H. and Preiss, W. V., 2008. Understanding the 1720–1640 Ma Palaeoproterozoic Willyama Supergroup, Curnamona Province, southeastern Australia: implications for tectonics, basin evolution and ore genesis. *Precambrian Research,* **166**, 297–317.

Creaser, R. A., Price, R. C. and Wormald, P. R., 1991. A-type granites revisited: Assessment of a residual-source model. *Geology,* **19**, 163-166.

Creaser, R. A. and White, A. J. R., 1991. Yardea Dacite; large-volume, high-temperature felsic volcanism from the middle Proterozoic of South Australia. *Geology,* **19**, 48–51.

Crooks, A. F., 2001. Olary-Broken Hill domain boundary; MINGARY 1:100 000 map area, Curnamona Province. *MESA Journal,* **20**, 44-45.

Crooks, A. F. and Fricke, C. E., 2010. MINGARY map sheet. *South Australia. Geological Survey. Geological Atlas 1:100 000 series, sheet 7033, SI5402*.

D'Lemos, R. S., Brown, M. and Strachan, R. A., 1992. Granite magma generation, ascent and emplacement within a transpressional orogen. *Journal of the Geological Society of London,* **149**, 487–490.

Dutch, R. A., Hand, M. and Clark, C., 2005. Cambrian reworking of the southern Australian Proterozoic Curnamona Province; constraints from regional shear-zone systems. *Journal of the Geological Society of London,* **162**, 763-775.

Fanning, C. M., Teale, G. S. and Robertson, R. S., 2003. Is there a Willyama supergroup sequence in the Mount Painter Inlier? In: Peljo, M.C., compiler, Broken Hill Exploration Initiative: Abstracts from the July 2003 conference. *Geoscience Australia, Record*, **2003/13**, 38–41.

Flint, R. B., Blissett, A. H., Conor, C. H. H., Cowley, W. M., Cross, K. C., Creaser, R. A., Daly, S. J., Krieg, G. W., Major, R. B., Teale, G. S. and Parker, A. J., 1993. Mesoproterozoic. In: Drexel, J. F., Preiss, W. V. and Parker, A. J., editors, The geology of South Australia; Volume 1, The Precambrian. *Geological Survey of South Australia, Bulletin,* **54**, 106-169.

Forbes, C. J., Betts, P. G. and Lister, G. S., 2004. Synchronous development of Type 2 and Type 3 fold interference patterns; evidence for recumbent sheath folds in the Allendale area, Broken Hill, NSW, Australia. *Journal of Structural Geology,* **26**, 113-126.

Fricke, C. E., 2006. The Ninnerie Supersuite - Mesoproterozoic igneous rocks of the Curnamona Province. In: Korsch, R.J. and Barnes, R.G., editors, Broken Hill Exploration Initiative: Abstracts from the September 2006 conference. *Geoscience Australia, Record*, **2006/21**, 50-51.

Gibson, G., Drummond, B., Fomin, T., Owen, A., Maidment, D., Gibson, D., Peljo, M. and Wake-Dyster, K., 1998. Re-evaluation of crustal structure of the Broken Hill Inlier through structural mapping and seismic profiling. *Australian Geological Survey Organisation, Record,* **1998/11**, 55 pp.

Gibson, G. M. and Nutman, A. P., 2004. Detachment faulting and bimodal magmatism in the Palaeoproterozoic Willyama Supergroup, south-central Australia: keys to recognition of a multiply deformed Precambrian metamorphic core complex. *Journal of the Geological Society, London,* **161**, 55–66.

Giles, C. W., 1988. Petrogenesis of the Proterozoic Gawler Range Volcanics, South Australia. *Precambrian Research,* **40/41**, 407-427.

Goleby, B., Korsch, R. J., Fomin, T., Conor, C. H. H., Preiss, W. V., Robertson, R. S. and Burtt, A. C., 2006. The 2003-2004 Curnamona Province seismic survey. *Geoscience Australia, Record*, **2006/12**, 96 pp.

Korsch, R. J., Preiss, W. V., Blewett, R., Fabris, A., Neumann, N. L., Fricke, C. E., Fraser, G. L., Holzschuh, J. and Jones, L. E. A., 2009. The 2008 north-south oriented, deep seismic reflection transect across the Curnamona Province, South Australia. In: Korsch, R. J., editor, Broken Hill Exploration Initiative: Abstracts for the 2009 Conference. *Geoscience Australia, Record*, **2009/28**, 90–100.

Laing, W. P., 1996. Stratigraphic subdivision of the Willyama Supergroup - Olary Domain, South Australia. *MESA Journal,* **2**, 39–48.

Marjoribanks, R. W., Rutland, R. W. R., Glen, R. A. and Laing, W. P., 1980. The structure and tectonic evolution of the Broken Hill region, Australia. *Precambrian Research,* **13**, 209-240.

Neumann, N. L., Hore, S. and Fraser, G. L., 2009. New SHRIMP geochronology from the Mount Painter Province, South Australia. In: Korsch, R.J., editor, Broken Hill Exploration Initiative: Abstracts from the 2009 conference. *Geoscience Australia, Record*, **2009/28**, 136–139.

Noble, M. P., Fry, K., Betts, P. G., Forbes, C. J. and Lister, G. S., 2003. High temperature shear zones of the Curnamona Province. In: Peljo, M. C., compiler, Broken Hill Exploration Initiative; abstracts from the July 2003 conference. *Geoscience Australia, Record*, **2003/13**, 120–121.

Ogilvie, J. M., 2006. U-Pb detrital zircon dating of structural and stratigraphic relationships within Hidden Valley, Mount Painter Inlier, Northern Flinders Ranges: Implications for Proterozoic crustal evolution of Eastern Australia. Monash University, *B.Sc. (Hons) thesis (unpublished).*

Oliver, N. H. S., Mark, G., Marshall, L. J., Rubenach, M. J., Carew, M. J. and Pollard, P. J., 2001. Mineralisation, alteration and magmatism in the Eastern Fold Belt, Mount Isa Block, Australia: Geological Review and Field Guide, Geological Society of Australia. *Specialist Group in Economic Geology, Publication,* **5**, 103–122.

Page, R., Stevens, B. P. J., Conor, C., Preiss, W. V., Crooks, A., Robertson, R. S., Gibson, G. M. and Foudoulis, C., 2003. SHRIMP U-Pb geochronology in the Curnamona Province; improving the framework for mineral exploration. In: Peljo, M., compiler, Broken Hill Exploration Initiative; abstracts from the July 2003 conference. *Geoscience Australia, Record*, **2003/13**, 122–125.

Page, R. W., Conor, C. H. H., Stevens, B. P. J., Gibson, G. M. and Preiss, V. P., 2005. Correlation of Olary and Broken Hill Domains, Curnamona Province: possible relationship to Mt Isa and other northern Australian Pb-Zn-Ag-bearing successions. *Economic Geology,* **100**, 663–676.

Page, R. W. and Sun, S.-S., 1998. Aspects of geochronology and crustal evolution in the Eastern Fold Belt, Mt Isa Inlier. *Australian Journal of Earth Sciences,* **45**, 343–361.

Petrie, S., Conor, C.H.H. and Fricke, C.E., 2009. Mingary geophysical interpretation and investigation of the boundary between the Broken Hill and Olary Domains. In: Korsch, R. J., editor, Broken Hill Exploration Initiative: Abstracts for the 2009 conference. *Geoscience Australia, Record*, **2009/28**, 140–143.

Phillips, G. N., 1980. Water activity changes across an amphibolite-granulite facies transition, Broken Hill, Australia. *Contributions to Mineralogy and Petrology,* **75**, 377–386.

Preiss, V. P., 2009. The Curnamona Province: 1700 million years of tectonic evolution. In: Korsch, R.J., editor, Broken Hill Exploration Initiative: Abstracts for the 2009 conference. *Geoscience Australia, Record*, **2009/28**, 144–155.

Robertson, R. S., Preiss, W. V., Crooks, A. F., Hill, P. W. and Sheard, M. J., 1998. Review of the Proterozoic geology and mineral potential of the Curnamona Province in South Australia. In: Hodgson, I. and Hince, B., editors, Geology and mineral potential of major Australian mineral provinces. *Australian Geological Survey Organisation Record*, **17, 3**, 169-182.

Rutherford, L., Hand, M. and Barovich, K., 2007. Timing of Proterozoic metamorphism in the southern Curnamona Province: Implications for tectonic models and continental reconstructions. *Australian Journal of Earth Sciences,* **54**, 65–81.

Stevens, B. P. J., 2004. Constructing cross-sections through the Broken Hill Block. *Geological Survey of New South Wales, R.,* **GS2004/436 (unpublished)**.

Stevens, B. P. J., 2006. Advances in understanding Broken hill geology. In: Korsch, R. J. and Barnes, R. G., editors, Broken Hill Exploration Initiative: Abstracts from the September 2006 conference. *Geoscience Australia, Record*, **2006/21**.

Stevens, B. P. J., Barnes, R. G., Brown, R. E., Stroud, W. J. and Willis, I. L., 1988. The Willyama Supergroup in the Broken Hill and Euriowie blocks, New South Wales. In: Wyborn, L.A.I. and Etheridge, M.A., editors, *The early to middle Proterozoic of Australia.* Elsevier, **40-41**, 297-327.

Stevens, B. P. J., Page, R. W. and Crooks, A. F., 2008. Geochronology of Willyama Supergroup metavolcanics, metasediments and contemporaneous intrusions, Broken Hill, Australia. *Australian Journal of Earth Sciences,* **55**, 301–330.

Szpunar, M., Hand, M., Barovich, K. and Jagodzinski, L., 2006. Tectonic links between the Gawler Craton and Curnamona Province. In: Korsch, R.J. and Barnes, R.G., editors, Broken Hill Exploration Initiative: Abstracts for the September 2006 conference. *Geoscience Australia, Record,* **2006/21**, 176-177.

Teale, G. S., 1993. Mount Painter and Mount Babbage Inliers. In: Drexel, J. F., Preiss, W. V. and Parker, A. J. E., editors, The Geology of South Australia. Volume 1, The Precambrian, South Australia. *Geological Survey, Bulletin*, **54 (1)**, 93–100.

Webb, G. and Crooks, A., 2005. Metamorphic investigations of the Palaeoproterozoic metasediments of the Willyama Inliers, southern Curnamona Province - a new isograd map. *MESA Journal,* **37**, 53–57.

Willis, I. L., Brown, R. E., Stroud, W. J. and Stevens, B. P. J., 1983. The early Proterozoic Willyama Supergroup; stratigraphic subdivision and interpretation of high to low-grade metamorphic rocks in the Broken Hill Block, New South Wales. *Journal of the Geological Society of Australia,* **30**, 195-224.

Geology of the Neoproterozoic to Cambrian Adelaide Geosyncline and Cambrian Delamerian Orogen

W.V. Preiss

Geological Survey Branch, Primary Industries and Resources South Australia (PIRSA), GPO Box 1671, Adelaide, SA 5001, Australia

Wolfgang.Preiss@sa.gov.au

Introduction

The primary aim of the Gawler-Curnamona Link Line (09GA-CG1) deep reflection seismic survey was to establish the relationship between the perceived mineral-prospective Paleo- to Mesoproterozoic Gawler Craton (Hand et al., 2007) and Curnamona Province (Robertson et al., 1998; Conor and Preiss, 2008). These are separated by a zone of thick cover, with a minimum width of 170 km. This cover, ranging in age from Neoproterozoic to Holocene, obscures the critical relationship between the basement provinces (Szpunar et al., 2006).

The thickest cover is the Neoproterozoic to early Cambrian succession of the Adelaide Geosyncline. Numerous stratigraphic studies in the Flinders and Mount Lofty Ranges (see Preiss, 1987, 2000, and references therein), where these rocks crop out extensively, show that the cumulative thickness is considerably greater than ten kilometres, although the true total has been difficult to estimate because of great variation in thickness of individual packages in different parts of the Adelaide Geosyncline, and because the base of the succession is exposed only in a few places near the basin margins, but not in the depocentres. The Gawler-Curnamona Link Line seismic survey, the first to traverse the whole basin, confirms the great thickness of the cover succession and the great depth (up to 18 km) to basement in at least one of its depocentres, and provides new insights into syn- and post-depositional tectonics of the Adelaide Geosyncline along the transect. For example, it shows a number of major, crustal-penetrating faults and shear zones which are potential pathways for mineralising fluids within rocks of the Adelaide Geosyncline. One of these may be a reactivation of an original tectonic boundary between two basement provinces of different seismic character (Preiss et al., 2010).

Younger cover sediments in the vicinity of the seismic transect post-date the mid-Cambrian Delamerian Orogeny that deformed the Neoproterozoic to early Cambrian succession. These include: 1. Holocene alluvial and aeolian sand, clay and gravel, 2. Pleistocene alluvial fans, aeolian, lacustrine and wetland sediments and extensive calcrete, 3. Tertiary sand, clay and lignite of the Torrens Basin (up to hundreds of metres thick), and 4. local intermontane basins of Permian to Triassic age. At the northern extremity of the Flinders Ranges, Jurassic-Cretaceous sediments of the Eromanga Basin lap onto Proterozoic–Cambrian bedrock. No Permian or Mesozoic rocks are crossed in the Link Line transect.

The Adelaide Geosyncline is a complex of rifts and sags that are interpreted as partly intracontinental rifts and partly passive continental margin basins (Preiss, 2000). The Archean to Mesoproterozoic Gawler Craton to the west has a relatively thin but eastward-thickening wedge of Neoproterozoic to Cambrian platform cover, the Stuart Shelf (Figure 1). The Torrens Hinge Zone is a zone of transition between the platform and the rift and sag basins to the east. Northeast of the Adelaide Geosyncline, the Curnamona Province has similar thin platformal cover, to which the rarely cited term Coombalarnie Platform has been applied (Callen, 1990).

Sedimentation in the Adelaide Geosyncline is best described in terms of continuous sediment packages separated by sequence boundaries. Most of these packages and groupings of packages correspond to the currently used major lithostratigraphic divisions (Preiss et al., 1998; Preiss and Cowley, 1999), as shown in Figure 2. The chronostratigraphic terms Willouran, Torrensian, Sturtian, Marinoan, Ediacaran and Cambrian are used as a framework for historical accounts. The four original Neoproterozoic chronostratigraphic units all have type sections in South Australia (Mawson and Sprigg, 1950; Sprigg, 1952), as does the internationally-defined Ediacaran (Knoll et al., 2006).

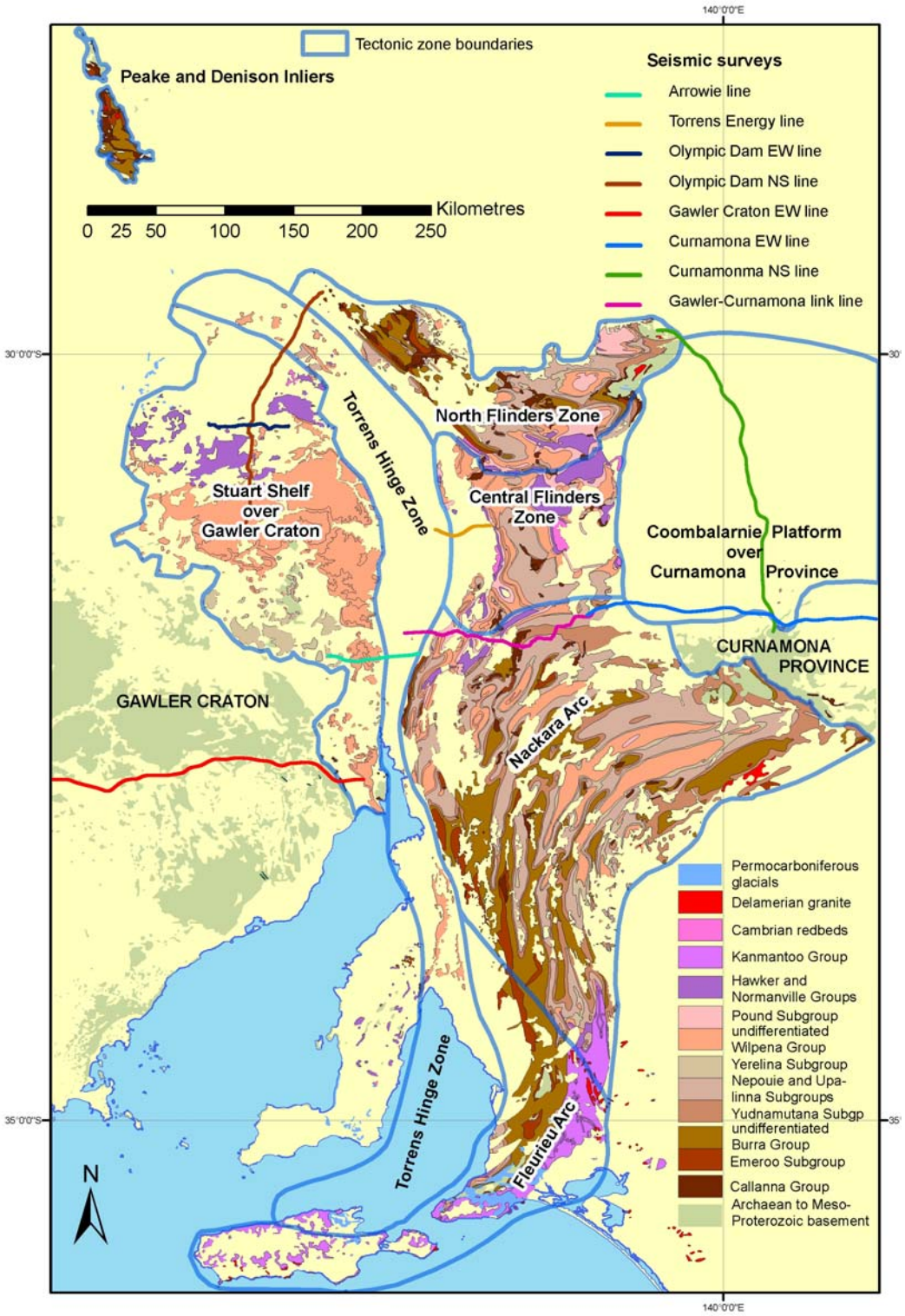

Figure 1. Neoproterozoic and Paleozoic geology of the Adelaide Geosyncline showing tectonic zones of the Delamerian Orogen and location of seismic surveys.

Chronostratigraphic units	Lithostratigraphic units, Flinders Ranges					Major events	Estimated Ages
	Supergroup	*Group*	*Subgroup*	*Selected Formations*	*Member*		
?mid-Cambrian	Moralana	Lake Frome				Redbeds	
Early Cambrian		Unnamed		Wirrealpa		marine limestone	
				Billy Creek		redbeds, tuffs	~510 Ma
		Hawker		Wilkawillina		archaeocyathan reefs	
				Parachilna		worm-burrows	
Marinoan / Ediacaran	Heysen	Wilpena	Pound	Rawnsley		thick sand sheet	
					Ediacara	metazoan fossils	
				Bonney		Redbeds	
			unnamed	Wonoka		submarine canyons	
				Bunyeroo		bolide impact layer	
			Sandison	ABC Range		transgression-regression	
				Brachina			
				Nuccaleena			
		Umberatana	Yerelina	Elatina		Glaciation	?635 Ma
							or 580 Ma
			Upalinna	Angepena		basin-margin redbeds	
Sturtian			Nepouie	Balcanoona		ooids, microbial reefs	
				Tapley Hill	Tindelpina	transgression-regression	~650 Ma
			Yudnamutana	Wilyerpa		deglaciation, rifting	~660 Ma
				Appila/Pualco		glaciation, rifting	
						major unconformity	
Torrensian	Warrina	Burra	Belair			Sag basin, deltas	
			Bungarider			Sag basin, deltas, deep-water dolomite	
			Mundallio	Skillogalee		paralic dolomite, magnesite	
					Kooringa	Burra Cu, felsic magma	~790 Ma
			Emeroo			major rifting, clastics minor mafic volcanism	
Willouran		Callanna	Curdimurka			major rifting, clastics, carbonates, evaporites minor mafic and	
				Rook		felsic volcanism	~800 Ma
			Arkaroola	Wooltana		mafic volcanism	827±6 Ma
				Wywyana		sag basin	
				Paralana			

Figure 2. Chronostratigraphic and lithostratigraphic subdivision of the Neoproterozoic–Cambrian Adelaide Geosyncline, showing a few of the formations, members and major events of the Flinders Ranges.

Neoproterozoic Sedimentation and Tectonics

During the Neoproterozoic, the continental crust of Australia was part of the Supercontinent Rodinia, which had amalgamated in a series of Paleo- and Mesoproterozoic orogenic episodes, the details and tectonic settings of which are still much debated.

Sedimentation in the Adelaide Geosyncline commenced in early Willouran time, with a mature, well-sorted, shallow-marine transgressive sand blanket that may have been a southern extension of the Centralian Superbasin, which was a large sag basin that developed in the centre of the continent during the Neoproterozoic. The Paralana Quartzite and its correlatives are thus probably approximate equivalents to the Heavitree Quartzite and other coeval

quartzites of central Australia. The Wywyana Formation, and equivalent carbonates, record a gradual shutting down of clastic supply with marine transgression.

Rifting, which eventually led to the breakup of Rodinia, commenced at ~827 ± 6 Ma, an event recorded by the intrusion of the Gairdner Dyke Swarm on the Gawler Craton and correlatives in the Curnamona Province (Wingate et al., 1998). The Beda Volcanics on the Stuart Shelf are probable extrusive equivalents. Adjacent to the Curnamona Province, mafic volcanics of this age were extruded over the basal sediment sand-carbonate package – the Wooltana Volcanics around the Mount Painter Inlier in the northwest, and the Wilangee Volcanics in the Barrier Ranges to the northeast in New South Wales. Rifting continued within the Adelaide Geosyncline during late Willouran and Torrensian time (~800-750 Ma), but had little effect on the Gawler Craton or Curnamona Province. The late Willouran Curdimurka Subgroup consists of evaporitic, mixed clastic and carbonate facies at least 6 km thick, and includes the ~800 Ma felsic volcanics of the Rook Tuff and Oodlawirra Volcanics (Fanning et al., 1986; Fabris et al., 2005). The Curdimurka Subgroup, probably with interbedded evaporite layers, was disrupted and became the source for diapiric breccias that later intruded younger parts of the succession.

Immature fluvial arkosic and pebbly sands characterise the base of the Burra Group, consistent with an active rift setting. This was followed by marine transgression, depositing sandy silt and local dolomite in a western graben (Gladstone Trough), bounded to the east by the uplifted Manoora Horst. The latter was an active fault block bounded to the west by the Clare–Spalding Fault and to the east by the north-northwest- striking Kooringa–Kingston fault system, which is part of the G2 Corridor (O'Driscoll, 1983). Deposits of the mid-Torrensian Mundallio Subgroup are sand-dominated in the Gladstone Trough, with minor dolomite, but interfinger northward and eastward with the magnesite-bearing Skillogalee Dolomite, which attains great thicknesses and forms strong reflections in the seismic transect (Preiss et al., 2010). Local ~790 Ma felsic magmatism at Burra was responsible for hydrothermal copper mineralisation (Drexel, 2008; Preiss et al., 2009).

The widespread late Torrensian Bungarider Subgroup transgresses over the horsts and grabens, and thus reflects incipient sag conditions, though the basin margins were probably still active extensional faults. The earliest Sturtian Belair Subgroup overlies the Bungarider Subgroup with an, at least locally, erosive sequence boundary, but is more restricted in distribution due to differential erosion at the major, mid-Sturtian unconformity. Both subgroups are dominated by siltstone and deep-water dolomite, with tongues of deltaic sandstone.

The ~660 Ma Sturtian glaciation left widespread glacial, glaciomarine and fluvioglacial deposits of the Yudnamutana Subgroup upon the mid-Sturtian unconformity in the Adelaide Geosyncline, but these sediments extend only a short distance west onto the Gawler Craton and east onto the Curnamona Province. Glaciation accompanied the last major phase of rifting, which produced northwest-trending grabens encircling, and defining the margins of, the Curnamona Province. The thickness of the Yudnamutana Subgroup increases markedly into the grabens, across a series of down-stepping extensional faults. The MacDonald Fault, defining the southwestern margin of the Kalabity Inlier of the Curnamona Province, was one such active rift fault during the Sturtian glaciation (Preiss, 2006).

The interglacial Nepouie and Upalinna Subgroups record widespread sag-phase conditions. Post-glacial transgression led to the first significant inundation of the Stuart Shelf, with laminated carbonaceous siltstone of the Tapley Hill Formation being deposited widely across the Adelaide Geosyncline in deep marine shelf conditions. It did not, however, extend onto the Benagerie Ridge of the Curnamona Province, which remained elevated until onlapped by the Upalinna Subgroup of the Coombalarnie Platform. Upward shallowing led to deposition of ooid shoals, stromatolite bioherms and a microbial reef near the basin margins. Sea level was generally lower during sedimentation of the early Marinoan Upalinna Subgroup, which deposited redbeds at basin margins.

The Yerelina Subgroup consists of deposits of the Elatina glaciation, the age of which has been variously interpreted as either 635 Ma (Hoffman and Schrag, 2002; Knoll et al., 2006) or 580 Ma (Calver et al., 2004). A wide variety of facies represent thin aeolian (Stuart Shelf), and thicker fluvioglacial and glaciomarine (Flinders Ranges) environments (Williams et al., 2008). Thick,

outer shelf successions with dropstones and interfingering sandstones characterise the Yerelina Subgroup in the eastern Nackara Arc and North Flinders Zones.

Apart from the basal cap dolomite of the Nuccaleena Formation, the Ediacaran-age Wilpena Group is clastic dominated. The Sandison Subgroup (Dyson, 1992) represents a major transgress-regressive cycle. The overlying Bunyeroo Formation, a deep-water mudstone, contains a bolide impact debris layer (Williams and Gostin, 2005). Calcareous siltstone and limestone of the Wonoka Formation contain evidence of submarine canyons (Giddings et al., 2010). The Pound Subgroup at the top of the Neoproterozoic succession consists of the Bonney Sandstone redbeds and the white Rawnsley Quartzite (Forbes, 1971; Jenkins, 1981). The Ediacara Member of the Rawnsley Quartzite contains the Ediacara assemblage of metazoan fossils (Jenkins, 1981; Gehling, 2000).

Early Cambrian deposition followed a major hiatus throughout the Adelaide Geosyncline (Gravestock et al., 1995). Cambrian sediments in the Flinders Ranges, on the Stuart Shelf and on the Curnamona Province are assigned to the Arrowie Basin. Transgressive, worm-burrow sandstone passes up to various shallow and deep-water limestone facies, including archaeocyathan reefs, of the Hawker Group. Redbeds of the Billy Creek Formation, including felsic tuffs, overlie the Hawker Group, followed by the marine Wirrealpa Limestone, then the thick, generally upward-coarsening redbed clastics of the Lake Frome Group. In the south, renewed rifting along arcuate, generally northeast-striking extensional faults produced the deeply subsiding Kanmantoo Trough (Jago et al., 2003), which was filled rapidly with turbiditic and lesser shallow-water siliciclastic sediments within only a few million years. If this trough is due to backarc extension (Powell et al., 1994), it implies a change from a passive continental margin to the east in the Neoproterozoic to an active margin in the early Cambrian.

Delamerian Orogeny, ~515-490 Ma

Deformation

The Delamerian Orogen in South Australia (Figure 1) is divided into three belts of arcuate folds – the Fleurieu and Nackara Arcs in the south and the North Flinders Zone in the north (Rutland et al., 1981). A zone of less intense deformation, the Central Flinders Zone, separates the northern and southern belts and consists of broad dome and basin structures. The complex fold patterns of the Delamerian Orogen resulted from interaction of northwest-directed contraction with the rifted eastern margin of the Gawler Craton and western margin of the Curnamona Province.

The Fleurieu Arc of the Mount Lofty Ranges and Kangaroo Island records the earliest deformation and maximum shortening, with northwest-directed thrusts against a southeastern promontory of the Gawler Craton, which resulted from multiple Neoproterozoic and Cambrian rift events. These earliest structures are overprinted to the north by north-south folds, faults and cleavages of the Nackara Arc, which developed in a sinistral transpressional regime, with the Kooringa–Kingston fault system as the master strike-slip fault, as the deformation propagated northward. The northeastern arm of the Nackara Arc curves toward the Curnamona Province, at the southwestern margin of which domal, fault-bounded basement inliers resulted from fold interference (Preiss and Conor, 2001).

The boundary between the Nackara Arc and Central Flinders Zone is not sharply defined, but marks a substantial thickening of the Neoproterozoic succession toward the southeast. Aeromagnetic data indicate that basement is shallower beneath the Central Flinders Zone, where the cover underwent much less Delamerian shortening than in the fold arcs to the north and south. This thickening is clearly displayed on the seismic section (Preiss et al., 2010).

Delamerian magmatism

An arcuate belt of early to late syntectonic I-type, and less common S-type, granites between ~515 Ma and 505 Ma follows the trend of the Fleurieu and Nackara Arcs near the eastern limit of outcrop, and extends southeast into western Victoria. These are possibly related to west-dipping subduction beneath the orogen. After considerable exhumation of the orogen, A-type

magmas at ~490 Ma were intruded into upper crustal levels, in a belt of similar distribution to the synorogenic magmas (Foden et al., 2002).

Metamorphism

Metamorphic grade in cover rocks during the Delamerian Orogeny ranged from essentially unmetamorphosed on the cratons (Stuart Shelf and Coombalarnie Platform), to upper amphibolite facies in the eastern Fleurieu Arc. Lower amphibolite facies is recorded in basal Adelaidean metasedimentary rocks around the Mount Painter Inlier (McLaren et al., 2006) and the southwestern Kalabity Inlier (Rutherford et al., 2006; Dutch et al., 2005), and the grade of Delamerian metamorphism may have been even higher deeper in the basement. Most of the remainder of the Delamerian Orogen consists of metasedimentary rocks at low to mid-greenschist facies.

Post-Delamerian magmatic and hydrothermal activity

Post-Delamerian events include intrusion of Early Ordovician felsic dykes in the Radium Hill area (Jagodzinski et al., 2006) and intrusion of granites and high-temperature veins in the Mount Painter Inlier at ~440 Ma (Elburg et al., 2003). The high-level hydrothermal system of the Radium Ridge Breccias and Mount Gee Sinter (Drexel and Major, 1987) are probably Permo-Carboniferous in age (Idnurm and Heinrich, 1993).

Neotectonics

As a result of the onset of late Cenozoic east-west compression of Australia, much of the deeply eroded Delamerian mountain chain has been uplifted, at least partly on reactivated Delamerian and older faults. Such faults include the faults bounding the Cenozoic St Vincent Basin near Adelaide, the Morgan, Burra and Mongolata Faults of the Mid-North, and the Crystal Brook and Wilkatana Faults of the southwestern Flinders Ranges. In the northeastern Flinders Ranges, the Paralana and Lady Buxton Faults were similarly responsible for neotectonic uplift, while the Mundi Mundi Fault forms the western boundary of the Barrier Ranges in NSW. All these are thrust faults that dip east and west beneath the uplifted regions, reflecting deep structures in the crust that can now be imaged on seismic sections.

References

Callen, R.A., 1990. CURNAMONA, South Australia, Sheet SH/54-14. *South Australia. Geological Survey. 1:250 000 series – Explanatory Notes.*

Calver, C.R., Black, L.P., Everard, J.L. and Seymour, D.B., 2004. U-Pb age constraints on late Neoproterozoic glaciation in Tasmania. *Geology*, **32**, 893-896.

Conor, C.H.H. and Preiss, W.V., 2008. Understanding the 1720-1640 Ma Palaeoproterozoic Willyama Supergroup, Curnamona Province: implications for tectonics, basin evolution and ore genesis. *Precambrian Research*, **166**, 297–317.

Drexel, J.F. and Major, R.B., 1987. Geology of the uraniferous breccias near Mount Painter, South Australia, and revision of rock nomenclature. *Geological Survey of South Australia, Quarterly Geological Notes*, **104**, 14-24.

Drexel, J.F., 2008. Review of the Burra Mine project, 1980–2008 - a progress report. *Primary Industries and Resources Department South Australia. Report Book*, **2008/16**.

Dutch, R.A., Hand, M. and Clark, C., 2005. Cambrian reworking of the southern Australian Proterozoic Curnamona Province: constraints from regional shear-zone systems. *Journal of the Geological Society, London*, **162**, 763-775.

Dyson, I.A., 1992. Stratigraphic nomenclature and sequence stratigraphy of the lower Wilpena Group, Adelaide Geosyncline: the Sandison Subgroup. *Geological Survey of South Australia, Quarterly Geological Notes*, **122**, 2-13.

Elburg, M.A., Bons, P., Foden, J. and Brugger, J., 2003. A newly defined Late Ordovician magmatic-thermal event in the Arkaroola area, northern Flinders Ranges, South Australia. *Australian Journal of Earth Sciences*, **50**, 611-631.

Fabris, A., Constable, S., Conor, C., Woodhouse, A., Hore, S. and Fanning, M., 2005. Age, origin, emplacement and mineral potential of the Oodla Wirra Volcanics, Nackara Arc, central Flinders Ranges. *MESA Journal* **37**, 44–52.

Fanning, C.M., Ludwig, K.R., Forbes, B.G. and Preiss, W.V., 1986. Single and multiple grain U-Pb zircon analyses for the early Adelaidean Rook Tuff, Willouran Ranges, South Australia. In: 8th Australian Geological Convention, Adelaide, 1986. *Geological Society of Australia. Abstracts,* **15**, 71-72.

Foden, J.D., Elburg, M.A., Turner, S.P., Sandiford, M., O'Callaghan, J.O. and Mitchell, S., 2002. Granite production in the Delamerian Orogen, South Australia. *Journal of the Geological Society, London,* **159**, 557-575.

Forbes, B.G., 1971. Stratigraphic subdivision of the Pound Quartzite (late Precambrian, South Australia). *Royal Society of South Australia Transactions*, **95**, 219–225.

Gehling, J.G., 2000. Sequence stratigraphic context of the Ediacara Member, Rawnsley Quartzite, South Australia: a taphonomic window into the Neoproterozoic biosphere. *Precambrian Research*, **100**, 65-95.

Giddings, J.A., Wallace, M.W., Haines, P.W. and Mornane, K., 2010. Submarine origin for the Neoproterozoic Wonoka canyons, South Australia. *Sedimentary Geology*, **223**, 35-50.

Gravestock, D.I., Alley, N.F., Benbow, M.C., Cowley, W.M., Farrand, M.G., Flint, R.B., Gatehouse, C.G., Krieg, G.W. and Preiss, W.V., 1995. Early and Middle Palaeozoic. In: Drexel, J.F. and Preiss, W.V., editors, The Geology of South Australia. Vol.2, The Phanerozoic. South Australia. *Geological Survey Bulletin* **54(2)**, 2–61.

Hand, M., Reid, A. and Jagodzinski, E., 2007. Tectonic framework and evolution of the Gawler Craton, South Australia. *Economic Geology*, **102**, 1377-1395.

Hoffman, P.F., and Schrag, D.P., 2002. The snowball Earth hypothesis: Testing the limits of global change. *Terra Nova*, **14**, 129–155.

Idnurm, M and Heinrich, C.A., 1993. A palaeomagnetic study of hydrothermal activity and uranium mineralisation at Mt Painter, South Australia. *Australian Journal of Earth Sciences*, **40**, 87-101.

Jago, J.B., Gum, J.C., Burtt, A.C., and Haines, P.W., 2003. Stratigraphy of the Kanmantoo Group: a critical element of the Adelaide Fold Belt and the Palaeo-Pacific plate margin, Eastern Gondwana. *Australian Journal of Earth Sciences*, **50**, 343-363.

Jagodzinski, E.A., Frew, R.A., Szpunar, M., Conor, C., Crooks, A.F. and Burtt, A., 2006. Compilation of SHRIMP U-Pb geochronological data for the Curnamona Province and Adelaide Geosyncline, South Australia, 2006. *South Australia. Department of Primary Industries and Resources. Report Book,* **2006/6**.

Jenkins, R.J.F., 1981. The concept of an "Ediacaran Period" and its stratigraphic significance in Australia. *Royal Society of South Australia Transactions,* **105**,179-194.

Knoll, A.H., Walter, M.R., Narbonne, G.M., and Christie-Blick, N., 2006. The Ediacaran Period: A new addition to the geologic time scale. *Lethaia*, **39**, 13–30.

Mawson, D. and Sprigg, R.C., 1950. Subdivision of the Adelaide System. *Australian Journal of Science*, **13**, 69-72.

McLaren, S., Sandiford, M., Powell, R., Neumann, N. and Woodhead, J., 2006. Palaeozoic intraplate crustal anatexis in the Mount Painter province, South Australia: timing, thermal budgets and the role of crustal heat production. *Journal of Petrology*, **47**, 2281-2302.

O'Driscoll, E.S.T., 1983. Deep tectonic foundations of the Eromanga Basin. *APEA Journal*, **23**, 5-17.

Powell, C.McA., Preiss, W.V., Gatehouse, C.G., Krapez, B. and Li, Z.X., 1994. South Australian record of a Rodinia epicontinental basin and its mid-Neoproterozoic breakup (~700 Ma) to form the Palaeo-Pacific Ocean. *Tectonophysics*, **237**, 113-140.

Preiss, W.V., 1987 (Compiler). The Adelaide Geosyncline - late Proterozoic stratigraphy, sedimentation, palaeontology and tectonics. *South Australia Geological Survey, Bulletin,* **53**, 105p.

Preiss, W.V., Dyson, I.A., Reid, P.W. and Cowley, W.M., 1998. Revision of lithostratigraphic classification of the Umberatana Group. *MESA Journal*, **9**, 36-42.

Preiss, W.V. and Cowley, W.M., 1999. Genetic stratigraphy and revised lithostratigraphic classification of the Burra Group in the Adelaide Geosyncline. *MESA Journal*, **14**, 30-40.

Preiss, W.V., 2000. The Adelaide Geosyncline of South Australia, and its significance in continental reconstruction. *Precambrian Research*, **100**, 21-63.

Preiss, W.V., 2006. Old Boolcoomata Conglomerate Member of the Benda Siltstone – Neoproterozoic glacial sedimentation in terrestrial and marine environments in an active rift basin. *MESA Journal*, **41**, 15-23.

Preiss, W.V. and Conor, C.H.H., 2001. Origin and nomenclature of the Willyama Inliers. *MESA Journal*, **21**, 47-49.

Preiss, W.V., Drexel, J.F. and Reid, A.J., 2009. Definition and age of the Kooringa Member, Skillogalee Dolomite: host for Neoproterozic (~790 Ma) porphyry-related copper mineralisation at Burra. *MESA Journal*, **55**, 11-25.

Preiss, W.V., Korsch, R.J., Blewett, R.S., Fomin, T., Cowley, W.M., Neumann, N.L. and Meixner, A.J., 2010. Geological interpretation of deep seismic reflection line 09GA-CG1: the Curnamona Province-Gawler Craton Link Line, South Australia. *Geoscience Australia, Record,* **2010/10**, this volume.

Robertson, R.S., Preiss, W.V., Crooks, A.F., Hill, P.W. and Sheard, M.J., 1998. Review of the Proterozoic geology and mineral potential of the Curnamona Province in South Australia. *AGSO Journal of Australian Geology and Geophysics,* **17**, 169-182.

Rutland, R.W.R., Parker, A.J., Pitt, G.M., Preiss, W.V. and Murrell, B., 1981. The Precambrian of South Australia. In: Hunter, D.R., editor, Precambrian of the Southern Hemisphere. *Developments in Precambrian Geology Series,* **2**, 309-360, Elsevier, Amsterdam.

Rutherford, L., Hand, M. and Mawby, J., 2006. Delamerian-aged metamorphism in the southern Curnamona Province, Australia; implications for the evolution of the Mesoproterozoic Olarian Orogeny. *Terra Nova*, **18**, 138-146.

Sprigg, R.C., 1952. Sedimentation in the Adelaide Geosyncline and the formation of the continental terrace. In: Glaessner, M.F. and Rudd, E.A., editors, *Sir Douglas Mawson Anniversary Volume.* University of Adelaide, Adelaide, 153-159.

Szpunar, M., Hand, M., Barovich, K. and Jagodzinski, L., 2006. Tectonic links between the Gawler Craton and Curnamona Province. In: Korsch, R.J. and Barnes, R.G., editors, Broken Hill Exploration Initiative: Abstracts for the September 2006 conference. *Geoscience Australia, Record,* **2006/21**, 176-177.

Williams, G.E. and Gostin, V.A., 2005. Acraman–Bunyeroo impact event (Ediacaran), South Australia, and its environmental consequences: twenty-five years on. *Australian Journal of Earth Sciences*, **52**, 607-620.

Williams, G.E., Gostin, V.A., McKirdy, D.M. and Preiss, W.V., 2008. The Elatina glaciation, late Cryogenian (Marinoan Epoch), South Australia: Sedimentary facies and palaeoenvironments. *Precambrian Research*, **163**, 307-331.

Wingate, M.T.D., Campbell, I.H., Compston, W. and Gibson, G.M., 1998. Ion-probe U–Pb ages for Neoproterozoic basaltic magmatism in south-central Australia and implications for the break-up of Rodinia. *Precambrian Research,* **87**, 135-159.

Geological interpretation of deep seismic reflection and magnetotelluric line 08GA-C1: Curnamona Province, South Australia

R.J. Korsch[1], W.V. Preiss[2], R.S. Blewett[1], A.J. Fabris[2], N.L. Neumann[1], C.E. Fricke[2], G.L. Fraser[1], J. Holzschuh[1], P.R. Milligan[1] and L.E.A. Jones[1]

[1]Onshore Energy & Minerals Division, Geoscience Australia, GPO Box 378, Canberra, ACT 2601, Australia
[2]Geological Survey Branch, Primary Industries and Resources South Australia (PIRSA), GPO Box 1671, Adelaide, SA 5001, Australia

Russell.Korsch@ga.gov.au

Introduction

Deep seismic reflection surveys in the Paleoproterozoic to Mesoproterozoic Curnamona Province (Fricke et al., 2010), acquired in 1996-97 (seismic lines 96AGS-BH1A and 96AGS-BH1B; Gibson et al., 1998) and 2003-04 (seismic line 03GA-CU1; Goleby et al., 2006) were combined to provide a single, 400 km long transect across the entire Curnamona Province from the Darling Basin in the east to the Flinders Ranges in the west (Korsch et al., 2006a). In 2008, as part of its Onshore Energy Security Program, Geoscience Australia, in conjunction with Primary Industries and Resources South Australia (PIRSA), acquired 262 km of vibroseis-source deep seismic reflection data as a single traverse in the Curnamona Province in South Australia. This line, 08GA-C1, was oriented approximately north-south (Figures 1 to 3); it tied to seismic line 03GA-CU1 in the south, ran to the east of Lake Frome along the Benagerie Ridge, and ended to the northeast of the Mount Painter and Mount Babbage Inliers. Crustal-scale, magnetotelluric data were also collected along the seismic route. Here, we report the results of an initial geological interpretation of this seismic line.

Aims of the Seismic Survey

The main aim of the current seismic survey was to determine the crustal architecture of this part of the Curnamona Province, which has high potential for uranium and geothermal exploration. The seismic line traversed the eastern part of the South Australian Heat Flow Anomaly, with the aim of providing insights into the large-scale character and composition of this crustal-scale, geochemical and thermal anomaly. In particular, the Mount Painter Inlier contains the most radiogenic granites known in Australia (Neumann et al., 2000).

Within the Curnamona Province, the seismic line crossed areas which have a high potential for a range of U and Th mineral systems. This includes the Benagerie Ridge, which does not crop out, but does contain igneous rocks of equivalent age to the ~1590 Ma Hiltaba Suite-Gawler Range Volcanics event in the Gawler Craton, suggesting potential for IOCGU-type mineralisation within this area. Further south, in the Willyama Inlier, Paleoproterozoic basement hosts the granite-related U-Th Crocker Well deposit and the Radium Hill U deposit. Young cover rocks overlying the basement host three significant palaeochannel/sandstone-hosted U deposits, Honeymoon near Kalkaroo, and Beverley and Four Mile, east of Mount Painter. The seismic lines will provide the regional-scale architecture of these different mineral systems.

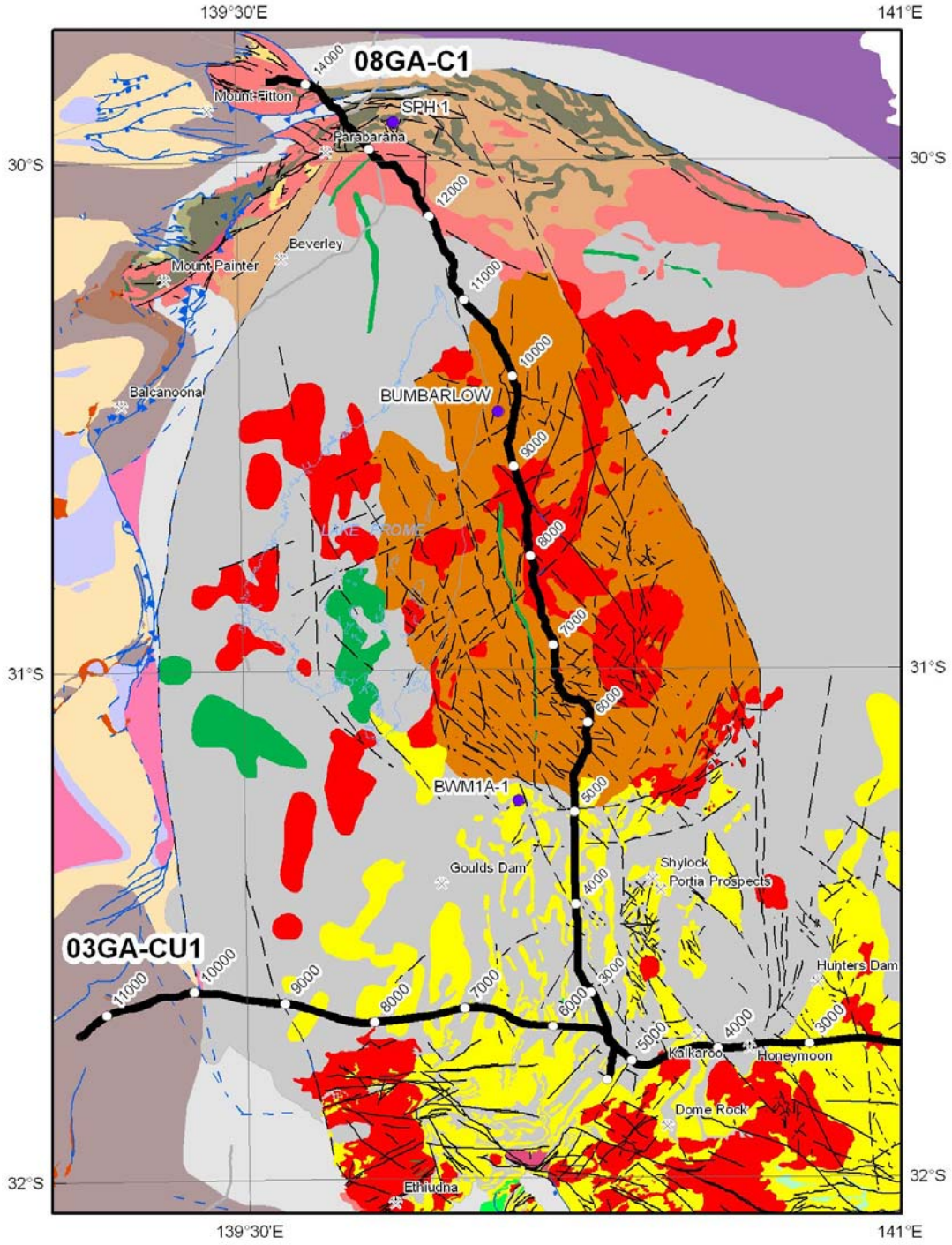

Figure 1. Map showing the solid geology of the Curnamona Province in South Australia, including the Moolawatana Domain in the north around Mt Painter (after Cowley, 2006, which also contains the legend). Also shown are the locations of the deep seismic reflection transects 03GA-CU1 and 08GA-C1, with CDP stations labelled, and the locations of drillholes referred to in the text.

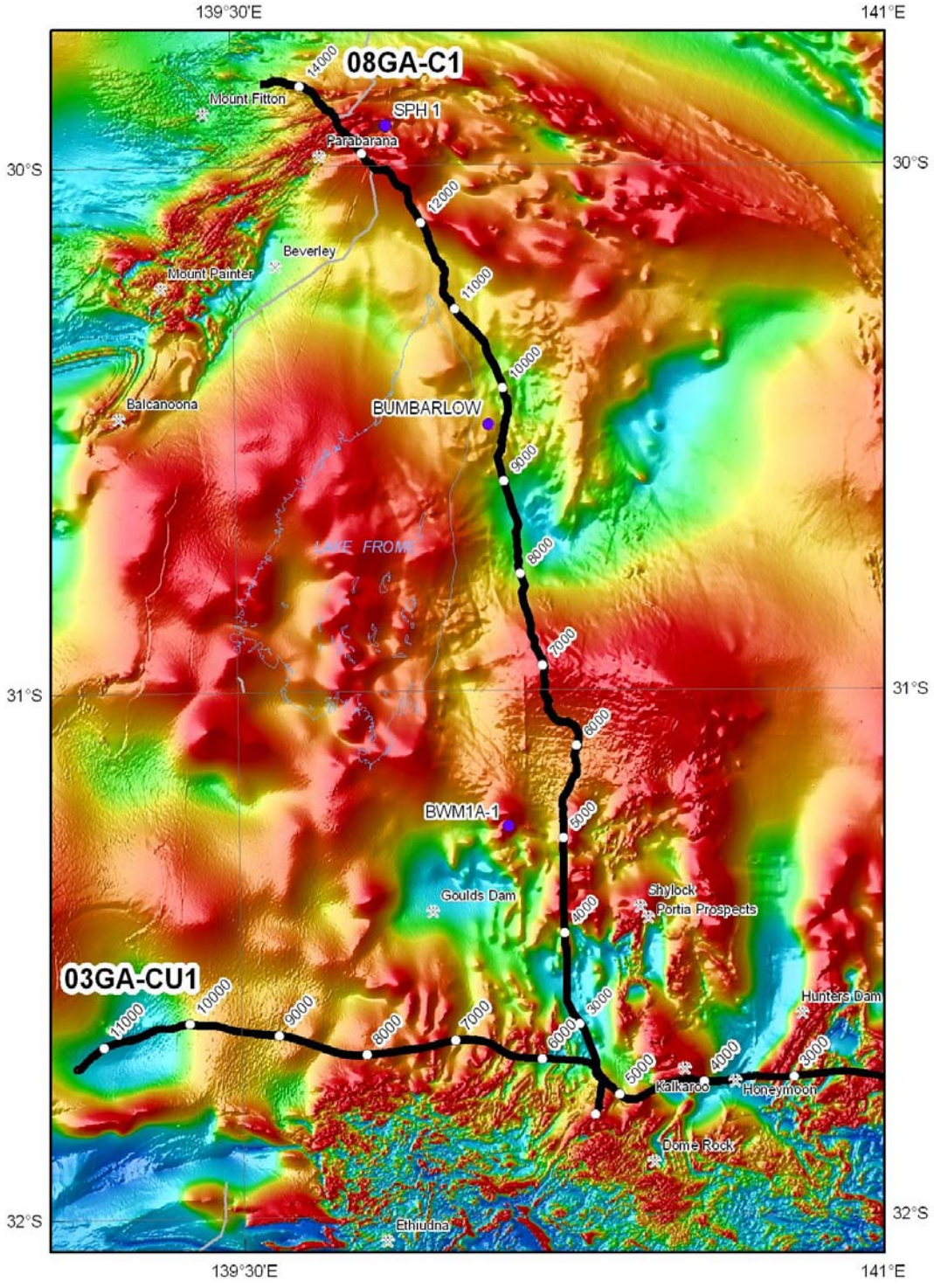

Figure 2. Map showing regional aeromagnetic data for the Curnamona Province in South Australia (warm colours are high magnetic intensities, cool colours are low magnetic intensities). Also shown are the locations of the deep seismic reflection transects 03GA-CU1 and 08GA-C1, with CDP stations labelled, and the locations of drillholes referred to in the text.

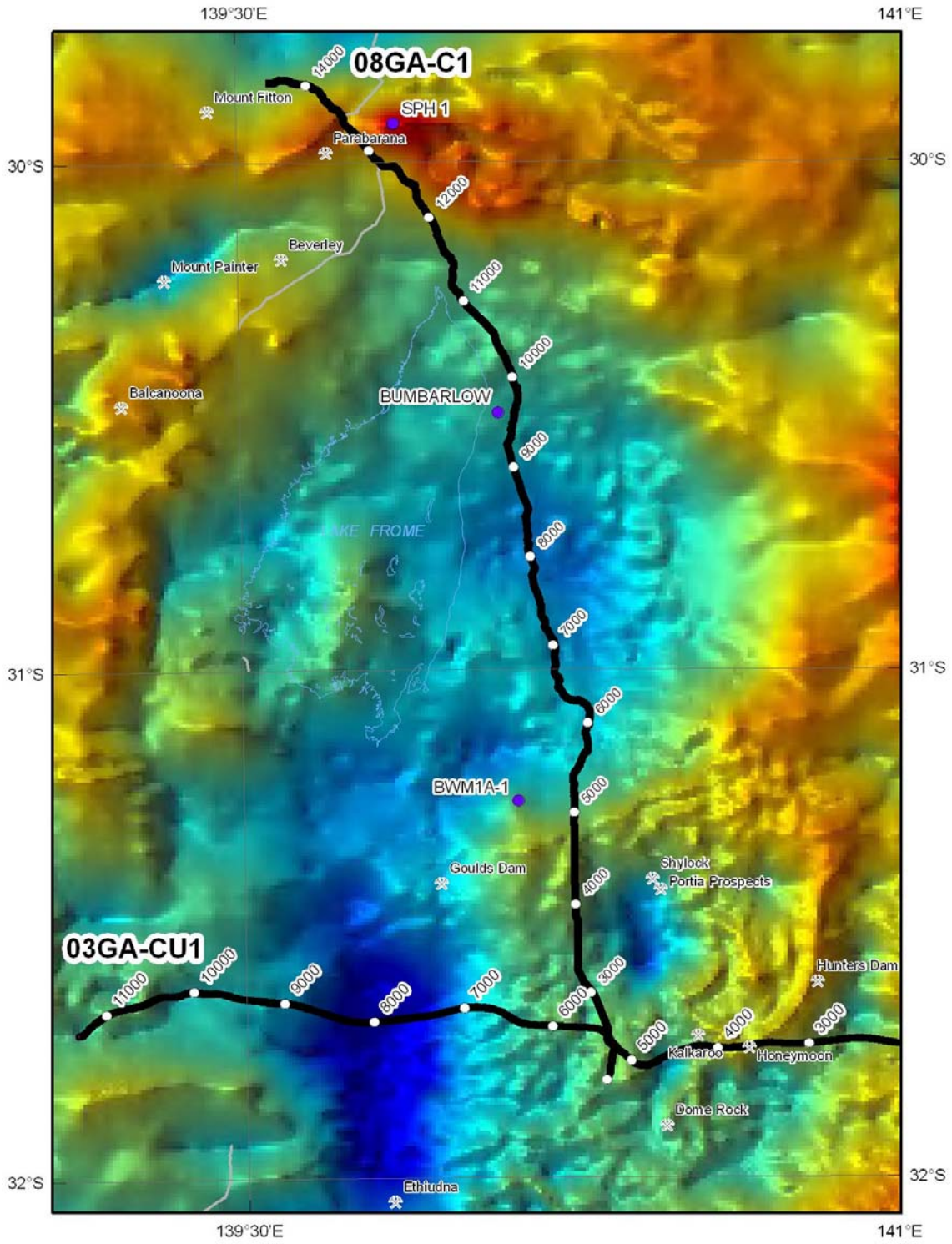

Figure 3. Map showing a regional gravity image for the Curnamona Province in South Australia (warm colours are gravity highs, cool colours are gravity lows). Also shown are the locations of the deep seismic reflection transects 03GA-CU1 and 08GA-C1, with CDP stations labelled, and the locations of drillholes referred to in the text.

The Mount Painter Inlier hosts the Paleozoic Mount Gee U system, a poorly understood hematite-rich breccia system, with some similarities to the Mesoproterozoic Olympic Dam system. The seismic line across and between the Mount Painter and Mount Babbage Inliers will aim to elucidate the regional structure that may have controlled Proterozoic to Paleozoic U mineral systems in the inliers.

Seismic Acquisition and Processing

Seismic line 08GA-C1 was acquired in June and July 2008, with project management undertaken by the Seismic Acquisition and Processing Project from Geoscience Australia. A summary of acquisition parameters is given in Fomin et al. (2010).

For seismic line 08GA-C1, 75-fold seismic reflection data were acquired to 20 s two-way time, using three Hemi-60 (60,000 lb) peak force vibrators. A Sercel 388SN recording system was used to record and correlate the seismic data. Three sweeps, 6-64 Hz, 12-96 Hz, 8-72 Hz, each 12 s long, with an 80 m vibration point interval, were selected as source acquisition parameters for this survey. Data were processed in the DISCO/FOCUS seismic processing package. The final processing flow for seismic line 08GA-C1 is summarised in Fomin et al. (2010).

Magnetotelluric acquisition and processing

Magnetotelluric (MT) data were acquired for Geoscience Australia by contract along the north-south 08GA-C1 Curnamona seismic traverse from November 2008 to January 2009. Twenty-five sites were spaced at an average of 10 km apart, and five-component broadband data were recorded with a frequency bandwidth of 0.001 Hz to 250 Hz and dipole lengths of 100 m. Details of the acquisition and processing of the magnetotelluric data are provided by Thiel et al. (2010).

Preliminary geological interpretation of seismic line 08GA-C1

Almost the entire route of the seismic traverse was over concealed basement, with only a few drillholes which could be used as control points. Overall, the crust in the vicinity of the seismic section is relatively reflective, although the central part of the section contains an upper crust which has very low reflectivity (Figure 4). The lower two-thirds of the crust contain strong subhorizontal reflections. The Moho is not sharply defined, but is interpreted to occur at the base of the reflective package at about 13 s two-way travel time (TWT), which is at a depth of about 40 km. The upper mantle beneath the Moho is essentially nonreflective.

The highly reflective crust can be tracked from the southern end of the seismic section, northwards, past the tie with seismic line 03GA-CU1, for a distance of about 200 km (to approximately CDP 13000). In the northernmost part of the section, where rocks of the Mount Painter and Mount Babbage Inliers (part of the Moolawatana Domain; Conor and Preiss, 2008) are exposed close to the section, the crust has a marked lower reflectivity compared to that of the rest of the line. The contrast in crustal reflectivity suggests that the crust beneath the Moolawatana Domain is different to that beneath the Willyama Supergroup of the Curnamona Province in the south. Although not well imaged, a crustal-scale, south-dipping boundary between the Moolawatana Domain and the Curnamona Province is inferred (Figure 4). A zone of dipping reflections in the upper mantle at about CDP 9500 indicates where this structure cuts the Moho. The reflective middle to lower crust beneath the Willyama Supergroup does not come to the surface in the plane of the seismic section, and is referred to as the Yarramba Seismic Province (Korsch et al., 2010). It is feasible that the crust below the Moolawatana Domain is the same as that below the Adelaide Rift System in the western half of the Curnamona-Gawler Link Line (09GA-CG1; Preiss et al., 2010), in which case it would be termed the Warrakimbo Seismic Package (Korsch et al., 2010).

Willyama Supergroup

The Curnamona Province consists predominantly of the Paleoproterozoic (~1720-1640 Ma) Willyama Supergroup and coeval magmatic rocks. These rocks were deformed and metamorphosed during the ~1600 Ma Olarian Orogeny, which was followed by an early

Mesoproterozoic magmatic event. In South Australia, the Curnamona Province is mostly under cover of Neoproterozoic to Cenozoic sedimentary rocks (Preiss, 2009).

In the southernmost part of the seismic section, the Willyama Supergroup contains reflections with apparent dips to the south (between CDPs 2000 and 3800, Figure 4). We consider these to be thrusts; associated folded reflections are interpreted as hangingwall antiforms. We correlate these structures with structures that have apparent dips to the east in seismic line 03GA-CU1, which were interpreted to be D3 structures formed during the Olarian Orogeny (Korsch et al., 2006b); field mapping by PIRSA and GSNSW shows that the folds associated with these structures verge to the northwest, and have faulted western limbs, as confirmed by the seismic data.

Farther to the north, between CDPs 3800 to 5200, there are a series of planar reflections with apparent dips to the north. In places, folds occur above the planar reflections; these folds are interpreted to be hangingwall antiforms that sit on thrusts, which have an apparent south-directed sense of movement. These folds are relatively open but it is unclear how these thrusts relate to the Olarian D3 structures farther south. One possibility is that they represent Olarian D2 structures.

The late structures overprint the earlier structures, which are difficult to observe in the seismic section. This is because the seismic image is one of the present day architecture of the crust; later structures tend to be the best imaged because they overprint and deform earlier structures, but are not deformed by later events. It is also difficult to image steeply dipping structures, and also those that are highly deformed.

Benagerie Ridge

Mesoproterozoic felsic and mafic volcanic rocks from the Benagerie Ridge in the northwestern part of the Curnamona Province are not exposed at the surface, but have been intersected in several drillholes (Fricke, 2009). These A-type volcanics are bimodal, and have a SHRIMP age of 1582 ± 4 Ma (Fanning et al., 1998). There is approximately a 10 Ma period of time between the cessation of the D3 deformation during the Olarian Orogeny and extrusion of the subhorizontal Benagerie Volcanics over exhumed greenschist facies rocks of the Willyama Supergroup (Korsch et al., 2006b). The Benagerie Volcanics, which are equivalent in age to the Hiltaba Suite-Gawler Range Volcanics, host of the giant Olympic Dam IOCGU deposit in the Gawler Craton, are of interest to base metal and uranium explorers.

In the seismic section, there are two nonreflective packages, separated by a set of strong reflections (at about CDP 5300), which have an apparent dip gently to the north. The Benagerie Volcanics are relatively flat-lying and form the upper, nonreflective package, which we interpret to have a maximum thickness of ~0.5 s TWT (~1.5 km). The lower, relatively nonreflective package is up to 2.3 s TWT (~ 7 km) thick. Below this, a more reflective package, consisting of the deformed and metamorphosed rocks of the Willyama Supergroup, can be traced from the surface at the southern end of the seismic line, beneath the lower nonreflective package, to near the northern end of the line (CDP 12800, Figure 4).

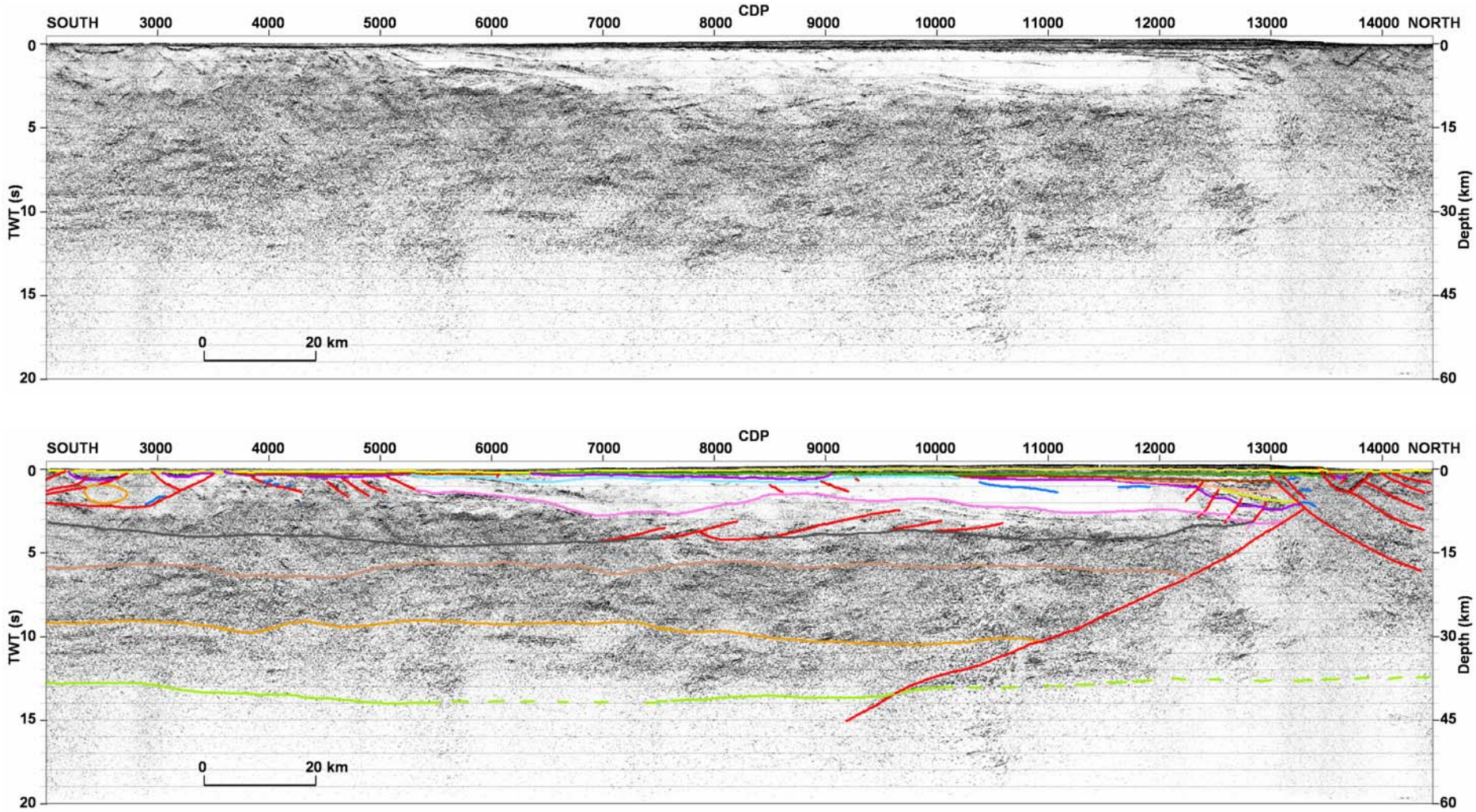

Figure 4. Migrated seismic section for line 08GA-C1 in South Australia. Display shows the vertical scale equal to the horizontal scale, assuming a crustal velocity of 6000 m s^{-1}.

At this stage, the correlation of the lower, nonreflective package to other rock packages in the Curnamona Province is unknown. Nevertheless, the youngest package of metasedimentary rocks in the Curnamona Province is the Dalnit Bore Metasediments, which has a maximum depositional age of 1642 ± 5 Ma (Page et al., 2005), and was considered to have been deposited contemporaneously with air-fall volcanism at this time. This leaves a gap of about 20 Ma before the onset of the Olarian Orogeny at about 1620 Ma. Stevens (2006), following the model of McLaren et al. (2005), implied the presence of an insulating blanket of pelitic metasediments; this was possibly deposited between 1640 Ma and 1620 Ma. Forbes et al. (2008) also suggested that sedimentation continued to at least 1620 Ma (and possibly even to 1600 Ma). Thus, we speculate that the lower, nonreflective package consists of a monotonous package of pelitic metasedimentary rocks deposited in the interval 1640-1620 Ma. This package also would have been deformed by the Olarian Orogeny, prior to eruption of the Benagerie Volcanics at ~1585 Ma. South of the Benagerie Volcanics, the Willyama Supergroup is greenschist metamorphic grade, whereas the Benagerie Volcanics appear to be essentially unmetamorphosed, leading Korsch et al. (2006b) to imply that up to 10 km of sediment was removed by erosion prior to 1585 Ma. Much of this package could be preserved as the nonreflective layer beneath the Benagerie Volcanics.

The drillhole BWM1A-1 occurs ~10 km to the west of the seismic section, and contains dipping metasedimentary rocks beneath a younger Neoproterozoic sedimentary package. It is difficult to project this drillhole onto the seismic section using aeromagnetic data, but it is possible that it intersected the lower, nonreflective package, rather than part of the Willyama Supergroup (*sensu stricto*).

Bumbarlow 1 Drillhole

The Bumbarlow 1 drillhole is located ~4 km to the west of CDP 9600 on the seismic traverse (Figure 1). This drillhole penetrated a succession of Mesozoic sedimentary rocks, followed initially by a succession of clastic sedimentary rocks and then a succession of interbedded mafic volcanic rocks and clastic sedimentary rocks (both of unknown affinity and age), before ending in low-grade metasedimentary rocks (grey-black shale with a cleavage). The lower, interbedded, sedimentary and mafic volcanic succession has a relatively disrupted reflectivity pattern, possibly due to the irregular distribution of volcanic rocks in the subsurface. Sandstone from above the uppermost basalt has yielded a SHRIMP zircon maximum depositional age of 1555 Ma (Fraser and Neumann, 2010), whereas a sandstone beneath the lowest basalt has a maximum depositional age of 1595 Ma (Fraser and Neumann, 2010). Thus, the low-grade metasedimentary rocks at the base of the hole appear to represent the lower, nonreflective package.

Moolawatana Domain

The northernmost part of the seismic section crosses Mesoproterozoic rocks of the Mount Painter and Mount Babbage Inliers, which occur beneath a thin cover of Mesozoic to Cenozoic sediment, and which form part of the Moolawatana Domain (Conor and Preiss, 2008). These rocks have been shown to be younger than any rocks in the rest of the Curnamona Province (Fanning et al., 2003; Neumann et al., 2009). In outcrop, the rocks are heavily faulted, with the main fault pattern having an apparent dip to the northwest.

In that part of the seismic section which is immediately south of the Paralana Fault (CDPs 13450 to 13000), there is a package of moderately reflective rocks, bound to the south by a northwest-dipping fault zone (CDPs 13000 to 13100); this package overthrusts the margin of a Neoproterozoic basin. Within this package, calcsilicate rocks of unknown affinity have been intersected in the SPH1 drillhole.

The Terrapinna Corridor separates the Mount Painter Inlier from the Mount Babbage Inlier. It contains Neoproterozoic Sturtian glacial rocks, which in the vicinity of the seismic line, have been mapped between CDPs 13520 and 13700. These rocks are not obvious on the seismic section and are probably relatively thin.

Neoproterozoic to Cambrian Basins

In the southern part of the seismic line, several remnants of Neoproterozoic and/or Cambrian sedimentary basins are preserved beneath a thin cover of Cenozoic sediment. The thickest of the remnant basins, also imaged on the tie line 03GA-CU1 (Goleby et al., 2006) is ~600 ms TWT (~1500 m) thick, using a seismic velocity of 5000 m s^{-1}.

The Neoproterozoic and Cambrian succession thickens significantly in the northern part of the line (CDPs 10200 to 13000), where it occurs at depth adjacent to the Moolawatana Domain. The base of the Neoproterozoic succession is difficult to map, but could be as deep as ~2.4 s TWT (~ 6 km). The sedimentary succession also shows significant growth towards the north, implying the possible existence of an original syn-depositional, extensional fault. This thick component of the basin has been disrupted by syn-depositional to post-depositional faults. Also, a major unconformity has been interpreted within the Neoproterozoic succession at a depth of about 1.3 s TWT (~3.2 km); we interpret this to be the unconformity at the base of the Umberatana Group, which has been mapped in outcrops in the Flinders Ranges to the west. The Neoproterozoic to Cambrian succession is currently of interest as a thermal blanket and also as a resource for geothermal energy.

The original Neoproterozoic basin-bounding fault, with an apparent dip to the south, is now located deeper in the crust, with the original basin margin that was near the surface having been destroyed by later deformation. The present, near-surface boundary is a thrust fault (at ~CDP 13,000) with an apparent dip to the north, and has thrust calcsilicate rocks over the Neoproterozoic to Cambrian succession. Zircons from a sample from drillhole SPH1 have a SHRIMP age of ~1560 Ma (Fraser and Neumann, 2010), indicating that these rocks have a Moolawatana Domain affinity, rather than that of the Willyama Supergroup. Note that this thrust is not active, as it is covered by essentially flat-lying Mesozoic and Cenozoic sediment. This implies that the juxtaposing of the calcsilicate rocks onto the Neoproterozoic succession occurred during either the Delamerian (~520-490 Ma), Benambran (~455-440 Ma) or Tabberabberan (~395-380 Ma) Orogenies.

Mesozoic and Cenozoic Basins

Much of the basement in the northern part of the seismic section has a cover of Mesozoic to Cenozoic sediment, which reaches a maximum thickness of about 575 m in the vicinity of CDP 12800. The Cenozoic sediments are important because they are the host of the Beverley and Four Mile uranium deposits to the west of the seismic section.

Paralana Fault

To the southwest of the seismic section, the Paralana Fault is an active thrust fault, which is thrusting Mesoproterozoic rocks of the Moolawatana Domain over Pliocene and Quaternary sediments (Célérier et al., 2005). The high heat flow, distribution of current seismicity, and the location of the Paralana hot springs on the plains adjacent to the range front, all attest to the active nature of this region. The Paralana Fault occurs at the range front and dips 25° to the west, beneath the northern Flinders Ranges. In the seismic section, the Paralana Fault is imaged as a zone of reflections with an apparent dip to the northwest.

Preliminary interpretation of the magnetotelluric results

Crustal-scale magnetotelluric data were collected along the seismic line (Thiel et al., 2010). One feature of a two dimensional model of the TM and TE modes (Figure 5) is the high near-surface conductivity values in the central part of the section, which correlate with conductive surface sediments. The depth of this conductive zone increases towards the north, consistent with the northward thickening of the subhorizontal sedimentary package. At the southern end of the line, there is a zone of high conductivity, which extends to considerable depth. The crustal-scale, south-dipping boundary between the Curnamona Province and the Moolawatana Domain, interpreted in the seismic data (Figure 4), appears also to be a major gradient in the MT model, with conductive crust to the south of the boundary, and resistive crust to the north (Figure 5).

Three-dimensional inversion of the gravity data shows that there is a significant change in density across the boundary, with denser crust occurring to the north (Chopping et al., 2010).

The MT model shows several resistive zones in the upper half of the Curnamona Province (e.g., features A and B on Figure 5), underlain by more conductive material in the lower crust, but the geological interpretation of these features is uncertain.

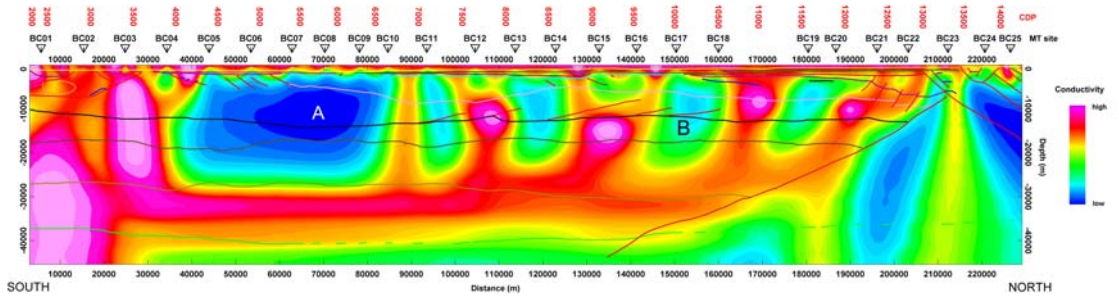

Figure 5. Two dimensional model of TM and TE modes for the magnetotelluric data (see details in Thiel et al., 2010). Line work from the interpretation of the seismic section is overlain on the model.

Tectonic Implications

The southern part of seismic transect 08GA-C1 has a reasonably well-defined Moho at ~13 s TWT (~40 km depth), with a strongly reflective middle to lower crust, termed the Yarramba Seismic Province, above a nonreflective upper mantle. In the northern quarter of the seismic section, however, the lower crust (possibly equivalent to the Warrakimbo Seismic province to the southwest) is only weakly reflective, and the location of the Moho is not obvious (Figure 4). This implies that the crust in this region is significantly different to that farther to the south, and raises the possibility of an ancient crustal boundary between the two regions. This boundary could correlate with the major crustal boundary observed in the in the Curnamona-Gawler Link line (09GA-CG1; Preiss et al., 2010).

In the southern part of the seismic transect, there are a series of south-dipping thrusts cutting the Willyama Supergroup. This is consistent with mapped fold trends to the south, as the northwest-verging F3 folds in outcrops of the Willyama Supergroup are consistent with apparent north-directed D3 thrusting observed in the seismic transect. These late structures overprint the earlier structures, which are difficult to observe in the seismic section.

The Benagerie Volcanics are interpreted to be a relatively subhorizontal sheet, up to 4 km thick, with a gently undulating base. Rocks of the Willyama Supergroup can be tracked from the south to beneath both the volcanics and a lower, nonreflective package of unknown affinity.

The Neoproterozoic sedimentary rocks are associated with crustal extension related to the breakup of the Rodinian supercontinent. The original basin-bounding fault possibly represents reactivation of the ancient crustal boundary between the Curnamona Province and the Moolawatana Domain. Minor contractional deformation of the Neoproterozoic succession has inverted the basin in places, and is inferred to be Delamerian in age. Nevertheless, the active Paralana Fault indicates that shortening across it is occurring today.

Conclusions

The Moho under the Curnamona Province is at ~40 km depth, and is slightly undulating in the south. The northern limit of the Curnamona Province is defined by a possible boundary between two different types of lower crust, with the crust in the north below the Moolawatana Domain (possibly the Warrakimbo Seismic Province) being overthrust by sub-Curnamona crust (the Yarramba Seismic Province) in the south. A sediment pile up to 6 km thick occurs in the northern part of the seismic transect, and contains Neoproterozoic, Cambrian, Mesozoic and

Cenozoic rocks. Structural remnants of a Neoproterozoic basin occur in the southern part of the line. These rocks are important thermal blankets, and are of interest in geothermal exploration. In the north, the Neoproterozoic-Cambrian rocks are covered by Mesozoic to Cenozoic sediments, which are important hosts for uranium mineralisation and geothermal energy systems.

Acknowledgements

We thank Natalie Kositcin and Simon van der Wielen for their comments on the manuscript.

References

Célérier, J., Sandiford, M., Lundbek Hansen, D. and Quigley, M., 2005. Modes of active intraplate deformation, Flinders Ranges, Australia. *Tectonics*, **24**, TC6006, doi:1029/2004TC001679.

Chopping, R., Williams, N.C., Meixner, A.J. and Roy, I.G., 2010. 3D potential-field inversions and alteration mapping in the Gawler Craton and Curnamona Province, South Australia. *Geoscience Australia, Record,* **2010/10**, this volume.

Conor, C.H.H. and Preiss, W.V., 2008. Understanding the 1720-1640 Ma Palaeozoic Willyama Supergroup, Curnamona Province, Southeastern Australia: implications for tectonics, basin evolution and ore genesis. *Precambrian Research*, **166(1-4)**, 297-317.

Cowley, W.M., 2006. Solid geology of South Australia: peeling away the cover. *MESA Journal*, **43**, 4-15.

Fanning, C.M., Ashley, P.M., Cook, N.D.J., Teale, G.S. and Conor, C.C.H., 1998. A geochronological perspective of crustal evolution in the Curnamona Province. In: Gibson, G.M., editor, Broken Hill Exploration Initiative: Abstracts of papers presented at the fourth annual meeting in Broken Hill. *Australian Geological Survey Organisation, Record,* **1998/25**, 30-35.

Fanning, C.M., Teale, G.S., and Robertson, R.S., 2003. Is there a Willyama Supergroup sequence in the Mount Painter Inlier? In: Peljo, M., compiler, Broken Hill Exploration Initiative: abstracts of papers presented at the July 2003 conference in Broken Hill. *Geoscience Australia, Record*, **2003/13**, 38-41.

Fomin, T., Holzschuh, J., Nakamura, A., Maher, J., Duan, J. and Saygin, E., 2010. 2008 Gawler-Curnamona-Arrowie (L189) and 2009 Curnamona-Gawler link (L191) seismic surveys – acquisition and processing. *Geoscience Australia, Record,* **2010/10**, this volume.

Forbes, C.J., Betts, P.G., Giles, D. and Weinberg, R., 2008. Reinterpretation of the tectonic context of high-temperature metamorphism in the Broken Hill Block, NSW, and its implications on the Palaeo- to Meso-Proterozoic evolution. In: Cawood, P.A. and Korsch, R.J., editors, Assembling Australia: Proterozoic building of a continent. *Precambrian Research*, **166(1-4)**, 338-349.

Fraser, G.L. and Neumann, N.L., 2010. Compilation of SHRIMP U-Pb geochronological data, Gawler Craton, Curnamona Craton, and Mt Painter Province, South Australia, 2008-2010. *Geoscience Australia, Record,* in preparation.

Fricke, C.E., 2009. 1590 Ma magmatism in the Curnamona Province: Mineral potential of the Ninnerie Supersuite. In: Korsch, R.J., editor, Broken Hill Exploration Initiative: Abstracts for the 2009 Conference. *Geoscience Australia, Record*, **2009/28**, 42-44.

Fricke, C.E., Preiss, W.V. and Neumann, N.L. 2010. Curnamona Province: a Paleo- to Mesoproterozoic time slice. *Geoscience Australia, Record,* **2010/10**, this volume.

Gibson, G., Drummond, B., Fomin, T., Owen, A., Maidment, D., Gibson, D., Peljo, M. and Wake-Dyster, K., 1998. Re-evaluation of crustal structure of the Broken Hill Inlier through structural mapping and seismic profiling. *Australian Geological Survey Organisation, Record,* **1998/11**, 55 pp.

Goleby, B.R., Korsch, R.J., Fomin, T., Conor, C.H.H., Preiss, W.V., Robertson, R.S. and Burtt, A.C., 2006. The 2003-2004 Curnamona Province seismic survey. *Geoscience Australia, Record,* **2006/12**, 96 pp.

Korsch, R.J., Fomin, T., Conor, C.H.H., Stevens, B.P.J., Goleby, B.R., Robertson, R.S. and Preiss, W.V., 2006a. A deep seismic reflection transect across the Curnamona Province from the Darling Basin to the Flinders Ranges. In: Korsch, R.J. and Barnes, R.G.,

editors, 2006. Broken Hill Exploration Initiative: Abstracts for the September 2006 Conference. *Geoscience Australia, Record,* **2006/21**, 102-109.

Korsch, R.J., Preiss, W.V., Conor, C.H.H., Goleby, B.R., Fomin, T., Robertson, R.S. and Burtt, A.C., 2006b. Tectonic implications based on the deep seismic reflection data from the Curnamona Province, South Australia. In: Goleby, B.R., Korsch, R.J., Fomin, T., Conor, C.H.H., Preiss, W.V., Robertson, R.S. and Burtt, A.C., 2006. The 2003-2004 Curnamona Province seismic survey. *Geoscience Australia, Record*, **2006/12**, 73-80.

Korsch, R.J., Fomin, T., Conor, C.H.H., Stevens, B.P.J., Goleby, B.R., Robertson, R.S. and Preiss, W.V., 2007. Geodynamic implications of a deep seismic reflection transect across the Curnamona Province. In: SGTSG Deformation on the Desert Conference, Alice Springs 9-13 July 2007. *Geological Society of Australia, Specialist Group in Structural Geology and Tectonics, Abstract Volume*, p.46.

Korsch, R.J., Preiss, W.V., Blewett, R.S., Cowley, W.M., Neumann, N.L., Fabris, A.J., Fraser, G.L., Dutch, R., Fomin, T., Holzschuh, J., Fricke, C.E., Reid, A.J., Carr, L.K. and Bendall, B.R., 2010. Deep seismic reflection transect from the western Eyre Peninsula in South Australia to the Darling Basin in New South Wales: Geodynamic implications. *Geoscience Australia, Record,* **2010/10**, this volume.

McLaren, S., Sandiford, M. and Powell, R., 2005. Contrasting styles of Proterozoic crustal evolution: a hot-plate tectonic model for Australian terranes. *Geology*, **33**, 673-676.

Neumann, N., Sandiford, M. and Foden, J., 2000. Regional geochemistry and continental heat flow: implications for the origin of the South Australian Heat Flow anomaly. *Earth and Planetary Science Letters,* **183**, 107-120.

Neumann, N., Hore, S. and Fraser, G., 2009. New SHRIMP geochronology from the Mount Painter Province, South Australia. In: Korsch, R.J., editor, Broken Hill Exploration Initiative: Abstracts for the 2009 Conference. *Geoscience Australia, Record*, **2009/28**, 136-139.

Page, R.W., Stevens, B.P.J. and Gibson, G.M., 2005. Geochronology of the sequence hosting the Broken Hill Pb-Zn-Ag orebody, Australia. *Economic Geology*, **100**, 633-661.

Preiss, W.V., 2009. The Curnamona Province – 1700 million years of tectonic evolution. In: Korsch, R.J., editor, Broken Hill exploration initiative: Abstracts for the 2009 Conference. *Geoscience Australia, Record*, **2009/28**, 144-155.

Preiss, W.V., Korsch, R.J., Blewett, R.S., Fomin, T., Cowley, W.M., Neumann, N.L. and Meixner, A.J., 2010. Geological interpretation of deep seismic reflection line 09GA-CG1: the Curnamona Province-Gawler Craton Link Line, South Australia. *Geoscience Australia, Record,* **2010/10**, this volume.

Stevens, B.P.J., 2006. Advances in understanding Broken Hill geology. In: Korsch, R.J. and Barnes, R.G., compilers, Broken Hill Exploration Initiative: Abstracts from the September 2006 conference. *Geoscience Australia, Record*, **2006/21**, 166-175.

Thiel, S., Milligan, P.R., Heinson, G., Boren, G., Duan, J., Ross, J., Adam, H., Dhu, T., Fomin, T., Craven, E., and Curnow, S., 2010. Magnetotelluric acquisition and processing, with examples from the Gawler, Curnamona and Link transects in South Australia. *Geoscience Australia, Record,* **2010/10**, this volume.

Geological interpretation of seismic reflection lines 08GA-C1 and 09TE-01: Arrowie Basin, South Australia

L.K. Carr[1], R.J. Korsch[1], J. Holzschuh[1], R.D. Costelloe[1], A.J. Meixner[1], C. Matthews[2] and B. Godsmark[3]

[1]*Onshore Energy & Minerals Division, GPO Box 378, Canberra, ACT 2601, Australia*
[2]*Torrens Energy Limited, PO Box 506, Unley, SA 5061, Australia*
[3]*Formerly Torrens Energy Limited, PO Box 506, Unley, SA 5061, Australia*

Lidena.Carr@ga.gov.au

Introduction

Many of the onshore sedimentary basins in Australia are underexplored with respect to hydrocarbons. To date only the Cooper-Eromanga basin system is a major commercial oil and natural gas producer, although this has recently been complemented by commercialisation of coal seam gas resources in the Bowen and Surat basins in Queensland. With domestic oil production in steady decline, and increasing offshore exploration costs, the Onshore Energy Security Program was funded by the Australian Government with ~$59 million over five years (2006-2011). This program, conducted by Geoscience Australia (GA), aims to provide precompetitive geoscience data and assessments of the potential for onshore energy resources including hydrocarbons, uranium, thorium and geothermal energy.

As part of the Onshore Energy Security Program, deep seismic reflection data have been acquired across several frontier sedimentary basins to stimulate petroleum exploration in onshore Australia. In 2008, Geoscience Australia, in conjunction with Primary Industries and Resources South Australia (PIRSA), acquired a 60 km long deep-seismic line (08GA-A1) across the western part of the Arrowie Basin, immediately to the west of the central Flinders Ranges (Figures 1 to 3). This part of the basin is of interest for petroleum exploration, but has received almost no attention for hydrocarbon exploration since the shallow Wilkatana wells were drilled in the 1950s, to a maximum depth of ~670 m. About 15 km to the south of the seismic line, some of these wells encountered non-commercial bituminous hydrocarbons in the Cambrian succession (SANTOS, 1957). The Cambrian source rocks are considered to have previously generated oil, and in some places are still within the oil generation and preservation window (McKirdy, 1994). In 2009, as part of their geothermal exploration program, Torrens Energy Limited acquired a 41 km long seismic line (09TE-01) at Parachilna, about 90 km to the north of the Arrowie Basin 08GA-A1 line (Figures 1-3).

Seismic line 08GA-A1 was acquired in June 2008, with project management undertaken by the Seismic Acquisition and Processing Project from Geoscience Australia. A summary of acquisition parameters is given in Fomin et al. (2010). For this seismic line, 75-fold seismic reflection data were acquired to 20 s two-way time, using three Hemi-60 (60,000 lb) peak force vibrators. A Sercel 388SN recording system was used to record and correlate the seismic data. Three sweeps, 6-64 Hz, 12-96 Hz, 8-72 Hz, each 12 s long, with an 80 m vibration point interval, were selected as source acquisition parameters for this survey. Data were processed in the DISCO/FOCUS seismic processing package. The final processing flow for seismic line 08GA-A1 is summarised in Fomin et al. (2010). Seismic line 09TE-01 was acquired for Torrens Energy Limited and originally the data were processed commercially. Subsequently, R.D.

Costelloe from Geoscience Australia reprocessed the data, focussing in particular on the deep data below the Arrowie Basin and Adelaide Rift System.

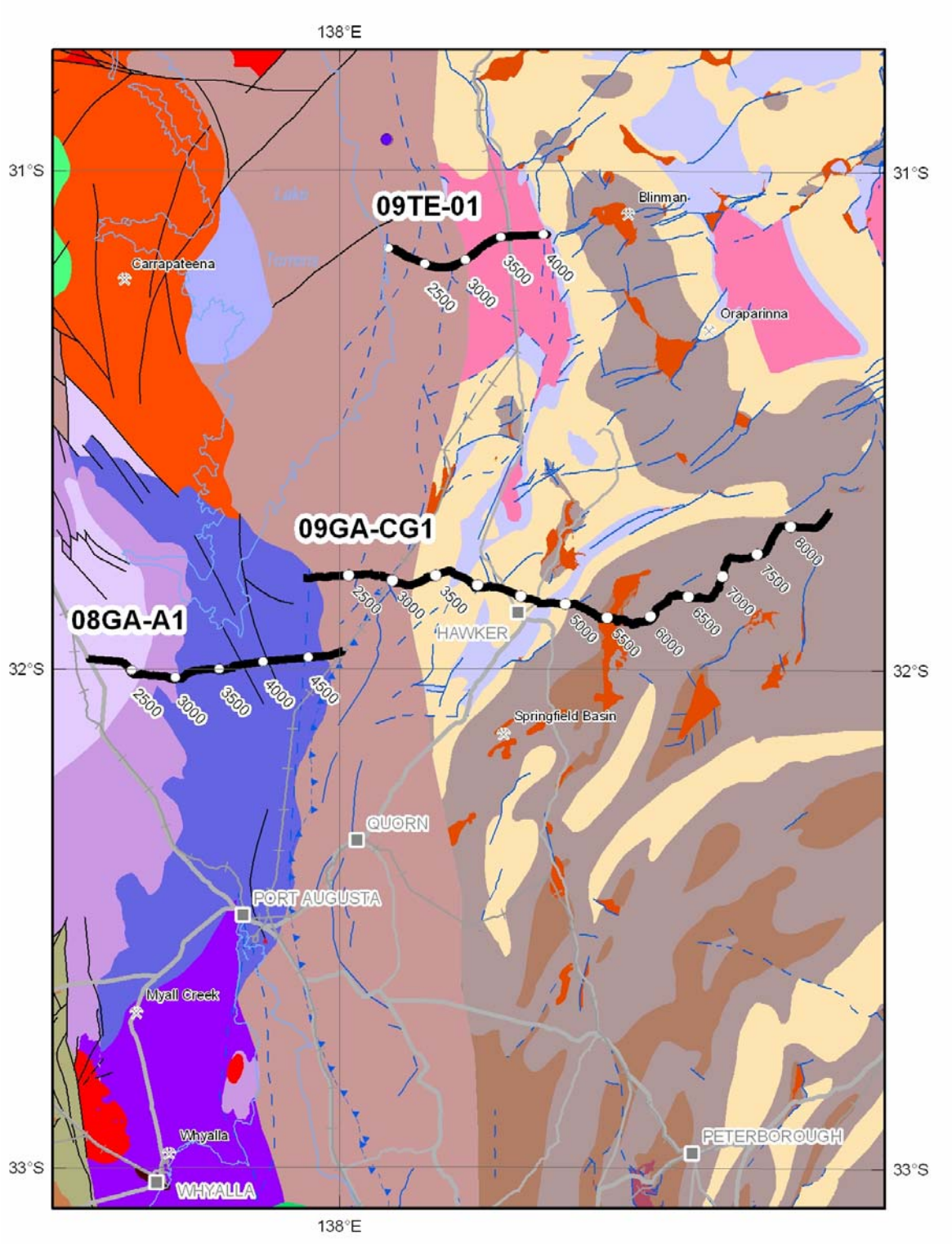

Figure 1. Solid geology map (after Cowley, 2006, which also contains the legend) showing the locations of seismic lines 08GA-A1 and 09TE-01 in the western Arrowie Basin, South Australia. Numbers on the lines represent CDP locations.

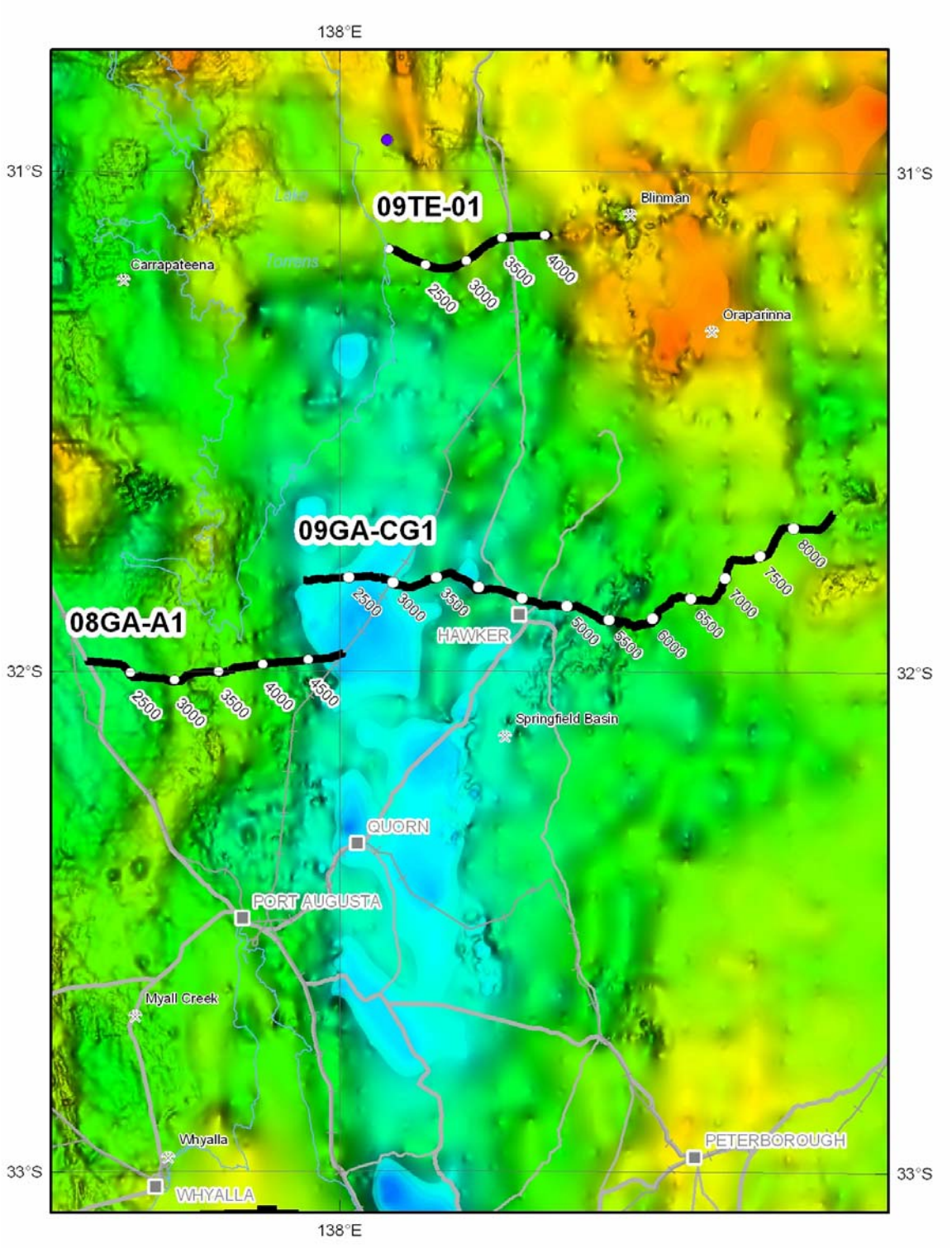

Figure 2. Gravity image showing the locations of seismic lines 08GA-A1 and 09TE-01 in the western Arrowie Basin, South Australia (warm colours are gravity highs, cool colours are gravity lows).

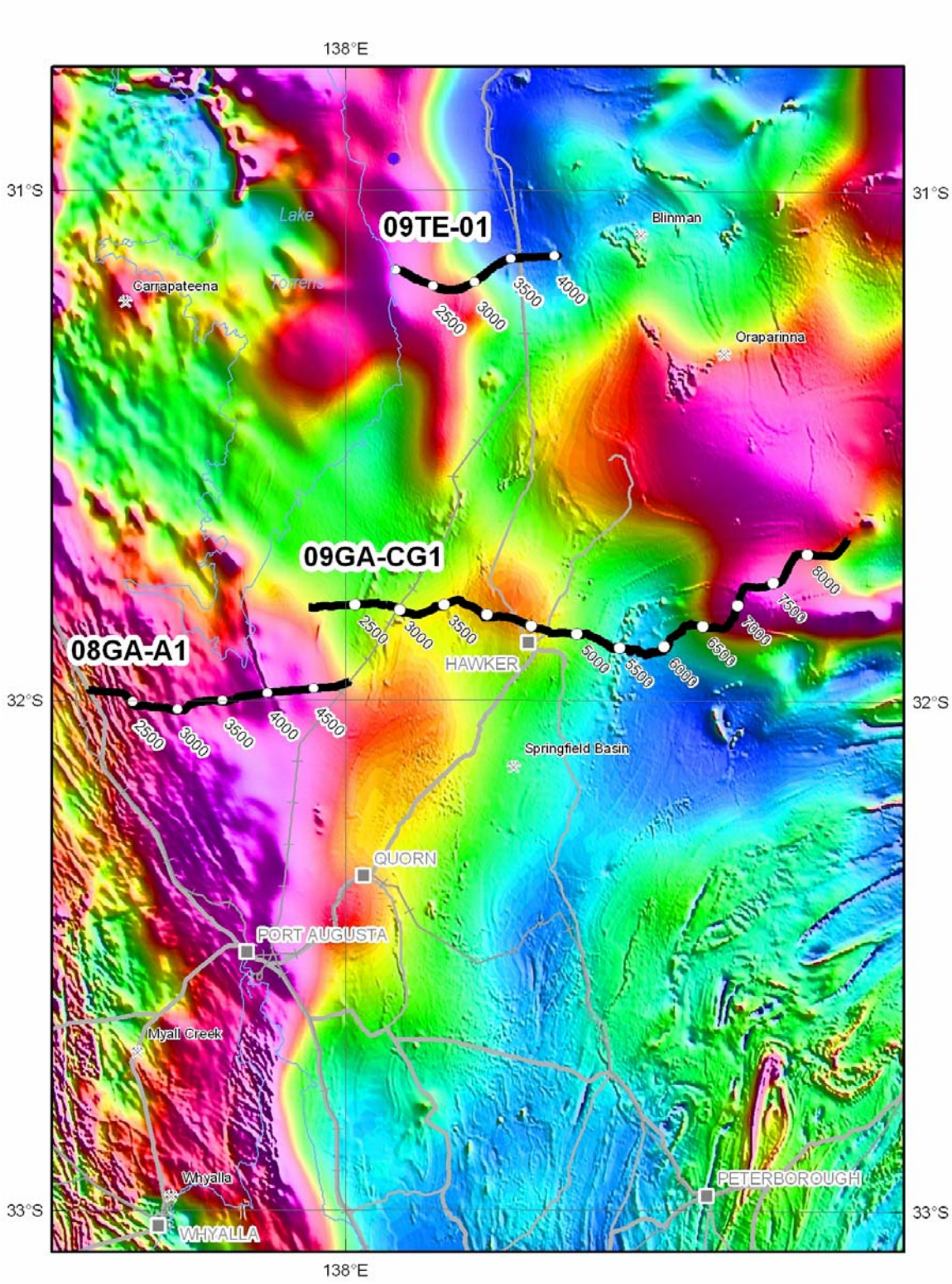

Figure 3. Total magnetic intensity image showing the locations of seismic lines 08GA-A1 and 09TE-01 in the western Arrowie Basin, South Australia (warm colours are high magnetic intensities, cool colours are low magnetic intensities).

Arrowie Basin, South Australia

The Arrowie Basin in South Australia represents the last phase of sedimentation in the Neoproterozoic to Cambrian Adelaide Rift System which, in the vicinity of the seismic lines described here, consists of five major structural components: (from west to east) the Stuart Shelf, the Torrens Hinge Zone, the central Flinders Ranges, and the Moorowie and Yalkalpo Sub-basins to the east of the Flinders Ranges and extending into westernmost New South Wales (PIRSA, undated). Initially, extension in the Rodinian supercontinent resulted in the Neoproterozoic succession being derived through erosion of the supercontinent and deposited, in a predominantly shallow marine environment, in the active Adelaide Rift System. A series of transgressive and regressive cycles, due to continued rifting, followed initial sedimentation. Later, deepening accommodation space during the post-rift sag phase, resulted in the accumulation of carbonate and clastic sediments. Sedimentation continued into the Cambrian, with the term Arrowie Basin being given to this part of an essentially continuous succession. Deposition ceased at the onset of contractional deformation at the start of the Delamerian Orogeny in the Late Cambrian.

In the vicinity of the seismic lines, the western part of the Arrowie Basin forms part of the essentially undeformed Stuart Shelf (in the west) and the Torrens Hinge Zone (a zone of faulting and folding in the east). The Torrens Hinge Zone occurs immediately to the west of the highly folded component of the Adelaide Rift System in the Flinders Ranges. In both seismic sections, a near-complete Neoproterozoic succession has been interpreted, but there appears to be a variable thickness of the Cambrian succession, due to localised deformation, uplift and erosion. Depositional successions on the Stuart Shelf overlie the northeastern-most part of the Gawler Craton. The Neoproterozoic sediments deposited on the shelf are thin, flat-lying and largely undeformed. The Torrens Hinge Zone, described by Preiss (1987) as the locus of rifting, is characterised by an area of sediment thickening and some deformation, and is the transition zone from the thinner, undeformed Neoproterozoic and Cambrian successions on the Stuart Shelf, to the markedly thicker successions in the uplifted Flinders Ranges.

Seismic line 08GA-A1

Seismic line 08GA-A1 (Figures 1-3) crossed the Cambrian Arrowie Basin, which is underlain by a Neoproterozoic succession of the Adelaide Rift System. The seismic line shows that the basin (Figures 4 and 5) is asymmetrical, varying in thickness from about 700 m in the west, up to about 3800 m in the east. There is very limited stratigraphic control in this region, with the Wilkatana wells, about 15 km to the south of the seismic section, where most end in the Cambrian succession. Recent industry drilling (TDKH1A, 1002 m total depth) to the south of the seismic line, intersected part of the Neoproterozoic succession. Several sequence boundaries, mapped using sequence stratigraphic principles, are tentatively correlated with the sequence boundaries between the major Neoproterozoic stratigraphic groups in the Adelaide Rift System, which have been mapped in outcrop in the Flinders Ranges to the east.

The east-dipping Yadlamalka Fault (ca. CDP 4000, Figure 5) is a post-depositional thrust fault defining the eastern limit of the Stuart Shelf, to the east of which is the Torrens Hinge Zone. To the south of the seismic line, recent mineral exploration drilling intersected the Beda Volcanics (part of the basal Neoproterozoic Callanna Group) in the hanging wall of the thrust, indicating that there has been at least 1200 m of pre-Cenozoic throw on the fault. A narrow linear magnetic high on the aeromagnetic image (Figure 3) is interpreted to represent the upthrust Beda Volcanics on the eastern side of the Yadlamalka Fault.

The Callanna Group forms a highly reflective lowermost package in the basin; much of the reflectivity is due to the presence of the mafic Beda Volcanics. The Group has been interpreted across the entire section, and has a relatively constant thickness, varying from 200 ms two-way travel time (TWT, ~500 m) in the west to 300 ms TWT (~750 m) in the east. Above the Callanna Group, the Burra Group varies in thickness across the section, and its upper part has been removed by erosion to the west of CDP 2300 (Figure 5), below the Cenozoic unconformity. It is a reflective package in the west, but is less reflective to the east of the Yadlamalka Fault. It also has an erosional upper surface beneath the unconformably overlying Umberatana Group. The Umberatana Group thickens towards the east, where its upper surface is terminated below the

Cenozoic unconformity at CDP 2600. To the west of the Yadlamalka Fault, the uppermost unit in the Neoproterozoic, the Wilpena Group, has had its upper part removed by erosion below the Cenozoic unconformity (Figure 5).

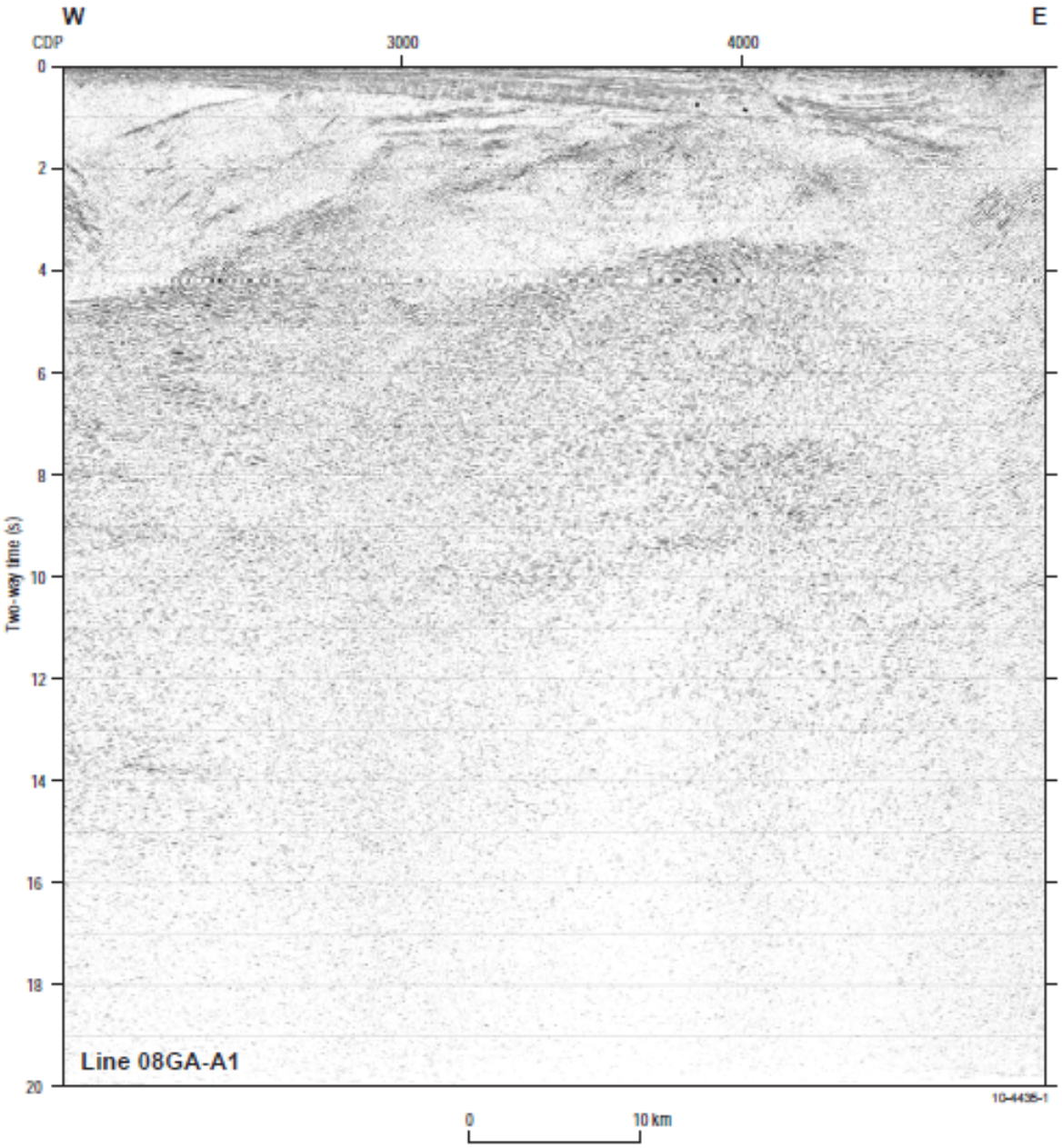

Figure 4. Uninterpreted migrated seismic section of the line 08GA-A1 across the western Arrowie Basin.

In this seismic section, only a thin remnant of the Cambrian succession is preserved, occurring to the east of the Yadlamalka Fault. It is into this succession that the Wilkatana wells were drilled to the south of the seismic line. The presence of bituminous hydrocarbons at depths of less than 670 m in these wells indicates that a considerable thickness of sediment has been eroded from this area.

In the easternmost part of the seismic section, a series of east-dipping thrust faults disrupt the stratigraphic section. These faults might be related, in part, to the currently active, east-dipping, Wilkatana Fault, which occurs immediately east of the seismic line and is associated with the recent uplift of the Flinders Ranges (Quigley et al., 2006). Further to the east, the Neoproterozoic succession thickens dramatically (e.g., Preiss et al., 2010).

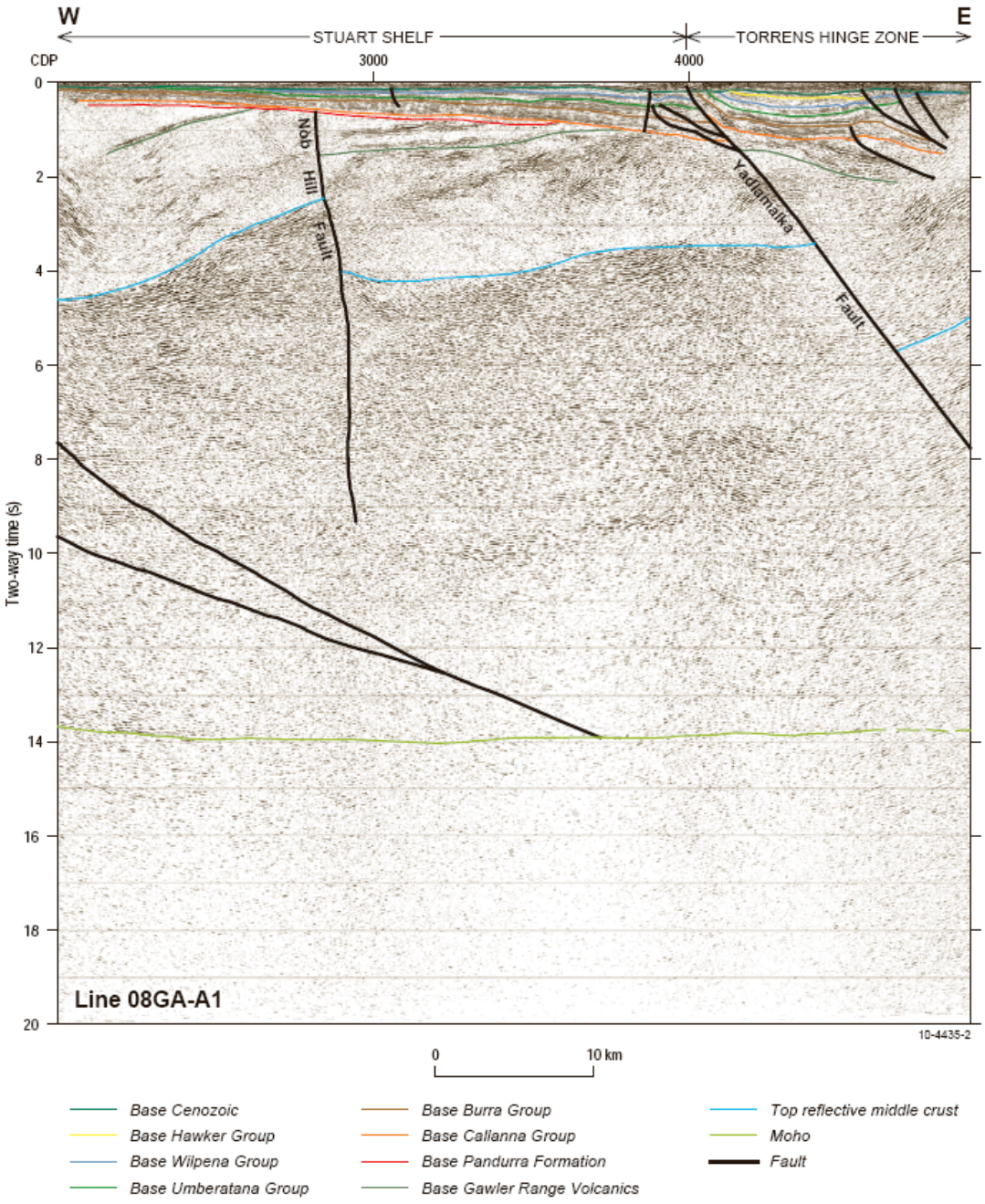

Figure 5. Interpreted migrated seismic section of the line 08GA-A1 across the western Arrowie Basin.

Below the Neoproterozoic succession, strong, subhorizontal to gently-dipping reflections are interpreted to represent the Mesoproterozoic (ca. 1585 Ma) Gawler Range Volcanics (Figure 5). These volcanics have been disrupted by faulting, and then in part eroded, prior to initiation of sedimentation in the Adelaide Rift System at about 830 Ma.

Below the Gawler Range Volcanics, there is a zone of low reflectivity about 3 s TWT (~9 km) thick. We interpret this to be equivalent to the folded and metamorphosed Wallaroo Group and equivalent units described in the 08GA-G1 seismic line by Fraser et al. (2010). The base of this package is defined by the top of a package of strong reflections forming the middle crust. A significant fault, here termed the Nob Hill Fault, occurs at about CDP 2800, and shows an extensional displacement of both the Gawler Range Volcanics and the top of the middle crust reflective package below the equivalents of the Wallaroo Group (Figure 5). The intensity of the

reflectivity decreases downwards in the crust, so that the lowermost part of the crust is only weakly reflective. Here, the middle to lower crust, which has not been traced to the surface in the seismic lines, is referred to as the Warrakimbo Seismic Province (Korsch et al., 2010). The Moho is poorly defined, and we infer it to occur at about 14 s TWT (~42 km) depth.

Forward modelling of the potential field data from along seismic line 08GA-A1 showed a good match with the geological interpretation of the seismic line (Figure 6). There is a gravity high in the middle of the seismic section, from CDP 2800 to 3800 (Figures 2 and 6). By assuming that the wedge of reflective material immediately below the Gawler Range Volcanics (Figures 5 and 6) consisted of mafic volcanics (density 2.84 gcm^{-3}), it was possible to match the modelled gravity curve with the observed one (Figure 6).

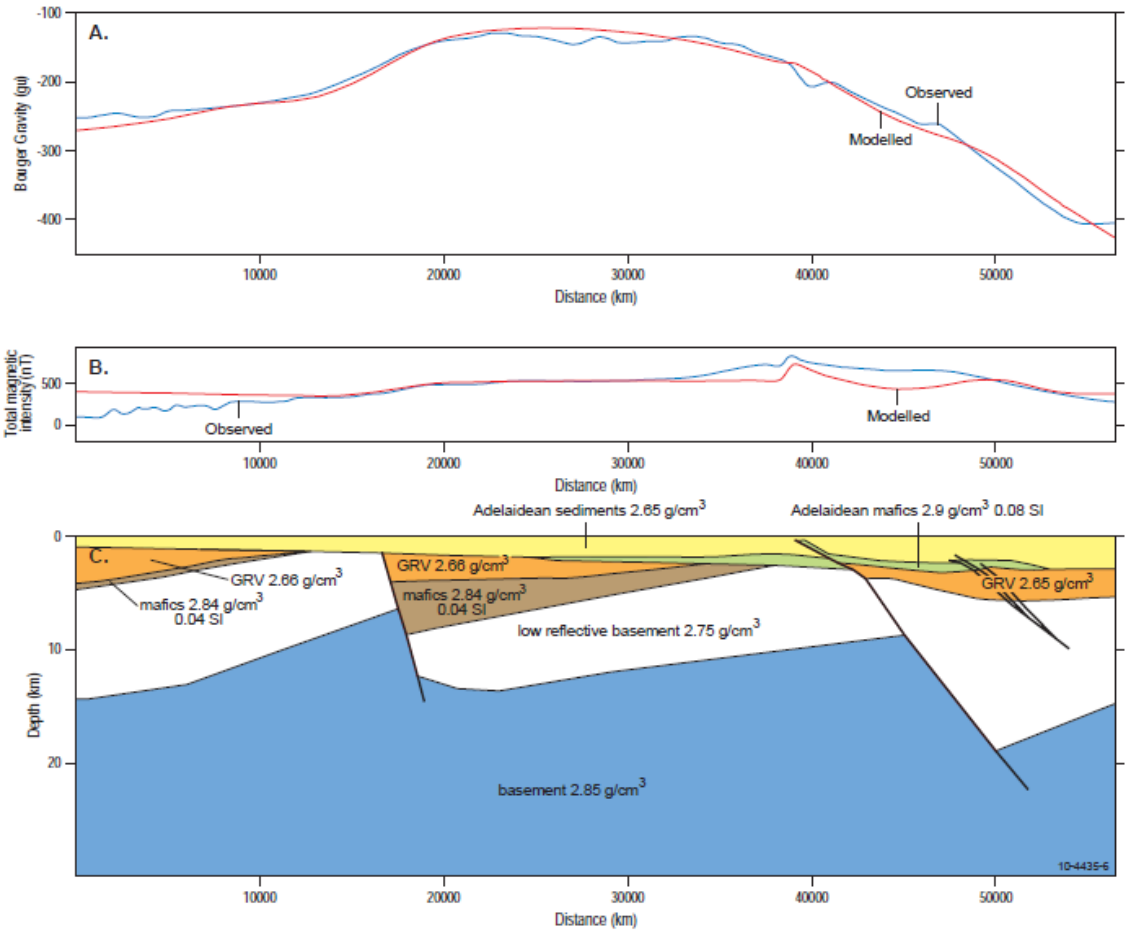

Figure 6. Forward model of the gravity and magnetic profile along the seismic line 08GA-A1. The upper panel shows the observed gravity signal in blue, and the modelled signal in red. The middle panel shows the observed magnetic signal in blue, and the modelled signal in red. The lower panel shows the density and magnetic values in the model, with the geometry being based on the interpretation of the seismic line (Figure 5).

Seismic line 09TE-01

In contrast to seismic line 08GA-A1, described above, the Parachilna seismic line (09TE-01) imaged a much thicker (up to 1500 m) Cambrian succession above the Neoproterozoic units (Figures 7 and 8). In this section, the Neoproterozoic-Cambrian succession is over 3500 m thick at the western end of the line and about 5800 m thick at the eastern end of the line. In this area, Cenozoic sediments are relatively thick, up to 430 m in places, and there is a significant angular unconformity at their base (Figure 7). The Callanna Group is interpreted to occur in the western part of this section, but it possibly terminates at about CDP 2500, and its strongly reflective character is not recognised to the east of this point.

The Treebeard 1A well (CDP ~2620) intersected 420 m of Cenozoic sediment, and then 1387 m of Cambrian Arrowie Basin before bottoming in the Wilkawillina Limestone of the Cambrian Hawker Group at a depth of 1807 m.

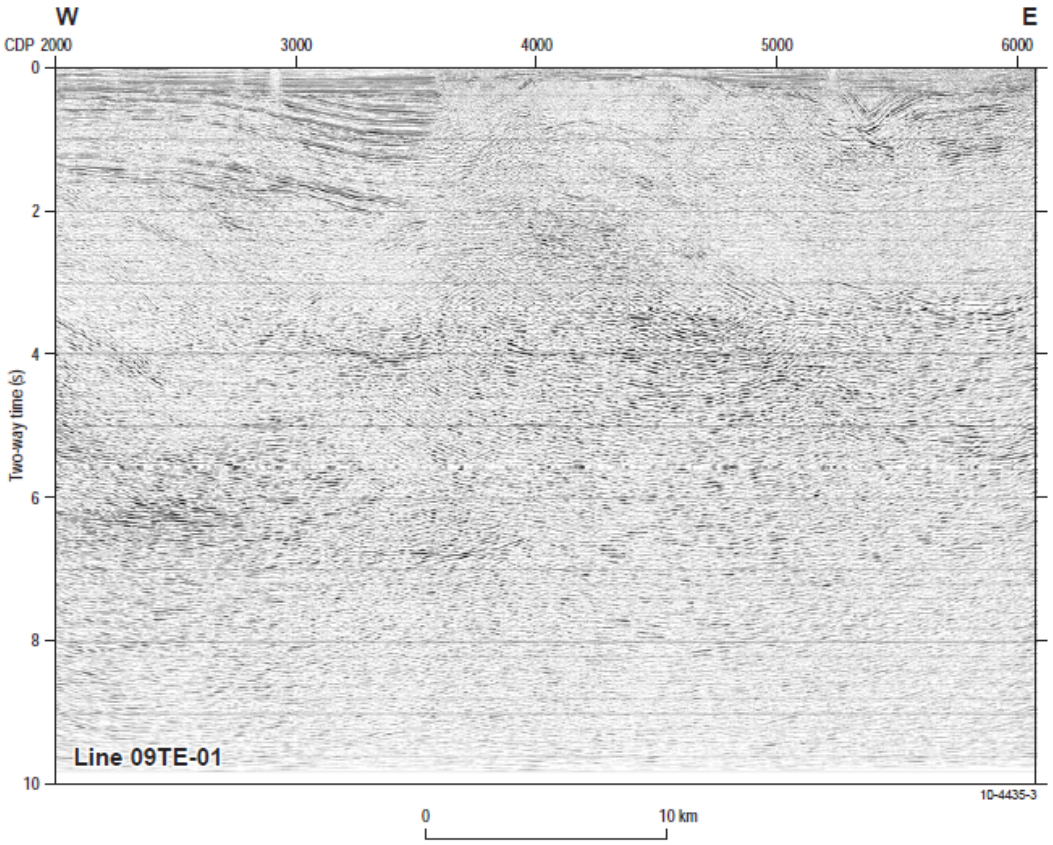

Figure 7. Uninterpreted migrated seismic section of the Torrens Energy Limited line 09TE-01 across the Arrowie Basin, near Parachilna.

In the western part of the seismic line, the relatively coherent sedimentary package is terminated by the east-dipping Ediacara Fault (Figure 8). To the east of the fault, the seismic reflectivity is low, although weak reflections define a relatively low-amplitude, long-wavelength anticline. It is possible that the low seismic reflectivity could be caused by a Neoproterozoic diapir, similar to those which are common in the Flinders Ranges to the east. This is supported by the presence of a thin (17 m thick), bedding parallel, diapiric unit, which has been observed in the Treebeard 1A well, to the west of the Ediacara Fault.

The seismic section indicates that the Ediacara Fault is a major structure, and that it has been reactivated in the Quaternary. Cenozoic sediments are uplifted in the hangingwall to the east of the fault; movement on the fault is also responsible for the recent uplift of the Ediacara Range to the north of the seismic section. Thus the Ediacara Fault can be considered to be the western

range-front fault in this area. Other faults in the section, to the east of the Ediacara Fault, also show minor displacement of the Cenozoic sediments. There is good seismic reflectivity near the eastern end of the line, where a steep-sided syncline is interpreted to preserve Cambrian Lake Frome Group in its core. This syncline in interpreted to be possibly a footwall syncline to a west-dipping thrust fault; it has a classic concentric geometry, with the fold amplitude decreasing with increasing depth. An alternative possibility is that this syncline could be part of a series of concentric folds above a decollement located near the base of the sedimentary succession, which were then cut by younger thrust faults.

Data for seismic line 09TE-01 were recorded to 10 s TWT (~30 km depth) and hence do not provide an image of the entire crust. Nevertheless, the geometry of the crust below the Neoproterozoic succession is very similar to that seen in line 08GA-A1, about 90 km to the south. Immediately below the basin is a zone of relatively weak reflections, which we correlate with the inferred Wallaroo Group in the southern section. We see no evidence for the Gawler Range Volcanics in this section. The base of this zone of reflectivity is again defined by the top of a package of strong reflections forming the middle crust, which we infer to be the Warrakimbo Seismic Province. Both this reflective package and the inferred Wallaroo Group are cut by east-dipping thrusts, one of which appears to be unconformably overlain by the Neoproterozoic succession.

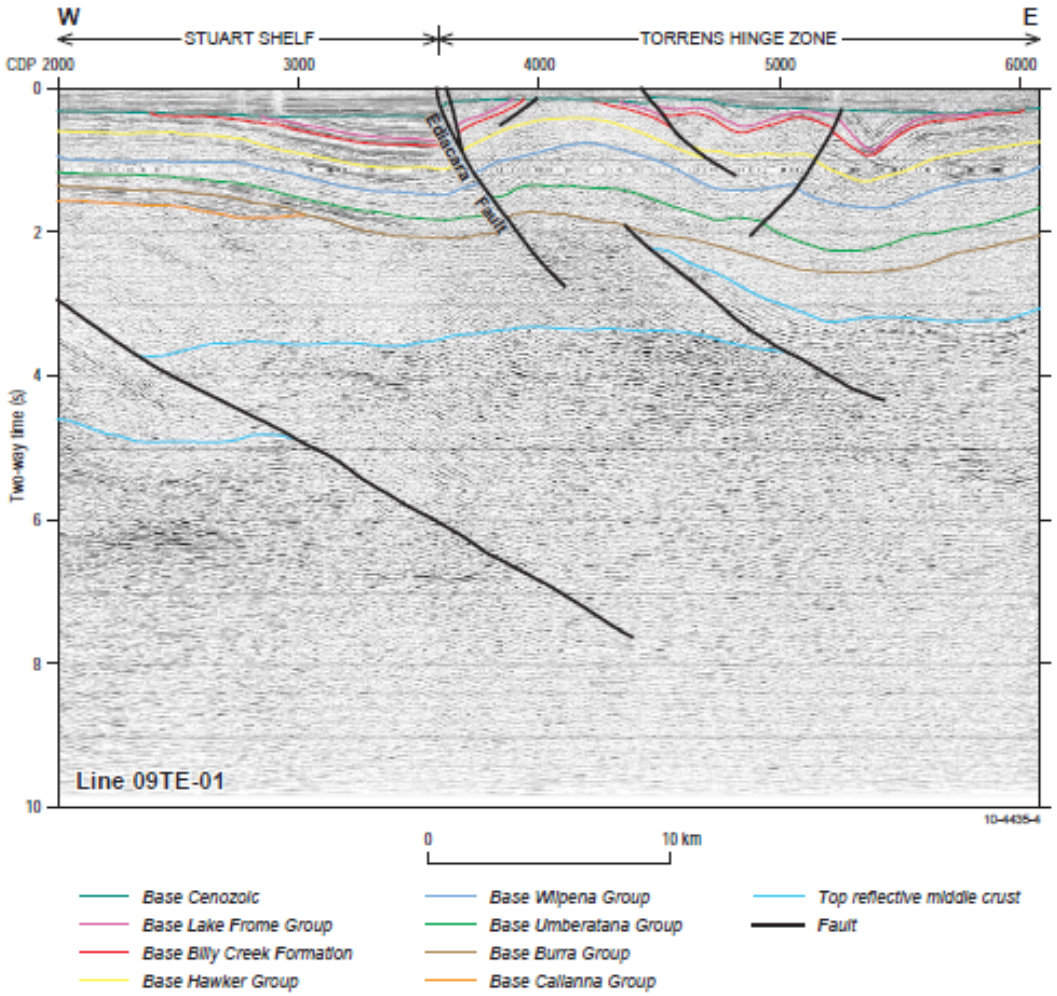

Figure 8. Interpreted migrated seismic section of the Torrens Energy Limited line 09TE-01 across the Arrowie Basin, near Parachilna.

High heat flow values have been recorded from sediments in wells drilled on the seismic line (115 mWm^{-2} in Melkor 1 at CDP ~2130, and 91 mWm^{-2} in Treebeard 1A at CDP ~2620; www.torrensenergy.com) making this area attractive for exploration for geothermal energy. Also, the nonreflective basement beneath the Arrowie Basin and Adelaide Rift System, interpreted to be the equivalent of the Wallaroo Group, would be expected to have a relatively low heat flow; hence the high heat flow values could be derived from high heat-producing granites of the Hiltaba Suite, which could be present in the nonreflective package, but not imaged seismically.

Conclusions

The two seismic sections across the western Arrowie Basin show a transition from the Stuart Shelf in the west to the Torrens Hinge Zone in the east. There is a relatively undeformed stratigraphic succession of Neoproterozoic to Cambrian age on the Stuart Shelf, whereas the Torrens Hinge Zone contains thrust faults and fault-related folds. The thrust faults cut the Cambrian succession, suggesting possible movement during the Delamerian Orogeny, with fault reactivation in the Quaternary, due to displacement of the overlying Cenozoic succession. Beneath the Neoproterozoic succession, the Gawler Range Volcanics, Wallaroo Group equivalents and a reflective middle crust, termed the Warrakimbo Seismic Province, have been imaged.

Acknowledgements

Acquisition of seismic line 08GA-A1 was undertaken in collaboration Primary Industries and Resources South Australia (PIRSA), and we thank them for their contributions. We thank Torrens Energy Limited for providing access to seismic line 09TE-01, and allowing us to publish our interpretation. We also thank Natalie Kositcin and Matilda Thomas for their reviews of the manuscript.

References

Cowley, W.M., 2006. Solid geology of South Australia: peeling away the cover. *MESA Journal*, **43**, 4-15.

Fomin, T., Holzschuh, J., Nakamura, A., Maher, J., Duan, J. and Saygin, E., 2010. 2008 Gawler-Curnamona-Arrowie (L189) and 2009 Curnamona-Gawler link (L191) seismic surveys – acquisition and processing. *Geoscience Australia, Record,* **2010/10**, this volume.

Fraser, G.L., Blewett, R.S., Reid, A.J., Korsch, R.J., Dutch R., Neumann, N.L., Meixner, T., Skirrow, R.G., Cowley, W., Szpunar, M., Preiss, W.V., Nakamura, A., Fomin, T., Holzschuh, J., Milligan P. and Bendall, B., 2010. Geological interpretation of deep seismic reflection and magnetotelluric line 08GA-G1: Eyre Peninsula, Gawler Craton, South Australia. *Geoscience Australia, Record,* **2010/10**, this volume.

Korsch, R.J., Preiss, W.V., Blewett, R.S., Fabris, A.J., Neumann, N.L., Fricke, C.E., Fraser, G.L., Holzschuh, J., Milligan, P.R. and Jones, L.E.A., 2010. Geological interpretation of deep seismic reflection and magnetotelluric line 08GA-C1: Curnamona Province, South Australia. *Geoscience Australia, Record,* **2010/10**, this volume.

McKirdy, D.M., 1994. Biomarker geochemistry of the early Cambrian oil show in Wilkatana-1: implications for oil generation in the Arrowie and Stansbury Basins. *PESA Journal*, **22**, 3–17.

PIRSA, undated. Petroleum and Geothermal in South Australia; the Arrowie Basin (and the Central Adelaide Geosyncline). Primary Industry and Resources South Australia (PIRSA),website: http://www.petroleum.pir.sa.gov.au/data/assets/pdf_file/0006/26916/prospectivity_arrowie.pdf (accessed 19 March 2010).

Preiss, W.V., complier, 1987. The Adelaide Geosyncline; late Proterozoic stratigraphy, sedimentation, palaeontology and tectonics. *Geological Survey of South Australia, Bulletin,* **53**, 438 pp.

Preiss, W.V., Korsch, R.J., Blewett, R.S., Fomin, T., Cowley, W.M., Neumann, N.L. and Meixner, A.J., 2010. Geological interpretation of deep seismic reflection line 09GA-CG1: the Curnamona Province-Gawler Craton Link Line, South Australia. *Geoscience Australia, Record,* **2010/10**, this volume.

Quigley, M.C., Cupper, M.L. and Sandiford, M., 2006. Quaternary faults of south-central Australia; palaeoseismicity, slip rates and origin. *Australian Journal of Earth Sciences*, **53(2),** 285-301.

SANTOS, 1957. Arrowie Basin: Wilkatana Well Completion Report numbers 1-19b. *Primary Industry and Resources South Australia, Open File Envelope* **No. 8577**.

Geological interpretation of deep seismic reflection line 09GA-CG1: the Curnamona Province-Gawler Craton Link Line, South Australia

W.V. Preiss[1], R.J. Korsch[2], R.S. Blewett[2], T. Fomin[1], W.M. Cowley[1], N.L. Neumann[1] and A.J. Meixner[2]

[1] *Geological Survey Branch, Primary Industries and Resources South Australia (PIRSA), GPO Box 1671, Adelaide, SA 5001, Australia*

[2] *Onshore Energy & Mineral Division, Geoscience Australia, GPO Box 378, Canberra, ACT 2601, Australia*

Wolfgang.Preiss@sa.gov.au

Introduction

In early 2009, Primary Industries and Resources South Australia (PIRSA) and Geoscience Australia (GA) acquired deep seismic reflection data along an east-west transect 144.44 km long across the Flinders Ranges, South Australia. This transect, referred to as the Curnamona Province-Gawler Craton Link Line Seismic Survey (09GA-CG1), commences about 10 km to the east of Lake Torrens, and runs eastwards, north of Hawker, to the easternmost Flinders Ranges (Figure 1). In the east, this line ties to the 2003-04 deep seismic reflection profile, the east-west Curnamona line (03GA-CU1; Goleby et al., 2006), which continued eastwards to the South Australian-New South Wales border. Seismic line 09GA-CG1 has provided new insights into the stratigraphy and tectonic architecture of a part of the Neoproterozoic–Cambrian Adelaide Geosyncline, in addition to its primary aim of elucidating the relationship, at depth, between the Curnamona Province and the Gawler Craton. This seismic line also has implications for the interpretation of the western end on seismic line 03GA-CU1.

The survey differs from most other seismic lines in South Australia, in traversing a region of substantial outcrop, which has been mapped at 1:100 000 scale or better. This provides a degree of geological control at the surface not available for other sections, and means that stratigraphic units recognised in outcrop can either be extrapolated to depth in the subsurface using the seismic data, or used as the surface control for interpreting underlying stratigraphic units.

Figures 1 to 3 show the location of the seismic transect in relation to the interpreted solid geology (Cowley, 2006) and regional geophysical data, and to the Arrowie Basin (08GA-A1) and Torrens Energy Parachilna (09TE-01) reflection seismic surveys (Carr et al., 2010). These seismic lines also image Adelaidean rocks, though mainly across the eastern Stuart Shelf and the Torrens Hinge Zone. All three seismic lines cross at least part of the Torrens Hinge Zone (Preiss, 2010).

Because transect 09GA-CG1 followed existing tracks through very hilly terrain, the line changes direction frequently. Much of the section is subparallel to the regional strike, and only relatively short sections are oriented at a high angle to the strike of bedding, fold axial traces and fault traces, as would be ideal. Figure 4 is an image of the deep seismic data, and Figure 5 shows our preliminary interpretation. Gravity and magnetic profiles along the seismic transect have

been forward modelled using boundaries interpreted from the seismic and plausible average petrophysical properties for major rock bodies (Figure 6).

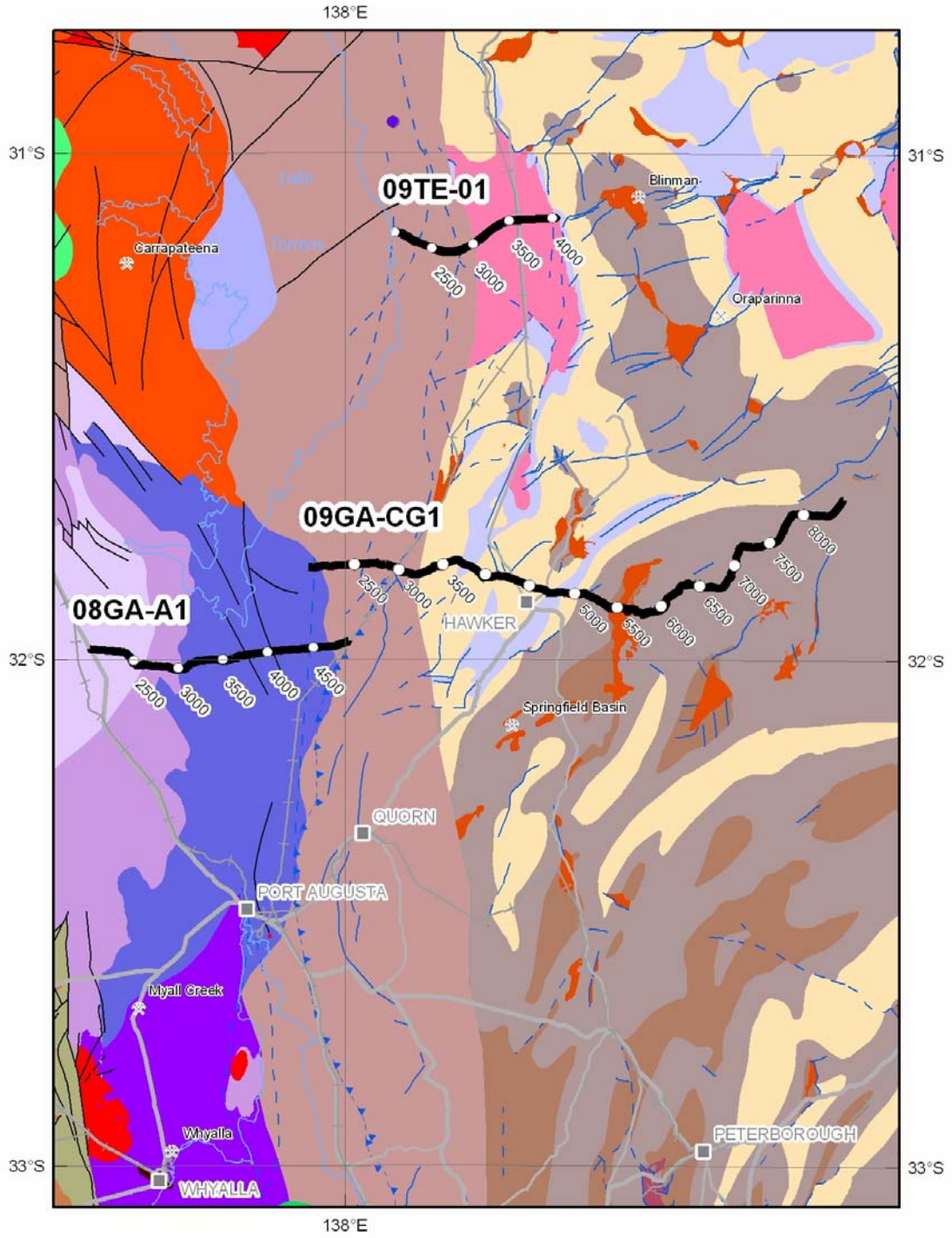

Figure 1. Solid geology map (after Cowley, 2006, which also contains the legend) showing the locations of seismic line 09GA-CG1 in the central Flinders Ranges. Also shown are the locations of seismic lines 08GA-A1 and 09TE-01 in the western Arrowie Basin, South Australia. Numbers on the lines represent CDP locations.

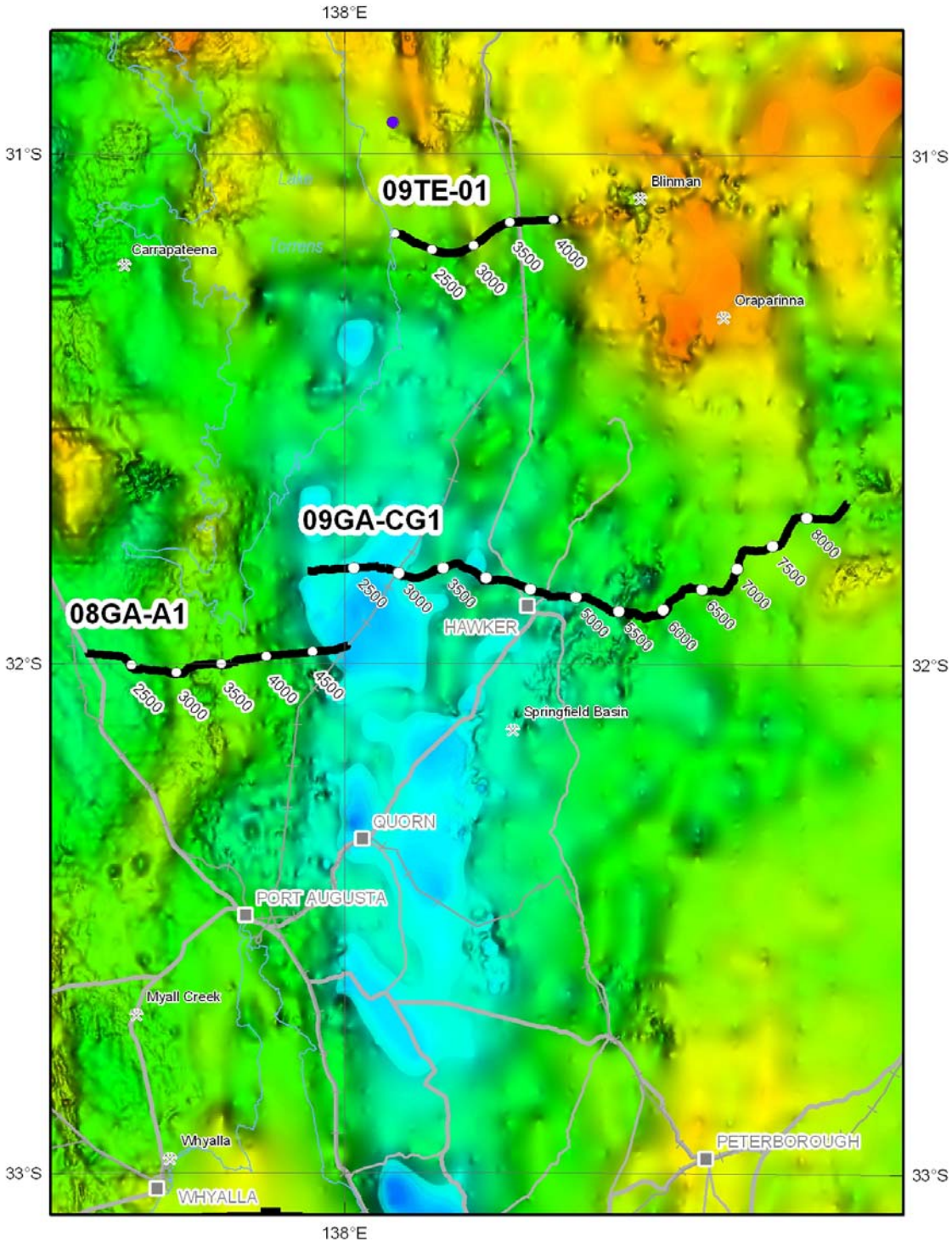

Figure 2. Gravity image showing the locations of seismic line 09GA-CG1 in the central Flinders Ranges (warm colours are gravity highs, cool colours are gravity lows). Also shown are the locations of seismic lines 08GA-A1 and 09TE-01 in the western Arrowie Basin, South Australia. Numbers on the lines represent CDP locations.

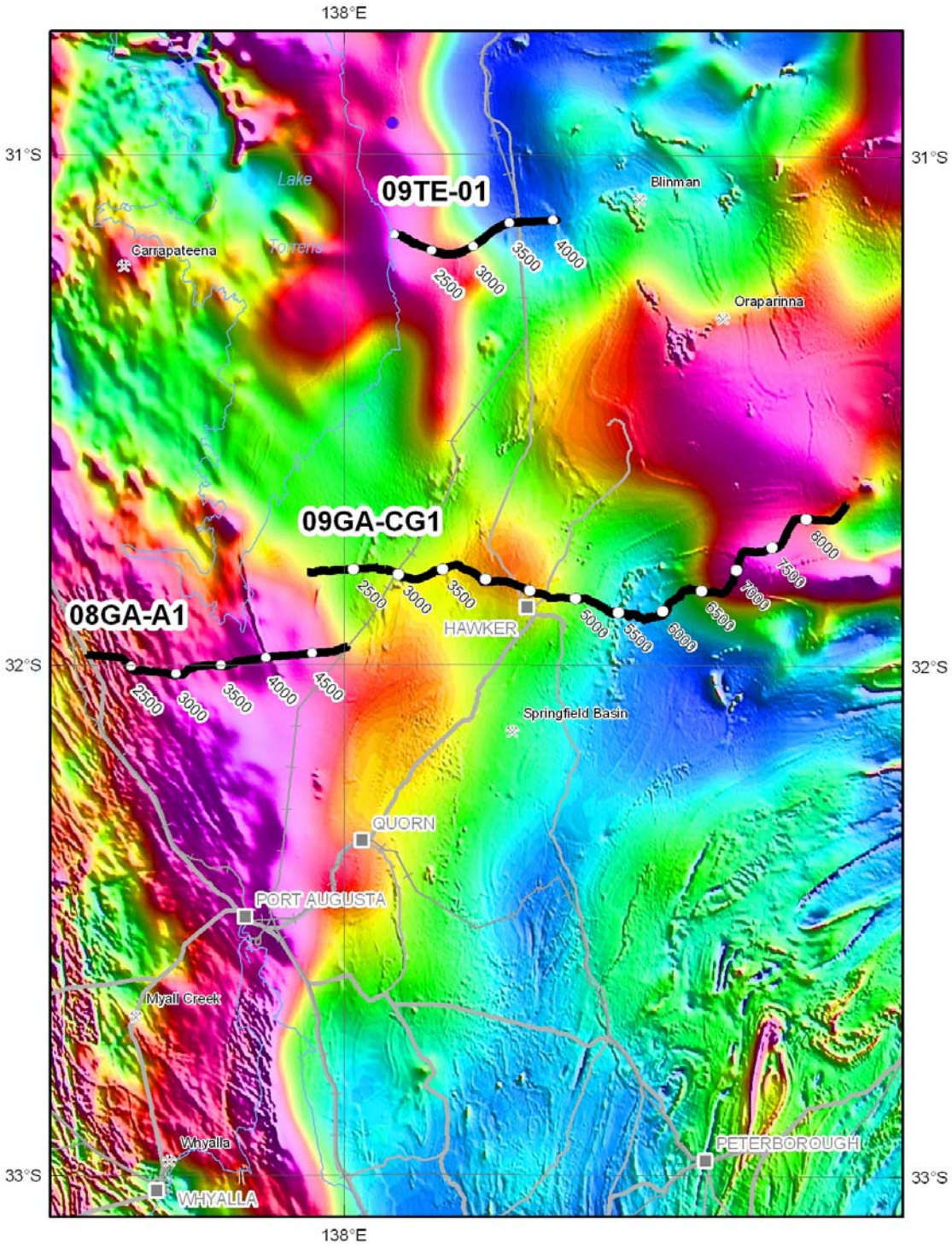

Figure 3. Enhanced regional total magnetic intensity image for part of the Flinders Ranges, showing the locations of seismic line 09GA-CG1 (warm colours are high magnetic intensities, cool colours are low magnetic intensities). Also shown are the locations of seismic lines 08GA-A1 and 09TE-01 in the western Arrowie Basin, South Australia. Numbers on the lines represent CDP locations.

Seismic Acquisition and Processing

Seismic line 09GA-CG1 was acquired in January 2009, with project management undertaken by the Seismic Acquisition and Processing Project from Geoscience Australia. A summary of acquisition parameters is given in Fomin et al. (2010).

For seismic line 09GA-CG1, 75-fold seismic reflection data were acquired to 20 s two-way time, using three Hemi-60 (60,000 lb) peak force vibrators. A Sercel 388SN recording system was used to record and correlate the seismic data. Three sweeps, 6-64 Hz, 12-96 Hz, 8-72 Hz, each 12 s long, with an 80 m vibration point interval, were selected as source acquisition parameters for this survey. Data were processed in the DISCO/FOCUS seismic processing package. The final processing flow for seismic line 08GA-C1 is summarised in Fomin et al. (2010).

Preliminary geological interpretation of seismic line 09GA-CG1

The geology in the vicinity of the seismic line is described by Preiss (2010). The entire seismic section consists of a folded succession of Neoproterozoic to Cambrian sedimentary, and lesser amounts of volcanic, rocks, below a thin, intermittent cover of Cenozoic sediment and alluvium. Below the Neoproterozoic to Cambrian succession, it is inferred that the Gawler Craton occurs at the western end of the section (for a description of the geology, see Reid et al., 2010), and that the Curnamona Province occurs at the eastern end (for a description of the geology, see Fricke et al., 2010).

Middle to lower crust

Seismic section 09GA-CG1 generally shows strong reflections in the upper to middle crust, especially at the eastern end of the line, but has a weakly to essentially nonreflective lower crust across much of the section (Figure 4). The Moho is poorly imaged; at the eastern end of the line, it is interpreted to occur immediately below a series of subhorizontal reflections, at about 13 s TWT (~39 km depth). In the centre of the section it is inferred to occur immediately below a short segment of moderate reflections at about 14 s TWT (~42 km depth). Elsewhere it has not been imaged.

A zone of crustal-penetrating, east-dipping, thrust faults (here termed the Aliena Fault Zone) are prominent in the seismic section (Figure 5). These faults project towards the surface between about CDP 5100 and CDP 6000, and appear to separate middle to lower crustal regions of very different seismic character. To the west of the westernmost crustal-penetrating fault (CDP 5100), the lower half of the crust is nonreflective, and has been termed the Warrakimbo Seismic Province by Korsch et al. (2010). This seismic province is also observed on the eastern part of the Eyre Peninsula seismic line (08GA-G1; Fraser et al., 2010) and on the Arrowie Basin seismic line (08GA-A1; Carr et al., 2010). East of the fault at CDP 5100, the lower crust is much more reflective, and has been termed the Yarramba Seismic Province by Korsch et al. (2010).

In seismic section 08GA-A1, there is a zone of low reflectivity about 3 s TWT (~9 km) thick, which occurs below the Gawler Range Volcanics (Carr et al., 2010), and is interpreted to be equivalent to the folded and metamorphosed Wallaroo Group and equivalent units described in the 08GA-G1 seismic line by Fraser et al. (2010). The equivalent unit appears to be absent in seismic line 09GA-CG1, and we interpret the Neoproterozoic succession in the western part of the section to sit directly on middle-lower crust of the Warrakimbo Seismic Province (Figure 5).

Neoproterozoic to Cambrian succession

The section shows a general eastward increase in the thickness of the Neoproterozoic and Cambrian cover, consistent with measured stratigraphic thicknesses at the surface. The base of the Neoproterozoic succession is difficult to pick, because there is no obvious angular unconformity present in the western part of the seismic section. A possible exception is the angular relationship at a depth of about 6 s TWT (~15 km) at the eastern end of the line, which has been tentatively taken as the basal unconformity. If, on the other hand, this discordance represents either an angular unconformity or a fault within lower Adelaidean rocks, then the depth to basement in this region could be even greater than ~18 km. To the west of the fault at

CDP 5100, the base of the Neoproterozoic succession is interpreted to be at the base of a series of relatively strong, subhorizontal reflections at about 4 s TWT (~10 km depth) (Figure 5), which we interpret to be, in part, the mafic Beda and Wooltana Volcanics, based on their reflectivity in the Arrowie Basin seismic line (08GA-A1), which has been confirmed by drilling. These reflections are relatively continuous, at about the same depth, for about 70 km across the western half of the succession.

To the east of the Aliena Fault Zone, there is a great thickness of the stratigraphic units, with some units showing significant thickening into the fault zone, indicating that the faults were active as syndepositional extensional structures. At about CDP 7600, the base of the Neoproterozoic succession is interpreted to occur at about 6 s TWT (~15 km depth), a significantly deeper level than for this horizon on the western side of the Aliena Fault Zone. Hanging wall anticlines and contractional offsets above some of the faults indicate that they were later reactivated, presumably during the late Cambrian Delamerian Orogeny, as thrusts.

As with other surveys which have partly traversed Adelaidean rocks (e.g., Preiss et al., 2004, 2006), thick carbonate packages are seen in seismic line 09GA-CG1 as a series of strong parallel reflections (Figure 5). A strong angular discordance midway down the Adelaidean succession can be related, with some confidence, to the base-of-Yudnamutana Subgroup unconformity, so that underlying units belong to the Burra Group. Between CDPs 6400 to 7600, erosion has removed over 2 s TWT (~5000 m) of stratigraphic section, prior to deposition of the Yudnamutana Subgroup (Umberatana Group). Within the Burra Group, a package of strong reflections is then identified as carbonates of the Mundallio Subgroup (Skillogalee Dolomite), and the nonreflective zone between these carbonates and the base-of-Yudnamutana Subgroup unconformity is the siltstone-dominated Bungarider Subgroup. A series of much less regular, strong reflections near the base of the succession are tentatively interpreted as mafic volcanics associated with the earliest onset of rifting (Beda and Wooltana Volcanics).

Seismic section 09GA-CG1 crosses a large anticline, centred on CDP 7000, with its geometry shown by the base of the Tapley Hill Formation (base of Nepouie Subgroup, Figure 5). The irregular shape of this anticline, particularly its western limb, is a result of the crooked-line geometry of the seismic line, which changes direction frequently, being alternately subparallel and perpendicular to the regional strike of the bedding.

Near the surface, the Neoproterozoic to Cambrian succession is very well imaged in places, with strong subparallel reflections (e.g., CDPs 2000-2400, CDPs 3100-3600, and from CDP 5800 to the eastern end of the line). Elsewhere, near-surface reflectivity is poor, in part due to very steep dips of the bedding (often over 80º), and to the possible presence of near-surface diapirs. Between CDPs 5400 and 5700, the seismic line crosses outcrops of the Worumba Diapir (Preiss, 1985). Poor reflectivity in this area supports the possibility of shallow diapirs being present elsewhere in the vicinity of the seismic section.

Surface mapping shows that the seismic line crosses some highly faulted regions (e.g., CDPs ~3000, 3900-4100 and 5400-5700). In these regions, the seismic image shows either many short, disconnected segments of reflections, or zones of very poor reflectivity. The disruption of the bedding by these minor faults has contributed to the lack of reflectivity, and no attempt was made to show these minor faults in this interpretation.

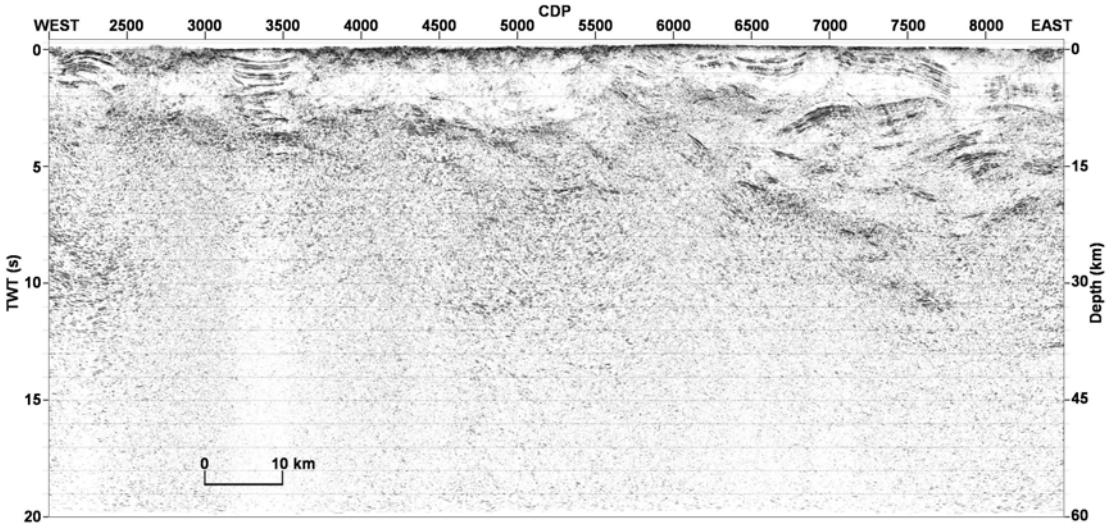

Figure 4. Uninterpreted migrated seismic section of the line 09GA-CG1 across the Flinders Ranges. Depth scale on right hand side assumes an average crustal velocity of 6000 m s^{-1}.

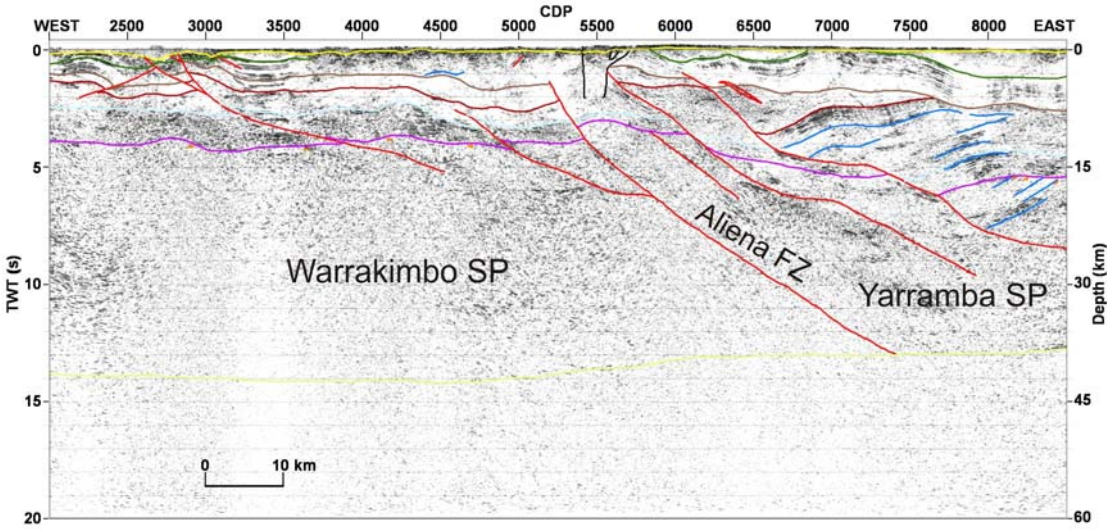

Figure 5. Preliminary interpretation of migrated seismic section of the line 09GA-CG1 across the Flinders Ranges. Depth scale on right hand side assumes an average crustal velocity of 6000 ms^{-1}.

Fault
Reflection (form line)
Base of Cenozoic
Base of Nepouie Subgroup
Base of Yudnamutana Subgroup
Base of Bungarider Subgroup
Base of Burra Group
Base of Neoproterozoic
Moho

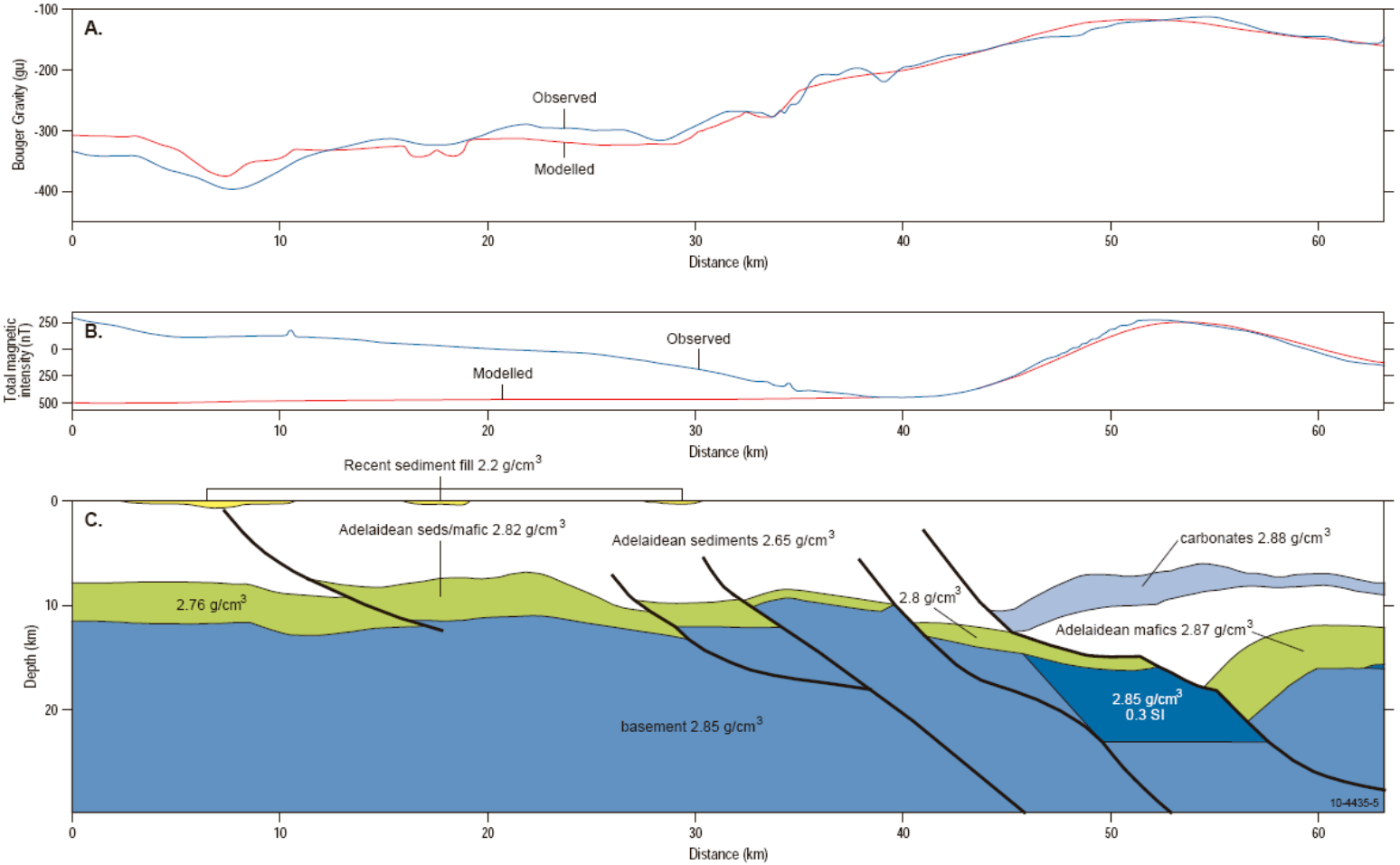

Figure 6. Forward model of the gravity profile along the seismic line 09GA-CG1. The upper panel shows the observed gravity signal in blue, and the modelled signal in red. The middle panel shows the observed magnetic signal; note that only the eastern half of the section has been forward modelled. The lower panel shows the density model, with geometry based on interpretation of the seismic line, and densities as shown.

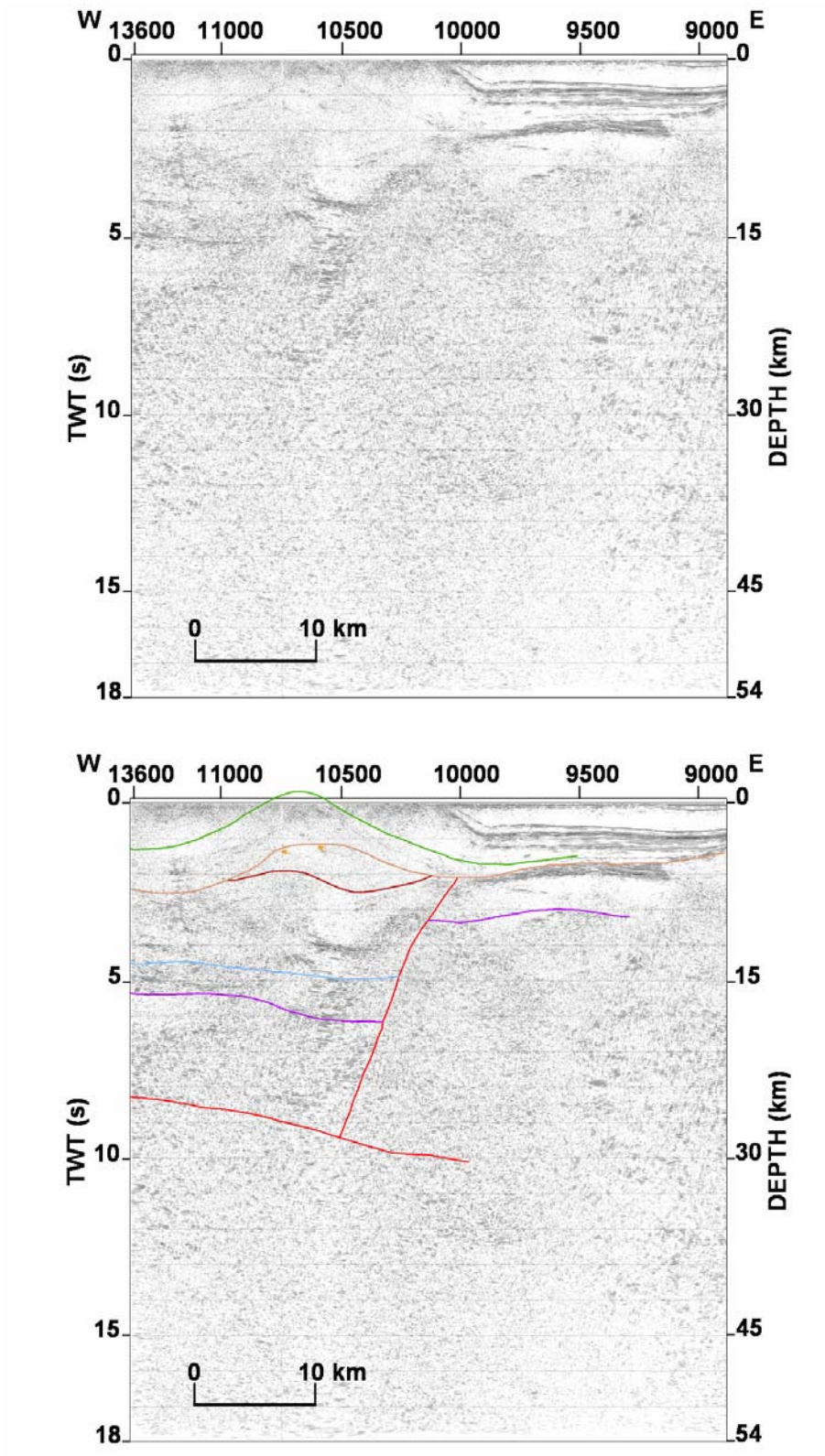

Figure 7. Migrated seismic section (top) and preliminary interpretation (bottom) of western portion of seismic section 03GA-CU1 across the Curnamona Province. Near its western end, this line tied to seismic section 09GA-CG1. Depth scale on right hand side assumes an average crustal velocity of 6000 m s^{-1}. Red = fault; green = base of Nepouie Subgroup; orange = base of Yudnamutana Subgroup; maroon = base of Bungarider Subgroup, light blue = base of Burra Group, purple = base of Neoproterozoic succession.

Forward modelling of potential field data

In the past, regional features of the potential field geophysical data have not been easy to reconcile with the known surface geology, but forward modelling of the gravity and magnetic profiles along the seismic line provides a reconciliation of these datasets (Figure 6). In particular, the gravity data, showing an overall increase from west to east along the seismic line, appear, at first sight, to contradict the known eastward increase in thickness of the sedimentary succession. Nevertheless, the gravity profile can be modelled successfully using dense dolomitic and mafic units within the Neoproterozoic succession. Observed lows in the gravity profile, relative to the regional profile (e.g., centred at about 7 km, 18 km, and 29 km from the western end of the seismic line, Figure 6), are modelled, in part, by relatively less-dense Cenozoic sediment (e.g., 2.2 g cm^{-3}) filling channels.

The Total Magnetic Intensity (TMI) image (Figure 3) shows near-surface high-frequency features, which can be easily related to the outcropping geology (slightly magnetic sedimentary beds, dolerite bodies and mafic volcanics). Broad low-frequency features clearly relate to deep-seated magnetic rock bodies. The magnetic high, near the eastern end of the seismic line (Figure 6), can be modelled using a magnetic susceptibility of 0.3 SI, which may possibly represent magnetic, mafic rocks in the basement (note, however, that the western end of the line was not forward modelled for the magnetic profile).

Implications for seismic line 03GA-CU1

Near its eastern end, seismic line 09GA-CG1 joined the western end of the east-west seismic line across the Curnamona Province (03GA-CU1), previously interpreted by Goleby et al. (2006). The reflectivity at the western end of 03GA-CU1 is relatively poor (Figure 7), whereas the eastern end of seismic line 09GA-CG1 is more reflective (Figure 5). Thus, it is now possible to continue the interpreted horizons from line 09GA-CG1 onto line 03GA-CU1.

Preiss et al. (2006) interpreted a Neoproterozoic to Cambrian basin, with a half graben geometry thinning to the east, in seismic line 03GA-CU1, from about CDP 10000 to about CDP 7700. The base of the Neoproterozoic succession is at about 3 s TWT (about 7500 m depth) (Figure 7). In contrast, the base of the Neoproterozoic succession at the western end of line 03GA-CU1 is interpreted to be significantly deeper, at about 5.3 s (about 13250 m depth). We resolve this difference in depth by inferring a west-dipping bounding fault on the eastern side of the thicker succession (Figure 7).

Near the western end of seismic line 03GA-CU1, reflections centred on CDP 10700 define an antiform at the surface, the Willippa Anticline (Figure 7), whereas reflections centred at about CDP 10400 define a synform at a depth of 2-3 s TWT. We reconcile this by inferring that there has been significant erosion of the Burra Group and development of an angular unconformity below the base of the Yudnamutana Subgroup (Figure 7).

Conclusions

Seismic section 09GA-CG1 crossed the Flinders Ranges, and imaged a major crustal-penetrating fault zone, the Aliena Fault Zone, which separates lower crust of very different seismic character. The crust to the west, the Warrakimbo Seismic Province below the Gawler Craton, is essentially nonreflective, whereas the lower crust to the east, the Yarramba Seismic Province below the Curnamona Province, is much more reflective. The upper crust consists of a Neoproterozoic and Cambrian succession overlain by thin Cenozoic sediment and alluvium. A major Neoproterozoic depocentre in the eastern part of the transect is bounded in the west by the Aliena Fault Zone, which at the time of deposition of the Neoproterozoic succession, was a crustal-scale extensional fault, and which was reactivated later, probably during the Delamerian Orogeny, as a thrust. The eastern limit of this depocentre can be traced onto the western end of seismic line 03GA-CU1. A strong angular discordance midway down the Adelaidean succession is interpreted to be the base-of-Yudnamutana Subgroup angular unconformity. The upper part of seismic section 09GA-CG1 contains broad zones which are essentially nonreflective; this is attributable to very steep dips of the bedding (often over 80º), and the possible presence of

near-surface diapirs. Forward modelling of the potential field data has assisted in constraining the interpretation of the seismic section.

Acknowledgements

We thank Natalie Kositcin and Lidena Carr for their reviews of the manuscript.

References

Carr, L.K., Korsch, R.J., Holzschuh, J., Costelloe, R.D., Meixner, A.J., Matthews, C. and Godsmark, B., 2010. Geological interpretation of seismic reflection lines 08GA-C1 and 09TE-01: Arrowie Basin, South Australia. *Geoscience Australia, Record,* **2010/10**, this volume.

Cowley, W.M., 2006. Solid geology of South Australia: peeling away the cover. *MESA Journal*, **43**, 4-15.

Fomin, T., Holzschuh, J., Nakamura, A., Maher, J., Duan, J. and Saygin, E., 2010. 2008 Gawler-Curnamona-Arrowie (L189) and 2009 Curnamona-Gawler link (L191) seismic surveys – acquisition and processing. *Geoscience Australia, Record,* **2010/10**, this volume.

Fraser, G.L., Blewett, R.S., Reid, A.J., Korsch, R.J., Dutch, R., Neumann, N.L., Meixner, A.J., Skirrow, R.G., Cowley, W.M, Szpunar, M., Preiss, W.V., Nakamura, A., Fomin, T., Holzschuh, J., Milligan, P.R. and Bendall, B.R., 2010. Geological interpretation of deep seismic reflection and magnetotelluric line 08GA-G1: Eyre Peninsula, Gawler Craton, South Australia. *Geoscience Australia, Record,* **2010/10**, this volume.

Fricke, C.E., Preiss, W.V. and Neumann, N.L. 2010. The Curnamona Province: a Paleo- to Mesoproterozoic time slice. *Geoscience Australia, Record,* **2010/10**, this volume.

Goleby, B.R., Korsch, R.J., Fomin, T., Conor, C.H.H., Preiss, W.V., Robertson, R.S. and Burtt, A.C., 2006. The 2003-2004 Curnamona Province seismic survey. *Geoscience Australia, Record,* **2006/12**, 96 pp.

Korsch, R.J., Preiss, W.V., Blewett, R.S., Cowley, W.M., Neumann, N.L., Fabris, A.J., Fraser, G.L., Dutch, R., Fomin, T., Holzschuh, J., Fricke, C.E., Reid, A.J., Carr, L.K. and Bendall, B.R., 2010. Deep seismic reflection transect from the western Eyre Peninsula in South Australia to the Darling Basin in New South Wales: Geodynamic implications. *Geoscience Australia, Record,* **2010/10**, this volume.

Preiss, W.V., 1985. Stratigraphy and tectonics of the Worumba Anticline and associated intrusive breccias. *South Australian Geological Survey, Bulletin*, **52**.

Preiss, W.V., 2010. Geology of the Neoproterozoic to Cambrian Adelaide Geosyncline and Cambrian Delamerian Orogen. *Geoscience Australia, Record,* **2010/10**, this volume.

Preiss, W.V., Korsch, R.J. and Totterdell, J.M., 2004. Gawler Craton cover succession: Stuart Shelf to Adelaide Geosyncline transition. In: Seismic Workshop Notes, Gawler Craton 2004 State of Play, 6 August 2004, Adelaide, 65-70.

Preiss, W.V., Fomin, T., Goleby, B.R., Korsch, R.J., Robertson, R.S., Conor, C.H.H. and Burtt, A.C., 2006. The Adelaidean and Cambrian cover succession of the Curnamona Province. In: Goleby, B.R., Korsch, R.J., Fomin, T., Conor, C.H.H., Preiss, W.V., Robertson, R.S. and Burtt, A.C., 2006. The 2003-2004 Curnamona Province seismic survey. *Geoscience Australia, Record*, **2006/12**, 49-61.

Reid, A., Szpunar, M. and Fairclough, M. 2010. Overview of the geology of the Gawler Craton, South Australia. *Geoscience Australia, Record,* **2010/10**, this volume.

Overview of the geology of the Gawler Craton, South Australia

A. Reid, M. Szpunar and M. Fairclough

Geological Survey Branch, Primary Industries and Resources South Australia, GPO Box 1671, Adelaide, SA 5001, Australia

Anthony.Reid@saugov.sa.gov.au

The Gawler Craton, South Australia, records a prolonged period of crustal growth, sedimentation and tectonothermal reworking which spans over half of Earth history. Review papers which cover the geology of the Gawler Craton include Daly et al. (1998), Ferris et al. (2002), Hand et al. (2007) and Payne et al. (2009), along with Bulletin 54, the Geology of South Australia (Drexel et al., 1993). Metallogenic aspects of the Gawler Craton, with emphasis on the Mesoproterozoic Olympic Dam IOCG deposit and associated mineral systems, are well covered in Daly et al. (1998), Skirrow et al. (2007) and references therein.

With the recent discovery of Mesoarchaean, c. 3150 Ma, gneissic basement in the Middleback Ranges (Fraser et al., 2010a), we can now confirm earlier suggestions (Daly and Fanning, 1990; Daly and Fanning, 1993) that the predominantly Neoarchean to early Mesoproterozoic rocks of the Gawler Craton were intruded into, or deposited upon an older basement. The distribution of this basement is poorly known, being confined at this stage to the northern Eyre Peninsula. Nevertheless, it may well be an important part of the middle to lower crust of the entire eastern Gawler Craton.

The better exposed and metallogenically significant Neoarchean to early Paleoproterozoic rocks of the Gawler Craton are organised into the Mulgathing and Sleaford Complexes, which likely form part of a formerly contiguous province now dismembered by Proterozoic tectonism. The komatiites, mafic and felsic volcanic rocks, BIF, carbonates and extensive clastic successions of these two complexes formed after c. 2560 Ma (Devils Playground Volcanics; Cowley and Fanning, 1991), and include rocks with maximum depositional ages which range from c. 2520 Ma, through to as young as c. 2485 Ma, based on recent work from the Mulgathing Complex (Jagodzinski et al., 2009). Sedimentation and magmatism was terminated by basin inversion that began at c. 2470 Ma and continued through to c. 2410 Ma, during the so-called Sleafordian Orogeny.

No geological activity is recorded within the Gawler Craton following the Sleafordian Orogeny until the intrusion of the precursor to the c. 2000 Ma Miltalie Gneiss. The intrusion of this granite heralds the beginning of a prolonged period of basin formation and growth over the interval c. 1870 to 1730 Ma, wherein large, lithologically complex basins formed across the entire Gawler Craton. In particular, the best known is the Hutchison Group, which occurs on the eastern Gawler Craton. Recent geochronology on the Hutchison Group shows that it was deposited between c. 1870 and 1730 Ma, with major input of c. 1790 Ma detritus to the basin marking a change in sediment provenance from the initial intracontinental rift. This change in provenance possibly indicates that the basin became involved with a proximal volcanic arc of some sort, possibly in a backarc setting (Szpunar et al., unpublished data).

At c.1850 Ma, a moderately isotopically-juvenile granitic batholith, termed the Donington Suite, was emplaced into the eastern Gawler Craton. This voluminous magmatic activity was accompanied in part by deformation and metamorphism, which is described only from southern Yorke Peninsula (Reid et al., 2008).

Subsequent to, or possibly synchronous with, deposition of the Hutchison Group, are a series of volcano-sedimentary basins, such as the c. 1760 Ma Wallaroo Group, which occur across the Gawler Craton. From the few drillholes into the northern Gawler Craton, geochronology shows that the sediments in this large region were also deposited at or around this time (Payne et al., 2006).

This depositional episode was followed by a major orogenic episode, which affected the entire Gawler Craton: the 1730-1690 Ma Kimban Orogeny. This high temperature, structurally complex orogen resulted in extensive reworking and magmatism (Parker, 1993; Dutch et al., 2008), and concluded with post-tectonic magmatism (Payne et al., 2010).

Latest Paleoproterozoic, c. 1660 to 1620 Ma, sedimentation and magmatism includes the Tarcoola Formation and associated basins in the central Gawler Craton, and the St Peter Suite in the southern Gawler Craton (Daly, 1993; Swain et al., 2008). Mesoproterozoic volcanic and intrusive rocks of the Gawler Range Volcanics and Hiltaba Suite form an extensive, and metallogenically significant, component of the Gawler Craton. Evidence for crustal thickening and deformation is preserved in the Gawler Craton synchronous with eruption of the Gawler Range Volcanics, which indicates significant partitioning of this early Mesoproterozoic tectonic event within the Gawler Craton, possibly controlled by large-scale shear zones such as the Karari Fault in the northern Gawler Craton (Hand et al., 2007, 2008). Lower temperature reworking, over the interval c. 1480-1450 Ma, is largely confined to regional-scale shear zones (Fraser and Lyons, 2006). This event largely terminated the tectonic development of the Gawler Craton.

Based upon geological and tectonic characteristics (delineated partly by geophysical data) and history, the Gawler Craton has been subdivided into several domains (Ferris et al., 2002; Fairclough et al, 2003). The Nuyts, Coulta, Cleve, Spencer and Moonta Domains are crossed by seismic line 08GA-G1, as summarised by Fraser et al. (2010b), and are not discussed further here. The Arrowie Basin seismic line 08GA-A1 (Carr et al., 2010), to the northeast, is situated in the adjacent Olympic Domain. This broadly corresponds spatially to the overlying Stuart Shelf, which is discussed in detail by Preiss (2010). The Domain is bound to the east by reworked equivalents corresponding approximately to the Torrens Hinge Zone. Basement to the Stuart Shelf crops out sporadically on Yorke Peninsula, but information to the north is limited to drillhole and mine exposures.

The Olympic Domain is an arcuate zone of Paleoproterozoic sedimentary and felsic igneous rocks and Mesoproterozoic granite, volcanic, quartz-rich sedimentary rocks and conglomerates. The oldest rocks known from the Olympic Domain form a schistose unit which occurs as enclaves within deformed granites. These rocks are strongly deformed, containing at least one foliation, and are thought to represent metasedimentary rocks of the Hutchison Group based on relationship with other units. The Hutchison Group is an extensive succession of shallow clastic and chemical marine sedimentary rocks, with minor acid and mafic volcanic rocks. The Group has been subdivided into three main successions.

Within the Olympic Domain, numerous drillholes intersect coarse-grained, deformed granite. U–Pb SHRIMP analysis of zircons from a number of drillholes in the region give crystallisation ages of c.1850-1860 Ma, hence this is considered to be part of the Donington Suite (Creaser, 1995; Jagodzinski, 2005). The unit is of batholithic extent, which supports a Donington Suite classification. In addition to the coarse-grained, deformed granite, two other distinct lithological types are present: felsic, medium-grained, equigranular granite and pegmatite; and intermediate to mafic lithologies, including tonalite, granodiorite and quartz monzonite.

Within the Olympic Dam region, overlying the Donington Suite, is a succession of intercalated, deformed felsic volcanic rocks and schists. This unit has not been dated, but is thought to correlate with either the Myola Volcanics (~1790 Ma; Fanning et al., 1988) or felsic volcanic rocks of the Wallaroo Group (~1740 Ma; Fanning et al., 1988), or possibly the Tidnamurkuna Volcanics (~1780 Ma; Fanning et al., 2007). Unconformably overlying the older granites, within the Olympic Domain, is a widespread succession of finely-laminated metasiltstone, feldspathic sandstone, calcsilicates and amphibolites. This succession is unconformably overlain by Gawler

Range Volcanics, and is correlated with the Wandearah Metasiltstone of the Wallaroo Group found on Yorke Peninsula.

The last major magmatic event observed in the area is the Hiltaba Suite–Gawler Range Volcanics magmatic event (1595–1575 Ma). The Gawler Range Volcanics cover an area of ~25 000 km^2 and are the dominant Proterozoic unit cropping out on the Gawler Craton. They consist of a series of dominantly felsic lavas and ignimbrites, with minor mafic lavas. The Hiltaba Suite intrudes the Gawler Range Volcanics and consists of mostly oxidised, K-feldspar-dominant granite. The discovery of the Olympic Dam Cu–U–Au–Ag orebody, hosted within the Roxby Downs Granite, a member of the Hiltaba Suite, has greatly increased the prospectivity of the Gawler Craton.

Unconformably overlying these older units is the Pandurra Formation, a thick succession of undeformed, arenaceous redbed sediments, which extends over a large part of the Olympic Domain. The Pandurra Formation has a minimum depositional age of 1424 ± 51 Ma based on Rb–Sr geochronology. Unconformably overlying the Pandurra Formation in the Cultana area are subaerial basalts of the Beda Volcanics and intercalated, coarse-grained fluvial clastics of the Backy Point Formation, both of Mesoproterozoic age.

References

Carr, L.K., Korsch, R.J., Holzschuh, J., Costelloe, R.D., Meixner, A.J., Matthews, C. and Godsmark, B. 2010. Geological interpretation of seismic reflection lines 08GA-C1 and 09TE-01: Arrowie Basin, South Australia. *Geoscience Australia, Record,* **2010/10**, this volume.

Cowley, W. M. and Fanning, C. M., 1991. Low-grade Archaean Metavolcanics in the northern Gawler Craton. *Geological Survey of South Australia, Quarterly Geological Notes,* **119 (2)**, 17.

Creaser, R.A., 1995. Neodymium isotopic constraints for the origin of Mesoproterozoic felsic magmatism, Gawler Craton, South Australia. *Canadian Journal of Earth Sciences*, **32**, 460-471.

Daly, S. and Fanning, C.M., 1990. Archaean geology of the Gawler Craton, South Australia. In: Glover, J.E. and Ho, S.E., Editors, 3rd *International Archaean Symposium*. Geoconferences (WA) Inc., Perth, pp. 91-92.

Daly, S.J., 1993. Tarcoola Formation. In: Drexel, J.F., Preiss, W.V. and Parker, A.J., editors, The geology of South Australia; Volume 1, The Precambrian. *Geological Survey of South Australia, Bulletin,* **54**, 68-69.

Daly, S.J. and Fanning, C.M., 1993. Archaean. In: Drexel, J.F., Preiss, W.V. and Parker, A.J., Editors, The geology of South Australia; Volume 1, The Precambrian. *Geological Survey of South Australia, Bulletin,* **54**, 32-49.

Daly, S.J., Fanning, C.M. and Fairclough, M.C., 1998. Tectonic evolution and exploration potential of the Gawler Craton, South Australia. *AGSO Journal of Australian Geology and Geophysics*, **17**, 145-168.

Drexel, J.F., Preiss, W.V. and Parker, A.J., Editors, 1993. The Geology of South Australia: Volume 1, The Precambrian. *Geological Survey of South Australia Bulletin*, **54**, 242 pp.

Dutch, R., Hand, M. and Kinny, P.D., 2008. High-grade Paleoproterozoic reworking in the southeastern Gawler Craton, South Australia. *Australian Journal of Earth Sciences*, **55**, 1063-1081.

Fairclough, M. C., Schwarz, M. P. and Ferris, G. M., 2003. Interpreted crystalline basement geology of the Gawler Craton. South Australia Geological Survey Special Map, 1:1 000 000.

Fanning, C. M., Flint, R. B., Parker, A. J., Ludwig, K. R. and Blissett, A. H., 1988. Refined Proterozoic evolution of the Gawler Craton, South Australia, through U-Pb zircon geochronology. *Precambrian Research*, **40/41**, 363-386.

Fanning, C. M., Reid, A. J. and Teale, G. S., 2007. A geochronological framework for the Gawler Craton, South Australia. *South Australia Geological Survey Bulletin* **55**.

Ferris, G.M., Schwarz, M.P. and Heithersay, P., 2002. The geological framework, distribution and controls of Fe-oxide and related alteration, and Cu-Au mineralisation in the Gawler Craton, South Australia. Part I: geological and tectonic framework. In: Porter, T.M.,

editor, Hydrothermal iron oxide copper-gold and related deposits: a global perspective. PGC Publishing, Adelaide, 9-31.

Fraser, G. and Lyons, P., 2006. Timing of Mesoproterozoic tectonic activity in the northwestern Gawler Craton constrained by $^{40}Ar/^{39}Ar$ geochronology. *Precambrian Research*, **151**, 160-184.

Fraser, G., McAvaney, S., Neumann, N., Szpunar, M. and Reid, A., 2010a. Early Mesoarchean crust in the eastern Gawler Craton, South Australia. *Precambrian Research, in press.*

Fraser, G.L., Blewett, R.S., Reid, A.J., Korsch, R.J., Dutch R., Neumann, N.L., Meixner, T., Skirrow, R.G., Cowley, W., Szpunar, M., Preiss, W.V., Nakamura, A., Fomin, T., Holzschuh, J., Milligan P. and Bendall, B., 2010b. Geological interpretation of deep seismic reflection and magnetotelluric line 08GA-G1: Eyre Peninsula, Gawler Craton, South Australia. *Geoscience Australia, Record,* **2010/10**, this volume.

Hand, M., Reid, A. and Jagodzinski, E., 2007. Tectonic framework and evolution of the Gawler Craton, South Australia. *Economic Geology*, **102**, 1377-1395.

Hand, M., Reid, A., Szpunar, M., Direen, N.G., Wade, B., Payne, J. and Barovich, K., 2008. Crustal architecture during the early Mesoproterozoic Hiltaba-related mineralisation event: are the Gawler Range Volcanics a foreland basin fill? *MESA Journal*, **51**, 19-24.

Jagodzinski, E., Reid, A. and Fraser, G., 2009. Compilation of SHRIMP U-Pb geochronological data for the Mulgathing Complex, Gawler Craton, South Australia, 2007-2009. South Australia. *Department of Primary Industries and Resources, Report Book*, **2009/16**.

Jagodzinski, E.A., 2005. Compilation of SHRIMP U-Pb geochronological data, Olympic Domain, Gawler Craton, South Australia, 2001-2003. *Geoscience Australia, Record,* **2005/20**, 211.

Parker, A.J., 1993. Kimban Orogeny. In: Drexel, J.F., Preiss, W.V. and Parker, A.J., Editors, The geology of South Australia; Volume 1, The Precambrian. *Geological Survey of South Australia, Bulletin,* **54**, 71-82.

Payne, J., Barovich, K. and Hand, M., 2006. Provenance of metasedimentary rocks in the northern Gawler Craton, Australia: Implications for Palaeoproterozoic reconstructions. *Precambrian Research*, **148**, 275-291.

Payne, J.L., Ferris, G., Barovich, K.M. and Hand, M., 2010. Pitfalls of classifying ancient magmatic suites with tectonic discrimination diagrams: An example from the Paleoproterozoic Tunkillia Suite, southern Australia. *Precambrian Research*, **177**, 227-240.

Payne, J.L., Hand, M., Barovich, K., Reid, A.J. and Evans, D.A.D., 2009. Correlations and reconstruction models for the 2500-1500 Ma evolution of the Mawson Continent. In: Reddy, S.M., Mazumder, R., Evans, D.A.D. and Collins, A.S., editors, Palaeoproterozoic supercontinents and global evolution. *Geological Society, London, Special Publication,* **323,** 319-355.

Preiss, W.V., 2010. Geology of the Neoproterozoic to Cambrian Adelaide Geosyncline and Cambrian Delamerian Orogen. *Geoscience Australia, Record,* **2010/10**, this volume.

Reid, A., Hand, M., Jagodzinski, E., Kelsey, D. and Pearson, N.J., 2008. Palaeoproterozoic orogenesis within the southeastern Gawler Craton, South Australia. *Australian Journal of Earth Sciences*, **55**, 449-471.

Skirrow, R.G., Bastrakov, E.N., Barovich, K., Fraser, G.L., Creaser, R.A., Fanning, C.M., Raymond, O.L. and Davidson, G.J., 2007. The Olympic Cu-Au province: timing of hydrothermal activity, sources of metals, and the role of magmatism. *Economic Geology*, **102**, 1441-1470.

Swain, G., Barovich, K., Hand, M., Ferris, G. and Schwarz, M., 2008. Petrogenesis of the St Peter Suite, southern Australia: Arc magmatism and Proterozoic crustal growth of the South Australian Craton. *Precambrian Research*, **166**, 283-296.

Geological interpretation of deep seismic reflection and magnetotelluric line 08GA-G1: Eyre Peninsula, Gawler Craton, South Australia

G.L. Fraser[1], R.S. Blewett[1], A.J.Reid[2], R.J. Korsch[1], R. Dutch[2], N.L. Neumann[1], A.J. Meixner, R.G. Skirrow, W.M. Cowley[2], M. Szpunar[2], W.V. Preiss[2], T. Fomin[1], J. Holzschuh[1], S. Thiel[3], P.R. Milligan[1], B.R. Bendall[4]

[1]Onshore Energy & Minerals Division, Geoscience Australia, GPO Box 378, Canberra, ACT 2601, Australia
[2]Geological Survey Branch, Primary Industries and Resources South Australia (PIRSA), GPO Box 1671, Adelaide, SA 5001, Australia
[3]Tectonics, Resources and Exploration (TRax), School of Earth and Environmental Sciences, University of Adelaide, Adelaide, SA, 5005, Australia
[4] Petroleum Geology Branch, Primary Industries and Resources South Australia (PIRSA), GPO Box 1671, Adelaide, SA 5001, Australia

Geoff.Fraser@ga.gov.au

Introduction

In 2008, as part of the Onshore Energy Security Program (OESP), Geoscience Australia, in conjunction with Primary Industries and Resources South Australia (PIRSA), acquired deep seismic reflection data along an east-west transect of 253 km across northern Eyre Peninsula, South Australia. This transect (08GA-G1) starts northeast of Whyalla and runs westwards, past the northern end of the Middleback Ranges and north of Lake Gilles, to a westernmost extent northwest of Wudinna (Figure 1). In addition to the deep seismic reflection data, wide angle seismic reflection and magnetotelluric data were also collected along this transect. Details of acquisition parameters and data processing methods are provided by Fomin et al. (2010) and Thiel et al. (2010). Here, we report the results of these geophysical surveys, with a particular emphasis on the seismic reflection data, and present preliminary geological interpretations.

Aims of the Seismic Survey

The location and orientation of the 08GA-1 seismic survey were selected in order to investigate the crustal architecture of the eastern part of the Gawler Craton. The surface geology of northern Eyre Peninsula exhibits a broadly north-south trending structural grain, and has been subdivided into five tectonic domains (Ferris et al., 2002); from east to west these are the Moonta, Spencer, Cleve, Coulta and Nuyts Domains (Figure 1). The seismic line is oriented approximately perpendicular to strike and crosses each of these domains. The line also crosses the western boundary of the South Australian Heat Flow Anomaly (SAHFA). The SAHFA (Neumann et al., 2000) is defined by a relatively small number of heat flow measurements that reveal heat flow values on eastern Eyre Peninsula that are approximately double (~100 mWm^{-2}) the Proterozoic crustal average, dropping to more typical values (~60 mWm^{-2}) in the west (Figure 1).

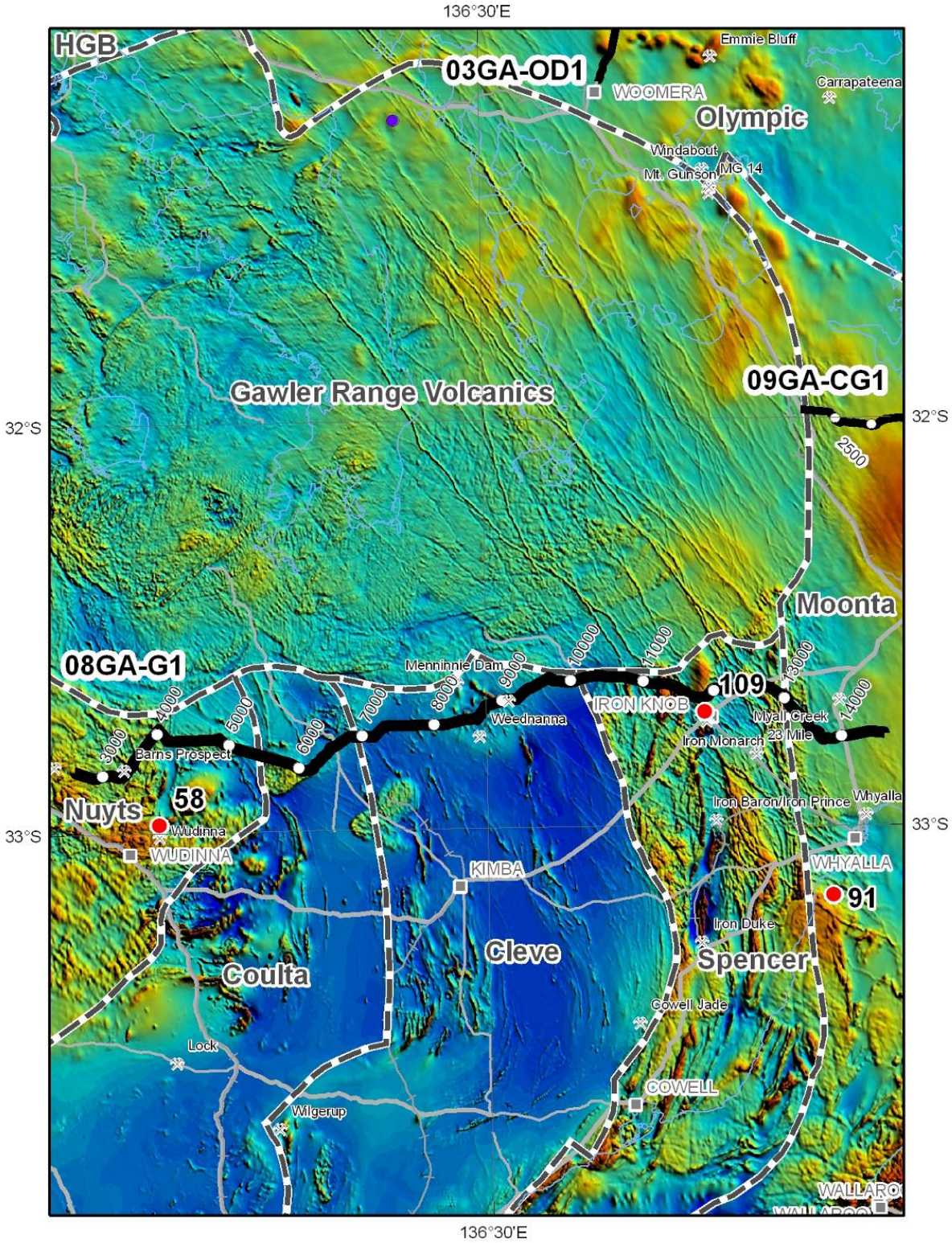

Figure 1. Map showing aeromagnetic data for the northern Eyre Peninsula, with subdivision into domains after Ferris et al. (2002) (warm colours are high magnetic intensities, cool colours are low magnetic intensities). The bold black lines show the location of the east-west seismic reflection transect 08GA-G1, with CDP stations labelled, and parts of the seismic lines 03GA-OD1 and 09GA-CG1. Red dots show the locations of heat-flow measurements, with heat-flow values given in mWm^{-2}. Also shown are the locations of mines and prospects. HGB – Harris Greenstone Belt.

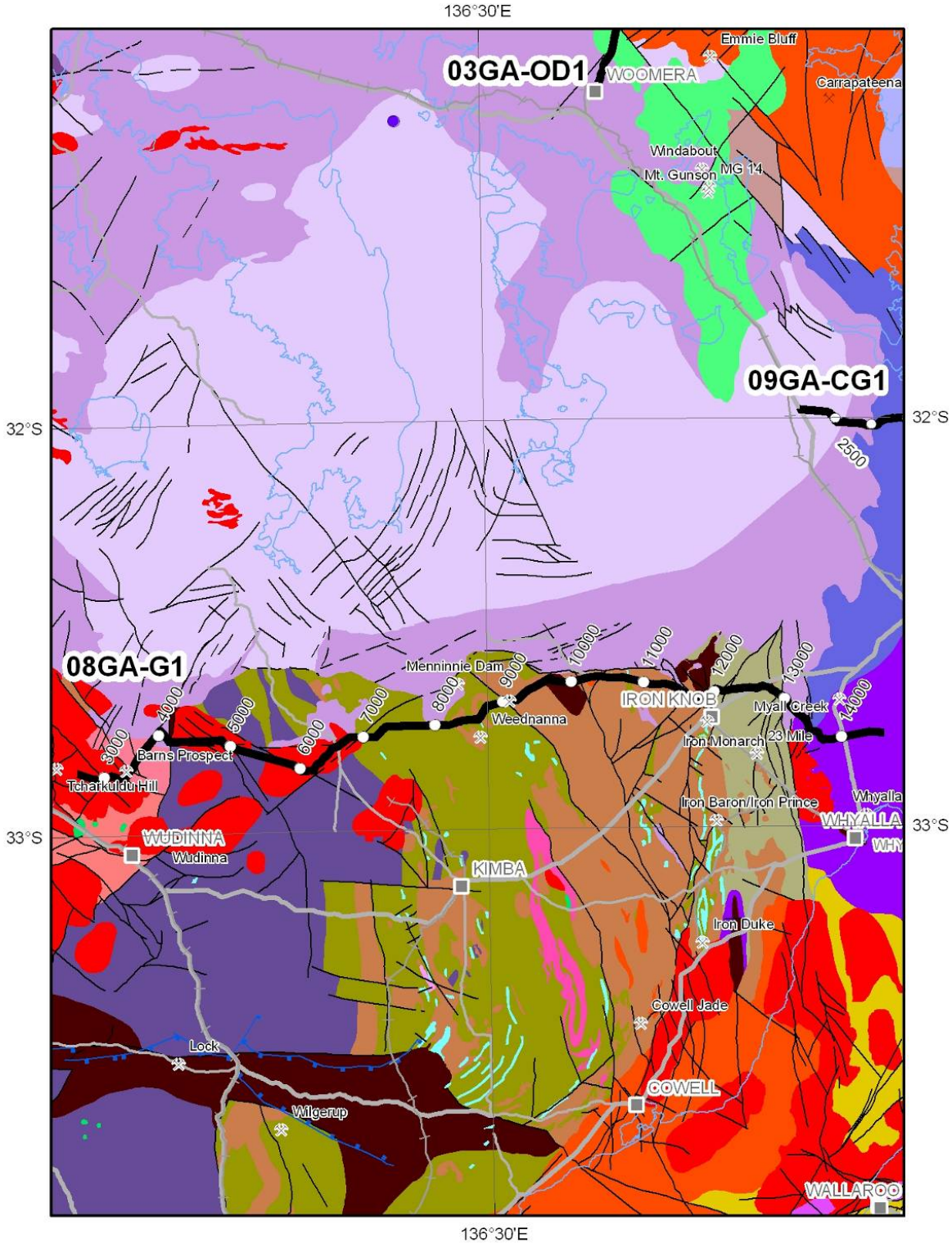

Figure 2. Map showing the solid geology of the Eyre Peninsula in South Australia (after Cowley, 2006, which also contains the legend). The bold lines show the location of the east-west seismic reflection transect 08GA-G1, with CDP stations labelled, and parts of the seismic lines 03GA-OD1 and 09GA-CG1. Also shown are the locations of mines and prospects.

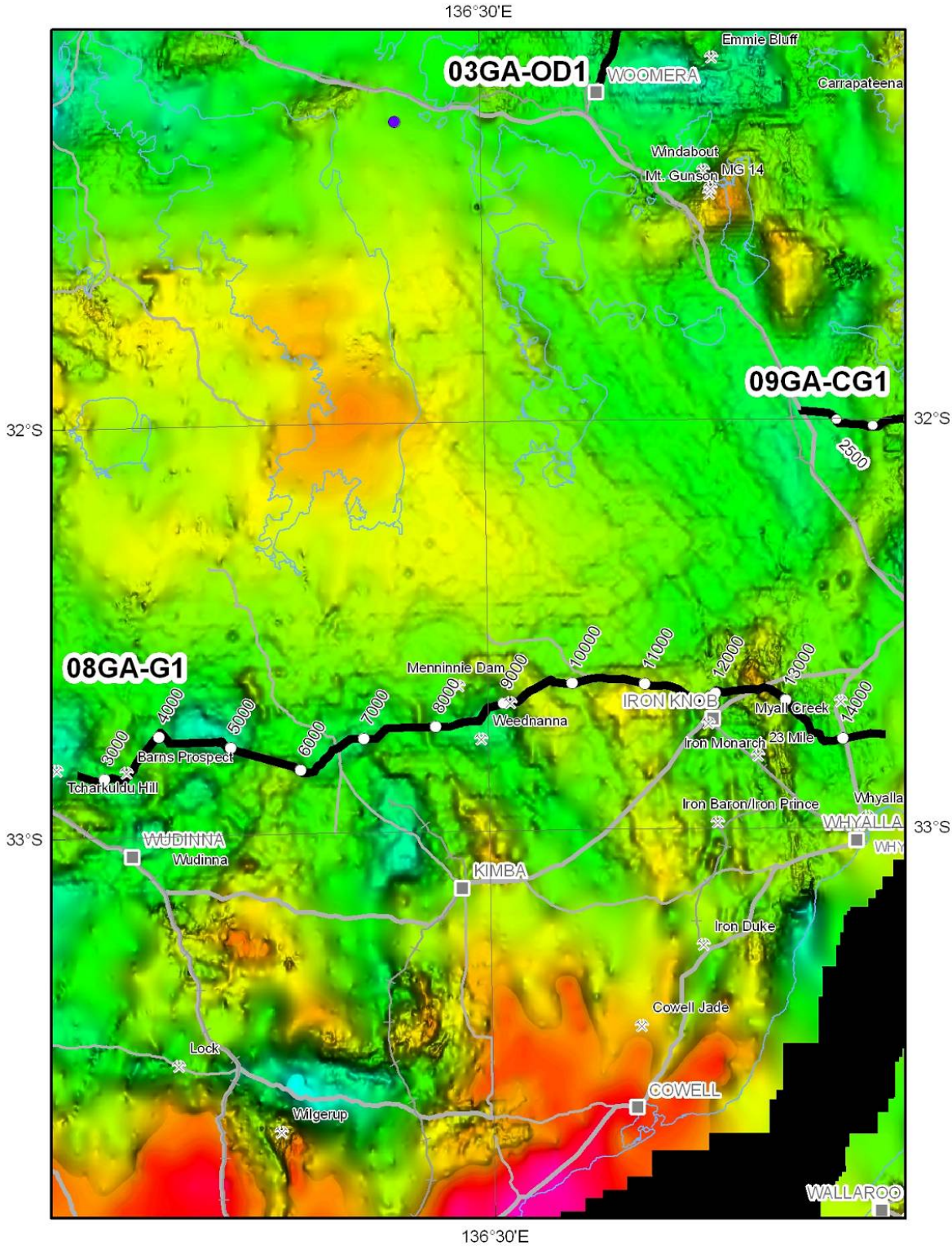

Figure 3. Map showing regional gravity data for the northern Eyre Peninsula in South Australia (warm colours are gravity highs, cool colours are gravity lows). The bold lines show the location of the east-west seismic reflection transect 08GA-G1, with CDP stations labelled, and parts of the seismic lines 03GA-OD1 and 09GA-CG1. Also shown are the locations of mines and prospects.

The dramatic increase in heat flow in the east has been shown to arise from crustal enrichment in radiogenic heat producing elements (U, Th, K) (Neumann et al., 2000), but the origin of such enrichment, and the exact position and nature of the heat-flow boundary, have not been well established. The radiogenically enriched crust in the eastern part of the Gawler Craton has been suggested as a control on differing styles of mineralisation across the Craton (Hand et al., 2007). Specifically, the Olympic IOCG±U province is situated along the eastern side of the craton, within radiogenically enriched crust, and hosts the world's largest U deposit, Olympic Dam. The SAHFA is also a focus for geothermal exploration and development. In contrast, the central Gawler Craton, with lower radiogenic element abundance, hosts several Au-deposits and prospects, in a belt known as the Central Gawler Gold Province (Drown, 2003; Ferris and Schwarz, 2003; Fraser et al., 2007). The across-strike, east-west orientation of the seismic line provides crustal geometries that can be compared with existing tectonic models. For example, the model of Betts and Giles (2006) interprets a collisional suture in the position of the Kalinjala Mylonite Zone on eastern Eyre Peninsula. Such tectonic models have implications for the geodynamic setting of known mineral systems and for prospectivity for undiscovered mineral and energy resources.

Preliminary geological interpretation of seismic line 08GA-G01

Overview

The crust imaged by the seismic transect (Figure 4) can be divided into two regions of different seismic character. The central and western portion of the section (from the western end of the line to CDP 10,000) shows a very nonreflective upper crust in the top ~2 s TWT (6 km), underlain by a much more reflective middle to lower crust characterised by predominantly east-dipping reflections. This middle to lower reflective crust has not been tracked to the surface in the seismic line, and has been termed the Yeltana Seismic Province by Korsch et al. (2010). The Moho is poorly imaged across this central portion of the section, although it is interpreted to lie at ~14 s TWT (42 km depth). In the east (CDP 10,000 to eastern end of the line), the crust is not as clearly layered, and the middle crust is less reflective than in the central part of the section. Again, the middle to lower crust in this region has not been traced to the surface in either this seismic lines or in the Arrowie Basin line (08GA-A1; Carr et al., 2010) or in the Curnamona-Gawler Link line (09GA-CG1; Preiss et al., 2010); it has been called the Warrakimbo Seismic Province by Korsch et al. (2010). The Moho is interpreted at ~14 s TWT (42 km depth). The upper mantle beneath the Moho is essentially nonreflective across the entire section.

The less reflective middle crust in the east of the section corresponds to the region east of the Middleback Ranges, in the Moonta and Spencer Domains, where surface geology is dominated by Paleoproterozoic metasedimentary and volcanic rocks, and farther to the east, across the Roopena Fault, by relatively flat-lying Pandurra Formation and lower Adelaidean sedimentary rocks. The central zone of nonreflective upper crust and strongly reflective middle to lower crust spans the Cleve and Coulta Domains, where the surface geology is dominated by Hutchison Group metasedimentary rocks and felsic gneisses, including the Sleaford Complex (~2450 Ma) and Miltalie Gneiss (~2000 Ma). Most, if not all, of the gneisses in this central zone have experienced high-grade metamorphism, partial melting and granitic intrusions during the Kimban Orogeny (~1730 Ma). The boundary between this central zone and the less reflective crust to the east is interpreted as an east-dipping structure that can be traced from the middle to the lower crust from beneath the vicinity of the Kalinjala Mylonite Zone (see discussion of terminology below).

In the following sections we describe in more detail, from east to west, the major features of the seismic line.

Moonta Domain

Mesoproterozoic and Neoproterozoic cover successions

Surface geology on the eastern end of the line, east of CDP 13900, consists of an eastwards-thickening wedge of near flat-lying Neoproterozoic Backy Point Formation and Beda Volcanics.

These units unconformably overlie sandstones and conglomerates of the Mesoproterozoic Pandurra Formation, which crop out between CDP 13900 and 13500. In the seismic section, the Pandurra Formation is interpreted to thicken eastwards, reaching a thickness of ~0.5 s TWT at the eastern end of the section, corresponding to a thickness of >1000 m. Strong seismic reflections at the base of the Pandurra Formation are interpreted as a thin layer of Gawler Range Volcanics (GRV). The middle to lower crust beneath the GRV is poorly constrained. It is relatively weakly reflective down to ~4 s TWT (~12 km depth), and slightly more reflective below this level.

Between CDP 13500 and 13000, the seismic transect trends northwest and follows the boundary between the Pandurra Formation to the northeast, and the Paleoproterozoic Moonabie Formation to the southwest. Also present at the surface along this segment are basaltic Roopena Volcanics, which are part of the lower GRV. A region of very low seismic reflectivity between ~0.4 and 0.8 TWT between CDPs 13000 and 13300 is interpreted as a Hiltaba Suite granite, extending northwards at depth from its near-surface extent on the solid geology map of Cowley (2006).

The north-south-striking Roopena Fault is crossed by the seismic line between CDP 12900 and 13000. This fault separates relatively flat-lying Meso- and Neoproterozoic cover successions to the east from uprightly-folded Paleoproterozoic Broadview Schist to the west. On the seismic section, this fault is not well-imaged in the near-surface, but is interpreted to dip steeply to the east, on the basis of a zone of low reflectivity which truncates shallow-dipping reflections on either side. This near-surface fault zone can be traced down to east-dipping planar reflections between 4 and 5 s TWT (12 to 15 km depth). The poorly reflective zone from 1-4 s TWT (3-12 km depth) could possibly be the equivalent of the lower Wallaroo Group.

Spencer Domain

Geological mapping (Fairclough and Curtis, 2008) shows the poorly-exposed Broadview Schist to extend westwards from the Roopena Fault to the eastern edge of the Baxter Hills (CDP 11900). This corresponds to a region of low reflectivity in the top ~0.5-1 s TWT of the seismic section. The base of the Broadview Schist is interpreted to correspond to an undulating surface of higher reflectivity between two east-dipping faults. The Bouguer gravity field shows a distinct high to the west of the Roopena Fault (Figures 3, 5). Forward modelling of the Bouguer gravity signal (see Figure 5) requires a near-surface feature with distinctly higher density (~2.95 g.cm^{-3}) than that inferred for the average underlying gneissic basement. The origin of this density anomaly is unknown. It may be a distinctly more mafic component of the shallow basement, it may be a gabbroic intrusion, or it may represent a large, relatively non-magnetic alteration system.

Middleback Ranges-Baxter Hills region

At ~CDP 11900 the seismic transect passes between the Middleback Ranges to the south and the Baxter Hills to the north. At this position, the top of reflective crust steps up from ~1 s TWT in the east to ~0.4 s TWT to the west. This step-up occurs across a zone of relatively-planar, steeply east-dipping reflections, interpreted as an east-dipping fault or shear zone. This fault can be traced to ~2 s TWT and is interpreted to link with a deep crustal structure extending into the middle crust.

The Baxter Hills consist predominantly of east-dipping conglomerates and sandstones of the Corunna Conglomerate. These are not imaged in the seismic line, consistent with the map pattern that shows the seismic line skirting the southern margin of the outcrop extent, which thickens to the north.

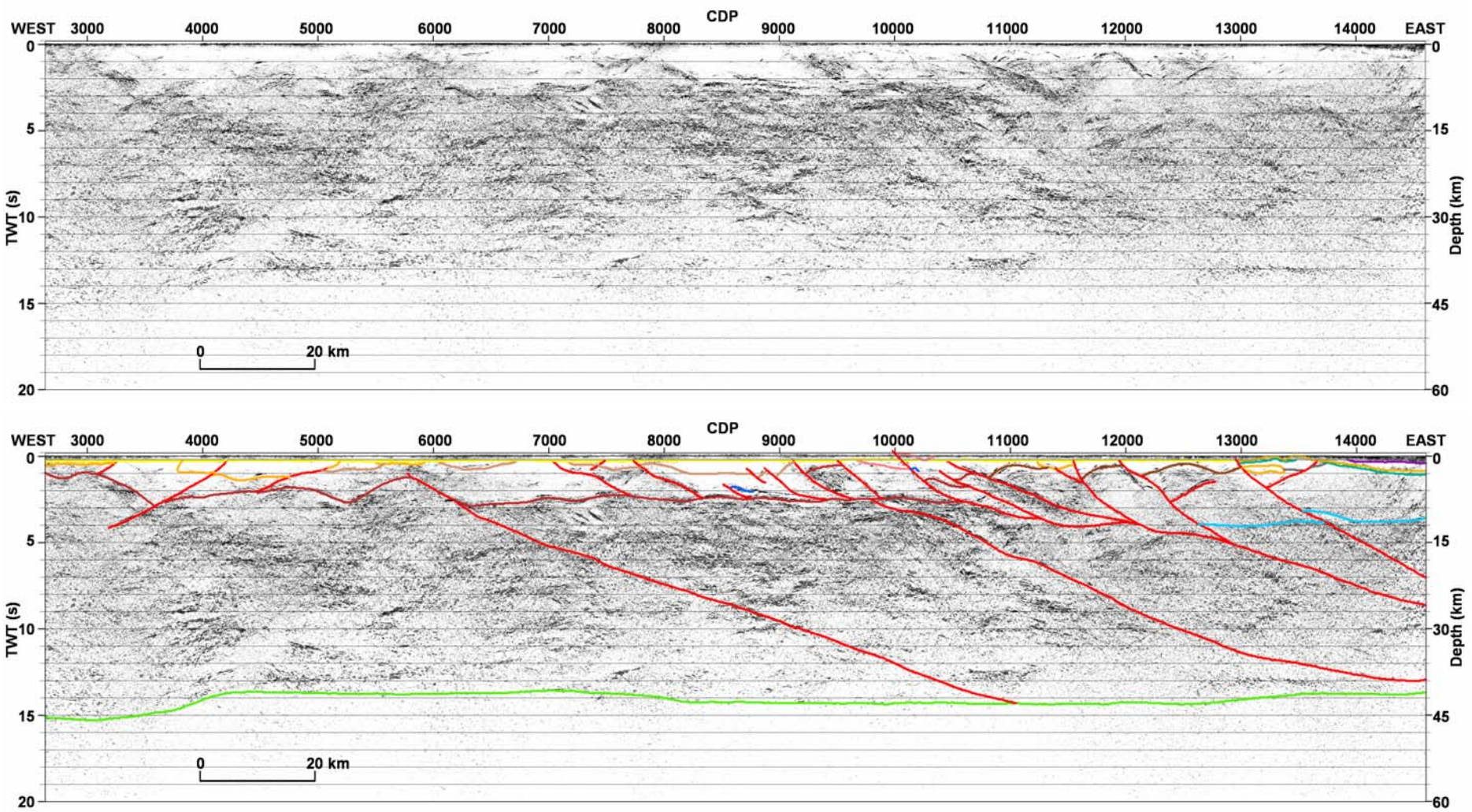

Figure 4. Migrated seismic section (upper panel) with interpretation (lower panel) for line 08GA-G1 in South Australia. Display shows the vertical scale equal to the horizontal scale, assuming a crustal velocity of 6000 m s^{-1}.

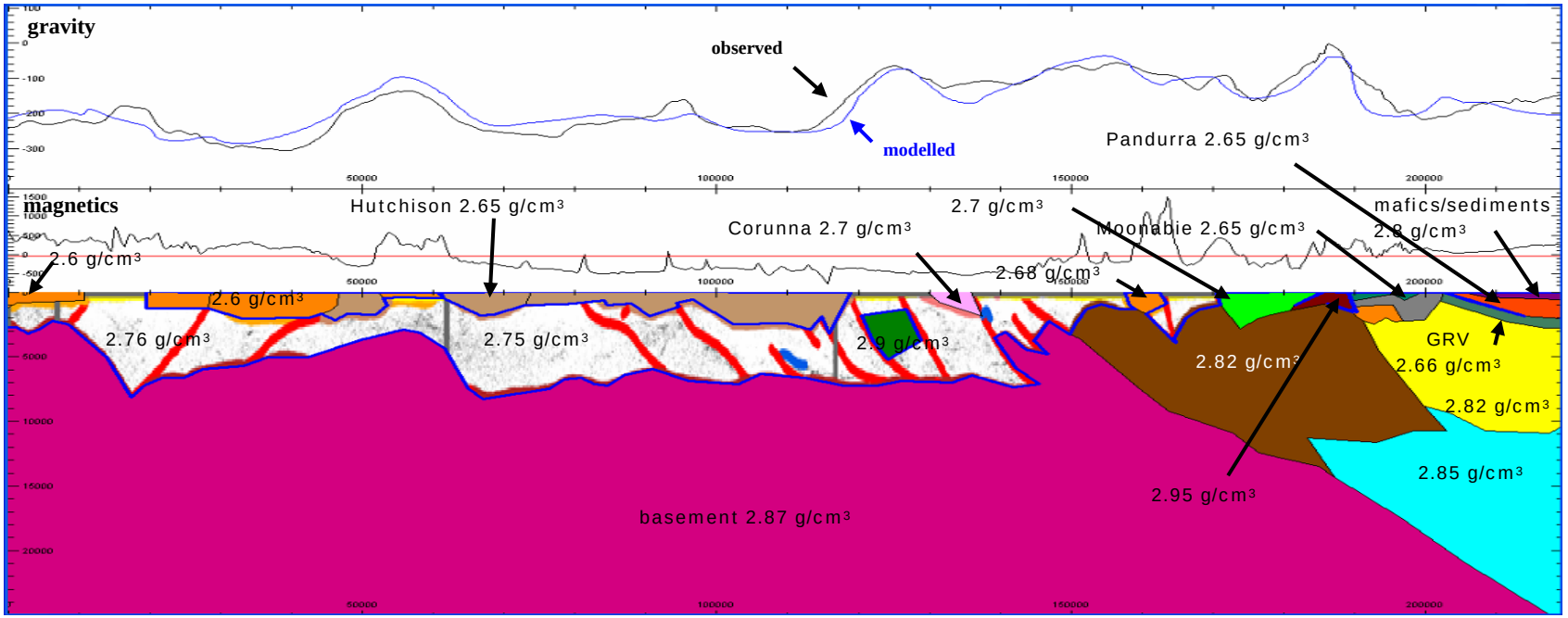

Figure 5. Forward model of the gravity profile along the seismic line 08GA-G1. The upper panel shows the observed gravity signal in black, and the modelled signal in blue. The middle panel shows observed magnetic signal. The lower panel shows the density model, with geometry based on interpretation of the seismic line, and densities as shown.

The Middleback Ranges consist of clastic and chemical sediments (dolomite, BIF) of the Middleback Subgroup, folded by doubly-plunging north-south trending tight to isoclinal folds, wrapping around a basement core of Mesoarchean (~3150 Ma) Cooyerdoo Granite (Fraser et al., 2010). Outcrop extent of the Middleback Subgroup and Cooyerdoo Granite is not crossed by the seismic line which passes immediately to the north. In the seismic line, reflective basement at ~0.4 s TWT at CDP 11800 is interpreted as "sub-Cooyerdoo" basement, acknowledging the evidence for pre-3150 Ma crust preserved in inherited zircons and Paleoarchean depleted mantle model ages from the Cooyerdoo Granite (Fraser et al., 2010).

Lake Gilles region

West of the Baxter Hills, the uppermost ~0.5 s TWT is only weakly reflective between CDP 11900 and 10000. Within this region, the Burkitt Granite crops out between CDP ~11500 and 11200. This is an undeformed, hornblende-bearing granite with high U content and high heat production (17 μWm^{-3}; Neumann et al., 2000). The Burkitt Granite has proven difficult to date due to the high U content of the zircons, and consequent radiation damage, with an imprecise age of ~1740 Ma indicating it is broadly coeval with the Kimban Orogeny (Fraser et al., 2010). Host rocks to the Burkitt Granite are at least as old as late Archean. Exposed gneiss to the east of the Burkitt Granite has yielded zircon ages of ~3150 Ma as well as metamorphic zircon ages of ~2500 Ma (Fraser et al., 2010). West of the Burkitt Granite, along the northern shore of Lake Gilles, a succession of interlayered felsic and mafic orthogneisses and paragneisses crops out. The age of these gneisses is constrained by a single U-Pb zircon age from a layer-parallel leucogranite with an age of ~2530 Ma (Fraser et al., 2010), suggesting these gneisses pre-date the Sleaford Orogeny.

Kalinjala Mylonite Zone

The Kalinjala Mylonite Zone (KMZ) was defined originally by Parker (1980) at Port Neill, over 150 km south of the seismic line. At Port Neill, the KMZ strikes northeast and is subvertical (mean dip 80–85° west; Parker, 1980). Parker (1980) traced the KMZ northwards via scattered outcrop and via a prominent aeromagnetic anomaly that appears as a steep gradient "west of the Middleback Ranges". The map in Parker (1980) shows the KMZ striking north-northeast adjacent to the western side of the Middleback Ranges, and offset by a north-northwest-striking fault that passes through the vicinity of Lake Gilles.

Ferris et al. (2002) state that the KMZ "separates the Cleve Domain from the Spencer Domain", and show this boundary trending north-northwest on northern Eyre Peninsula, passing through Lake Gilles. Thus, in the vicinity of the seismic line GA08-G1, the KMZ, as depicted by Ferris et al. (2002), is farther west than originally depicted by Parker (1980), and corresponds to a sharp north-northwest-trending boundary separating relatively magnetic rocks to the east from much less magnetic rocks to the west (Figure 1). This prominent magnetic boundary has also been equated with the KMZ by Reid et al. (2008). While we acknowledge differing interpretations of the northern extension of the KMZ, here we follow the usage of Ferris et al. (2002) and Reid et al. (2008).

In the vicinity of the seismic line, the north-northwest-striking KMZ swings to a northeasterly strike immediately south of where the seismic line crosses it at CDP 10400. The KMZ is not well imaged in the uppermost 0.6 s TWT, where the crust is essentially nonreflective, but is well imaged as an east-dipping planar structure from 0.6 to 3.0 s TWT (corresponding to depths from ~2 to ~9 km). A similar, subparallel structure is imaged slightly further west, reaching the surface at CDP 10000, and is interpreted as a splay of the KMZ. This structure bounds the eastern side of the Uno Range, composed of Corunna Conglomerate, which is predominantly gently east-dipping but, at its easternmost extent, is interpreted to be a footwall syncline below a thrust fault. This is consistent with limited field observations of steep west dips and overturned easterly dips in the vicinity of this interpreted fault zone (Morgan, 2007). The two splays of the KMZ are interpreted to mark a major change in the seismic character of the middle to lower crust, from relatively unreflective to the east to considerably more reflective to the west, marking the boundary between the middle to lower crustal Yeltana Seismic Province in the west, and the Warrakimbo Seismic Province in the east (Korsch et al., 2010).

Cleve and Coulta Domains

West of the KMZ, the seismic line traverses the Cleve Domain. The surface geology in this domain is dominated by metasedimentary rocks of the Paleoproterozoic Hutchison Group, but also includes felsic gneisses and granites. Recent geochronology (Fraser and Neumann, 2010) shows that these gneisses and granites are syn-Kimban Orogeny (~1740–1715 Ma), although many of the gneisses contain older inherited zircon, suggestive of either ~Sleaford-age (~2500–2450 Ma) or Miltalie Gneiss-aged (~2000 Ma) protoliths. Sedimentary rocks of the Hutchison Group include quartzite, BIF and dolomite. In the vicinity of the seismic line, outcrop of Hutchison Group is dominated by quartzites, which crop out south of the line near Wilcherry Hill and Weednanna Hill, and to the north of the line near Peter Pan Dam on Buckleboo Station. In magnetic images, the Cleve Domain is dominated by a uniformly low magnetic response, apart from narrow, folded, magnetic marker horizons, which are interpreted as BIFs of the Hutchison Group. In the seismic line, the Hutchison Group is interpreted as regions of very low seismic reflectivity, extending from the surface to variable depths between ~0.5 and 1.0 s TWT (up to ~3 km thickness), and distributed discontinuously across the Cleve Domain. The Hutchison Group is interpreted to overlie felsic gneisses of both ~Sleaford-age (~2500–2450 Ma) and Miltalie Gneiss-age (~2000 Ma), which were deformed, metamorphosed, and, in some cases, partially melted, during the Kimban Orogeny (~1740–1715 Ma). These gneisses are recognised in the seismic line as being slightly more reflective than the Hutchison Group, although still relatively weakly reflective. The Hutchison Group and the interleaved and underlying gneisses together form a weakly reflective upper crust, which extends to ~2 s TWT (~6 km depth), and is underlain by much more reflective middle and lower crust across the Cleve and Coulta Domains. Several east-dipping faults are imaged across the Cleve Domain; these sole-out along the subhorizontal boundary between upper and middle crust at ~2s TWT (~6 km depth). There is a distinct gravity high near the eastern side of the Cleve Domain, between CDP 9600 and 9200 (Figures 3, 5). This gravity high is centred over a region of high seismic reflectivity at depths of ~1 to 2 s TWT (depth of 3 to 6 km), and is bounded on either side by east-dipping faults or shear zones. Forward modelling of this gravity high (Figure 5) suggests that this region of unusually reflective upper crust is significantly denser than its surroundings (density ~2.9 g.cm^{-3}).

The western part of the Cleve Domain is intruded by granite plutons of the ~1590 Ma Hiltaba Suite. The seismic line crosses one of these granites, the Buckleboo Granite, between CDP 6700 and 5500, and another between CDP 5200 and 4200. On the seismic line, these granites appear as regions of uniformly weak reflectivity, difficult to distinguish from adjacent metasedimentary rocks of the Hutchison Group, and are restricted to the upper ~0.6 s TWT (depth of ~1.5 km).

Nuyts Domain

The westernmost portion of the seismic line crosses into the Nuyts Domain, a poorly exposed region characterised by a higher magnetic response than the adjacent Cleve and Coulta Domains, and with a distinctive blotchy magnetic pattern, which is interpreted to represent granite plutons. At the craton-scale, the Nuyts Domain is interpreted to be dominated by granites of the ~1615 Ma St Peter Suite (Cowley, 2006; Swain et al., 2008). The eastern boundary of the Nuyts Domain, as defined by Ferris et al. (2002) (Figure 1), appears in magnetic images as a north-south trending linear feature, interpreted as a fault at CDP 5400. In the seismic line, this fault is not clearly imaged in the near surface, but a crustal-scale, east-dipping structure is interpreted at depth. There is a distinct gravity high immediately west of the Nuyts-Coulta domain boundary (Figures 3, 5). Although outcrop in the Nuyts Domain is sparse, the seismic line crosses migmatitic felsic gneisses at Little Pinbong Rockhole at CDP 3400. Recent geochronology (Fraser and Neumann, 2010) shows that these gneisses are late-Kimban in age (~1715 Ma). Also present in this region are numerous undeformed plutons of the Hiltaba Suite, forming prominent local landmarks such as Mt Wudinna. Forward modelling of the gravity profile requires relatively low density rocks in the near surface across much of the Nuyts Domain, interpreted to be granites, most likely of the Hiltaba Suite. In the seismic line, west-dipping faults are interpreted to reach the surface at CDP ~5200 and ~4200.

Preliminary interpretation of the magnetotelluric results

Inverse modelling of magnetotelluric data collected along the seismic line shows a very resistive crust between 5-40 km with resistivities exceeding 10^5 Ohm.m overlain by a conductive cover in the top few kilometres with resistivities below 10 Ohm.m (Figure 6). A crustal conductor with resistivities of 10-100 Ohm.m extends from the surface to depths of around 40 km and is located underneath broadband sites epa02 to epa09. The conductor narrows towards the surface to a few kilometres width at maximum. The feature is robust for a variety of parameter models tested. Similarly, a crustal conductor can be seen underneath the western stations eyrBB01 to eyrBB03, which extends to depths of around 50 km. This conductor in the west is situated within the Nuyts Domain. The central crustal conductor is located near the boundary between the Coulta and Cleve Domains. There is no obvious deep crustal feature interpreted in the seismic data in this location. The central conductor in the MT model is consistent with being the northern extension of the Eyre Peninsula Conductivity Anomaly (EPCA) (Figure 7) that has been defined further south (White and Milligan, 1984; Kusi et al., 1998; Thiel et al., 2005), although the geological origin of this feature remains uncertain.

This model does not show any major feature on eastern Eyre Peninsula that would correlate with the change in seismic character or major east-dipping structures interpreted in that region.

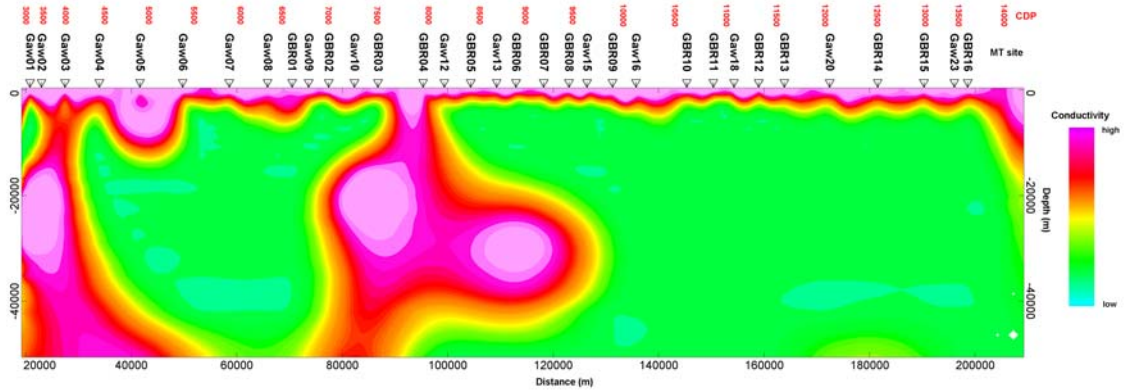

Figure 6. Two dimensional inverse model of the magnetotelluric profile across Eyre Peninsula, west (left) to east (right) (see details in Thiel et al., 2010).

Tectonic Implications

The first-order geometric features revealed by the seismic survey show a layered crust beneath the Cleve Domain of central Eyre Peninsula, in which seismically nonreflective upper crust overlies distinctly more reflective middle and lower crust of the Yeltana Seismic Province. The upper crust is interpreted as a combination of felsic gneisses and metasedimentary rocks of the Hutchison Group, deformed and metamorphosed during the Kimban Orogeny. The base of the nonreflective upper crust is defined by a relatively sharp transition to higher reflectivity at ~2 s TWT (depth of ~6 km). In the eastern part of the seismic section, in the Spencer Domain, the transition from low to higher reflectivity is much closer to the surface, and is interpreted to indicate the presence of shallower mid-crustal basement in the east. Velocity modelling of wide-angle seismic reflection data (Figure 8) produces a similar picture, with high velocity basement shallowing between the Cleve and Spencer Domains. The middle and lower crust forming the Warrakimbo Seismic Province at the eastern end of the line has a lower and more uniform seismic reflectivity compared to that beneath the Cleve Domain.

The boundary between the regions of differing seismic character is a zone in which major east-dipping structures, interpreted as splays of the Kalinjala Mylonite Zone, can be traced into the middle and lower crust. The presence of a boundary region in the vicinity of the Kalinjala Mylonite Zone, as interpreted from the seismic data, is consistent with a variety of other geophysical, geological and isotopic datasets which suggest a change in surface geology, crustal composition and geological history across this zone.

For example, gravity data show a long wavelength increase over the Spencer Domain compared with the Cleve Domain. Both inverse modelling of the regional gravity field (Chopping et al., 2010) and forward modelling of the gravity profile along the seismic line (Figure 5), require shallower basement beneath the Spencer Domain. Forward modelling of the gravity profile suggests that although relatively dense basement is present at shallower levels to the east of the KMZ, the density of this basement is, on average, slightly lower than the middle to lower crust to the west.

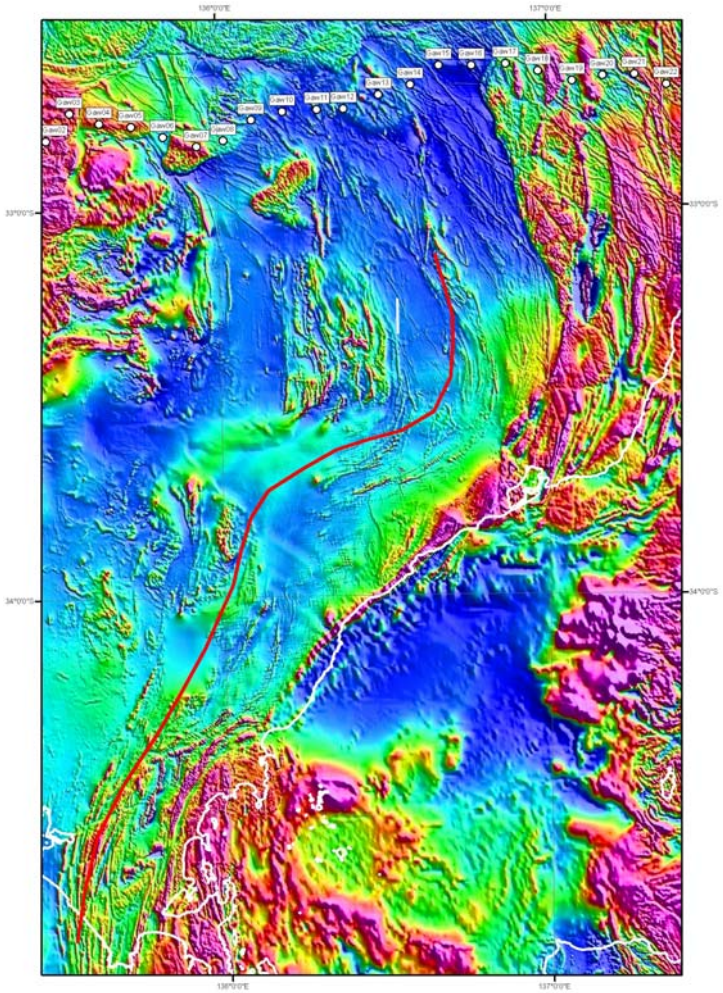

Figure 7. The axis of the previously-mapped Eyre Peninsula Conductivity Anomaly (red) overlain on an enhanced image of the total magnetic intensity (Milligan et al., 2004). The EPCA axis appears to follow trends in the Hutchison Group, and its extension north may result in the conductive anomaly observed in the MT data near site GAW11.

A significant change in surface geology is also evident across the KMZ. Gneissic and granitic rocks in the Cleve Domain exhibit evidence for high-grade metamorphism, partial melting, pervasive intense ductile deformation and granite intrusion during the Kimban Orogeny. In contrast, to the east of the KMZ, sedimentary and volcanic rocks of the Broadview Schist, McGregor Volcanics and Moonabie Formation were deposited prior to the Kimban Orogeny and, although uprightly folded, have been metamorphosed to significantly lower grades than the gneisses to the west. Outcrops of Mesoarchean crust have been found only to the east of the KMZ, and similarly, ~1850 Ma Donington Suite granites also are found only east of the KMZ. Conversely, Kimban-aged granites are not present to the east of the KMZ, with the possible exception of the Burkitt Granite, but are common to the west.

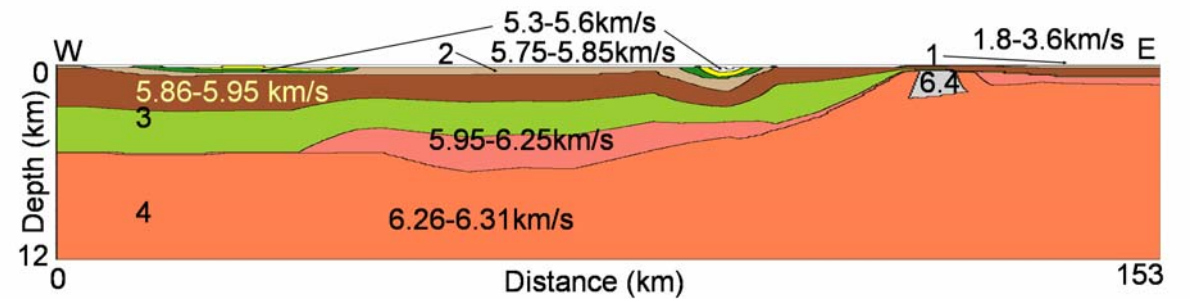

Figure 8. Velocity model of the upper crust derived from wide-angle data along the central part of the Gawler transect.

The location and geometry of the east-dipping seismic boundary between the Cleve and Spencer Domains provide new constraints on the underlying reasons for the observed changes in gravity, magnetic-intensity, metamorphic grade, stratigraphy, heat flow and mineralisation-style across this region. This boundary zone is inferred to separate deep crustal blocks of different composition and age, namely the Yeltana Seismic Province to the west and the Warrakimbo Seismic Province to the east. Nevertheless, when, how and how often the boundary has been tectonically active remain subject to interpretation. Geological evidence suggests this boundary was active during the Kimban Orogeny, with metamorphic grade variation suggesting an overall extensional component of movement at this time. This conflicts with previous interpretations that regard the KMZ as a dextral, transpressional structure during the Kimban Orogeny (Vassallo and Wilson, 2002). There is also evidence for subsequent thrust movement, perhaps broadly synchronous with the Olarian Orogeny, as suggested by offset of the Corunna Conglomerate on the eastern side of the Uno Range.

In the seismic section, the surface expression of the Roopena Fault is interpreted to link to a major east-dipping structure. This structure is likely to have acted as a controlling feature in the development of the Neoproterozoic Adelaide Geosyncline. Small fault scarps along the Roopena Fault indicate reverse-sense reactivation of this structure during the Quaternary (Crone et al., 2003).

Conclusions

Interpretation of seismic line GA08-G1 infers that a crustal-scale, east-dipping fault zone separates crust of different seismic character beneath the central versus the eastern Eyre Peninsula. The boundary zone broadly corresponds to the Kalinjala Mylonite Zone, forming the boundary between the Cleve and Spencer Domains at the surface and the Yeltana and Warrakimbo Seismic Provinces in the middle to lower crust. This insight from the seismic interpretation complements other geological datasets, which suggest a change in crustal age, density, geological history, radiogenic heat production, and mineralisation-style across the same structural zone. The seismic data, therefore, provide evidence for a structural and tectonic control underlying the patterns observed in a variety of disparate datasets. The timing and kinematics of movement within the structural zone remain open to interpretation. Nevertheless, the identification and interpreted geometry of this zone allow for improved constraints on geologically testable models, including energy and mineral exploration models.

Acknowledgements

We thank Paul Henson and Natalie Kositcin for their reviews of the manuscript.

References

Betts, P.G. and Giles, D., 2006. The 1800–1100 Ma tectonic evolution of Australia. *Precambrian Research*, **144**, 92–125.

Carr, L.K., Korsch, R.J., Holzschuh, J., Costelloe, R.D., Meixner, A.J., Matthews, C. and Godsmark, B. 2010. Geological interpretation of seismic reflection lines 08GA-C1 and 09TE-01: Arrowie Basin, South Australia. *Geoscience Australia, Record,* **2010/10**, this volume.

Chopping, R., Williams, N.C., Meixner, A.J. and Roy, I.G., 2010. 3D potential-field inversions and alteration mapping in the Gawler Craton and Curnamona Province, South Australia. *Geoscience Australia, Record,* **2010/10**, this volume.

Cowley, W.M., 2006. Solid geology of South Australia: peeling away the cover. *MESA Journal*, **43**, 4-15.

Crone, A.J., De Martini, P.M., Machette, M.N., Okumura, K. and Prescott, J.R., 2003. Paleoseismicity of two historically quiescent faults in Australia: Implications for fault behaviour in stable continental regions. *Bulletin of the Seismological Society of America*, **93**, 1913–1934.

Drown, C.G., 2003. The Barns gold prospect – discovery in an emerging district. *MESA* Journal, **28**, 4 -9.

Fairclough, M.C. and Curtis, S.O., 2008. PORT AUGUSTA 1:120 000 Geological Map, sheet SI 53-04. *Primary Industries and Resources South Australia.*

Ferris, G.M., Schwarz, M.P. and Heithersay, P., 2002. The Geological Framework, Distribution and Controls of Fe-oxide Cu-Au Mineralisation in the Gawler Craton, South Australia. Part I – Geological and Tectonic Framework. In: Porter, T. M., editor, *Hydrothermal Iron Oxide Copper-Gold and Related Deposits: A Global Perspective, Volume 2*. PGC Publishing, Adelaide, 9–31.

Ferris, G.M. and Schwarz, M.P., 2003. Proterozoic gold province of the central Gawler Craton. *MESA Journal*, **30**, 4–12.

Fomin, T., Holzschuh, J., Nakamura, A., Maher, J., Duan, J. and Saygin, E., 2010. 2008 Gawler-Curnamona-Arrowie (L189) and 2009 Curnamona-Gawler link (L191) seismic surveys – acquisition and processing. *Geoscience Australia, Record,* **2010/10**, this volume.

Fraser, G.L., Skirrow, R.G., Schmidt-Mumm, A. and Holm, O., 2007. Mesoproterozoic gold in the Central Gawler Craton, South Australia: Geology, Alteration, Fluids, and Timing. *Economic Geology*, **102**, 1511–1539.

Fraser, G.L, McAvaney, S., Neumann, N.L., Szpunar, M., Reid, A.J., 2010. Discovery of Mesoarchean crust in the eastern Gawler Craton, South Australia. *Precambrian Research, in press.*

Fraser, G.L. and Neumann, N.L., 2010. Compilation of SHRIMP U-Pb geochronological data, Gawler Craton, Curnamona Craton, and Mt Painter Province, South Australia, 2008-2010. *Geoscience Australia, Record, in preparation.*

Hand, M., Reid, A.J. and Jagodzinski, E., 2007. Tectonic framework of Evolution of the Gawler Craton, Southern Australia. *Economic Geology*, **102**, 1377–1395.

Korsch, R.J., Preiss, W.V., Blewett, R.S., Cowley, W.M., Neumann, N.L., Fabris, A.J., Fraser, G.L., Dutch, R., Fomin, T., Holzschuh, J., Fricke, C.E., Reid, A.J., Carr, L.K. and Bendall, B.R., 2010. Deep seismic reflection transect from the western Eyre Peninsula in South Australia to the Darling Basin in New South Wales: Geodynamic implications. *Geoscience Australia, Record,* **2010/10**, this volume.

Kusi, R., White, A., Heinson, G. and Milligan, P., 1998. Electromagnetic induction studies in the Eyre Peninsula, South Australia. *Geophysical Journal International*, **132**, 687–700.

Milligan, P.R. and Franklin, R., 2004. Magnetic Anomaly Map of Australia (Fourth ed.), 1:5 000 000 scale, Geoscience Australia, Canberra.

Morgan, L.M., 2007. Depositional history of the Corunna Conglomerate: Tectonic implications of an evolving Palaeo- to Mesoproterozoic depocentre in the Gawler Craton, South Australia. *Unpublished Honours Thesis*, Monash University.

Neumann, N., Sandiford, M. and Foden, J., 2000. Regional geochemistry and continental heat flow: implications for the origin of the South Australian Heat Flow anomaly. *Earth and Planetary Science Letters,* **183**, 107-120.

Parker, A.J., 1980. The Kalinjala mylonite zone, eastern Eyre Peninsula. *Geological Survey of South Australia, Quarterly Geological Notes*, **76**, 6–11.

Preiss, W.V., Korsch, R.J., Blewett, R.S., Fomin, T., Cowley, W.M., Neumann, N.L. and Meixner, A.J., 2010. Geological interpretation of deep seismic reflection line 09GA-CG1: the Curnamona Province-Gawler Craton Link Line, South Australia. *Geoscience Australia, Record,* **2010/10**, this volume.

Reid, A. J., McAvaney, S. O. and Fraser, G. L., 2008. Nature of the Kimban Orogeny across northern Eyre Peninsula. *MESA Journal*, **51**, 25–34.

Swain, G., Barovich, K., Hand, M., Ferris, G. and Schwarz, M., 2008. Petrogenesis of the St Peter Suite, southern Australia: Arc magmatism and Proterozoic crustal growth of the South Australian Craton. *Precambrian Research*, **166**, 283–296.

Thiel, S., Heinson, G. and White, A., 2005. Tectonic evolution of the southern Gawler Craton, South Australia, from electromagnetic sounding. *Australian Journal of Earth Sciences*, **52**, 887-896.

Thiel, S., Milligan, P.R., Heinson, G., Boren, G., Duan, J., Ross, J., Adam, H., Dhu, T., Fomin, T., Craven, E., and Curnow, S., 2010. Magnetotelluric acquisition and processing, with examples from the Gawler, Curnamona and Link transects in South Australia. *Geoscience Australia, Record,* **2010/10**, this volume.

Vassallo, J.J. and Wilson, C.J.L., 2002. Palaeoproterozoic regional-scale non-coaxial deformation: an example from eastern Eyre Peninsula, South Australia. *Journal of Structural Geology,* **24**, 1–24.

White, A., and Milligan, P.R., 1984. A crustal conductor on the Eyre Peninsula, South Australia. *Nature*, **310**, 219–222.

3D potential-field inversions and alteration mapping in the Gawler Craton and Curnamona Province, South Australia

R. Chopping, N.C. Williams, A.J. Meixner and I.G. Roy

Onshore Energy & Minerals Division, Geoscience Australia, GPO Box 378, Canberra, ACT 2601, Australia

richard.chopping@ga.gov.au

Introduction

Inversions of potential-field (gravity or magnetic data) are techniques where a numerical algorithm identifies candidate physical property distributions (densities or magnetic susceptibilities) that reproduce observed gravity or magnetic data. The inversion property models provide a powerful insight into the subsurface geology of a region. The source of potential-field responses is entirely nonunique; coupled with the fact that many inverse models will fit observed data within measurement errors, means that 3D inversion results are highly nonunique, and meaningful results are only obtained by including both mathematical and geological constraints on the inversion algorithm. Despite the nonuniqueness of the results, inversions provide a quantitative estimate of the physical properties beneath a study area. These estimates of physical properties can be interpreted to extend our knowledge of subsurface geology away from known areas such as seismic lines, and to map alteration systems, even in areas of extensive cover.

This study used property inversions for gravity and magnetic data, which were conducted using commercially-available inversions software from the University of British Columbia–Geophysical Inversion Facility (UBC-GIF): *grav3d* (Li and Oldenburg, 1998a) and *mag3d* (Li and Oldenburg, 1996). Property inversions are those that produce a physical property model, rather than a geological model, from the inversion algorithm.

The data used were all publicly released gravity and magnetic grids for the region, available from the *Geophysical Archive Data Delivery System* (*GADDS*: http://www.geoscience.gov.au/gadds/). Examples of the gravity and magnetic data for the Gawler Craton and Curnamona Province in South Australia, with location of seismic lines mentioned in this study, are shown in Figures 1 and 2.

To mitigate the extreme nonuniqueness of inversions it is critical that available geological knowledge must be included as constraints on the inversion. In complex ancient terranes like the Gawler Craton, devising appropriate and reliable constraints is challenging. Geologically-constrained inversions will find candidate physical property models that are consistent with both the supplied geophysical data and the supplied geological data. Although constraints do not eliminate the nonuniqueness of inverse solutions, they soften its effect, and better reflect the subsurface. Furthermore, the nonuniqueness of inversion results requires inversions to be conducted in an iterative fashion, updating constraints as new or revised geological knowledge, such as seismic interpretations, become available.

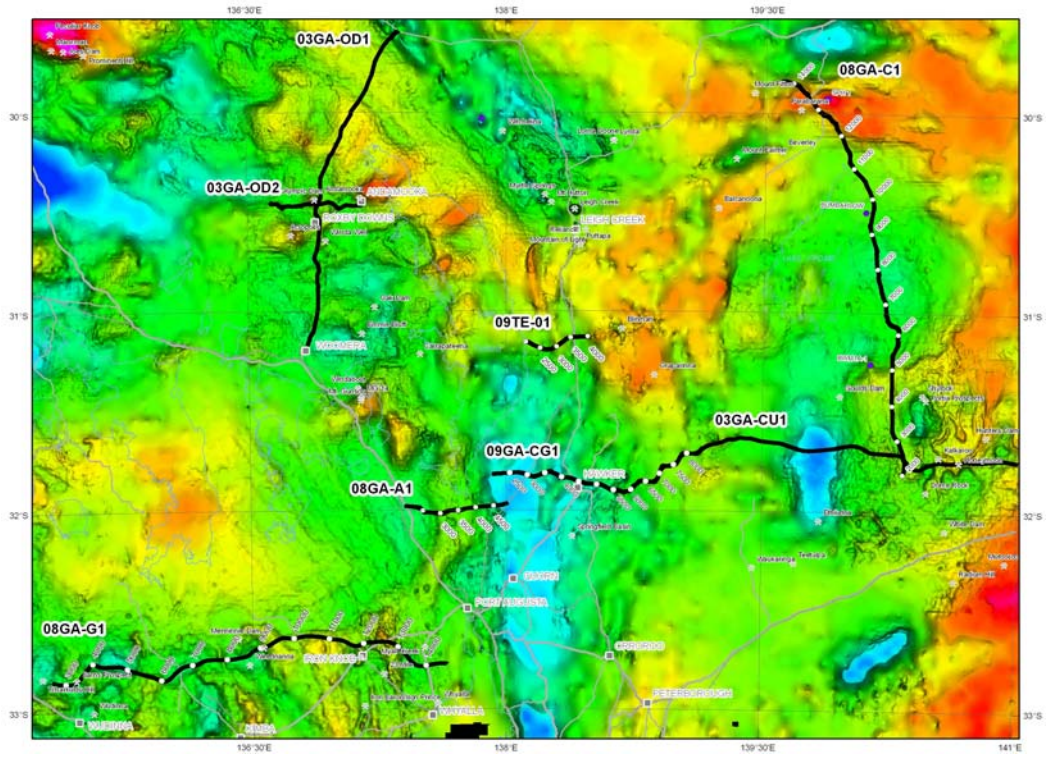

Figure 1. Gravity map for the study area in the Gawler Craton and Curnamona Province (warm colours are gravity highs, cool colours are gravity lows). Locations of seismic lines are depicted; for seismic interpretations see other papers in this volume.

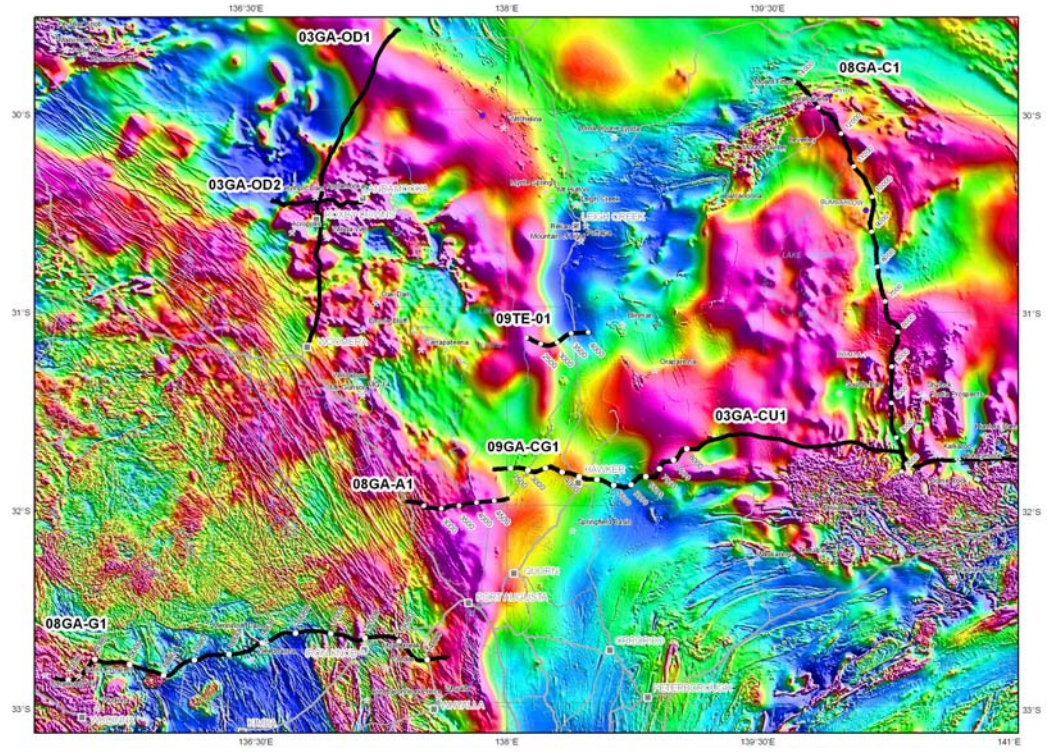

Figure 2. Total magnetic intensity map for the study area in the Gawler Craton and Curnamona Province (warm colours are high magnetic intensities, cool colours are low magnetic intensities). Locations of seismic lines are depicted; for seismic interpretations see other papers in this volume.

Constraints on an inversion do not depend just on geological information. Geological information must also be accompanied by physical property information to properly constrain an inversion. Generally, obtaining suitable, meaningful and abundant physical properties is the major difficulty in applying constraints to potential-field inversions. This study was limited by the paucity of physical property knowledge, however, even simple constraints, such as adding a constraint that the top layer of cells in the mesh are expected to be lower density due to weathering, improves the recovered inversion model (Figure 3).

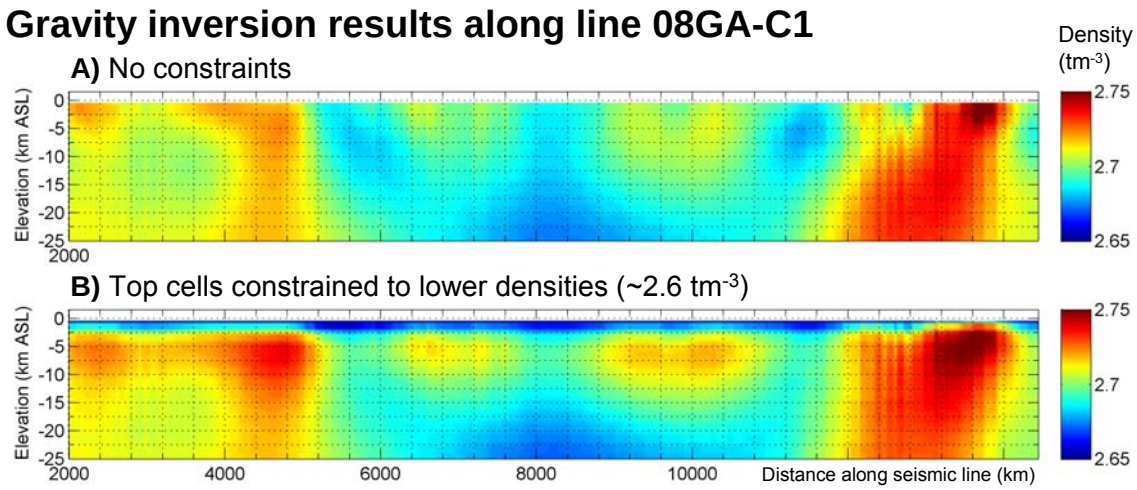

Figure 3. Comparison of A) default (unconstrained or constrained only by inversion smoothness parameters) and B) top layer of cells constrained to ~2.6 tm^{-3} *grav3d* inversions. Note the differences in recovered models, especially the higher density contrasts recovered in the basement beneath the lower density topmost layer of cells. These results are extracted along the 08GA-C1 seismic line from full 3D inversions.

Inversion methodology

A number of key steps are required in the preparation of potential-field inversions, and were applied in this study. These key steps, drawing heavily on the Williams et al. (2008) are:

1. Define study area.

This study area makes up the core of the inversion results. The core is surrounded on either side by an appropriate number of padding cells to prevent artefacts at the edges of the mesh volume. The core for this study is 600 x 510 x 25 km (east-west x north-south x height), and the padded core is 700 x 610 x 25 km.

2. Define regional area for regional-residual separation.

The regional-residual separation conducted for this study used the model-based, regional-residual separation of Li and Oldenburg (1998b). This requires a second inversion for the regional model, which also requires padding. The regional inversion required was 780 x 700 x 40 km; the padded regional inversion was 940 x 860 x 40 km.

3. Prepare grids of gravity, magnetic and topographic data, covering required areas.

Note that these data need to cover a significantly wider area than the core inversion. This is due to the requirement of padding for both the core and regional inversions. These data can be extracted from appropriate national compilations, or can be created by gridding available gravity, magnetic and topopgraphic information. These data also need to be upward-continued to approximately a height equal to that of the cell sizes to remove small features that cannot effectively be modelled in a volume of this size; for the regional inversion this is a height of 4 km, and for the core inversion it was 2 km.

4. Conduct model-based, regional-residual separation.

5. Apply constraints to the core inversion.

These constraints are applied using the techniques of Williams et al. (2009) and Williams (2009).

6. Conduct core inversion.

The core inversion for this study covered the area shown in Figures 1 and 2, and to a maximum depth of 25 km below Australian Height Datum. Cell dimensions were 2 x 2 km in lateral extent and 1 km in vertical extent. Due to the size of the corresponding inversion problems, the inversions for this study were conducted either using the Condor distributed computing network at Geoscience Australia (Litzkow et al., 1988) or the facilities at the National Computational Infrastructure (NCI: http://nci.org.au) at the Australian National University (ANU).

Inversion results

Although the inversion results are 3D volumes (Figure 4), for brevity and to best compare with other papers in this volume, we will present 2D sections extracted along two seismic lines: 08GA-C1 and 08GA-G1. The geological interpretations of these seismic lines are discussed in Korsch et al. (2010) and Fraser et al. (2010). Note that all inversion results will be further revised in the future; the preliminary results presented here are as of March 2009.

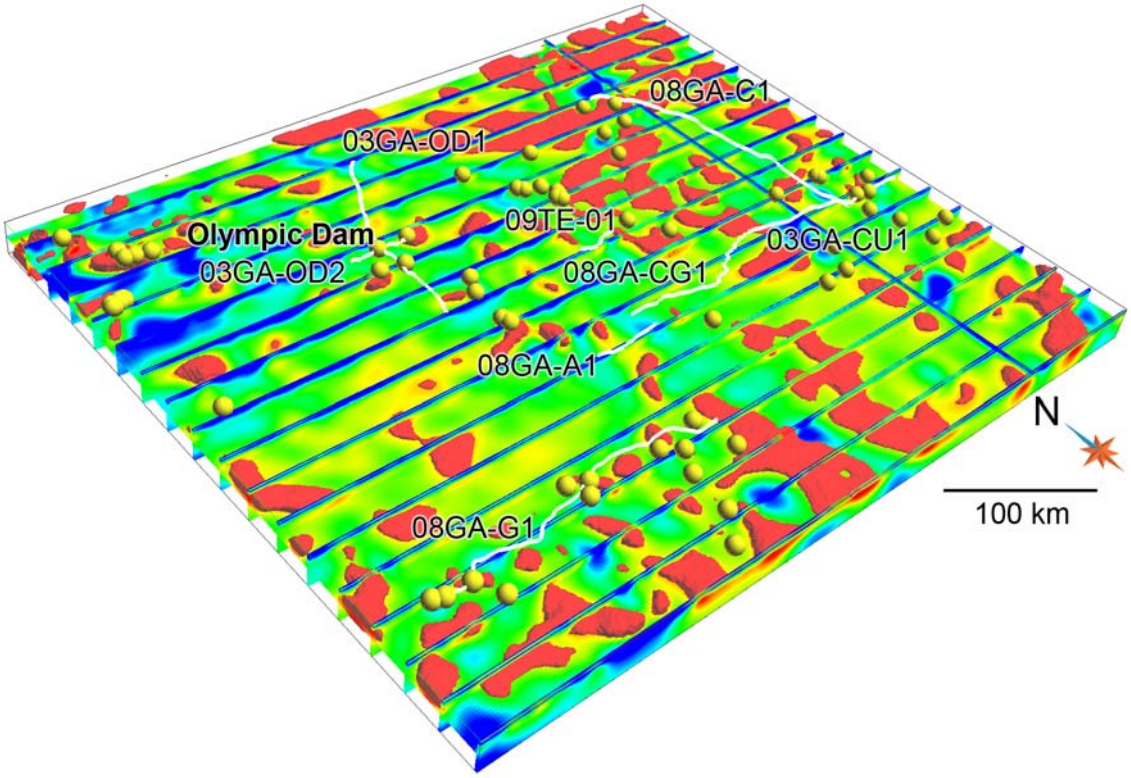

Figure 4. Gravity inversion for the study area in the Gawler Craton. Location of seismic lines and significant mineral occurrences (yellow spheres) are shown. Surfaces in red are isosurfaces (3D contours) of the highest densities recovered in the inversion. East-west sections at ~30 km spacing, horizontal (depth) slice is at 10 km depth. Of note is the band of high-density crust intersecting the northern portion of line 08GA-C1 (Figure 5 and discussed below).

08GA-C1

The most significant feature apparent in the inversion results for line 08GA-C1 is the separation between higher density crust to the north and lower density crust to the south, at approximately CDP 12000 (Figure 5). This reflects the differences between the Mt Painter Inlier and the Curnamona Province, and is a feature visible both in the seismic reflection data and the magnetotelluric results (Korsch et al., 2010). Crust towards the southern end of the line (CDP ~5000) is also dense, corresponding to shallower basement (Korsch et al., 2010).

08GA-G1

In contrast to the 08GA-C1 line, the inversion results along line 08GA-G1 are dominated by significantly more discrete anomalies (Figure 6). The anomalous zones are smoothed in the depth direction by the inversion algorithm (a feature of *grav3d* and *mag3d* inversions). These anomalies are the result of small discrete near-surface bodies (Fraser et al., 2010) and obscure the major feature recovered in the inversion, which is an indication of the slightly denser basement becoming significantly closer to the surface to the east of CDP ~9000.

Forward-modelling of the gravity response along 08GA-G1 (Fraser et al., 2010) indicates that the basement to the east of CDP 9500 is slightly less dense than the basement to the west, it is also located on an east-dipping fault (possibly a thrust fault). Neither of these features are particularly well resolved in the seismic image. To best understand the extent of these features to the north and south, use of the latest seismic interpretation and forward modelling results is required.

Alteration mapping

Mineralogy primarily controls the magnetic susceptibilities and densities of crystalline basement rocks (Carmichael, 1989; Guéguen and Palciauskas, 1994). Although the mineralogy of a rock may be quite complex, the densities and magnetic susceptibilities of the common rock-forming minerals (for example, feldspar, quartz, pyroxene) dominate the gross property values of unaltered rocks. Some alteration end-members, such as hematite, sulfides or magnetite, show significant property contrasts to the common rock-forming minerals. As chemical alteration, by definition, changes the mineralogy of a rock, rocks altered to contain significant proportions of magnetite, sulphides or hematite can show significant physical property contrasts to unaltered host rocks.

Two methods have been developed to map alteration systems: a qualitative and a quantitative method (Williams and Chopping, 2009). The qualitative method interprets alteration trends on plots of magnetic susceptibility versus density and assigns each cell as either unaltered or altered to one of many alteration end-members (Chopping and van der Wielen, 2009). In contrast, the quantitative method seeks to solve a system of three linear equations and produces a quantitative estimate of the abundances of host and all alteration assemblages (Williams and Dipple, 2007). For brevity, this discussion is limited to highlighting the mapping of magnetite in the subsurface using the quantitative alteration mapping method.

Mapping of magnetite in the Gawler Craton highlights some features which are of a very large scale and are therefore more likely to be associated with more iron-rich primary lithologies, as well as highlighting some smaller-scale features which are likely to be the result of hydrothermal alteration (Figure 7). Specifically, the magnetite alteration map (Figure 8) highlights Olympic Dam and prospects surrounding it. Previous studies (Williams and Dipple, 2007) have also indicated the existence of hematite and/or sulfides around these prospects and elsewhere.

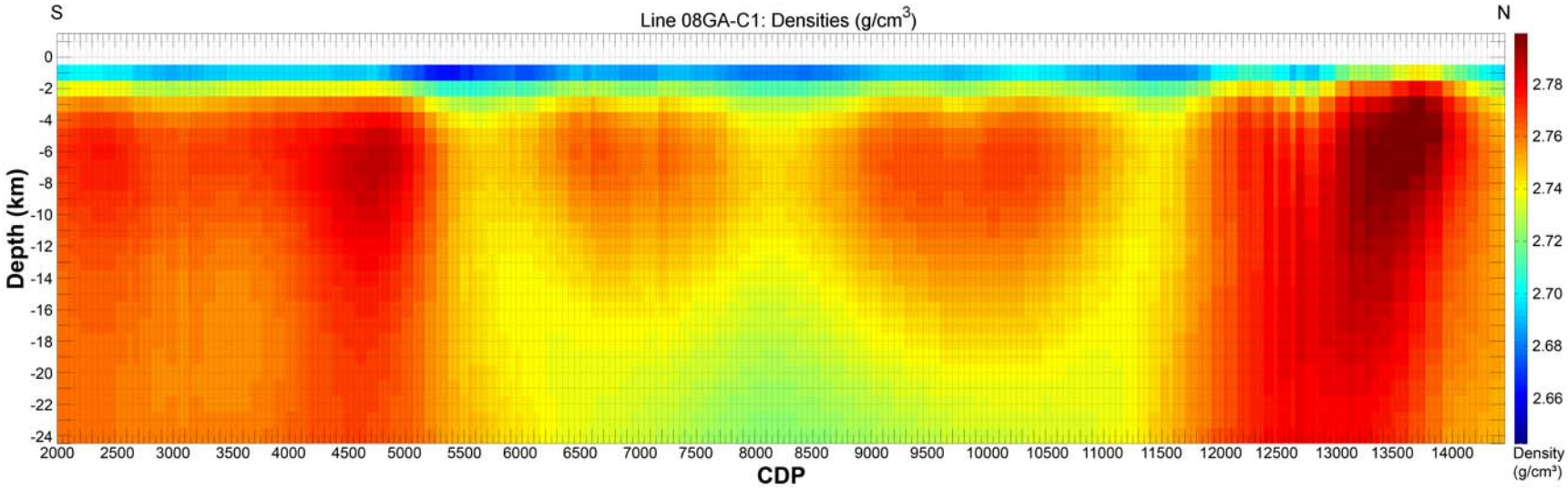

Figure 5. Gravity inversion results extracted along line 08GA-C1.

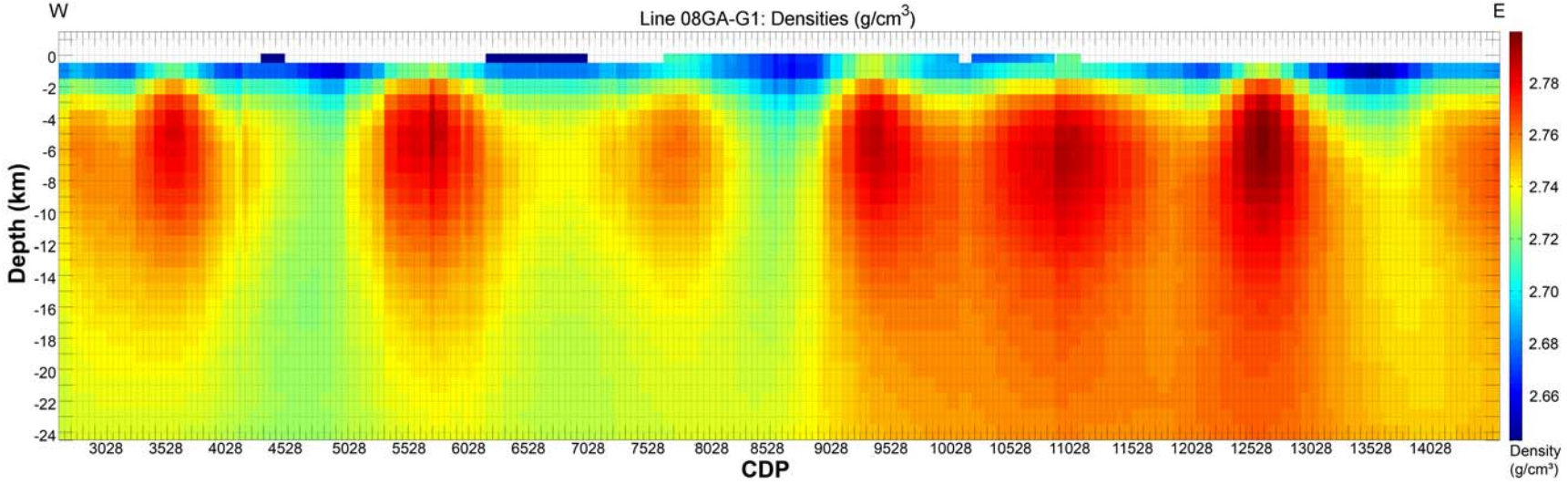

Figure 6. Gravity inversion results extracted along line 08GA-G1.

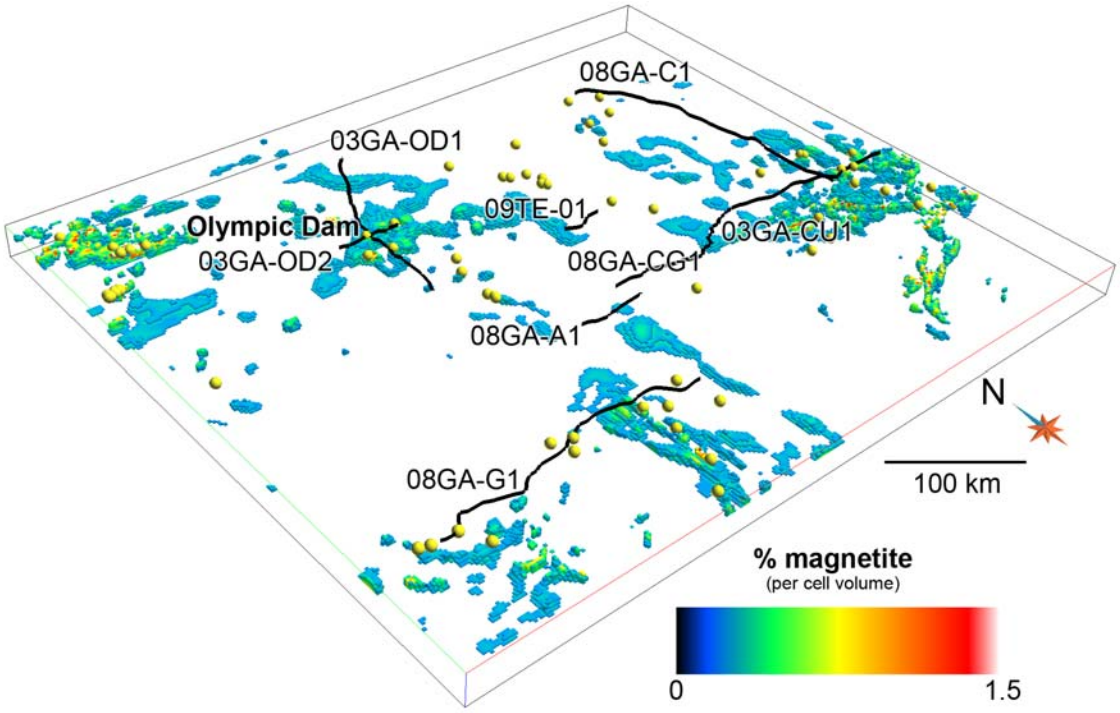

Figure 7. Alteration mapping results highlighting percent magnetite recovered by the gravity and magnetic inversions in the Gawler Craton. Locations of seismic lines and significant mineral occurrences (yellow spheres) are highlighted. The displayed cells are all those with >0.3% magnetite per cell volume. Cells are further coloured by the percentage magnetite they contain.

Conclusions

Although no inversion result can be viewed as final, property inversions in the Gawler Craton and Curnamona Province allow us to better understand the full 3D geometries of features interpreted in the seismic data, as well as extending our knowledge away from the seismic lines. Furthermore, the use of inversions provide useful insights into chemical alteration, including in regions under significant cover. As always, further work is required to fully refine the inversions, especially in regions with small, near-surface anomalies, which obscure more broad general features in the inversions.

Acknowledgements

We thank Natalie Kositcin and Anthony Schofield for their comments on the manuscript.

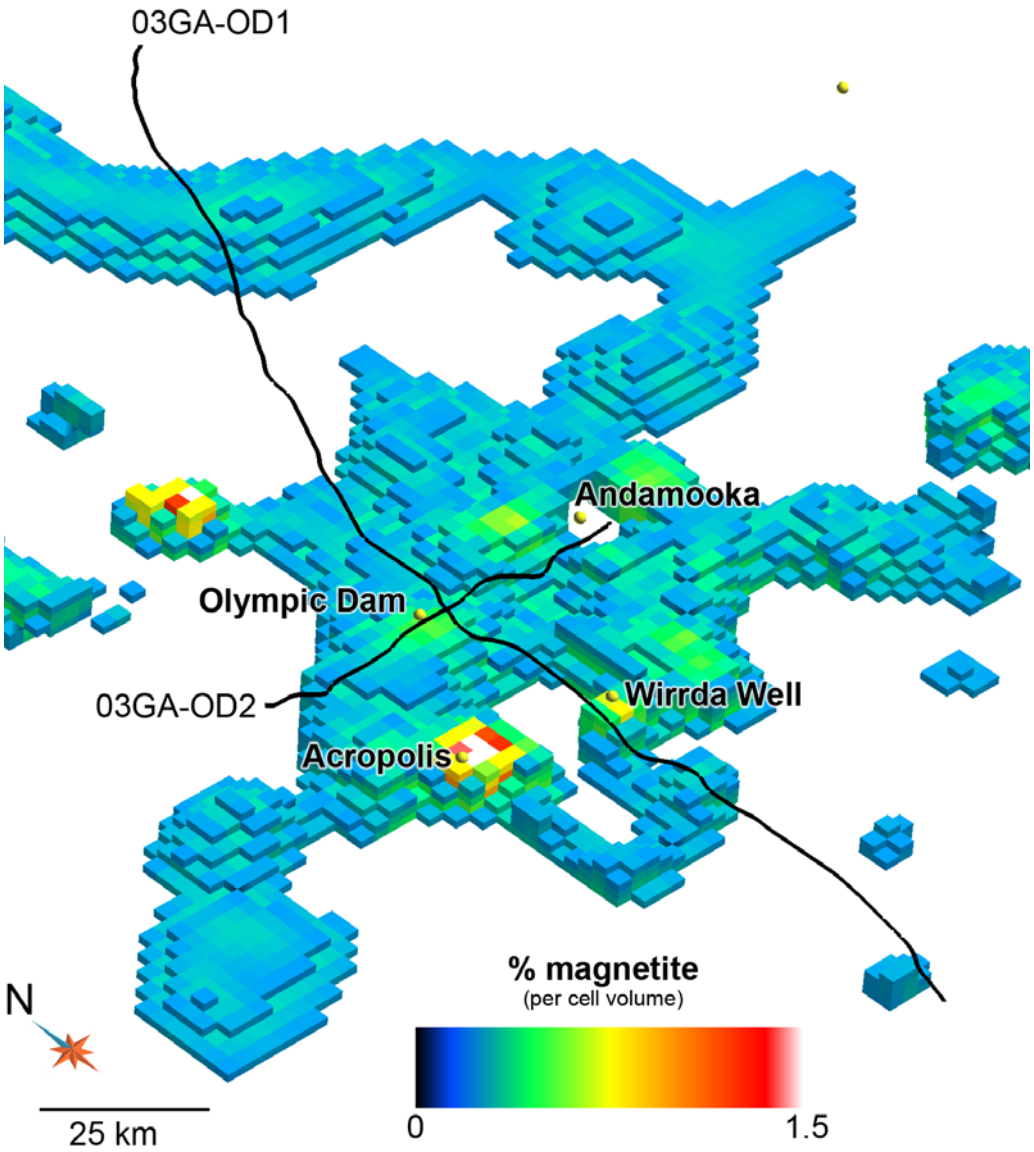

Figure 8. Alteration mapping results highlighting percent magnetite recovered by the gravity and magnetic inversions in the vicinity of Olympic Dam. As per Figure 7, the displayed cells are all those with >0.3% magnetite per cell volume. Cells are further coloured by the percentage magnetite they contain. Although it appears Andamooka is not associated with magnetite alteration, this is an artefact of the perspective view displayed here.

References

Carmichael, R.S., 1989. *Practical Handbook of Physical Properties of Rocks and Minerals*. CRC Press, 741pp.

Chopping, R. and van der Wielen, S.E., 2009. Querying potential field inversions for signatures of chemical alteration: An example from Cobar, NSW. In: Proceedings of the 20th International Geophysical Conference and Exhibition, Adelaide. *Preview (Australian Society of Exploration Geophysicists),* **138**, 85.

Fraser, G.L., Blewett, R.S., Reid, A.J., Korsch, R.J., Dutch, R., Neumann, N.L., Meixner, A.J., Skirrow, R.G., Cowley, W., Szpunar, M., Preiss, W.V., Nakamura, A., Fomin, T., Holzschuh, J., Milligan, P. and Bendall, B., 2010. Geological interpretation of deep seismic reflection and magnetotelluric line 08GA-G1: Eyre Peninsula, Gawler Craton, South Australia. *Geoscience Australia, Record,* **2010/10**, this volume.

Guéguen, Y. and Palciasuskas, V., 1994. *Introduction to the Physics of Rocks*. Princeton University Press, 294p.

Korsch, R.J, Preiss, W.V., Blewett, R.S., Fabris, A.J., Neumann, N.L., Fricke, C.E., Fraser, G.L., Holzschuh, J., Milligan, P.R. and Jones, L.E.A., 2010. Geological interpretation of deep seismic reflection and magnetotelluric line 08GA-C1: Curnamona Province, South Australia. *Geoscience Australia, Record,* **2010/10**, this volume.

Li, Y. and Oldenburg, D.W., 1996. 3-D inversion of magnetic data. *Geophysics*, **61(2)**, 394-408.

Li, Y. and Oldenburg, D.W., 1998a. 3-D inversion of gravity data. *Geophysics*, **63(1)**, 109-119.

Li, Y. and Oldenburg, D.W., 1998b. Separation of regional and residual magnetic field data. *Geophysics*, **63(2)**, 431-439.

Litzkow, M.J., Livny, M. and Mutka, M.W., 1988. Condor – A Hunter of Idle Workstations. *Proceedings of the 8th International Conference of Distributed Computing Systems*, 104-111.

Williams, N.C. and Dipple, G.M., 2007. Mapping subsurface alteration using gravity and magnetic inversion models. In: Milkereit, B., editor, *Proceedings of Exploration 07: Fifth Decennial International Conference on Mineral Exploration*, 461-472.

Williams, N.C, Lane, R., Oldenburg, D.W., Lelievre, P., Phillips, N. and Jones, F., 2008. A workflow for preparing and applying UBC-GIF gravity and magnetic inversions. In: Williams, N.C., *Geologically-constrained UBC-GIF gravity and magnetic inversions with examples from the Agnew-Wiluna greenstone belt, Western Australia.* Ph.D. thesis, University of British Columbia, 478pp. http://hdl.handle.net/2429/2744/.

Williams, N.C., 2009. An automated sparse constraint model builder for UBC-GIF gravity and magnetic inversions. In: Proceedings of the 20th International Geophysical Conference and Exhibition, Adelaide. *Preview (Australian Society of Exploration Geophysicists),* **138**, 60-61.

Williams, N.C. and Chopping, R., 2009. Mapping alteration in 3D using potential field data. In: Chopping, R. and Henson, P.A., editors, 3D map and supporting geophysical studies in the North Queensland region. *Geoscience Australia, Record,* **2009/29**, 68-79.

Williams, N.C., Lelievre, P. and Oldenburg, D.W., 2009. Constraining gravity and magnetics inversions for mineral exploration using limited geological data. In: Proceedings of the 20th International Geophysical Conference and Exhibition, Adelaide. *Preview (Australian Society of Exploration Geophysicists),* **138**, 85-86.

Deep seismic reflection transect from the western Eyre Peninsula in South Australia to the Darling Basin in New South Wales: Geodynamic implications

R.J. Korsch[1], W.V. Preiss[2], R.S. Blewett[1], W.M. Cowley[2], N.L. Neumann[1], A.J. Fabris[2], G.L. Fraser[1], R. Dutch[2], T. Fomin[1], J. Holzschuh[1], C.E. Fricke[2], A.J. Reid[2], L.K. Carr[1] and B.R. Bendall[2]

[1]Onshore Energy & Minerals Division, Geoscience Australia, GPO Box 378, Canberra, ACT 2601, Australia
[2]Primary Industries and Resources South Australia (PIRSA), GPO Box 1671, Adelaide, SA 5001, Australia

Russell.Korsch@ga.gov.au

Introduction

In 2008 and 2009, Geoscience Australia, through its Onshore Energy Security Program, in conjunction with Primary Industries and Resources South Australia (PIRSA), acquired a total of 720.5 km of vibroseis-source, deep seismic reflection data in southern South Australia. This consisted of four separate profiles, namely, a 253.48 km long profile in the southern Gawler Craton (Fraser et al., 2010a), a 60.4 km long profile across the western Arrowie Basin (Carr et al., 2010), a 262.16 km long, north-south oriented profile in the Curnamona Province in South Australia (Korsch et al., 2009, 2010) and a 144.44 km long profile which links the Gawler Craton to the Curnamona Province (Preiss et al., 2010).

Prior to these deep seismic surveys, in 1996-97 a consortium consisting of the Geological Survey of New South Wales (Industry & Investment NSW) and the Australian Geodynamics Cooperative Research Centre, acquired 295 km of explosive (dynamite) source deep seismic reflection data in the Curnamona Province in New South Wales from the South Australian border eastwards to the Darling Basin (Gibson et al., 1998). In 2003-04, another consortium consisting of PIRSA, the Predictive Mineral Discovery Cooperative Research Centre (***pmd****CRC*) and Geoscience Australia acquired 198 km of vibroseis source deep seismic reflection data in the Curnamona Province in South Australia from the New South Wales border to the Flinders Ranges (Goleby et al., 2006).

The data from the original 1996-97 seismic survey were reprocessed using current seismic processing techniques (Fomin et al., 2006; Korsch et al., 2006), and these were combined with the 2003-04 data to form a single ~400 km long transect across the Curnamona Province from the Darling Basin in the east to the Flinders Ranges in the west (Korsch et al., 2006a). We are now able to combine these seismic lines with those lines acquired in 2008-09, which have an approximate east-west orientation, to form a single east-west traverse ~800 km long (Table 1, Figure 1). Note that the two western seismic profiles do not link physically to the rest of the transect.

Table 1. Summary of seismic lines used to form the east-west transect.

LINE	AREA	LENGTH	SOURCE	FOLD (NOMINAL)
08GA-G1	Gawler Craton (northern Eyre Peninsula)	253.48 km	Vibroseis	75
08GA-A1	Arrowie Basin (west of Flinders Ranges)	60.4 km	Vibroseis	75
09GA-CG1	Central Flinders Ranges	144.44 km	Vibroseis	75
03GA-CU1	Curnamona Province, SA	197.6 km	Vibroseis	60
96AGS-BH1A	Broken Hill Domain, Curnamona Province, NSW	52.96 km	Explosives	10
96AGS-BH1B	Broken Hill Domain - Murray Basin - Darling Basin	162.0 km	Explosives	10

Seismic Acquisition and Processing

The transect described here consists of two sets of vibroseis data (both 60 fold and 75 fold, Table 1) collected about five years apart, and 10 fold dynamite seismic data collected in 1996-97, which were reprocessed in 2005-06. Despite the differences in acquisition and processing parameters (compare Goleby et al., 2006; Korsch et al., 2006a; Fomin et al., 2010), it is possible to reuse old, low fold seismic data by utilising new processing techniques. Korsch et al. (2006a) demonstrated the comparability in the resolution of reprocessed dynamite and new vibroseis data. Thus, the various datasets have been combined into a coherent east-west transect, which can be interpreted in terms of the geodynamic evolution of the region.

Regional Geology along the Eyre Peninsula-Darling Basin Transect

At the surface, although mostly covered by Cenozoic sediment and alluvium, the Eyre Peninsula-Darling Basin transect crosses part of the Gawler Craton, Adelaide Rift System, Curnamona Province, Koonenberry Belt and Darling Basin (Figure 2). In the west, the transect crosses the Gawler Craton, which consists of Mesoarchean (~3150 Ma granites, Fraser et al., 2010b) to Mesoproterozoic sedimentary, volcanic, metamorphic and granitic rocks (Reid et al., 2010). To the east, Neoproterozoic and Cambrian rocks of the Adelaide Rift System (Preiss, 2010) conceal both the eastern margin of the Gawler Craton and the western margin of the Curnamona Province (Figure 2). The Curnamona Province consists of Paleoproterozoic and Mesoproterozoic sedimentary, volcanic and granitic rocks, metamorphosed up to granulite facies (Fricke et al., 2010). The eastern part of the transect crosses the Neoproterozoic-early Paleozoic Koonenberry Belt (Greenfield et al., 2010) and the late Silurian-Devonian Darling Basin (Stewart and Alder, 1995).

Concept of Seismic Provinces

At the surface, discrete areas of similar geology are referred to generally as *provinces* (where *craton* and *basin* are specific types of provinces). Provinces can be subdivided into *domains*. In some seismic sections, however, where rocks forming the middle to lower crust are not able to be tracked to the surface, there are no geological constraints on their age or lithological composition. We use the term *seismic province* to refer to a discrete volume of middle to lower crust, which cannot be traced to the surface, and whose crustal reflectivity is different to that of an adjoining seismic province.

In the Eyre Peninsula-Darling Basin transect, we recognise at least four discrete middle to lower crustal seismic provinces, which are, from west to east, the Yeltana, Warrakimbo, Yarramba and Tandou Seismic Provinces. These are described below, and in Korsch et al. (2010), Carr et al. (2010), Preiss et al. (2010) and Fraser et al. (2010).

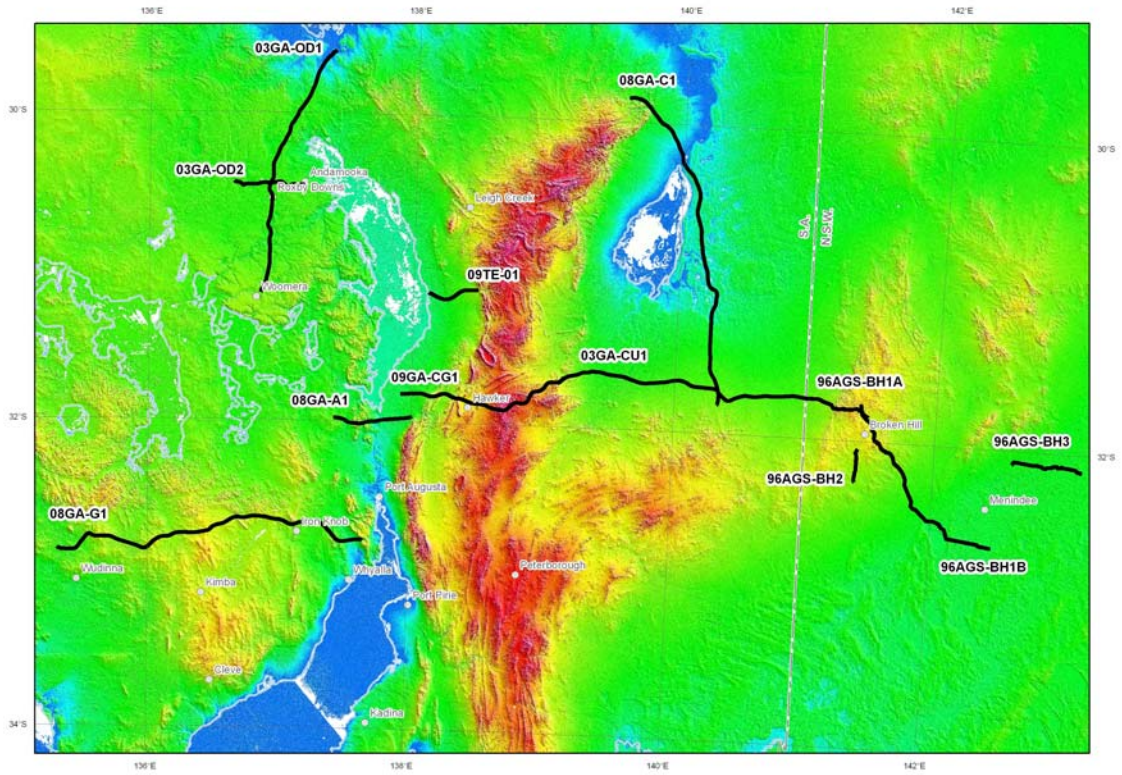

Figure 1. Map showing the digital elevation model and the locations of the deep seismic lines in South Australia and New South Wales, which form the east-west transect (warm colours are topographic highs, cool colours are topographic lows). Also shown are other deep seismic reflection lines in the region.

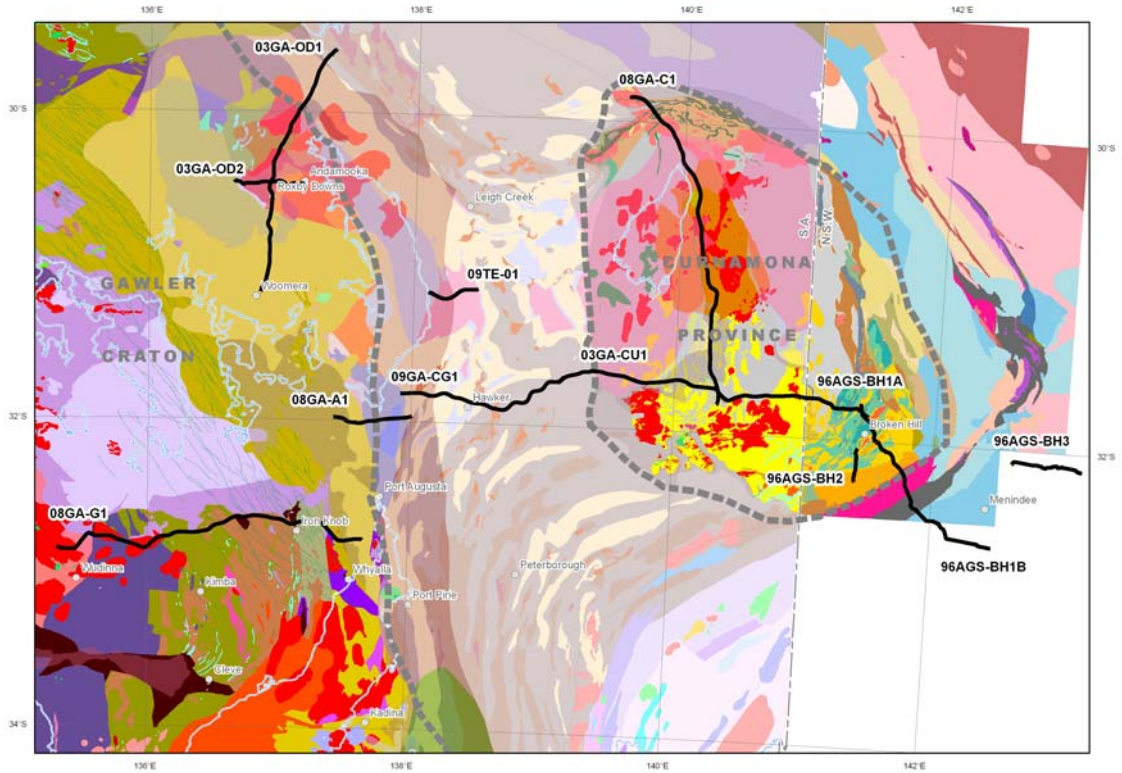

Figure 2. Map showing the solid geology of the area covered by the east-west transect (after Cowley, 2006, which also contains the legend), the inferred boundaries at the surface of the Gawler Craton and Curnamona Province (dashed lines), and the locations of the deep seismic lines in South Australia and New South Wales.

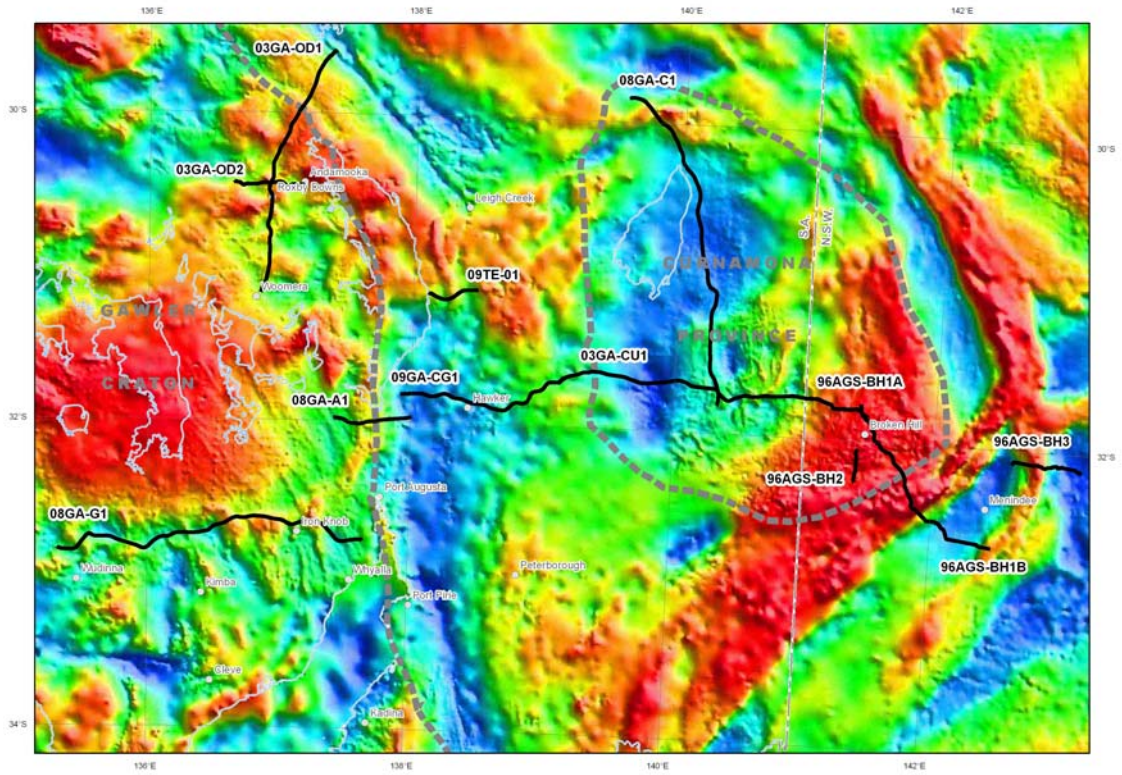

Figure 3. Gravity image of the area covered by the east-west transect, the inferred boundaries at the surface of the Gawler Craton and Curnamona Province, and the locations of the deep seismic lines in South Australia and New South Wales (warm colours are gravity highs, cool colours are gravity lows).

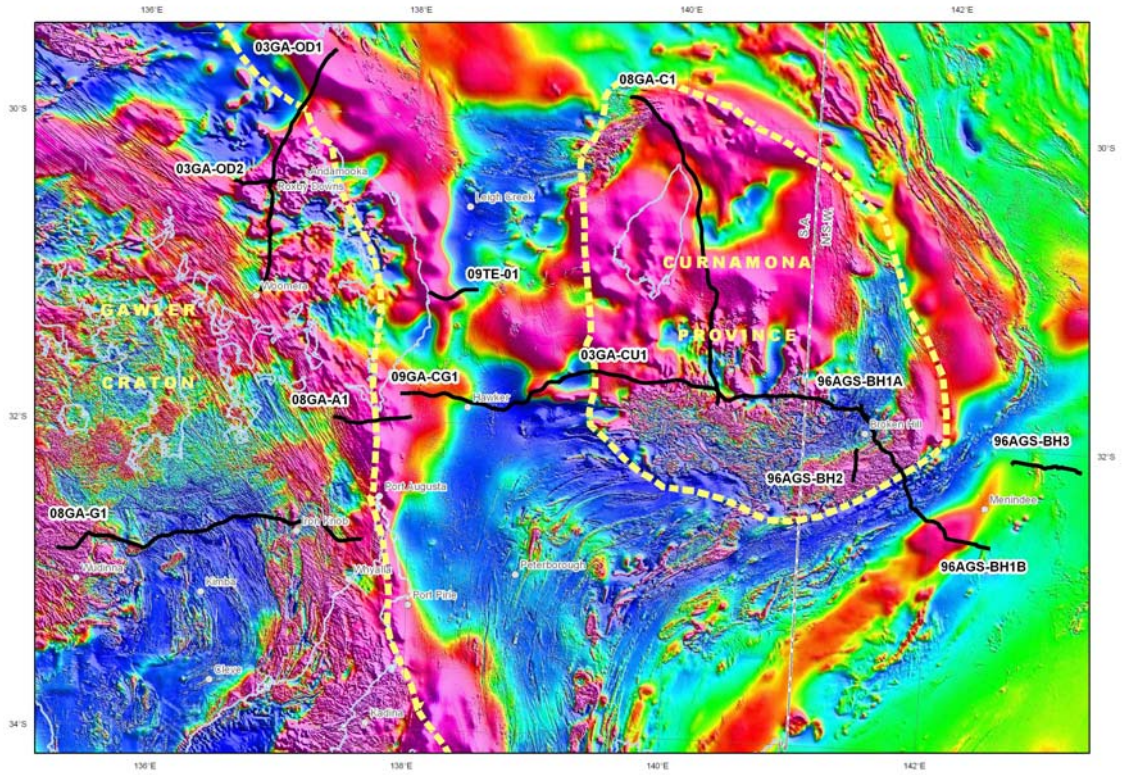

Figure 4. Total magnetic intensity image of the area covered by the east-west transect, the inferred boundaries at the surface of the Gawler Craton and Curnamona Province, and the locations of the deep seismic lines in South Australia and New South Wales (warm colours are high magnetic intensities, cool colours are low magnetic intensities).

Eyre Peninsula-Darling Basin Deep Seismic Transect

The combination of several deep seismic profiles into a single, east-west transect has provided insights into the crustal architecture and geodynamic evolution of several provinces in southern Australia.

Gawler Craton

In seismic line GA08-G1, a crustal-scale, east-dipping fault zone separates upper crust of different seismic character on the central Eyre Peninsula compared to the eastern Eyre Peninsula. The fault zone corresponds broadly to the Kalinjala Mylonite Zone, forming the boundary between the Cleve and Spencer Domains at the surface (Fraser et al., 2010a), across which there are marked changes in gravity, magnetic intensity, metamorphic grade, stratigraphy, heat flow and style of mineralisation. In particular, to the west of the Kalinjala Mylonite Zone, high-grade metamorphism, partial melting, pervasive intense ductile deformation and granite intrusion predominate during the Kimban Orogeny (~1740-1715 Ma). Protolith ages of these Kimban aged gneisses are either ~2500 Ma (Sleaford Orogeny) or ~2000 Ma (Miltalie Gneiss). There is no evidence of ~1850 Ma Donington Suite granites (Fraser et al., 2010a). By comparison, to the east of the Kalinjala Mylonite Zone, the Broadview Schist, McGregor Volcanics and Moonabie Formation were deposited prior to the Kimban Orogeny and, although deformed into upright folds, have been metamorphosed to significantly lower grades than the gneisses to the west of the mylonite zone. Mesoarchean crust (Cooyerdoo Granite, c. 3150 Ma, Fraser et al, 2010b) is present, along with granites of the Donington Suite. No Sleaford or Miltalie-aged protolith ages have been found to the east of the Kalinjala Mylonite Zone.

The movement history of the Kalinjala Mylonite Zone remains subject to speculation (see Fraser et al., 2010a). Geological evidence suggests this boundary was active at least during the Kimban Orogeny, with the variation in metamorphic grade across the fault suggesting extensional movement at this time. This could have been a continuation of the extensional event which started with basin formation and deposition of the Broadview Schist, McGregor Volcanics and Moonabie Formation. There is also evidence for subsequent reactivation, with thrust movement perhaps occurring during the Olarian Orogeny, ca. 1600 Ma.

The frontal splay of the Kalinjala Mylonite Zone occurs at the surface at about CDP 10000, and the mylonite zone forms part of an imbricate set of faults which sole onto a deep crustal-penetrating fault, extending to the eastern edge of the seismic section at ~9 s TWT (~27 km depth), with a geometry suggestive of a west-directed, thick-skinned, thrust belt. The frontal splay marks a sharp change in the magnetic character, with highly magnetic rocks to the east and weakly magnetic rocks to the west (Figure 4).

To the west of the Kalinjala Mylonite Zone, in the Cleve Domain, there is a series of near-surface, east-dipping faults between CDPs 7000 and 9500, which appear to sole onto a detachment surface at the top of the reflective middle crust at about 2.5-3 S TWT (~7.5-9 km depth). These faults were possibly extensional faults during deposition of the Hutchison Group, and our interpretation suggests that possibly they were reactivated subsequently as thrusts, with a geometry suggestive of a west-directed, thin-skinned, thrust belt in this region.

At the western end of seismic line 08GA-G1, in the Nuyts Domain, west of CDP 5200, there is a change in polarity of the faults in the upper crust, with the faults becoming predominantly west-dipping.

Middle-lower crust below Gawler Craton

The Kalinjala Mylonite Zone also separates deep crustal blocks of different composition and probably of different age. To the west of the mylonite zone, the middle to lower crust is more reflective, and characterised by predominantly east-dipping reflections. This middle to lower reflective crust has not been traced to the surface in the seismic line, and is here termed the Yeltana Seismic Province (named after a property south of seismic line 08GA-G1). The subhorizontal detachment surface, which forms the floor thrust to the inferred thin-skinned thrust belt, defines the upper boundary of the Yeltana Seismic Province (Figure 6).

To the east of the Kalinjala Mylonite Zone, the crust is not as clearly layered, and the middle crust is less reflective than in the central part of the section. Again, the middle to lower crust in this region has not been traced to the surface, and is here called the Warrakimbo Seismic Province (named after a property south of seismic line 09GA-CG1).

The timing of juxtaposition of the Yeltana and Warrakimbo Seismic Provinces across the Kalinjala Mylonite Zone is unknown, but could be significantly older than the age of movement on the mylonite zone at the surface, which is known to be at least as old as the Kimban Orogeny (ca. 1740-1715 Ma). As the Kalinjala Mylonite Zone represents a major crustal boundary, it raises the possibility of early amalgamation of terranes to form the deep crust beneath this part of South Australia.

Further to the east, the Warrakimbo Seismic Province is interpreted to occur at depth on the Arrowie Basin seismic line (08GA-A1; Carr et al., 2010) and the Curnamona Province-Gawler Craton Link seismic line (09GA-CG1, Preiss et al., 2010). In the Arrowie Basin seismic line, beneath the Neoproterozoic succession of the Adelaide Rift System and the Gawler Range Volcanics, a nonreflective package about 3 s TWT (~9 km) thick is inferred to be equivalent to the Wallaroo Group (Figure 6). The base of this package is marked by a significant increase in reflectivity, marking the top of a reflective middle crust. Reflectivity then gradually decreases downwards in the crust, so that it is extremely difficult to pick the boundary between the lower crust and upper mantle, but is inferred to be at about 14 s TWT (~42 km depth). Both the reflective middle crust and the nonreflective lower crust are referred to as the Warrakimbo Seismic Province.

The middle to lower crust on the western half of the Curnamona Province-Gawler Craton Link seismic line (09GA-CG1; Figure 6) has a similar reflectivity to that seen on the Arrowie Basin seismic line, and is also referred to as the Warrakimbo Seismic Province. One notable difference is that the upper crustal nonreflective package (equivalent to the Wallaroo Group) appears to be absent, with Neoproterozoic rocks of the Adelaide Rift System sitting directly on the Warrakimbo Seismic Province (Figure 6). Thus, the middle to lower crust below the Gawler Craton on the eastern Eyre Peninsula continues eastwards to at least the middle of the Flinders Ranges.

Curnamona Province

The Curnamona Province consists of the Paleoproterozoic (~1720-1640 Ma) Willyama Supergroup and coeval magmatic rocks (Fricke et al., 2010). These rocks were deformed and metamorphosed during the ~1600 Ma Olarian Orogeny, which was followed by an early Mesoproterozoic magmatic event (Benagerie Volcanics, Fricke et al., 2010). Seismic line 03GA-CU1 in South Australia (Goleby et al., 2006) and lines 96AGS-BH1A and 96AGS-BH1B in New South Wales (Gibson et al., 1998), form a linked transect cross the Curnamona Province (Korsch et al., 2006a). In New South Wales, the transect crosses outcrops of the rocks in the Redan and Broken Hill Domains, but in South Australia, the Curnamona Province is mostly under cover of Neoproterozoic to Cenozoic sedimentary rocks.

In the eastern two-thirds of seismic line 03GA-CU1, west of the South Australia-New South Wales border, there is an upper crustal thrust belt, with east-dipping thrusts, cutting the Willyama Supergroup. This thrust belt sits on an interpreted decollement defined by strong reflectivity at 2-3 s TWT (~6-9 km depth), which we consider to be the depth limit of the Willyama Supergroup. This decollement can be tracked westwards across the seismic section almost to a Neoproterozoic-Cambrian basin (~CDP 7500 on Figure 6). The high-level thrust belt propagated westwards, with the amount of displacement dying out to the west, and the shortening being accommodated into broad wavelength folds in the near surface. This is consistent with observed fold trends at the surface, as the northwest-verging F3 folds in outcrops of the Willyama Supergroup are consistent with apparent west-directed thrusting observed in the seismic transect. Also, this geometry is very similar to that predicted by Davies and Anderson (2000) in their schematic cross section across the Olary Block.

The original interpretation of the seismic transect in New South Wales by Gibson et al. (1998) indicated that the dominant features seen in the seismic data were a series of reflections that

had an apparent dip to the southeast. These reflections were interpreted to represent shear zones, some of which were inferred to cut deep into the crust (e.g., Mundi Mundi Fault, Figure 6). The direction of tectonic transport was mainly to the northwest, indicating that these shear zones were predominantly thrust faults. A short, high-resolution seismic line to the east of Broken Hill (05GA-BH1) has provided a much improved image of the upper 1 s TWT (~3 km) of the crust, including the region between the Stephens Creek and Globe-Vauxhall Shear Zones (Korsch et al., 2006b). This seismic line confirmed the apparent southeast dip and thrust geometry of the shear zones.

Gibson et al. (1998) considered the Mundi Mundi Fault to be an important structure that possibly marked the boundary between the Broken Hill and Olary Domains. Reprocessing of the 1996-97 seismic data has resulted in an improved seismic section which images dipping structures not detected in the original processing (Figure 6). For example, there is a series of dipping reflections to the west of, but parallel to, the reflections defining the Mundi Mundi Fault; these reflections are interpreted to be a shear zone, and it extends the limit of the zone of crustal-penetrating, southeast-dipping shear zones further to the west.

Towards the southeast of the seismic transect, the southeast-dipping shear zones extend at least to the Rockwell Shear Zone, but the Redan Fault, which marks the southeastern limit of the Curnamona Province, appears to dip to the northwest.

Middle-lower crust below Curnamona Province

In South Australia, the eastern part of seismic line 03GA-CU1 has a well-defined Moho at ~13 s TWT (~40 km depth), with a strongly reflective middle to lower crust above a nonreflective upper mantle (Figure 6). In the western half of this seismic section, the Moho is not as well defined, but appears to be undulating and slightly deeper than the eastern half (Figure 3). Below the interpreted decollement at 2-3 s TWT (~6-9 km depth), the middle to lower crust is much more reflective than the upper crust. This zone of strong reflectivity continues into New South Wales on seismic lines 96AGS-BH1A and 96AGS-BH1B (Figure 6).

The zone of strong middle to lower crustal reflectivity, observed on the western end of seismic line 03GA-CU1 can be traced onto seismic line 09GA-CG1 to as far west as a zone of crustal-penetrating, east-dipping, thrust faults (termed the Aliena Fault Zone), which project towards the surface between about CDP 5100 and CDP 6000, and appear to separate middle to lower crustal regions of very different seismic character. To the west of the westernmost crustal-penetrating fault (CDP 5100), the lower half of the crust is nonreflective, and is termed the Warrakimbo Seismic Province (see above). East of the fault at CDP 5100, the lower crust is much more reflective, and is here termed the Yarramba Seismic Province (named after a property to the north of seismic line 03GA-CU1). We consider that this seismic province can be tracked at depth beneath the entire exposed part of the Curnamona Province (Figure 6). The Aliena Fault Zone represents a major crustal boundary, with significantly different lower to middle crust on either side, indicating that it could represent a zone across which there was an amalgamation of terranes, prior to deposition of the Willyama Supergroup, to form the deep crust beneath this part of South Australia.

Superimposed on the crustal reflectivity patterns described above, in seismic line 03GA-CU1, there are a series of crustal-scale, narrow zones which we interpret as faults with apparent dips to the east. Some of these appear to cut almost the entire crust, from just below the Neoproterozoic basins to the Moho (Figure 6). We interpret these faults to be crustal-penetrating structures which occur entirely within the Yarramba Seismic Province.

Koonenberry Belt to Darling Basin

East of the Redan Fault, seismic line 96AGS-BH1B crosses the Neoproterozoic to Early Paleozoic Koonenberry Belt, which is generally nonreflective. Farther to the east, the easternmost ~45 km of the seismic line crosses the Menindee Trough of the Darling Basin, which is imaged as a series of subhorizontal reflections up to 2 s TWT (~6 km thick).

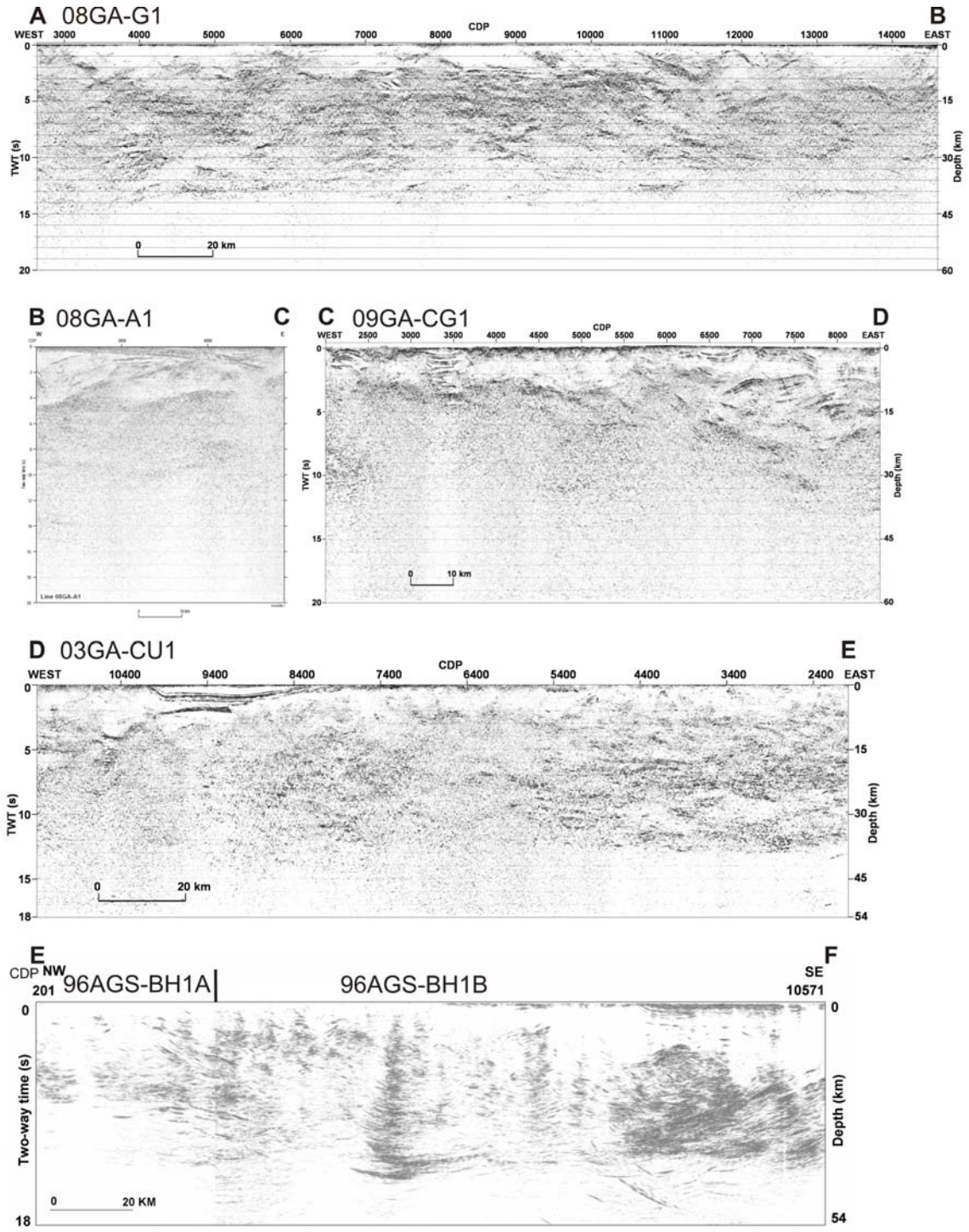

Figure 5. Display of seismic sections forming the transect from the western Eyre Peninsula to the Darling Basin. Display shows the vertical scale equal to the horizontal scale, at a crustal velocity of 6000 km s-1. Horizontal scale is based on 1 CDP equal 20 m. Note that seismic lines 96AGS-BH1A and 96AGS-BH1A are a different display, as semblance filtering has been applied to the section.

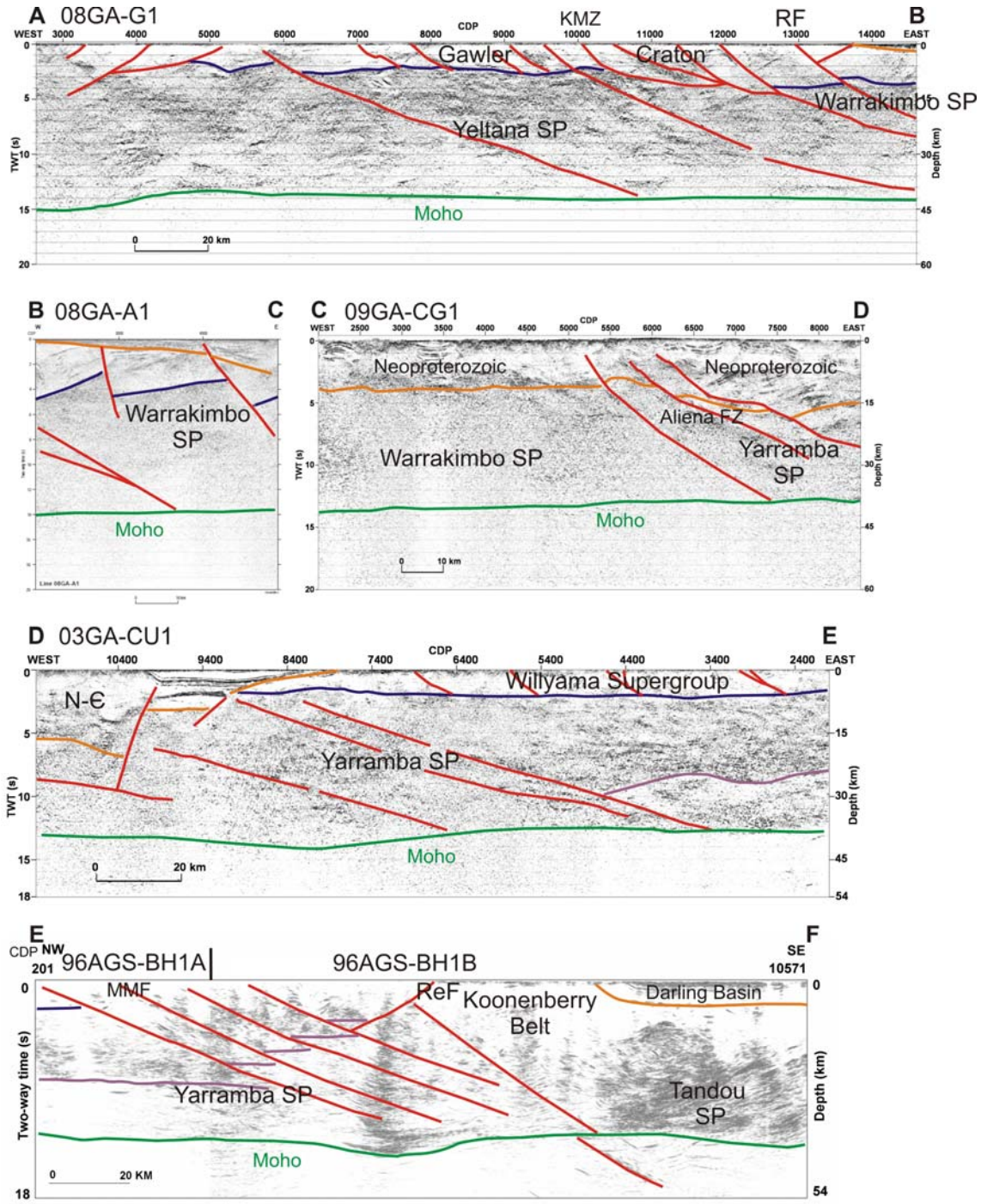

Figure 6. Interpretations of seismic sections forming the transect from the western Eyre Peninsula to the Darling Basin. Display shows the vertical scale equal to the horizontal scale, at a crustal velocity of 6000 km s-1. Horizontal scale is based on 1 CDP equal 20 m. KMZ = Kalinjala Mylonite Zone, RF = Roopena Fault, ReF = Redan Fault, MMF = Mundi Mundi Fault. Red = faults, orange = base of Neoproterozoic succession (and base of Darling Basin on lowest section), blue = top of reflective middle crust, purple = base of reflective middle crust.

Middle-lower crust below Koonenberry Belt and Darling Basin

At the surface, the boundary between the Curnamona Province and the Neoproterozoic-Paleozoic rocks of the Koonenberry Belt and Darling Basin is the northwest-dipping Redan Fault. Crust of very different reflectivity occurs beneath the Koonenberry Belt and Darling Basin compared with that under the Curnamona Province, with the crust to the east being much more reflective (Figure 6). The reflective packages representing the subsurface to the Curnamona Province and the Koonenberry Belt appear to be separated by a major structure that has an apparent dip to the southeast, and which defines the eastern limit of the Yarramba Seismic Province. To the east, the highly reflective middle to lower crust is here termed the Tandou Seismic Province (named after Tandou Lake, which was skirted by seismic line 96AGS-BH1B).

The boundary between the Yarramba and Tandou Seismic Provinces coincides approximately with strong, east-dipping reflections which penetrate the mantle to about 17 s TWT (~51 km), and possibly represents a crustal suture, with the Tandou Seismic Province being thrust over the Yarramba Seismic Province. The Redan Fault appears to be a high-level, east-directed thrust above this suture, truncating the suture about 5 km below the surface.

Geodynamic Implications

The combined seismic profiles from the western Eyre Peninsula to the Darling Basin, covering a distance of about 800 km, provide a near complete cross-section of the crust across the Gawler Craton, Adelaide Rift System, Curnamona Province, Koonenberry Belt and Darling Basin, allowing us to examine the nature of the near-surface structures as well as the nature of the middle and lower crust across this region.

The entire region is dominated by east-dipping faults, some of which originated as basin-bounding extensional faults, but most appear also to have a thrust sense of movement overprinting the extension. In the Gawler Craton, an inferred shallow, thin-skinned thrust belt occurs to the west of an inferred thick-skinned thrust belt, in which the thrusts cut deep into the crust. The boundary between the two thrust belts, the Kalinjala Mylonite Zone, was active at least during the Kimban Orogeny, with extensional movement at that time. The thrust movement possibly occurred during the ~1600 Ma Olarian Orogeny.

The thin- and thick-skinned geometry is repeated to the east in the Curnamona Province. The thrusts are thick-skinned, and cut deep into the crust in the core of the orogen in the vicinity of Broken Hill, whereas to the west, principally in South Australia, the thrust belt is thin-skinned and consists of a series of thrusts that link onto a shallow detachment at a depth of ~6-9 km. Further west, the thrusts die out and the deformation is expressed as a series of folds above a subhorizontal decollement. In this province, the two thrust belts are seen to be part of a single, linked, westward-propagating thrust system. Because the thrust system includes individual folds and thrusts that are interpreted as F3, it is inferred to have formed late during the Olarian Orogeny, at about 1600 Ma.

Recognition of this 1600 Ma linked thrust system raises the question of what was to the east of the Curnamona Province at about 1600 Ma, because the Koonenberry Belt, and probably the Tandou Seismic Province, are much younger, and were probably sutured to the Curnamona province in the Paleozoic. The westward-propagating nature of the thrust system, and its size, indicate that it was driven by a major event, either backarc contraction related to subduction, a collision or intraplate deformation, the locus of which was to the east or southeast of the present limit of the Province. In the case of backarc contraction, the implication is that there was a continental-margin magmatic arc and subduction zone to the east. As the system was in contraction, the dip of the subduction zone was likely to be shallow, and thus the thrust system was a retroforeland thrust belt forming part of an accretionary orogen. In the collision scenario, the other half of the collisional orogen was located to the east, being either a continent or island arc, which was sutured to the eastern part of the Curnamona Province following closure of an ocean. In the intraplate deformation scenario, there would have been continental crust to the east.

The Olarian structures may have been reactivated during Neoproterozoic and/or Paleozoic (Delamerian) deformational events. Shear zones exhibiting this timing are well documented at the surface in the southern Curnamona Province (Rutherford et al., 2006). Also, Delamerian deformation is seen towards the eastern end of the transect, in the Koonenberry Belt, and to the west, in the Adelaide Rift System, where Neoproterozoic rocks are strongly deformed.

At least four discrete seismic provinces have been recognised in the middle to lower crust along the seismic transect. All of these seismic provinces are bounded by east-dipping, crustal-penetrating fault zones which extend to the Moho. Each seismic province has a very different seismic reflectivity to the adjacent seismic province, suggesting that each is a unique piece of middle to lower crust, consisting of different lithologies and with a different geological history and structural architecture. As the seismic provinces have not been traced to the surface, age control is poor, but they are inferred to be older that the upper crustal rocks above them. Timing of amalgamation of the seismic provinces with each other, prior to the deposition of the sedimentary packages mapped at the surface, is also essentially unconstrained.

Conclusions

Deep seismic reflection profiling in southern Australia over the last 15 years has enabled several profiles to be combined into a single east-west transect, covering a distance of about 800 km, from the western Gawler Craton in South Australia to the Darling Basin in New South Wales. The transect provides a near complete cross-section of the crust across the Gawler Craton, Adelaide Rift System, Curnamona Province, Koonenberry Belt and Darling Basin, allowing us to examine the nature of the entire crust across this region.

Across the seismic transect, the upper crust is dominated by east-dipping faults, some of which originated as basin-bounding extensional faults. Nevertheless, most of these faults appear also to have a thrust sense of movement overprinting the extension, and in places appear to form linked thin-skinned or thick-skinned thrust belts. At least four discrete seismic provinces have been recognised in the middle to lower crust along the seismic transect. All of these seismic provinces are bounded by east-dipping, crustal-penetrating fault zones which extend to the Moho. Each seismic province has a very different seismic reflectivity to the adjacent seismic province, suggesting that each is a unique piece of middle to lower crust, consisting of different lithologies and with a different geological history and structural architecture.

Acknowledgements

We acknowledge the many geoscientists who have made contributions to the previous seismic surveys in the Gawler Craton, Curnamona Province and Koonenberry Belt: Tim Barton, Colin Conor, Barry Drummond, Martin Fairclough, David Gibson, George Gibson, Bruce Goleby, David Johnstone, Jim Leven, Patrick Lyons, David Maidment, Kingsley Mills, Andrew Owen, Matti Peljo, Stuart Robertson, Barney Stevens and Kevin Wake-Dyster. We thank Paul Henson and Natalie Kositcin for their comments on the manuscript.

References

Carr, L.K., Korsch, R.J., Holzschuh, J., Costelloe, R.D., Meixner, A.J., Matthews, C. and Godsmark, B., 2010. Geological interpretation of seismic reflection lines 08GA-C1 and 09TE-01: Arrowie Basin, South Australia. *Geoscience Australia, Record,* **2010/10**, this volume.

Davies, B. and Anderson, H., 2000. Olarian waves: deformation, fluids and alteration in the Western Willyama. In: Peljo, M., compiler, Broken Hill Exploration Initiative: Abstracts presented at the May 2000 conference in Broken Hill. *Australian Geological Survey Organisation, Record*, **2000/10**, 29-32.

Fomin, T., Korsch, R.J. and Goleby, B.R., 2006. Combining data from dynamite and vibroseis sources: deep seismic transect in the Curnamona Province, Australia. 12th International Symposium on Deep Seismic Profiling of the Continents and Their Margins. Shonan Village Center, Hayama, Japan, 24-29 September 2006, p. 69.

Fomin, T., Holzschuh, J., Nakamura, A., Maher, J., Duan, J. and Saygin, E., 2010. 2008 Gawler-Curnamona-Arrowie (L189) and 2009 Curnamona-Gawler link (L191) seismic surveys – acquisition and processing. *Geoscience Australia, Record,* **2010/10**, this volume.

Fraser, G.L., Blewett, R.S., Reid, A.J., Korsch, R.J., Dutch, R., Neumann, N.L., Meixner, A.J., Skirrow, R.G., Cowley, W.M, Szpunar, M., Preiss, W.V., Nakamura, A., Fomin, T., Holzschuh, J., Milligan, P.R. and Bendall, B.R., 2010a. Geological interpretation of deep seismic reflection and magnetotelluric line 08GA-G1: Eyre Peninsula, Gawler Craton, South Australia. *Geoscience Australia, Record,* **2010/10**, this volume.

Fraser, G.L, McAvaney, S., Neumann, N.L., Szpunar, M., Reid, A.J., 2010b. Discovery of Mesoarchean crust in the eastern Gawler Craton, South Australia. *Precambrian Research*, in press.

Fricke, C.E., Preiss, W.V. and Neumann, N.L. 2010. Curnamona Province: a Paleo- to Mesoproterozoic time slice. *Geoscience Australia, Record,* **2010/10**, this volume.

Gibson, G., Drummond, B., Fomin, T., Owen, A., Maidment, D., Gibson, D., Peljo, M. and Wake-Dyster, K., 1998. Re-evaluation of crustal structure of the Broken Hill Inlier through structural mapping and seismic profiling. *Australian Geological Survey Organisation, Record* **1998/11,** 55 pp.

Greenfield, J.E., Gilmore, P.J. and Mills, K.J., compilers. Explanatory notes for the Koonenberry Belt geological maps. *Geological Survey of New South Wales, Bulletin*, **35**, in press.

Goleby, B.R., Korsch, R.J., Fomin, T., Conor, C.H.H., Preiss, W.V., Robertson, R.S. and Burtt, A.C., 2006. The 2003-2004 Curnamona Province seismic survey. *Geoscience Australia, Record*, **2006/12**, 96 pp.

Korsch, R.J., Fomin, T., Conor, C.H.H., Stevens, B.P.J., Goleby, B.R., Robertson, R.S. and Preiss, W.V., 2006. A deep seismic reflection transect across the Curnamona Province from the Darling Basin to the Flinders Ranges. In: Korsch, R.J. and Barnes, R.G., compilers, 2006a. Broken Hill Exploration Initiative: Abstracts for the September 2006 Conference. *Geoscience Australia, Record,* **2006/21**, 102-109.

Korsch, R.J., Fomin, T. and Stevens, B.P.J., 2006b**.** Preliminary results of a high resolution seismic reflection survey at Broken Hill. *Geoscience Australia, Record*, **2006/21**, 110-115.

Korsch, R.J., Preiss, W.V., Blewett, R.S., Fabris, A.J., Neumann, N.L., Fricke, C.E., Fraser, G.L., Holzschuh, J. and Jones, L.E.A., 2009. The 2008 north-south oriented, deep seismic reflection transect across the Curnamona Province, South Australia. In: Korsch, R.J., editor, Broken Hill Exploration Initiative: Abstracts for the 2009 Conference. *Geoscience Australia, Record,* **2009/28**, 90-100.

Korsch, R.J., Preiss, W.V., Blewett, R.S., Fabris, A.J., Neumann, N.L., Fricke, C.E., Fraser, G.L., Holzschuh, J., Milligan, P.R. and Jones, L.E.A., 2010. Geological interpretation of deep seismic reflection and magnetotelluric line 08GA-C1: Curnamona Province, South Australia. *Geoscience Australia, Record,* **2010/10**, this volume.

Preiss, W.V., 2010. Geology of the Neoproterozoic to Cambrian Adelaide Geosyncline and Cambrian Delamerian Orogen. *Geoscience Australia, Record,* **2010/10**, this volume.

Preiss, W.V., Korsch, R.J., Blewett, R.S., Fomin, T., Cowley, W.M., Neumann, N.L. and Meixner, A.J., 2010. Geological interpretation of deep seismic reflection line 09GA-CG1: the Curnamona Province-Gawler Craton Link Line, South Australia. *Geoscience Australia, Record,* **2010**, this volume.

Reid, A., Szpunar, M. and Fairclough, M. 2010. Overview of the geology of the Gawler Craton, South Australia. *Geoscience Australia, Record,* **2010/10**, this volume.

Rutherford, L., Hand, M. and Mawby, J., 2006. Delamerian-aged metamorphism in the southern Curnamona Province, Australia; implications for the evolution of the Mesoproterozoic Olarian Orogeny. *Terra Nova*, **18**, 138-146.

Stewart, J.R. and Alder, J.D., 1995. Darling Basin. In: New South Wales petroleum potential. *New South Wales Department of Mineral Resources, Coal and Petroleum Geology Branch, Bulletin*, **1**, 37-56.

Recent deep seismic reflection surveys in the Gawler Craton and Curnamona Province, South Australia: Implications for regional energy systems

N.L. Neumann[1], R.S. Blewett[1], G.L. Fraser[1], P. Henson[1], W.V. Preiss[2], R.J. Korsch[1], W.M. Cowley[2] and A.J. Reid[2]

[1]Onshore Energy & Minerals Division, Geoscience Australia, GPO Box 378, Canberra, ACT 2601, Australia
[2]Geological Survey Branch, Primary Industries and Resources South Australia (PIRSA), GPO Box 1671, Adelaide, SA 5001, Australia

Narelle.Neumann@ga.gov.au

Introduction

Between mid-2008 and early 2009, Geoscience Australia, in conjunction with Primary Industries and Resources South Australia (PIRSA), acquired ~720 km of new deep seismic reflection data in the southern Gawler Craton and Curnamona Province, South Australia, as part of the Onshore Energy Security Program. The main aim of the seismic surveys was to image the crustal architecture of the Gawler Craton and Curnamona Province, and the overlying Adelaide Rift System, in order to evaluate the uranium, geothermal and petroleum potential of the region. Seismic data were collected along a number of transects (Figures 1 to 3): 1) north-south Curnamona line (08GA-C1; ~262 km length); 2) Curnamona-Gawler Link line (09GA-CG1; ~144 km length); 3) Arrowie Basin line (08GA-A1; ~60km) and 4) Eyre Peninsula line (08GA-G1; ~253 km). In 2009, Torrens Energy acquired the 41 km long Parachilna seismic line (09TE-01), about 90 km to the north of the Arrowie Basin line, as part of their geothermal exploration program, which was also integrated into this study. Collectively, these lines, together with the Olympic Dam and Curnamona seismic reflection data collected in 2003 (03GA-OD1, 03GA-OD2 and 03GA-CU1), provide seismic transects which can be used to characterise the crustal architecture and inferred geodynamics of this region. This architecture and geodynamic interpretation can then be integrated with other geological and geophysical data sets to evaluate energy and other mineral systems at a regional scale.

Here, we focus on the interpretation of the seismic data with regards to the regional extent and crustal geometry of the Olympic iron oxide-copper-gold+uranium (IOCG+U) Province within the Gawler Craton (e.g., Skirrow et al., 2002), and the South Australia Heat Flow Anomaly (e.g., Neumann et al., 2000) for geothermal energy system plays.

Crustal character of the Olympic IOCG+U Province

The Olympic IOCG+U Province along the eastern side of the Gawler Craton was defined by Skirrow et al. (2002), and includes the Mount Woods Inlier, the Olympic Dam region and the Moonta-Wallaroo region (Figure 1). Two seismic transects were collected previously in the Olympic Dam region (03GA-OD1 and 03GA-OD2), to image the crustal architecture of the giant IOCG+U Olympic Dam deposit (Figure 4). Using these data, Lyons and Goleby (2005) interpreted the Olympic Dam deposit to lie above the boundary between two distinct crustal blocks – one interpreted to be Archean-Paleoproterozoic in the southwest and the other as Meso-Neoproterozoic crust to the northeast (Figure 4).

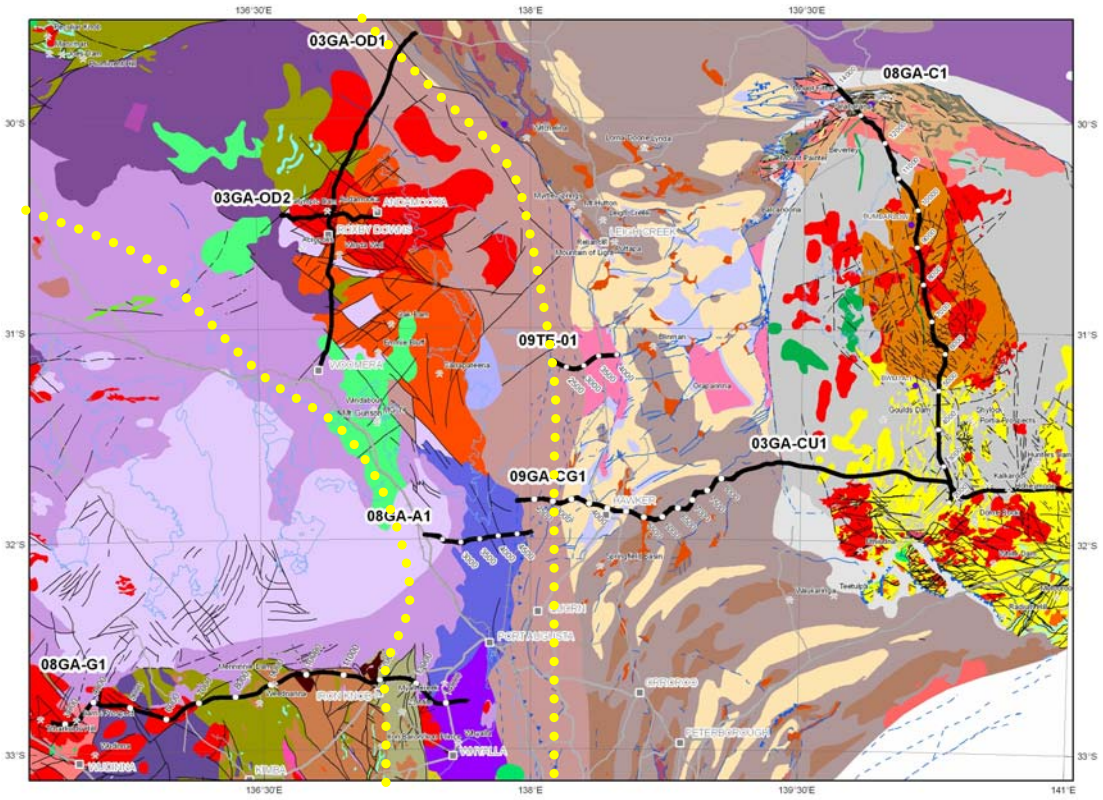

Figure 1. Solid geology of central South Australia (from Cowley, 2006, which also contains the legend) with the locations, names and CDP stations of the deep seismic reflection transects. The dashed yellow lines indicate the approximate boundaries of the Olympic IOCG+U Province within the study area (from Skirrow et al., 2002).

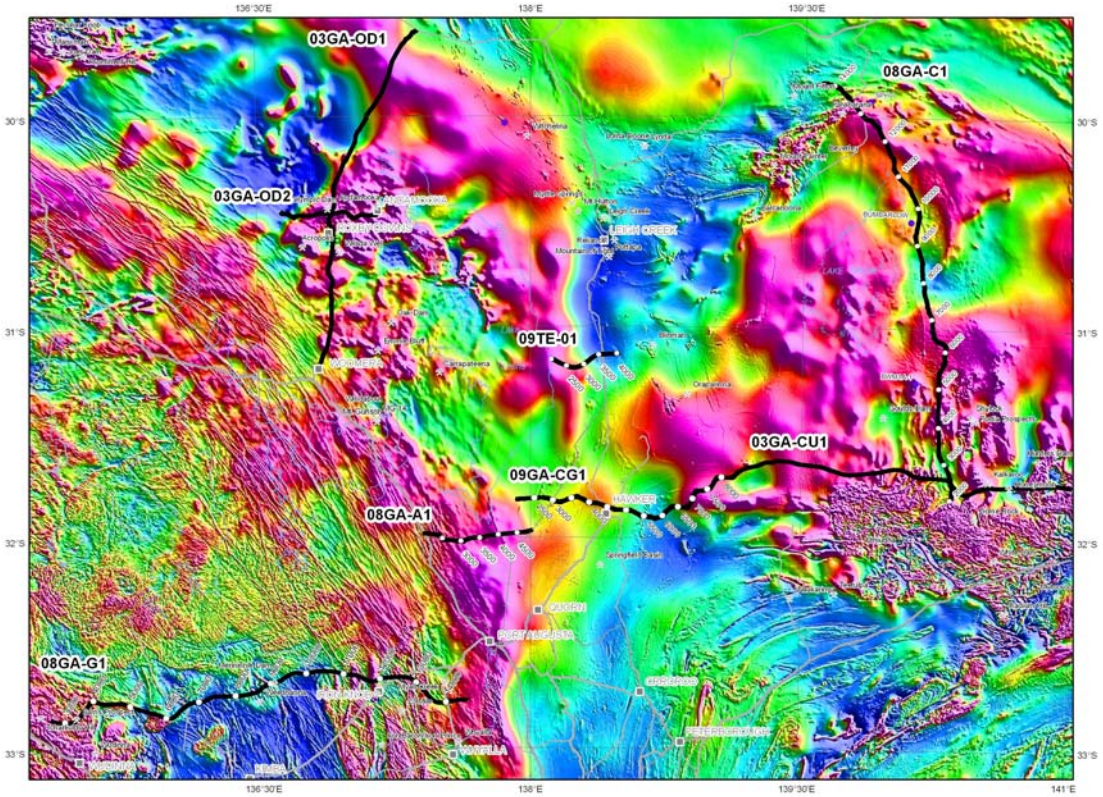

Figure 2. Enhanced TMI (total magnetic intensity) of central South Australia, with the locations, names and CDP stations of the deep seismic reflection transects (warm colours are high magnetic intensities, cool colours are low magnetic intensities).

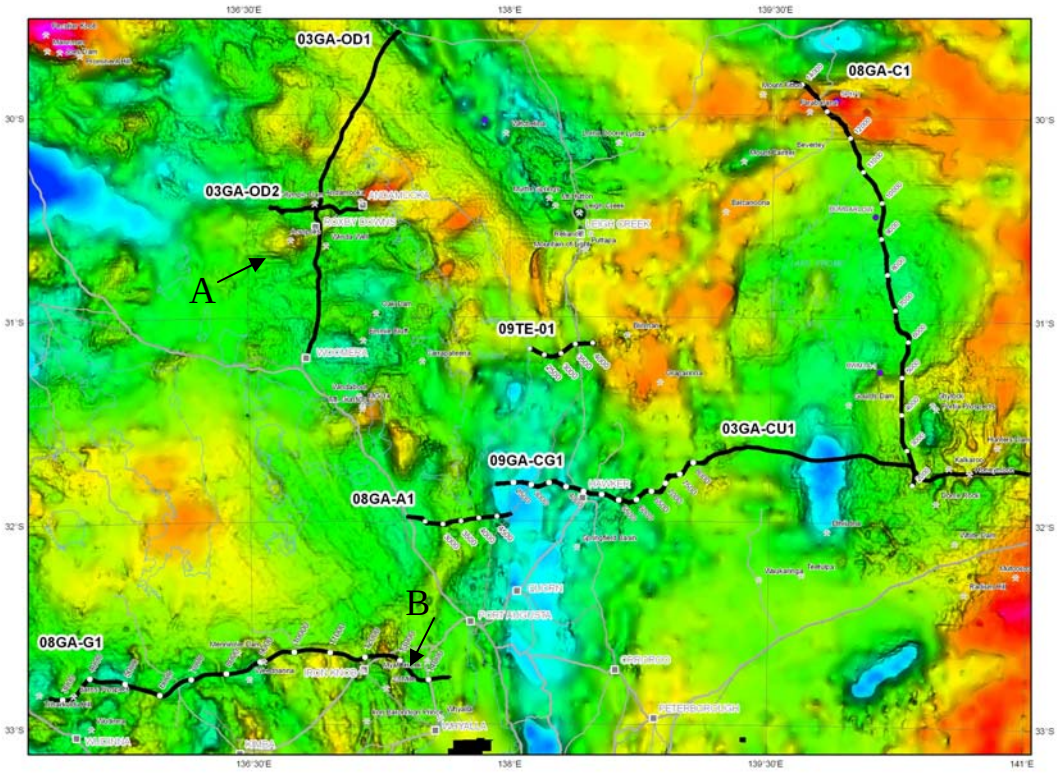

Figure 3. Bouguer gravity image of central South Australia, with the locations, names and CDP stations of the deep seismic reflection transects. Warm colours represent gravity high regions, cool colours represent gravity low regions. A is the Acropolis prospect (which is associated with significant magnetite alteration) and B is a dense body located in the Roopena region. Note other ovoid density anomalies, many of which are due to alteration systems depositing iron, chiefly magnetite (see Chopping et al., 2010).

The boundary between these two blocks corresponds to the Elizabeth Creek Fault, a northeast dipping fault which intersects the surface ~30 km southwest of the deposit. Another feature identified within the transects is a middle- to lower crustal region which is ~40-50 km wide and has a relatively lower amplitude and coherency, referred to as a 'bland zone', directly beneath the deposit (Figure 4; Lyons and Goleby, 2005; Drummond et al., 2006). In the region below Olympic Dam, the Moho is poorly defined in the seismic data. Coincident with this seismic bland zone, is a conductivity anomaly mapped in magnetotelluric data that extends from the Moho to the upper crust (Heinson et al., 2006).

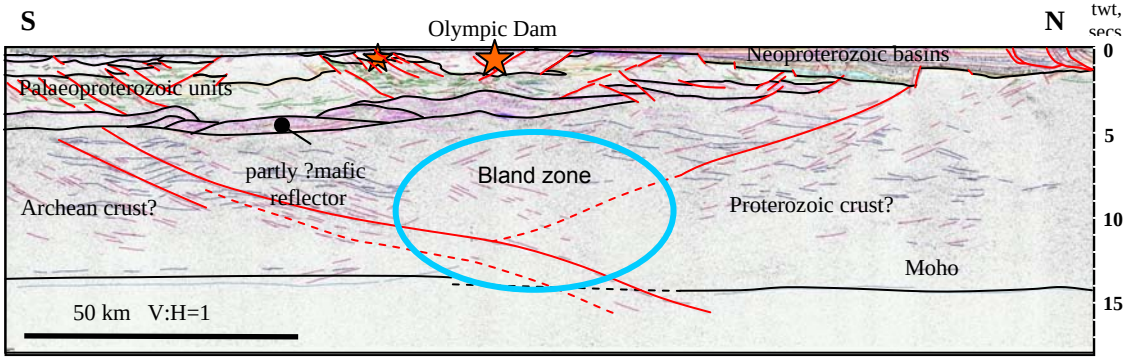

Figure 4. Seismic data and interpretation for the Olympic Dam region (03GA-OD1) showing some of the key architectural components of the IOCG+U mineralisation system (from Lyons and Goleby, 2005). The key components include a major boundary (fault) between different aged crustal domains, and normal (extensional) offset of the Moho by this structure, and a seismic bland zone interpreted to be due to lower crustal alteration.

Both the Eyre Peninsula (08GA-G1) and the Arrowie Basin (08GA-A1) seismic lines cross the Olympic IOCG province (Figures 1 to 3), in the region between known IOCG mineralisation at Olympic Dam in the north, and the Moonta-Wallaroo mineral district in the south. These seismic lines provide architectural information along strike from the Olympic Dam deposit, and they share some of the key features seen in the seismic data from the Olympic Dam region.

A major structure of pre-Adelaidean age is imaged in the Arrowie Basin line (Figure 1; Carr et al., 2010). This structure (ca. 2700 CDP on 08GA-A1), informally termed the Nob Hill Fault, shares many features of the Elizabeth Creek Fault. It is a crustal–scale east-dipping extensional fault, linking into a low-amplitude bland zone in the middle- to lower crust, below which the Moho is poorly imaged. The Nob Hill Fault has a similar orientation to the Elizabeth Creek Fault, and it may represent the southeastern continuation of this fault system. This would suggest that the Elizabeth Creek Fault is part of a laterally continuous, craton-scale fault system, and that regions along this structural corridor might be favourable for IOCG+U mineralisation. Although the thickness of Neoproterozoic and younger cover stratigraphy in the vicinity of the Arrowie line is at least 700 m, these cover rocks thin to the northwest, indicating that this may be a favourable region of high IOCG+U mineralisation potential. No magnetotelluric data exist in the region around the Arrowie Basin line to test the continuation of the conductivity anomaly observed beneath Olympic Dam.

Further along strike to the south, the Eyre Peninsula line (08GA-G1) also intersects the Olympic IOCG+U Province of Skirrow et al. (2002). The Kalinjala Mylonite Zone (KMZ) in the eastern part of the Eyre Peninsula is also an east-dipping crustal-scale structure (see Fraser et al., 2010), and may represent a further extension of this craton-scale fault system. In detail, the trend of the KMZ may be offset from the Elizabeth Creek Fault system by northeast–southwest trending structures, or is a parallel fault system which continues north underneath the Gawler Range Volcanics. Within the hangingwall of the KMZ and immediately west of the Roopena Fault (Fraser et al., 2010), there is a body which is 5 km wide of unusually high gravity (Figure 3), which is also weakly to nonmagnetic (Figure 2). The body strikes northwest, transecting the regional north-northwest strike, so is likely to be either intrusive in origin, or a basement high. The body has similar dimensions and gravity response to the alteration system at Acropolis (Figure 3), which is a dense and magnetic body (Williams et al., 2004). Fraser et al. (2010) model the Eyre Peninsula gravity body with a density of 2.95 g/cm^3, which is consistent with the following interpreted sources:

1) a dense mafic intrusive rock (~gabbro) that has been highly altered, resulting in the loss of magnetite, or
2) a felsic (~granite) or metasedimentary rock that is strongly hematite-altered, accounting for the nonmagnetic yet dense character.

If this body is caused by second alternative listed above, its position near the KMZ elevates the potential of this anomaly as an IOCG+U target.

Geothermal energy systems: the South Australia Heat Flow Anomaly

Hot Rock (HR) geothermal energy systems require high average geothermal gradients and good insulation by overlying basin packages. One of Australia's areas of highest geothermal gradient is associated with the South Australia Heat Flow Anomaly (SAHFA; Neumann et al., 2000), which is centred on the eastern Gawler Craton, Adelaide Rift System, and the western Curnamona Province (Figure 5). Although there are only a limited number of surface heat flow measurements in this region, the existing measurements define a broad (>250 km wide) zone of anomalously high surface heat flow (92 ± 10 mWm^{-2}; Neumann et al., 2000). More recent studies within the SAHFA region have added to the heat flow database and confirm the elevated values, with reports of 74-120 mWm^{-2} and 129 mWm^{-2} within the Torrens Energy geothermal exploration area (Matthews, 2009) and Petratherm's Paralana geothermal exploration area (Reid et al., 2009), respectively.

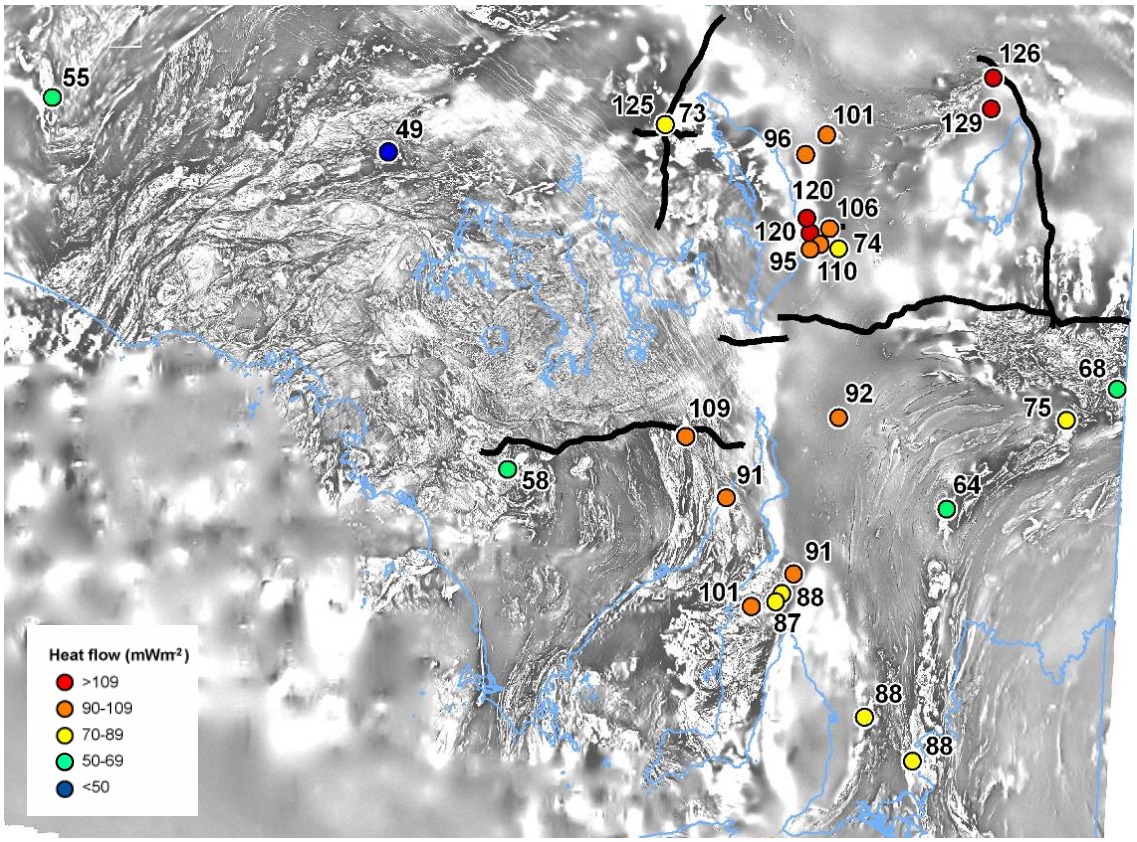

Figure 5. Map showing the location of existing heat flow measurements, and their value in mWm^{-2} (From Cull, 1982; Houseman et al., 1989; Matthews, 2009; Reid et al., 2009) on a Total Magnetic Intensity image. Also shown are the locations of the deep seismic reflection transects within this region.

Regional geochemical data sets indicate that this high heat flow zone correlates with elevated surface heat production values, which are predominantly hosted by Proterozoic granites. Comparisons suggest that the U and Th concentrations within the SAHFA crust are 2-3 times greater than would be expected, based on the global heat flow database (Neumann et al., 2000). Identifying the extent of these high heat-producing rocks, especially under cover in areas of sparse heat flow measurements can assist exploration in defining areas of high geothermal potential.

Characterising the middle to lower crust

Given that the SAHFA is a crustal feature, datasets including seismic reflection and gravity can be used to describe the large-scale characteristics of the crust in this region. The seismic character of a crustal column, in terms of the relative amplitude and the coherence of reflections, can distinguish one crustal domain from another. Similarly, the mass distribution varies with depth in the crust and laterally between different crustal domains. Regions of high gravity generally contain denser (mafic) rocks than those with low gravity, which generally contain less dense (felsic) rocks. Combining these two geophysical datasets permits identification of different crustal domains, and their intervening boundaries.

All of the seismic lines traverse the crustal-scale SAHFA (Figure 5) which, when integrated with gravity data, provides insights into the large-scale character and composition of this crustal-scale geochemical and thermal anomaly. In particular, the Eyre Peninsula line crosses the western margin of the SAHFA, from an area with lower heat flow in the west to higher heat flow in the east, and the Arrowie, Parachilna and Curnamona-Gawler Link lines occur within this high heat flow zone (Figure 5). The 2003 east-west Curnamona line (which links to the Curnamona-Gawler Link line on its western end) crosses the proposed eastern margin of the SAHFA, as

does the new north-south Curnamona line, which crosses the northern extent of the Mount Painter Province, which contains the most radiogenic granites known within Australia.

The seismic character and gravity response of the middle- to lower crust changes across the Eyre Peninsula line (Fraser et al., 2010), from crust with stronger seismic reflections and higher density in the west, to less seismically reflective and less dense crust in the east. The boundary between these two crustal blocks corresponds to the east-dipping KMZ. This boundary also approximates the change in surface heat flow (Figure 5) as well as heat production values within Hiltaba Granites (calculated from U, Th and K concentrations), from lower values in the west to higher values in the east (Neumann et al., 2000). This fault zone may thus represent the boundary between less radiogenic and more radiogenic middle- to lower crust and, if so, suggests that the area to the east of the KMZ has a greater potential for geothermal systems.

To the east, the characteristically less seismically reflective middle- to lower crust continues beneath the Arrowie, Parachilna and Curnamona-Gawler Link lines, until ca. CDP 5400 in the Curnamona-Gawler Link line, where the middle- to lower crust becomes more seismically reflective. This change in reflectivity occurs across a major crustal-scale fault that also dips to the east (Preiss et al., 2010). This fault may represent the eastern boundary of the more radiogenic middle- to lower crust. A similar change in seismic character is described in the north-south Curnamona line, with the lower crust in the northern part of the transect only weakly reflective, whereas in the southern part of line, the middle- to lower crust is strongly reflective (Korsch et al., 2010).The SAHFA is therefore mapped between these east-dipping crustal-scale faults, defining a corridor of higher geothermal potential.

Characterising overlying basin packages

As well as characterising compositional changes in the nature of the middle- to lower crust, and thus heat production capacity, across the SAHFA, both seismic and gravity data can be used to determine the location, regional extent and thickness of overlying basin packages, which are another important ingredient in HDR geothermal systems. Basin packages including the Gawler Range Volcanics and Neoproterozoic-Cambrian successions of the Adelaide Rift System have been imaged in the Arrowie, Parachilna and Curnamona-Gawler Link seismic lines, and are up to ~15 km thick.

Basins are commonly filled with relatively low density sedimentary rocks compared to the basement, which commonly contains relatively high density igneous rocks. This means that gravity lows are generally correlated with basins. However, this gravity relationship to basins does not always hold, and this is the case in the study area. Here, the basement is variable in its felsic-mafic ratio, and the overlying Neoproterozoic basin is variable in its sediment-mafic volcanic ratio. The deep seismic reflection data can be used to analyse the relationship between gravity and the nature of the crust. Comparison of the gravity signal and basin thickness determined from the 03GA-OD1 Olympic Dam seismic line illustrates that the main gravity signal in terms of density is derived from thick, dense, mafic volcanic successions in the lower part of the basin. The basement to the basin here consists of granites of the Hiltaba Suite and felsic rocks of the Gawler Range Volcanics (Lyons and Goleby, 2005), which are clearly less dense than the overlying basin.

Along the Gawler-Curnamona Link line, the seismic data show an asymmetric half graben basin up to ~10 km thick in the hangingwall of a crustal-scale, east-dipping extensional fault (Preiss et al., 2010). This area of maximum basin thickness with abundant mafic volcanics, however, has a higher gravity response than the area immediately to the west, which is characterised by a thinner basin (~4 km) and a lower gravity signal (Figure 6). This suggests that the low gravity response across the western part of the line is associated with lower density basement rocks in the near surface rather than a thick basin succession. The low density in the basement is likely to be due to a high felsic-mafic ratio for this crustal column. It is felsic rocks, such as granites, that contain the high concentrations of heat producing elements, and these rock types tend to be associated with gravity lows. The gravity data (Figure 6) shows that this favourable corridor of possible heat-producing crust extends well to the south of the seismic lines, and so this low-gravity corridor in the area east and southeast of Port Augusta may be worthy of further consideration for a geothermal system play.

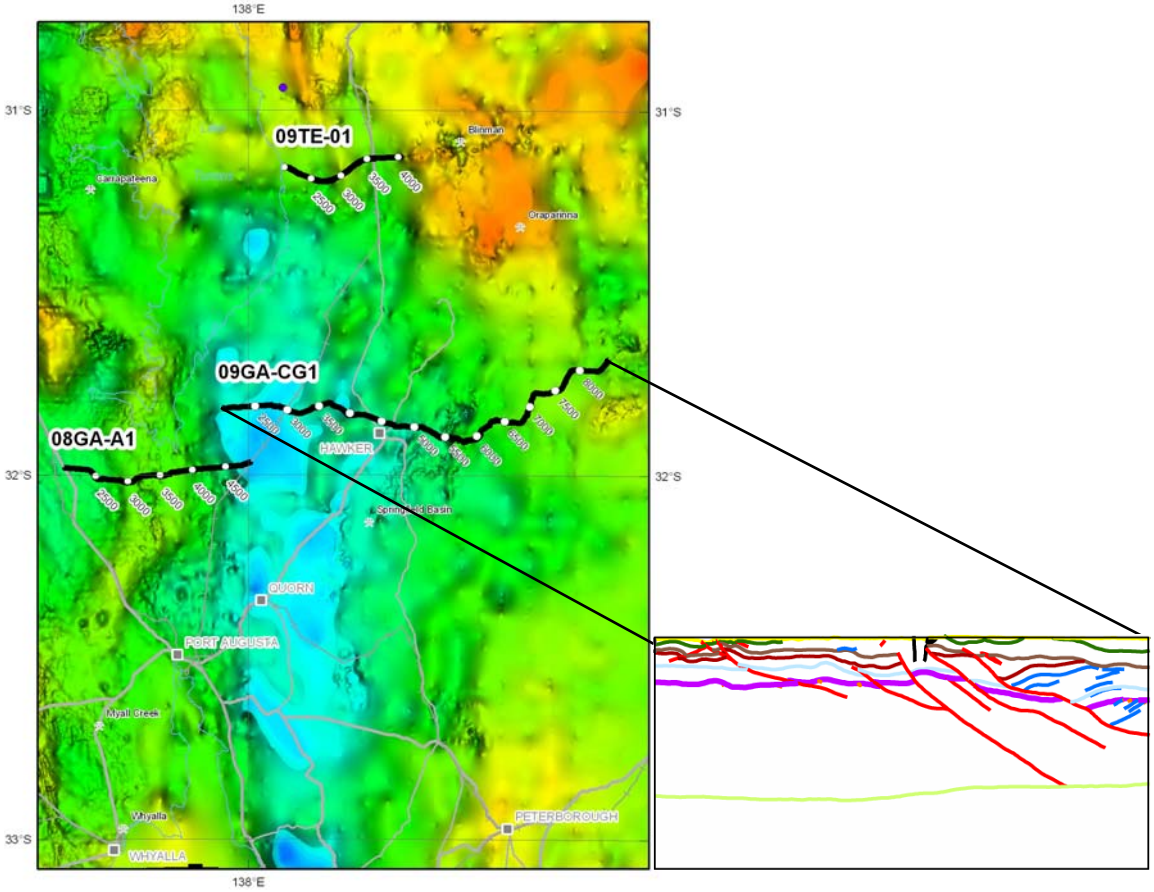

Figure 6. Map showing the gravity data and the interpreted seismic line in the Gawler-Curnamona Link line region (from Preiss et al., 2010). Note the low gravity response (blue colours) along the western part of the Gawler-Curnamona Link line, which is coincident with the location of relatively shallow basement (purple line) in the seismic section, and continues south past Port Augusta.

The seismic reflection data also image numerous fault systems within these basins. The presence of faults may influence hydraulic fracture stimulation models and fluid flow migration pathways within HR geothermal systems. Furthermore, the identification of stratigraphic packages or lithologies based on their seismic character may be used for thermal conductivity modelling within geothermal play systems.

Conclusions

The new seismic data, integrated with existing transects and other geophysical and geological data, provide new insights into the uranium and geothermal potential of the southern Gawler Craton, Curnamona Province and Adelaide Rift System. Along the Arrowie Basin line, the presence of an east-dipping crustal-scale structure, which also corresponds to a seismically non-reflective middle- to lower crust, suggests that crustal geometries similar to Olympic Dam are also preserved along strike to the southeast of this IOCG+U deposit. Some of these crustal components are also observed in the eastern Eyre Peninsula line, corresponding to the KMZ, suggesting another area of high IOCG+U potential. Integration of the surface heat flow with changes in seismic character of the crust suggests that the SAHFA is constrained to the east of the KMZ and is a broad north-south trending anomaly that may continue east as far as another crustal-scale structure imaged in the eastern part of the Gawler-Curnamona Link line. Within this high heat flow area, the seismic and gravity data can be used to identify both the thickness and fault geometry of basin packages, therefore providing a further guide for geothermal exploration.

Acknowledgements

We thank Roger Skirrow for many informative discussions on the characteristics and potential of the Olympic IOCG+U Province, and Lindsay Highet is acknowledged for preparing the figures. Roger Skirrow and Anthony Budd are thanked for their comments on the manuscript.

References

Carr, L.K., Korsch, R.J., Holzschuh, J., Costelloe, R.D., Meixner, A.J., Matthews, C. and Godsmark, B., 2010. Geological interpretation of seismic reflection lines 08GA-C1 and 09TE-01: Arrowie Basin, South Australia. *Geoscience Australia, Record,* **2010/10**, this volume.

Chopping, R., Williams, N.C., Meixner, A.J. and Roy, I.G., 2010. 3D potential-field inversions and alteration mapping in the Gawler Craton and Curnamona Province, South Australia. *Geoscience Australia, Record,* **2010/10**, this volume.

Cowley, W.M., 2006. Solid geology of South Australia: peeling away the cover. *MESA Journal*, **43**, 4-15.

Cull, K.P., 1982. An appraisal of Australian heat flow data. *BMR Journal of Australian Geology and Geophysics*, **7**, 11-21.

Drummond, B., Lyons, P., Goleby, B. and Jones, L., 2006. Constraining models of the tectonic setting of the giant Olympic Dam iron oxide-copper-gold deposit, South Australia, using deep seismic reflection data. *Tectonophysics,* **420**, 91-103.

Fraser, G.L., Blewett, R.S., Reid, A.J., Korsch, R.J., Dutch R., Neumann, N.L., Meixner, T., Skirrow, R.G., Cowley, W., Szpunar, M., Preiss, W.V., Nakamura, A., Fomin, T., Holzschuh, J., Milligan P. and Bendall, B., 2010. Geological interpretation of deep seismic reflection and magnetotelluric line 08GA-G1: Eyre Peninsula, Gawler Craton, South Australia. *Geoscience Australia, Record,* **2010/10**, this volume.

Heinson, G.S., Direen, N.G., and Gill, R.M. 2006. Magnetotelluric evidence for a deep-crustal mineralizing system beneath the Olympic Dam iron oxide copper-gold deposit, southern Australia. *Geology*, **34**, 573–576.

Houseman, G.A., Cull, J.P., Muir, P.M., and Paterson, H.L., 1989. Geothermal signatures and uranium ore deposits on the Stuart Shelf of South Australia. *Geophysics*, **54**, 158-170.

Korsch, R.J., Preiss, W.V., Blewett, R.S., Fabris, A.J., Neumann, N.L., Fricke, C.E., Fraser, G.L., Holzschuh, J., Milligan, P.R. and Jones, L.E.A., 2010. Geological interpretation of deep seismic reflection and magnetotelluric line 08GA-C1: Curnamona Province, South Australia. *Geoscience Australia, Record,* **2010/10**, this volume.

Lyons, P. and Goleby, B.R., 2005. The 2003 Gawler seismic survey: notes of the seismic workshop held at Gawler Craton State of Play 2004. *Geoscience Australia, Record,* **2005/19**, 85pp.

Matthews, C., 2009. Geothermal energy prospectivity of the Torrens Hinge Zone: evidence from new heat flow data. *Exploration Geophysics*, **40**, 288-300.

Neumann, N., Sandiford, M. and Foden, J., 2000. Regional geochemistry and continental heat flow: implications for the origin of the South Australian Heat Flow anomaly. *Earth and Planetary Science Letters,* **183**, 107-120.

Preiss, W.V., Korsch, R.J., Blewett, R.S., Fomin, T., Cowley, W.M., Neumann, N.L. and Meixner, A.J., 2010. Geological interpretation of deep seismic reflection line 09GA-CG1: the Curnamona Province-Gawler Craton Link Line, South Australia. *Geoscience Australia, Record,* **2010/10**, this volume.

Reid, P.W., Bendall, B.R. and McAllister, L., 2009. Developing large scale, base load EGS power: the Paralana project, South Australia. In: Korsch, R.J., editor, Broken Hill Exploration Initiative: Abstracts from the 2009 conference. *Geoscience Australia, Record*, **2009/28**, 156-160.

Skirrow, R.G., Bastrakov, E., Davidson, G., Raymond, O.L. and Heithersay, P., 2002. The geological framework, distribution and controls of Fe oxide Cu-Au mineralisation in the Gawler Craton, South Australia. Part II. Alteration and mineralisation. In: Porter, T.M., editor, *Hydrothermal iron oxide copper-gold and related deposits: A global perspective*. Adelaide, Porter GeoConsultancy Publishing, 33-47.

Williams, N.C., Lane, R., and Lyons, P., 2004. Regional constrained 3D inversion of potential field data from the Olympic Cu-Au-(U) province, South Australia. *Preview (Australian Society of Exploration Geophysicists)*, **109**, 30–33.